

TESIS DOCTORAL

2023

MATERIALES POLIMÉRICOS BIOBASADOS DERIVADOS DEL ÁCIDO ITACÓNICO CON ACTIVIDAD ANTIMICROBIANA

ALBERTO CHILOECHES SUÁREZ

Programa de Doctorado en Ciencias

Directora: Dra. Alexandra Muñoz Bonilla (CSIC-ICTP)

Codirectora: Dra. María del Coro Echeverría Zabala (CSIC-ICTP)

Tutora: Dra. Mercedes de la Fuente Rubio (UNED)

Han pasado ya cuatro años desde que empecé el doctorado. Cuatro años de trabajo duro y constancia, pero también de alegría y disfrute. Tras este largo camino, aquí estoy con mi tesis doctoral terminada. Pero este logro no ha sido gracias solo a mí, detrás siempre he tenido a gente que me apoyaba y confiaba.

En primer lugar, quiero agradecer al Ministerio de Universidades por la beca FPU18/01776, con la que se ha financiado esta tesis doctoral.

Agradecer profundamente al grupo de Ingeniería Macromolecular la oportunidad de poder desarrollar la tesis en este genial grupo. A la Dra. Marta Fernández que siempre estuvo ahí, para enseñar, para descubrir y para apoyarte en los momentos más difíciles, tanto en la ciencia como en la vida.

A mis directoras de tesis, Dra. Alexandra Muñoz y Dra. Coro Echeverría, por guiarme a lo largo de estos años y a progresar en la ciencia. Gracias a su esfuerzo y dedicación he podido completar este hito.

A mis compañeros de trabajo, Víctor, Pedro, Valentina, Alex, Carol e Iñaki, gracias por estar, sois los mejores con los que podría haber coincidido en el laboratorio. También a Sandrita, Castor y Adrián, que ya no están en nuestro laboratorio, pero que también fue un honor conocer.

También agradecer a la Dra. Anna Scotto d'Abusco, Alessia y Irene por su cálido acogimiento durante mi estancia en Roma, y enseñarme el mundo de las células. Al igual que a Ilaria y Clarisa, por su apoyo y amistada tanto en Roma como en Madrid.

Pero llegar aquí no hubiera sido posible, sin el apoyo constante de mi familia que siempre desde pequeño me han animado a continuar estudiando a pesar la dislexia. En especial quiero agradecer a mi Padre, que en paz descanse, su apoyo incondicional a estudiar, a pesar de no haber sido Guardia Civil, como él quería.

Por último, aunque no menos importante, a mis amigos Diego y Laura, que siempre están ahí cuando los necesito.

Gracias a todos, y a los que no he nombrado también, por su apoyo y amistad.

Índice

Resumen

Abstract

Acrónimos y abreviaturas

Lista de esquemas, figuras y tablas

Capítulo 1 Introducción y objetivos.....1

1.1 Introducción.....	3
1.1.1 Polímeros antimicrobianos.....	3
1.1.2 Polímeros y monómeros sostenibles de origen natural.....	10
1.1.3 Métodos de obtención de sistemas antimicrobianos biodegradables: Incorporación de polímeros antimicrobianos a matrices poliméricas biobasadas y biodegradables.....	18
1.1.4 Antecedentes e hipótesis.....	21
1.1.5 Referencias.....	24
1.2 Objetivos.....	33

Capítulo 2 Polímeros biobasados derivados del ácido itacónico.....35

2.1 Biobased polymers derived from itaconic acid bearing clickable groups with potent antibacterial activity and negligible hemolytic activity.....	37
2.1.1 Abstract.....	39
2.1.2 Introduction.....	40
2.1.3 Experimental Section.....	41
2.1.4 Results and discussion.....	48
2.1.5 Conclusions.....	58
2.1.6 Acknowledgments	58
2.1.7 References.....	59
2.1.8 Supporting Information.....	62
2.2 Antibacterial and compostable polymers derived from biobased itaconic acid as environmentally friendly additives for biopolymer.....	67
2.2.1 Abstract.....	69
2.2.2 Introduction.....	70
2.2.3 Experimental part.....	71
2.2.4 Results and discussion.....	76
2.2.5 Conclusions.....	85

2.2.6 Acknowledgments	86
2.2.7 References	87
Capítulo 3 Fibras electrohiladas de PLA y PBAT con polímeros biobasados antimicrobianos	91
3.1 PLA and PBAT-Based Electrospun Fibers Functionalized with Antibacterial Bio-Based Polymers	93
3.1.1 Abstract	95
3.1.2 Introduction	96
3.1.3 Results and discussion	97
3.1.4 Conclusions	107
3.1.5 Experimental part	107
3.1.6 Acknowledgments	111
3.1.7 References	112
3.1.8 Supporting Information	115
3.2 Electrospun Polylactic Acid-Based Fibers Loaded with Multifunctional Antibacterial Biobased Polymers	117
3.2.1 Abstract	119
3.2.2 Introduction	120
3.2.3 Experimental part	121
3.2.4 Results and Discussion	128
3.2.5 Conclusions	137
3.2.6 Acknowledgments	137
3.2.7 References	138
3.2.8 Supporting Information	141
3.3 Synergistic combination of antimicrobial peptides and cationic polyitaconates in multifunctional PLA fibers	143
3.3.1 Abstract	145
3.3.2 Introduction	146
3.3.3 Experimental part	148
3.3.4 Results and Discussion	153
3.3.5 Conclusions	162
3.3.6 Acknowledgments	162
3.3.7 References	164

Capítulo 4 Conclusiones.....	167
Anexo.....	171
Publicaciones científicas derivadas de esta tesis doctoral.....	173
Otras contribuciones.....	174

Resumen

Actualmente, la sociedad se está enfrentando a una emergencia sanitaria: la resistencia de las bacterias frente a los antibióticos. Esta resistencia hace que muchas infecciones no respondan a los tratamientos actuales, lo que está provocando un elevado número de muertes, además de un incremento del gasto en los sistemas sanitarios. Estas infecciones resistentes a antibióticos son especialmente críticas en entornos hospitalarios, siendo las infecciones relacionadas con cuidados sanitarios un problema de Salud Pública a nivel mundial, como por ejemplo las infecciones relacionadas con catéteres, ventilación mecánica, así como las asociadas a implantes, prótesis o apósticos. El uso de materiales con propiedades antimicrobianas en estos dispositivos y productos sanitarios, se muestra como una solución para reducir este tipo de infecciones. Igualmente, en la industria del envasado se emplean cada vez más envases activos con materiales antimicrobianos ya que las infecciones provocadas por intoxicaciones alimentarias son muy relevantes y generan gran alarma social.

Una de las soluciones que se plantean frente a este problema es el desarrollo y el uso de polímeros antimicrobianos que se presentan como una opción muy prometedora. Sin embargo, el origen fósil de los polímeros y su lenta biodegradación hacen necesario la búsqueda de alternativas más sostenibles. La presente tesis doctoral busca responder a esta necesidad dirigiendo el esfuerzo hacia el desarrollo de polímeros antimicrobianos a partir de polímeros biobasados o de origen natural, en concreto a partir del ácido itacónico. El ácido itacónico es un compuesto de origen natural considerado como uno de los compuestos químicos obtenidos de la biomasa de alto valor añadido más prometedores para la producción de múltiples productos y derivados. El ácido itacónico es polimerizable y funcionalizable lo que permite añadir diferentes funcionalidades para la modulación de sus propiedades. Además, puede dar lugar a polímeros biodegradables.

Concretamente, este trabajo se ha centrado en la síntesis mediante polimerización radical de un polímero muy versátil derivado del ácido itacónico con dos grupos alquino. El polímero obtenido puede modificarse mediante química click de cicloadición azida-alquino catalizada con cobre (CuAAC). Utilizando esta técnica se han introducido varias moléculas con actividad biocida para la obtención de polímeros antimicrobianos biobasados, en concreto, se han incorporado grupos triazolio, tiazolio, N-halamina y el péptido antimicrobiano Temporin L. Además de incorporar grupos bioactivos

antimicrobianos, se ha modulado el carácter hidrófobo/hidrófilo de los polímeros ya que afecta directamente a su eficacia como antimicrobianos. Para ello se ha llevado a cabo la copolimerización con itaconatos apolares, así como el empleo de agentes alquilantes en reacciones de post-modificación.

En primer lugar, se prepararon copolímeros de itaconato de dimetilo e itaconato funcionalizado con grupos tiazolio y triazolio y empleando dos agentes alquilantes, de metilo y butilo. Se comprobó que los polímeros obtenidos eran muy eficientes frente a bacterias Gram-positiva y discretos frente a Gram-negativa, y dicha actividad dependía del balance hidrófobo-hidrófilo del copolímero. Los polímeros resultantes no eran tóxicos frente a glóbulos rojos humanos, se degradaban en condiciones de compostaje en menos de 80 días, y mantenían sus propiedades térmicas.

Con el objetivo de mejorar la actividad frente a bacterias Gram-negativa, se prepararon satisfactoriamente otros polímeros partiendo del poli(itaconato) con grupos alquino, al cual se incorporó mediante química click, por un lado, grupos N-halamina, y por otro lado, un péptido antimicrobiano, el Temporin L. Los polímeros resultantes tenían en su estructura dos tipos de funcionalidades biocidas, catiónicas de triazolio/tiazolio y N-halaminas o Temporin L, por lo que era de esperar una mayor actividad antimicrobiana. Sin embargo, estos polímeros presentaban problemas de solubilidad y agregación en disoluciones acuosas.

Todos los poli(itaconatos) con grupos antimicrobianos preparados se evaluaron posteriormente como aditivos o componentes en mezclas de polímeros biobasados/biodegradables de poli(ácido láctico) (PLA) y poli(butilén adipato-co-tereftalato) (PBAT), polímeros empleados habitualmente en la industria como alternativa a termoplásticos derivados del petróleo, y más concretamente en la industria del envasado y del material biosanitario. Se prepararon tanto films como fibras no tejidas de matrices de PLA y PBAT, con bajos contenidos de polímeros antimicrobianos sintetizados previamente, y funcionalizados con grupos tiazolio, triazolio, N-halamina y Temporin L. Los materiales obtenidos mostraron buena actividad antibacteriana, poniendo de manifiesto que la incorporación de los poli(itaconatos) biocidas aportaban dicha actividad al material final. Cabe reseñar que los grupos N-halamina y Temporin L mejoraban sustancialmente la actividad frente a bacterias Gram-negativa. Los materiales además, demostraron muy buenas propiedades de biocompatibilidad frente a fibroblastos, biodegradabilidad y buenas propiedades térmicas.

Por todo ello, los polímeros biobasados derivados del ácido itacónico desarrollados en esta tesis pueden ser una opción muy prometedora para impartir actividad antimicrobiana en materiales biobasados/biodegradables para aplicaciones tanto biomédicas como en el envasado, manteniendo el origen biobasado y la biodegradabilidad del producto.

Abstract

Currently, the society is facing a global health emergency: antibiotic resistant bacteria. This resistance causes that many infections do not respond to existing treatment which provokes a high number of deaths in addition to significant cost to national economies and their health systems. These antibiotic-resistant infections are especially critical in hospital environments with healthcare-related infections being a global public health problem, such as infections related to catheters, mechanical ventilation, as well as those associated with implants, prostheses or wound dressings. The use of materials with antimicrobial properties in these devices and medical products is shown as a solution to reduce this type of infections. Likewise, in the packaging industry, active packaging with antimicrobial materials is increasingly used as infections caused by food poisoning are very relevant and generate great social alarm.

One of the solutions proposed to address this problem is the development and use of antimicrobial polymers, which are presented as a very encouraging option. However, the fossil origin of polymers and their slow biodegradation make it necessary to search for more sustainable alternatives. This doctoral thesis seeks to respond to this need by directing efforts towards the development of antimicrobial polymers from biobased or natural-origin polymers, in particular from itaconic acid. Itaconic acid is a compound of natural origin considered one of the most promising chemical compounds obtained from biomass with high added value for the production of multiple products and derivatives. Itaconic acid is polymerizable and functionalizable, which allows different functionalities to be added and modulate its properties. In addition, it can give rise to biodegradable polymers.

Specifically, this thesis has focused on the synthesis via radical polymerization of a very versatile polymer derived from itaconic acid with two alkyne groups. The obtained polymer can be modified via copper-catalyzed azide-alkyne cycloaddition (CuAAC) click chemistry. Using this technique, several molecules with biocidal activity have been introduced to obtain biobased antimicrobial polymers, concretely, triazolium, thiazolium, N-halamine and the antimicrobial peptide Temporin L groups. In addition to the incorporation of bioactive antimicrobial groups, the hydrophobic/hydrophilic character of the polymers have been modulated because directly affects their effectiveness as antimicrobials. For this purpose, copolymerization with nonpolar itaconates has been carried out, as well as using alkylating agents in post-modification reactions.

Firstly, copolymers of dimethyl itaconate and itaconate functionalized with thiazolium and triazolium groups and using two alkylating agents, methyl and butyl, were prepared. It was found that the obtained polymers were very efficient against Gram-positive bacteria and modest against Gram-negative bacteria, and this activity depended on the hydrophobic-hydrophilic balance of the copolymer. The resulting polymers were not toxic to human red blood cells, degraded under composting conditions in less than 80 days, and maintained their thermal properties.

With the aim of improving the activity against Gram-negative bacteria, other polymers were successfully prepared starting from the polyitaconate with alkyne groups, to which was incorporated via click chemistry, on the one hand, N-halamine groups, and on the other hand an antimicrobial peptide, Temporin L. The resulting polymers had in their structure two types of biocidal functionalities, cationic triazolium/thiazolium and N-halamines or Temporin L, so a greater antimicrobial activity was expected. However, these polymers presented solubility and aggregation problems in aqueous solutions.

All prepared polyitaconates with antimicrobial groups were subsequently evaluated as additives or components in biobased/biodegradable polymer blends of poly(lactic acid) (PLA) and poly(butylene adipate-co-terephthalate) (PBAT), polymers commonly used in industry as an alternative to petroleum-derived thermoplastics, and more specifically in the packaging and bio-sanitary material industry. Both, films and nonwoven fibers, were prepared from PLA and PBAT matrices, with low contents of previously synthesized antimicrobial polymers functionalized with thiazolium, triazolium, N-halamine and Temporin L groups. The obtained materials showed good antibacterial activity, demonstrating that the incorporation of biocidal polyitaconates provided such activity to the final material. It should be noted that the N-halamine and Temporin L groups substantially improved the activity against Gram-negative bacteria. The materials also demonstrated very good biocompatibility properties against fibroblasts, biodegradability and good thermal properties.

For all these reasons, the biobased polymers derived from itaconic acid developed in this thesis can be a very promising option to impart antimicrobial activity in biobased/biodegradable materials for both, biomedical and packaging applications, maintaining the biobased origin and the biodegradability of the product.

Acrónimos y abreviaturas

¹³ C-NMR	– Resonancia magnética nuclear de carbón
¹ H-NMR	– Resonancia magnética nuclear de hidrógeno
<i>A. itaconicus</i>	– <i>Aspergillus itaconicus</i>
<i>A. niger</i>	– <i>Aspergillus niger</i>
<i>A. terreus</i>	– <i>Aspergillus terreus</i>
AIBN	– 2,2'-azobisisobutironitrilo
AMPs	– Péptidos antimicrobianos
APS	– Persulfato amónico
ASTM	– American Society for Testing and Materials
ATCC	– American Type Culture Collection
ATR	– Reflectancia total atenuada
ATRP	– Polimerización radical por transferencia de átomo
Boc-DMH-N3	– 3-(2-azidoetil)-5,5-dimetilhidantoin-1-carboxilato de <i>tert</i> -butilo
Bul	– 1-iodobutano
<i>C. albicans</i>	– <i>Candida albicans</i>
CALB	– Lipasa-B <i>Cándida antártica</i>
CFU	– Unidades formadoras de colonias
CLSI	– Clinical Laboratory Standards Institute
CO ₂ B	– CO ₂ producido en el blanco
CO ₂ P	– CO ₂ producido en las muestras
COSY	– Espectroscopia de correlación homonuclear
CRP	– Polimerización radical controlada
CTAB	– Bromuro de cetiltrimetilamonio
CuAAC	– Cicloadición azida-alquino catalizada con cobre
Đ	– Polidispersidad

DBO	– Demanda biología de oxígeno
DCC	– N,N'-diciclohexilcarbodiimida
DMAEMA	– Metacrilato de dimetilaminoetilo
DMAP	– 4-(dimetilamino)piridina
DMF	– N,N-dimetilformamida
DMH-Cl	– 3-(2-cloroethyl)-5,5-dimetilhidantoina
DMH-N ₃	– 3-(2-azidoethyl)-5,5-dimetilhidantoina
DMI	– Itaconato de dimetilo
DMSO	– Dimetil sulfóxido
DSC	– Calorimetría diferencial de barrido
DTGA/DTG	– Curvas de análisis termogravimétrico derivado
<i>E. faecalis</i>	– <i>Enterococcus faecalis</i>
EC	– <i>E. coli/Escherichia coli</i>
EDC	– 1-Etil-3-(3-dimetilaminopropil)carbodiimida
EDTA	– Ácido etilendiaminotetraacético
ESI	– Ionización de electrospray
EtOAc	– Acetato de etilo
EtOH	– Etanol
EVOH	– Copolímero etileno alcohol vinílico
FBS	– Suero fetal bovino
FE-SEM	– Microscopia electrónica de barrido de emisión de campo
FICI	– Índice de concentración inhibitoria fraccional
FTIR	– Espectroscopía infrarroja por transformada de Fourier
Hc ₅₀	– Concentración de antimicrobiano que induce el 50% de hemólisis
HR-MS	– Espectrometría de masas de alta resolución

IA	– Ácido itacónico
iPrOH	– Alcohol isopropílico
M2	– 2-(4-metiltiazol-5-il)etanol azida
M2Q	– 2-(4-metiltiazol-5-il)etanol azida cuaternizado
Mel	– Iodometano/Yoduro de metilo
MH	– Microdureza
M _{HCl}	– Concentración de HCl
MIC	– Concentración mínima de inhibición
M _{KOH}	– Concentración de KOH
M _n	– Peso molecular promedio en número
MRSA	– <i>Staphylococcus aureus</i> resistente a Meticilina
MS	– Espectrometría de masas
MTS	– 3-(4,5-dimetiltiazol-2-il)-5-(3-carboximetoxifenil)-2-(4-sulfofenil)-2H-tetrazolio
NHS	– N-Hidroxisuccinimida
NMR	– Resonancia magnética nuclear
OMS	– Organización Mundial de la Salud
P(Boc-DMHI)	– Poli(bis((1-(2-(3-(<i>tert</i> -butoxicarbonil)-4,4-dimetil-2,5-dioxoimidazolidin-1-il)ethyl)-1H-1,2,3-triazol-4-il)metil)itaconato)
P(DMHI)	– Poli(bis((1-(2-(4,4-dimetil-2,5-dioxoimidazolidin-1-il)ethyl)-1H-1,2,3-triazol-4-il)metil)itaconato)
P(DMHICI-Q)	– Poli(bis((1-(2-(4,4-dimetil-2,5-dioxoimidazolidin-1-il)ethyl)-1H-1,2,3-triazol-4-il)metil)itaconato) cuaternizado y clorado
P(DMHI-Q)	– Poli(bis((1-(2-(4,4-dimetil-2,5-dioxoimidazolidin-1-il)ethyl)-1H-1,2,3-triazol-4-il)metil)itaconato) cuaternizado
P(PrI)	– Poli(di(prop-2-in-1-il)itaconato)
P(PrI-co-DMI)	– Poli(di(prop-2-in-1-il)itaconate-co-dimetil itaconate)

- P(TTI-co-DMI) – Poli(bis((1-(2-(4-metiltiazol-5-il)ethyl)-1H-1,2,3-triazol-4-il) metil) itaconato-co-dimetil itaconato)
- P100 – Poli(di(prop-2-in-1-il) itaconato)
- P100T – Poli(bis((1-(2-(4-metiltiazol-5-il)ethyl)-1H-1,2,3-triazol-4-il) metil) itaconato)
- P100T-Me – Poli(bis((1-(2-(4-metiltiazol-5-il)ethyl)-1H-1,2,3-triazol-4-il) metil) itaconato) cuaternizado con yoduro de metilo
- P100T-Bu – Poli(bis((1-(2-(4-metiltiazol-5-il)ethyl)-1H-1,2,3-triazol-4-il) metil) itaconato) cuaternizado con yoduro de butilo
- P25 – Poli(di(prop-2-in-1-il) itaconate₂₅-co-dimetil itaconato₇₅)
- P25T – Poli(bis((1-(2-(4-metiltiazol-5-il)ethyl)-1H-1,2,3-triazol-4-il) metil) itaconato₂₅-co-dimetil itaconato₇₅)
- P25T-Me – Poli(bis((1-(2-(4-metiltiazol-5-il)ethyl)-1H-1,2,3-triazol-4-il) metil) itaconato₂₅-co-dimetil itaconato₇₅) cuaternizado con yoduro de metilo
- P25T-Bu – Poli(bis((1-(2-(4-metiltiazol-5-il)ethyl)-1H-1,2,3-triazol-4-il) metil) itaconato₂₅-co-dimetil itaconato₇₅) cuaternizado con yoduro de butilo
- P50 – Poli(di(prop-2-in-1-il) itaconate₅₀-co-dimetil itaconato₅₀)
- P50T – Poli(bis((1-(2-(4-metiltiazol-5-il)ethyl)-1H-1,2,3-triazol-4-il) metil) itaconato₅₀-co-dimetil itaconato₅₀)
- P50T-Me – Poli(bis((1-(2-(4-metiltiazol-5-il)ethyl)-1H-1,2,3-triazol-4-il) metil) itaconato₅₀-co-dimetil itaconato₅₀) cuaternizado con yoduro de metilo
- P50T-Bu – Poli(bis((1-(2-(4-metiltiazol-5-il)ethyl)-1H-1,2,3-triazol-4-il) metil) itaconato₅₀-co-dimetil itaconato₅₀) cuaternizado con yoduro de butilo
- P75 – Poli(di(prop-2-in-1-il) itaconate₇₅-co-dimetil itaconato₂₅)
- P75T – Poli(bis((1-(2-(4-metiltiazol-5-il)ethyl)-1H-1,2,3-triazol-4-il) metil) itaconato₇₅-co-dimetil itaconato₂₅)

P75T-Me	– Poli(bis((1-(2-(4-metiltiazol-5-il)etil)-1H-1,2,3-triazol-4-il) metil) itaconato ₇₅ -co-dimetil itaconato ₂₅) cuaternizado con yoduro de metilo
P75T-Bu	– Poli(bis((1-(2-(4-metiltiazol-5-il)etil)-1H-1,2,3-triazol-4-il) metil) itaconato ₇₅ -co-dimetil itaconato ₂₅) cuaternizado con yoduro de butilo
PA	– <i>P. aeruginosa/Pseudomonas aeruginosa</i>
PBAT	– Poli(butilén adipato-co-tereftalato)
PBS	– Tampón fosfato salino
PBSA	– Poli(butilén-succinato-co-adipato)
PCL	– Policaprolactona
PDMI/P0	– Poli(dimetil itaconato)
PEG	– Polietilenglicol
PET	– Polietileno tereftalato
PGA	– Poli(ácido glicólico)
PHAs	– Polihidroxialcanoatos
PIA	– Poli(ácido itacónico)
PLA	– Poli(ácido láctico)
PLLA	– Poli(ácido L-láctico)
PMDTA/PMDETA	– N,N,N',N'',N"-pentametildietilentriamina
PP	– Polipropileno
Prl	– Di(prop-2-in-1-il) itaconato
PTTI	– Poli(bis((1-(2-(4-metiltiazol-5-il)etil)-1H-1,2,3-triazol-4-il) metil) itaconato)
PTTI-Bu	– Poli(bis((1-(2-(4-metiltiazol-5-il)etil)-1H-1,2,3-triazol-4-il) metil) itaconato) butil
PTTI-Me	– Poli(bis((1-(2-(4-metiltiazol-5-il)etil)-1H-1,2,3-triazol-4-il) metil) itaconato) metil

PTTIQ	– Poli(bis((1-(2-(4-metiltiazol-5-il)ethyl)-1H-1,2,3-triazol-4-il) metil) itaconato) triazol cuaternizado
PTTIQ-AMP	– Poli(bis((1-(2-(4-metiltiazol-5-il)ethyl)-1H-1,2,3-triazol-4-il) metil) itaconato-co-AMP) triazol cuaternizado
PVDF	– Fluoruro de polivinilideno
Q-TOF LC/MS	– Cromatografía líquida de cuadrupolo tiempo de vuelo - espectrometría de masas
R _a	– Rugosidad media aritmética
RAFT	– Polimerización por trasferencia de cadena por adición-fragmentación reversible
RBC	– Células de glóbulos rojos
SA	– <i>S. aureus/Staphylococcus aureus</i>
scCO ₂	– Fluido supercrítico de dióxido de carbono
SD	– Desviación estándar
SE	– <i>S. epidermidis/Staphylococcus epidermidis</i>
SEC	– Cromatografía de exclusión por tamaño
SEM	– Microcopia electrónica de barrido
SSI	– Impregnación con solvente supercrítico
T _{d5}	– Temperatura descomposición a 5% de pérdida de peso
T _{dmax1}	– Temperatura máxima de descomposición paso 1
T _{dmax2}	– Temperatura máxima de descomposición paso 2
T _{dmax3}	– Temperatura máxima de descomposición paso 3
T _{dmax4}	– Temperatura máxima de descomposición paso 4
T _g	– Temperatura de transición vítrea
TGA	– Análisis termogravimétrico
THF	– Tetrahidrofurano
T _m	– Temperatura de fusión

T_{\max}	– Temperatura de degradación máxima
TTI	– Bis((1-(2-(4-metiltiazol-5-il)etil)-1H-1,2,3-triazol-4-il)metil) itaconato
UV	– Ultravioleta
UV-vis	– Ultravioleta-visible
V_{HCl}	– Volumen de HCl consumido en la valoración
V_{KOH}	– Volumen de KOH
VOCs	– Compuestos orgánicos volátiles
$\Sigma \text{CO}_2\text{B}$	– CO_2 acumulado en el blanco
$\Sigma \text{CO}_2\text{P}$	– CO_2 acumulado en las muestras
ζ	– Potencial Zeta

Lista de esquemas, figuras y tablas

Capítulo 1: Introducción y objetivos

Esquema 1. Formación de un 1,2,3-triazol 1,4-disustituido utilizando una azida y un alquino en presencia de cobre.....	14
Esquema 2. Mecanismo de reacción propuesto para la reacción CuAAC con un intermedio de reacción dinuclear de cobre.....	15
Esquema 3. Reactividad del polímero de ácido itacónico: a) aza-Michael y b) tia-Michael.....	17
Figura 1. Modelo de envoltura de una bacteria Gram-positiva y una Gram-negativa. Adaptada de la referencia 22.....	6
Figura 2. Representación general de un polímero catiónico antimicrobiano.....	7
Figura 3. Representación del mecanismo de acción de un polímero antimicrobiano catiónico.....	7
Figura 4. Estructura química de la vitamina B1 (a), de 2-(4-metiltiazol-5-il)etan-1-ol (b) y 1,2,3-triazol 1,4-disustituido (c).....	8
Figura 5. Estructura química de dimetilhidantoina (DMH) y una N-halamina derivada de la DMH.....	9
Figura 6. Los 12 compuestos de origen natural de gran valor añadido según el Departamento Nacional de Energía de Estados Unidos, entre ellos el ácido itacónico.....	11
Figura 7. Estructura química del ácido itacónico y del ácido metacrílico.....	12
Figura 8. Diagrama esquemático del funcionamiento del aparato de electrohilado rotatorio utilizado en esta tesis doctoral.....	20
Tabla 1. Parámetros del electrohilado y su efecto en las fibras.....	21

Capítulo 2: Polímeros biobasados derivados del ácido itacónico

2.1 Biobased polymers derived from itaconic acid bearing clickable groups with potent antibacterial activity and negligible hemolytic activity

Scheme 1. Synthesis of di(prop-2-yn-1-yl) itaconate (PrI)	43
Scheme 2. Synthesis of the antibacterial cationic copolymers derived from itaconic acid.....	50

Figure 1. $^1\text{H-NMR}$ spectra of (A) clickable monomer PrI and (B) monomer derivative TTI with thiazole and triazole groups in deuterated chloroform.....	49
Figure 2. FTIR spectra of the copolymers P50, P50T, P50T-Me and P50T-Bu.....	51
Figure 3. ^1H NMR spectra in DMSO-d_6 of the copolymers (A) P50 and (B) P50T.....	51
Figure 4. $^1\text{H-NMR}$ spectra in deuterated water of the copolymers (A) P75T-Me and (B) P75T-Bu.....	54

Figure 5. Hemolytic activity of the copolymers quaternized either with (A) methyl iodide or (B) butyl iodide.....57

Table 1. Molecular characteristics of the P(Prl-co-DMI) polymers synthesized with different molar feed ratios [Prl]/[DMI], final chemical compositions (polymer ratio [Prl]/[DMI]), number average molecular weights (\bar{M}_n) and molecular weight dispersity (D) determined by SEC in DMF as an eluent. \bar{M}_n and D values of the polymers after click reactions leading P(TTI-co-DMI) are also included.....52

Table 2. Zeta potential values (ζ) obtained for all the synthesized cationic copolymers.....55

Table 3. Antibacterial and hemolytic activity of the resulting cationic polymers derived from itaconic acid.....55

Supporting information

Scheme S1. Failed approaches 1 (A) and 2 (B) used to synthesize polymers derived from itaconic acid with thiazole and triazole groups.....62

Figure S1. ^{13}C -NMR spectra of (A) clickable monomer PrI and (B) monomer derivative TTI with thiazole and triazole groups in deuterated chloroform.....63

Figure S2. Copolymer P50T-Me. $^1\text{H-NMR}$ (400 MHz, DMSO- d_6), δ (ppm): 8.82 (2H, *H*-thiazole), 7.66 (2H, *H*-triazole), 5.24 (4H, O- CH_2 -triazole), 4.85 (4H, CH_2 -N), 4.15 (6H, N^+CH_3 triazole), 3.97 (6H, N^+CH_3 thiazole), 3.50 (4H, CH_2 -thiazole and 6H, -O- CH_3), 2.33 (6H, CH_3 -thiazole).....64

Figure S3. COSY-NMR spectrum in deuterated water of P50T-Me copolymer.....64

Figure S4. COSY-NMR spectrum in deuterated water of P50T-Bu copolymer.....65

2.2 Antibacterial and compostable polymers derived from biobased itaconic acid as environmentally friendly additives for biopolymers

Figure 1. Chemical structure of the antibacterial copolymers derived from itaconic acid used in this study.....72

Figure 2. Scheme of the used methodology to obtain antibacterial and compostable biopolymer films.....73

Figure 3. Biodegradation curves of the polymers derived from itaconic acid in comparison with microcrystalline cellulose sample.....78

Figure 4. DSC curves for the copolymer family P75, P75T and P75T-Me.....81

Figure 5. TGA and DTGA curves for the copolymer family P50, P50T and P50T-Me...82

Figure 6. a) TGA and b) DSC curves of PBAT and PBAT/P100T-Me films.....83

Figure 7. SEM micrographs of a) and b) PBAT film surface; c) and d) PBAT/P100T-Me film surface.....84

Figure 8. Pictures of the agar plates of MRSA after spreading 1 mL of inoculum in previous contact with PBAT film (left) and with PBAT/P100T-Me film (right), and incubation.....85

Table 1. Minimum inhibition concentration (MIC) values of the cationic polymers P(TTI-co-DMI)-Me against MRSA.....77

Table 2. Thermal properties of the cationic polymers obtained by TGA and DSC.....81

Capítulo 3: Fibras electrohiladas de PLA y PBAT con polímeros biobasados antimicrobianos

3.1 PLA and PBAT-based electrospun fibers functionalized with antibacterial bio-based polymers

Figure 1. Schematic representation of functionalized polymeric fibers with PTTI-Me and PTTI-Bu derivatives and their interactions with cells and bacteria.....97

Figure 2. SEM images of PLA, PBAT, PLA/PTTI and PBAT/PTTI electrospun fibers...98

Figure 3. a) Roughness R_a of the obtained fiber mats and films and b) roughness values compared to the fiber diameter (the red line is a linear trend line with corresponding R^2 value).....100

Figure 4. Contact angle measurements of the obtained fiber mats and films.....101

Figure 5. Cell viability of fibroblast seeded onto tested fibers and films assessed by MTS assay using cells seeded in well cell culture plate as negative control 100% viability. Cells adsorbed into the material surfaces are represented in blue, cells remained into cell culture plate are represented in gray. Results are expressed as mean \pm SEM of data obtained by three independent experiments.....105

Figure 6. SEM images of Human dermal primary fibroblasts growth for 24 h on a) PLA fiber mat, b) PBAT fiber mat, c) PBAT/PTTI-Bu fiber mat, and d) PBAT/PTTI-Me fiber mat.....106

Table 1. Antibacterial activity expressed as percentage of bacterial reduction (%) and Log reduction (Log) of tested fibers and films against, *S. aureus*, *MRSA* and *P. aeruginosa*. Surface charge of tested fibers and films expressed as $N^+ cm^{-2}$103

Supporting information

Figure S1. FTIR spectra of PLA and PBAT based fibers.....115

Figure S2. 1H NMR spectra and signal assignment of PTTI and PTTI-Me extracted in DMSO-d₆ from PLA/PTTI and PLA/PTTI-Me fiber mats.....115

Figure S3. FTIR spectra of PBAT based films.....116

3.2 Electrospun polylactic acid-based fibers loaded with multifunctional antibacterial biobased polymers

Figure 1. Synthesis route of the antibacterial biobased polymer P(DMHICl-Q).....129

Figure 2. FTIR spectra of the antibacterial biobased polymer P(DMHICl-Q) and its precursors P(PrI), P(Boc-DMHI) and P(DMHI-Q)130

Figure 3. SEM micrographs and its corresponding histograms of fiber diameters of a) PLA and b) PLA/P(DMHI) fiber mats.....131

Figure 4. Visual appearance and SEM images of the tested PLA and PLA/P(DMHICl-Q) fiber mats over time under composting conditions134

Figure 5. a) SEM image of PLA and PLA/P(DMHICI-Q) fibers taken at large 42 days of composting incubation. b) Average fiber diameter of PLA and PLA/P(DMHICI-Q) fiber mats over time under composting conditions.....136

Figure 6. Disintegration degree of PLA and PLA/P(DMHICI-Q) fiber mats over time under composting conditions.....136

Table 1. Antibacterial activity expressed as percentage of bacterial reduction (%) and Log reduction (Log) of PLA/P(DMHICI-Q) and PLA/P(DMHICI-Q) against, *S. epidermidis*, *S. aureus*, *P. aeruginosa* and *E. coli* after 30 min or 24 h of contact time.....133

Supporting information

Figure S1. ^1H -NMR spectra of (A) P(Boc-DMHI) and (B) P(DMHI-Q) polyitaconate derivatives obtained in DMSO- d_6 as solvent.....141

Figure S2. Pictures of the agar plates of *E. coli* (Gram-negative bacteria) and *S. epidermidis* (Gram-positive bacteria) bacterial colonies after spreading inoculum (at different dilutions) in previous contact with PLA fibers (control, left) and incubation during 24 h, and in contact with PLA/(P(DMHICI-Q) fibers and incubation during 30 min (middle) and 24 h (right).....142

3.3 Multifunctional PLA fibers loaded with antimicrobial peptides and cationic polyitaconates

Figure 1. Schematic representation of the synthesis of cationic biobased polyitaconate bearing thiazolium groups (PTTIQ) and of the conjugated structure, biobased polyitaconate bearing thiazolium and AMP (PTTIQ-AMP).....154

Figure 2. ^1H - NMR spectra of A) PTTIQ and B) PTTIQ-AMP biobased polymer.....155

Figure 3. FTIR spectra of PTTIQ, Temporin L peptide, and PTTIQ-AMP conjugated polymer.....156

Figure 4. SEM images of prepared fiber mats before (PLA and PLA/PTTIQ) and after (PLA + AMP and PLA/PTTIQ +AMP) scCO₂ impregnation with AMP.....158

Figure 5. FTIR spectra of non-impregnated fibers (PLA and PLA/PTTIQ) and of impregnated fibers with AMP (PLA+AMP and PLA/PTTIQ+AMP).....160

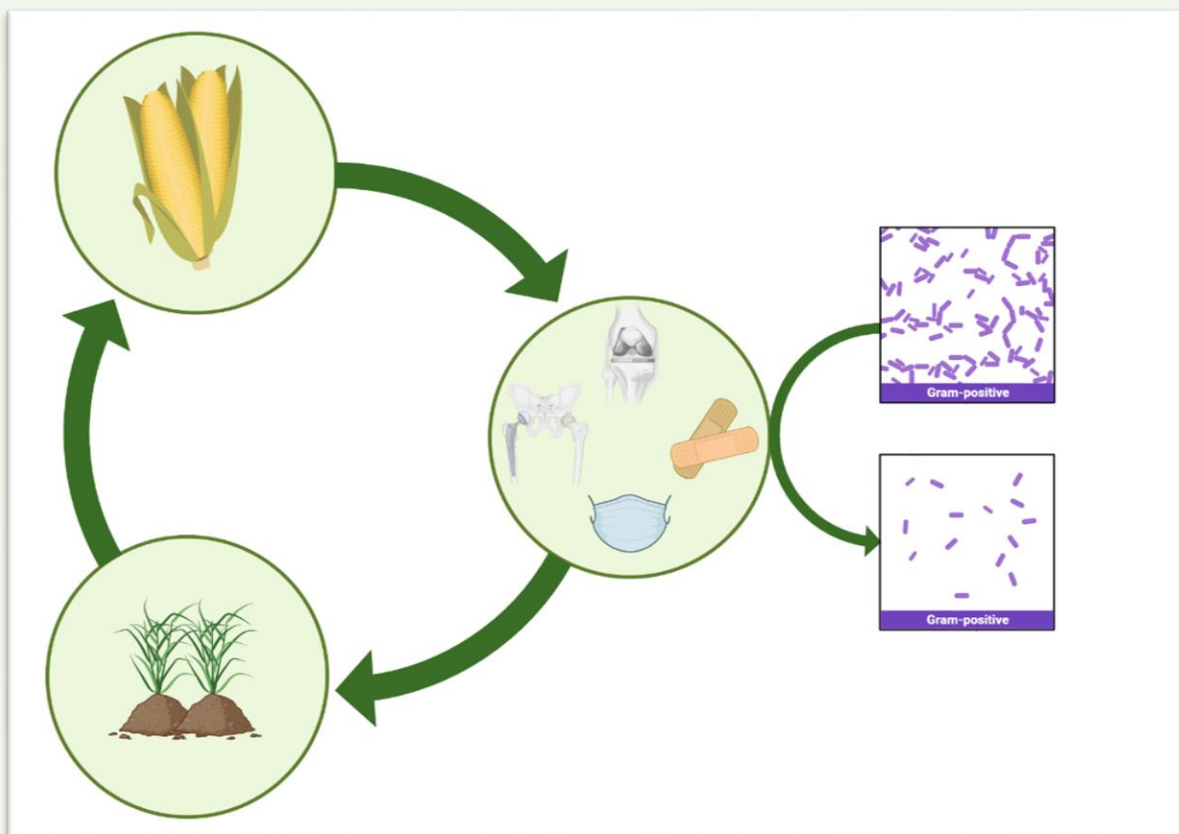
Figure 6. Photographs of disk diffusion assays on agar plates cultivated with Gram-negative *E. coli* of non-impregnated fibers (PLA and PLA/PTTIQ) and impregnated fibers with AMP (PLA+AMP and PLA/PTTIQ+AMP).....162

Table 1. MIC values of PTTIQ, Temporin L AMP and PTTIQ-AMP157

Table 2. Antimicrobial activity of non-impregnated fibers (PLA and PLA/PTTIQ) and of impregnated fibers with AMP (PLA+AMP and PLA/PTTIQ+AMP) against *E. coli* and *E. faecalis*.....161

Capítulo 1

Introducción y objetivos



1.1 Introducción

1.1.1 Polímeros antimicrobianos

El descubrimiento de los primeros antibióticos por Alexander Fleming en 1928^{1,2} fue un gran avance para el tratamiento de infecciones que hasta esa fecha no se podían curar. Desde entonces se han creado numerosos antibióticos para tratar casi cualquier infección. No obstante, las bacterias pueden adquirir resistencia a los antibióticos, provocando que estos compuestos dejen de tener actividad o que sea necesario aumentar la dosis, con el consiguiente aumento de la toxicidad. Esta resistencia se debe principalmente al abuso y al mal uso que se realiza a la hora de utilizar los antibióticos, ya sea tanto para uso humano como animal.³

La aparición de bacterias resistentes está generando un aumento de muertes por infecciones en el mundo y se estima que en 2019 se produjeron casi 5 millones de muertes asociadas a estas bacterias.⁴ Si no se logra el desarrollo de nuevos antibióticos la Organización Mundial de la Salud (OMS) prevé que en el año 2050 esta cifra pueda superar las 10 millones de muertes producidas por las bacterias resistentes a antibióticos.⁵ Las principales bacterias asociadas a infecciones mortales son: *Escherichia coli*, *Staphylococcus aureus*, *Klebsiella pneumoniae*, *Streptococcus pneumoniae* y *Pseudomonas aeruginosa*, entre otras.⁴

Por ello, es necesario crear nuevos tipos de antibióticos o agentes antimicrobianos para evitar la proliferación de nuevas variantes bacterianas con resistencia, que tengan un mecanismo de acción diferente al de los antibióticos actuales. Las principales rutas de acción de los antibióticos son: a) inhibición de la síntesis de la pared celular; b) inhibición de la síntesis de proteínas; c) inhibición de la síntesis de ácidos nucleicos; d) rotura de la membrana celular; y e) bloqueo de rutas metabólicas. Muchos de estos mecanismos de acción de los antibióticos pueden ser esquivados por las bacterias para evitar su erradicación, provocando la resistencia a los antibióticos.⁶ Las macromoléculas como los péptidos antimicrobianos (AMPs)⁷ y los polímeros tienen un enorme potencial como agentes antimicrobianos alternativos a los antibióticos. Los polímeros antimicrobianos son menos propensos a generar resistencias en las bacterias, debido a que el mecanismo de acción es diferente.⁸ Además, mantienen su actividad durante más tiempo, su toxicidad es menor, son más baratos y fáciles de producir.⁹ El empleo de polímeros antimicrobianos no solo se presenta como una alternativa prometedora al uso de antibióticos sino que también permite el desarrollo y preparación de materiales a partir

de estos polímeros que pueden servir como recubrimientos, para preparar hidrogeles o fabricar dispositivos médicos con actividad antimicrobiana.^{10,11}

Tipo de polímeros antimicrobianos

Existen diferentes estrategias para la eliminación y erradicación de bacterias mediante el empleo de polímeros antimicrobianos. Estos se pueden clasificar dependiendo de si la estrategia frente a la bacteria es pasiva o activa. La primera estrategia se basa en evitar que las bacterias se adhieran, proliferen y formen biofilm en la superficie de los materiales. Los polímeros antimicrobianos que tienen dicha acción pasiva son los polímeros antiadherentes (“antifouling”) que repelen e impiden así la adhesión de proteínas, microorganismos y otras biomoléculas en la superficie de los materiales. Estos polímeros están basados principalmente en polímeros hidrófilos no iónicos como el polietilenglicol (PEG), en polímeros con alta carga negativa o en polímeros ultrahidrófobos.^{12,13} El problema que tienen este tipo de sistemas es que no suelen ser eficientes a largo plazo, y los microorganismos acaban colonizando dichas superficies. La segunda estrategia se centra en eliminar de manera activa las bacterias inhibiendo su crecimiento o matando los microorganismos, ya sea por contacto directo o por liberación de un agente antimicrobiano. Dentro de esta estrategia podemos encontrar polímeros que por sí mismos son inactivos, pero a los que se les incorpora un agente antimicrobiano mediante mezclado físico. En este caso el modo de acción suele deberse a la difusión y liberación de las sustancias activas desde la matriz polimérica. Para la incorporación de estos componentes antimicrobianos se pueden utilizar técnicas como la extrusión en fundido, el electrohilado o la impregnación con fluidos supercríticos, o mediante disolución. Los principales agentes pueden ser otros polímeros antimicrobianos¹⁴, antibióticos¹⁵, aceites esenciales^{16,17} o nanopartículas metálicas,¹⁸⁻²¹ entre otros. Aunque muchos de estos sistemas son muy efectivos, pueden dar lugar a problemas de toxicidad y de contaminación ambiental, especialmente las nanopartículas metálicas, debido a su migración desde la matriz polimérica.²²

Otro grupo de polímeros antimicrobianos interesantes son los polímeros liberadores de biocidas, que tienen anclado químicamente los grupos biocidas que se liberan al medio actuando frente a los microorganismos. En este grupo destacan los polímeros con grupos halamina (liberadores de cloro)²³ y grupos liberadores de óxido nítrico,²⁴ así como polímeros con enlaces lábiles hidrolizables a un determinado pH o mediante la acción enzimática (enlaces carbonatos, éster, urea, carbinoamina).^{25,26} En

general, su actividad es muy alta cuando el agente es liberado en el lugar objetivo. No obstante, la actividad se pierde rápidamente con el tiempo y, además, el agente liberado puede producir toxicidad en el medio.

Pero sin duda, los polímeros antimicrobianos que más destacan de entre los que presentan una acción activa son aquellos que actúan mediante contacto directo, tales como los polímeros catiónicos, los fenólicos, los halogenados y los organometálicos.²⁷ En estos polímeros los grupos antimicrobianos están unidos a las cadenas poliméricas mediante enlaces químicos fuertes, lo que les confiere propiedades intrínsecas y permanentes o de larga duración, siendo más estables y seguros, y una alternativa más adecuada como solución al problema de desarrollo de resistencia por parte de las bacterias. De esta familia los más relevantes son los polímeros catiónicos debido a sus buenas propiedades.

Los polímeros catiónicos se han inspirado en los péptidos antimicrobianos (AMPs), que son las moléculas efectoras del sistema inmune innato. Los AMPs se encuentran en células procariotas que las utilizan para luchar en primera instancia contra bacterias. Estas contienen entre 8 y 100 aminoácidos, generalmente con una estructura de α -hélice. Principalmente contienen aminoácidos básicos (como arginina o lisina) y aminoácidos apolares (como alanina o leucina).²⁸ La distribución de estos aminoácidos a lo largo del AMP le confiere carácter anfifílico, indispensable para su actividad antimicrobiana.²⁹ A raíz de los AMPs, e inspirados en ellos, se han diseñado diversos sistemas de polímeros con propiedades antimicrobianas que imitan su estructura anfifílica y su carácter catiónico.^{10,30} Los principales grupos que confieren carga positiva a los polímeros son sales de amonio, fosfonio, guanidinio y sulfonio, mientras que su carácter hidrófobo suele aportarse mediante cadenas alquílicas de diferentes longitudes. Su mecanismo de acción se debe a una interacción disruptiva con las membranas bacterianas. Las ventajas que presentan son principalmente su alta eficiencia y amplio espectro, su menor tendencia a desarrollar resistencia y que no liberan biocidas al medio ambiente.

De todos los sistemas poliméricos antimicrobianos que se han destacado, los polímeros biocidas catiónicos son de los más prometedores y los más investigados a la hora de producir nuevos sistemas antimicrobianos para la lucha contra las infecciones. Teniendo en cuenta todo lo anterior, en esta tesis doctoral se han desarrollado nuevos polímeros catiónicos a partir de monómeros biobasados, por lo que a continuación se

profundizará en su modo de acción, así como en los parámetros que influyen en su actividad.

Polímeros antimicrobianos catiónicos y su mecanismo de acción

La actividad antimicrobiana de los polímeros catiónicos se produce gracias a las características comunes de las estructuras de la capa envolvente de las diferentes bacterias. La característica más importante presente en la envoltura bacteriana es su carga neta negativa. Las bacterias Gram-positiva y Gram-negativa poseen una carga negativa superficial que se debe principalmente a la composición fosfolipídica de la membrana citoplasmática. Además, en el caso de las bacterias Gram-positiva podemos encontrar los ácidos teicoicos y lipoteicoicos en la pared celular que contribuyen a la carga neta negativa.³¹ Por otro lado, las cargas negativas de las bacterias Gram-negativa provienen, también, de la presencia en la membrana externa de lipopolisacáridos (ver Figura 1).³²

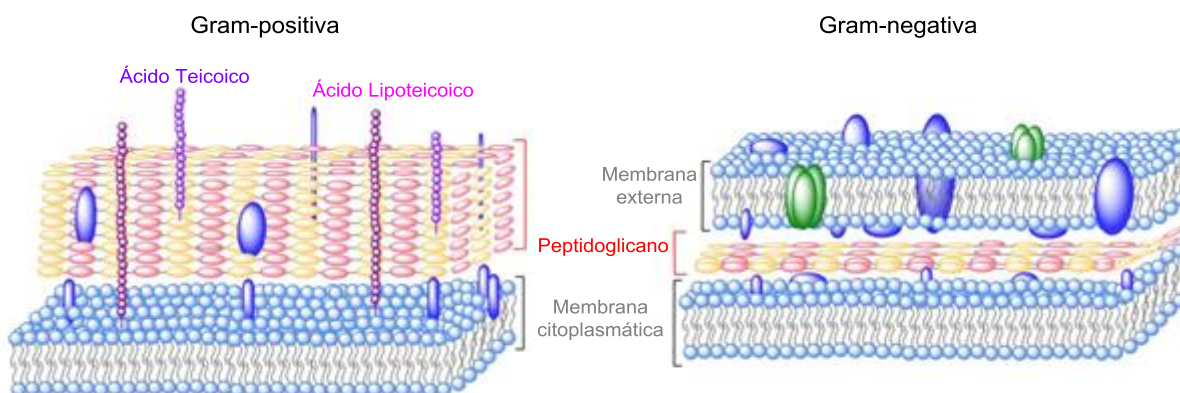


Figura 1. Modelo de envoltura de una bacteria Gram-positiva y una Gram-negativa. Adaptada de la referencia 31.

Debido a la naturaleza de la superficie de las bacterias cargadas negativamente, los polímeros antimicrobianos catiónicos se diseñan para interactuar con el recubrimiento externo de las bacterias mediante interacciones electrostáticas, pero además estos polímeros interaccionan con el interior lipídico de las membranas bacterianas a través de interacciones hidrófobas. Por ello, para que los polímeros tengan propiedades antimicrobianas deben tener un carácter hidrófilo-hidrófobo (Figura 2).

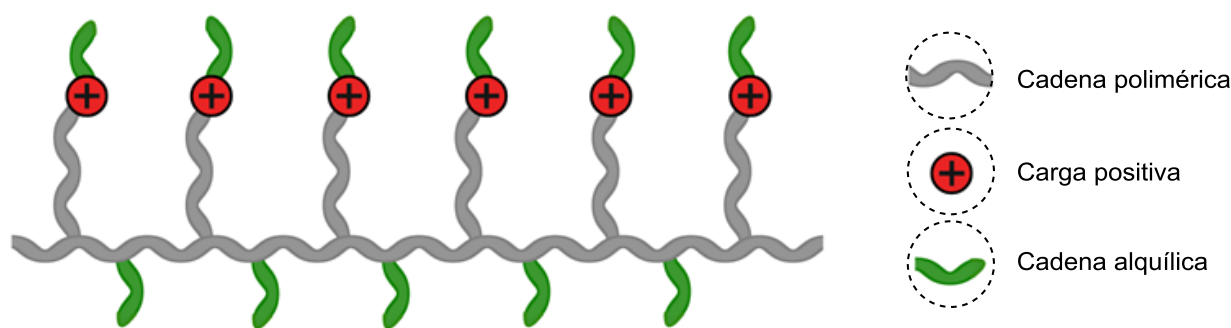


Figura 2. Representación general de un polímero catiónico antimicrobiano.

Los polímeros antimicrobianos catiónicos actúan de la siguiente manera: (1) se produce una rápida atracción electrostática del polímero catiónico con la superficie bacteriana; (2) la integración de las cadenas hacia el interior de las membranas bacterianas generada por su carácter apolar compromete su estabilidad produciéndose la formación de poros; y (3) se produce la muerte bacteriana por lisis mediante la fuga de material citoplasmático (Figura 3).³³

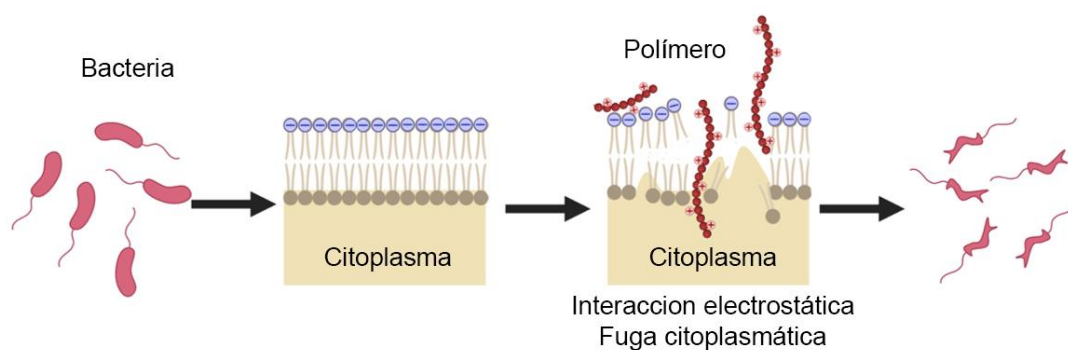


Figura 3. Representación del mecanismo de acción de un polímero antimicrobiano catiónico.

Teniendo en cuenta el mecanismo de acción de estos polímeros es importante diseñarlos para que tengan cargas positivas y segmentos apolares. Para incorporar grupos catiónicos, principalmente se utilizan grupos amina³⁴⁻³⁶ y fosfonio cuaternizados,³⁷ pero también se pueden utilizar heterociclos como piridina, imidazol, tiazol o triazol, cuyo nitrógeno está cuaternizado. Estos dos últimos grupos funcionales tienen un gran potencial. El 1,3-tiazol es un heterociclo que contiene azufre y nitrógeno y es utilizado en diferentes principios activos.³⁸ Concretamente, el compuesto 2-(4-metiltiazol-5-il)etan-1-ol (Figura 4b) presenta unas buenas propiedades antimicrobianas en polímeros, como ya se ha descrito en la literatura.³⁹ Este compuesto es parte de la vitamina B1 (Figura 4a), por lo que se trata de una sustancia biocompatible.⁴⁰ El otro heterociclo que puede poseer actividad antimicrobiana es el 1,2,3-triazol-1,4-disustituido.

Este se produce mediante la cicloadición azida-alquino catalizada con cobre (CuAAC), que se explicará más adelante. Este heterociclo está compuesto de tres nitrógenos (Figura 4c), y también se ha utilizado en la síntesis de compuestos antimicrobianos.⁴¹

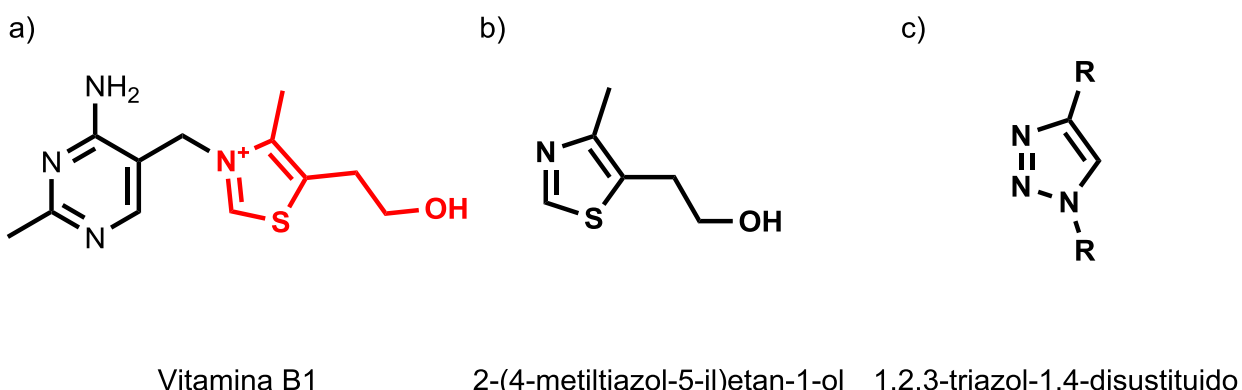


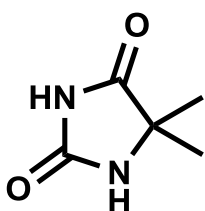
Figura 4. Estructura química de la vitamina B1 (a), de 2-(4-metiltiazol-5-il)etan-1-ol (b) y 1,2,3-triazol-1,4-disustituido (c).

Para lograr este carácter anfíflico hidrófilo-hidrófobo se puede proceder de varias formas, por ejemplo, mediante el uso de agentes alquilantes, normalmente haluros de alquilo. Estos tienen una gran influencia en los polímeros catiónicos. Además de ser los encargados de cuaternizar los grupos amino de los heterociclos proporcionando así la carga positiva, estos posibilitan ajustar el balance hidrófilo-hidrófobo con solo modificar la longitud de cadena apolar de estos agentes. No obstante, también se puede modificar ese balance mediante la copolimerización, variando la concentración de los monómeros apolares. Como ejemplos utilizados para regular el balance hidrófilo-hidrófobo se han usado monómeros como el acrilonitrilo o el metacrilato de butilo.⁴²⁻⁴⁴

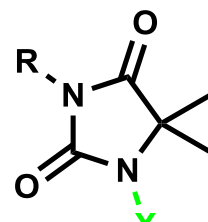
Otros polímeros antimicrobianos: N-halaminas

Otros polímeros con buena actividad antimicrobiana son los polímeros con N-halaminas en su estructura.⁴⁵ Las N-halaminas son compuestos químicos que tiene un grupo halógeno unido a una amina (ver figura 5). El mecanismo de acción es diferente de los anteriores. En este caso la actividad antimicrobiana se produce por la acción oxidativa de un halógeno (Cl^+ o Br^+) que se libera del polímero y actúa sobre un receptor biológico de la bacteria, como grupos tioles o amino de proteínas, produciendo una inhibición metabólica o inactivación de las bacterias.^{12,32}

Dimetilhidantoina



N-halamina



$X = Cl, Br$

Figura 5. Estructura química de dimetilhidantoina (DMH) y una N-halamina derivada de la DMH.

Las N-halaminas poliméricas son más estables, menos corrosivas, y tienden a generar menos compuestos halogenados, en comparación con las halaminas libres. Dado su potencial, los polímeros de N-halamina pueden usarse en una gran variedad de materiales tan diversos como recubrimientos de dispositivos médicos o en la industria textil. Sin embargo, no son polímeros de contacto directo como se ha comentado anteriormente, dado que el enlace es lábil y se liberan al medio los halógenos, por lo que estos polímeros deben ser recargados continuamente para que recuperen su actividad antimicrobiana.^{46–49}

Aplicaciones de los polímeros antimicrobianos

Los polímeros antimicrobianos catiónicos se utilizan para combatir las infecciones bacterianas, pero no solo en la industria biomédica, también tiene un gran potencial en otras industrias como la industria del empaquetado y envasado, o la industria textil.

Industria médica: Principalmente las bacterias pueden contaminar las superficies de los materiales biomédicos, catéteres, prótesis o apósticos, pudiendo provocar infecciones graves, incluso sepsis. A pesar de la tecnología actual, la mayoría de las infecciones producidas en los hospitales son debidas a estos dispositivos y hasta hora su tratamiento se basa en suministrar al paciente altas dosis de antibióticos. Alternativamente, los polímeros antimicrobianos pueden recubrir estos dispositivos y evitar así una posible infección.⁵⁰ Como ejemplo, Tiller *et al.* y Ghosh *et al.* recubrieron la superficie de diferentes materiales, como vidrio, metal o plásticos, con polímeros antimicrobianos catiónicos produciendo una gran reducción bacteriana en la mayoría de superficies probadas.^{51–54}

Industria del envasado de alimentos: El deterioro de los alimentos se debe, además de a factores ambientales, al crecimiento de microorganismos. Existen formas

tradicionales de conservar los alimentos como la congelación, ultracongelación, deshidratación, salazón, pasteurización, esterilización, etc. Pero en los últimos años, debido a la diversificación y globalización de los mercados se requiere un mayor tiempo de producción y distribución de los alimentos, surgiendo el término de “envases activos”, que hace referencia a envases que tienen actividad que favorecen la conservación de los alimentos y extienden su vida útil.^{55,56} Así, la incorporación de agentes antimicrobianos o polímeros antimicrobianos en el envasado podría alargar la vida útil de los alimentos. Como ejemplo, Friné *et al.* diseñaron envases de PLA que incorporaban carvacrol y timol para conferirle al envase propiedades antimicrobianas.⁵⁷ Además, Tripathi *et al.* recubrieron con quitosano diversos polímeros utilizados típicamente en envases alimentarios.⁵⁸

Industria textil: Los textiles que utilizamos actualmente poseen una gran área superficial que puede generar el crecimiento bacteriano, produciendo olores o decoloración. No solo eso, sino que también se pueden producir infecciones por bacterias en textiles utilizados en los hospitales.⁵⁹ Es por ello que se ha investigado en la incorporación de moléculas bioactivas en fibras y textiles, principalmente partículas de plata.⁶⁰ También se han incorporado polímeros antimicrobianos, por ejemplo Lin *et al.* consiguieron unir covalentemente polímeros catiónicos a diferentes fibras como algodón, lana, PET o nylon para producir fibras con propiedades antimicrobianas.⁶¹

No obstante, los polímeros antimicrobianos catiónicos generalmente son polímeros obtenidos a partir de monómeros que proceden del petróleo como el ácido metacrílico.^{39,62,63} Estos polímeros además de tener un origen fósil y no sostenible, no son biodegradables, lo que conlleva problemas medioambientales al final de su vida útil en muchas de sus aplicaciones mencionadas anteriormente. Para mitigar este problema, en los últimos años se está investigando en el desarrollo de polímeros antimicrobianos biobasados y/o biodegradables, y este es el marco en el que se integra esta tesis doctoral.

1.1.2 Polímeros y monómeros sostenibles de origen natural

Desde el descubrimiento de los primeros polímeros sintéticos a inicios del siglo XX, los polímeros se han convertido un material indispensable para el desarrollo de tecnologías y materiales que nos hacen la vida más fácil. A pesar de su gran distribución y versatilidad de usos, normalmente, los polímeros provienen de fuentes no renovables como el petróleo. A este aspecto negativo se les suma su gran durabilidad en el tiempo,

llegando a tardar cientos de años en descomponerse en la naturaleza. Actualmente solo se recicla el 5% de los polímeros producidos⁶⁴ debido a la mala gestión así como a la dificultad y el coste de los procesos en algunos productos, como por ejemplo envases multicapa o material biomédico. Esto provoca que los polímeros se acumulen en vertederos o acaben abandonados en el mar perjudicando la flora y fauna.⁶⁵

En los últimos años se ha incrementado los esfuerzos para el desarrollo y la implementación de polímeros y monómeros biodegradables de origen natural. Estos polímeros se pueden obtener de una forma sostenible y reutilizable sin recurrir al petróleo. Además, debido a su biodegradabilidad, estos polímeros podrían descomponerse en la naturaleza en menos de 3 meses, aportando además nutrientes a la tierra para generar de nuevo biomasa.

Ya en el año 2004, el Departamento Nacional de Energía de Estados Unidos publicó un informe con 12 compuestos químicos (Figura 6) obtenidos a partir de biomasa para la producción de productos y derivados de alto valor añadido, como polímeros.⁶⁶ Entre ellos se encuentra el ácido itacónico (IA). El IA se obtiene de la fermentación de los carbohidratos presentes en la biomasa gracias a los hongos de la familia *Aspergillus* (*A. terreus*, *A. itaconicus* o *A. niger*).⁶⁷

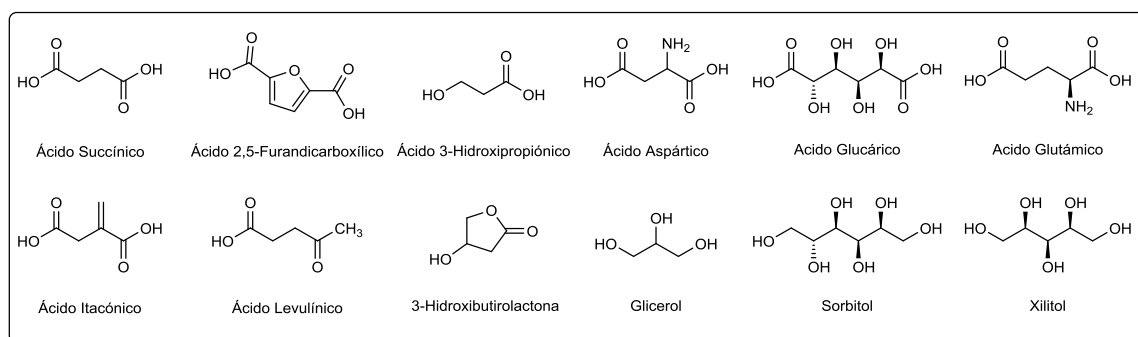


Figura 6. Los 12 compuestos de origen natural de gran valor añadido según el Departamento Nacional de Energía de Estados Unidos, entre ellos el ácido itacónico.

El ácido itacónico como monómero biobasado

El ácido itacónico (Figura 7) es un ácido dicarboxílico con una insaturación en posición α,β . Tanto su doble enlace, como sus dos grupos carboxilo brindan un sinfín de posibilidades de funcionalización, y de utilización como monómeros en reacciones de polimerización. Es insoluble en muchos disolventes orgánicos comunes, pero se disuelve fácilmente en agua o THF.

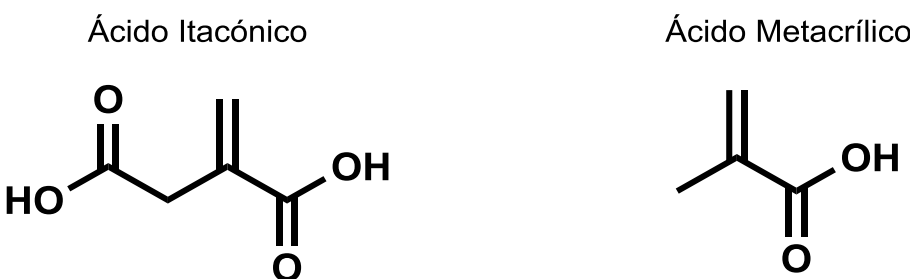


Figura 7. Estructura química del ácido itacónico y del ácido metacrílico.

El ácido itacónico tiene una estructura que se asemeja al ácido metacrílico o acrílico. Estos últimos compuestos provienen del petróleo, y son ampliamente utilizados en diversos materiales, sin embargo, sus derivados poliméricos no son biodegradables. Debido a su similitud estructural, el ácido itacónico podría ser un buen sustituto biobasado de los polímeros del ácido metacrílico. Además, presenta otras ventajas, como es su elevada temperatura de fusión, por lo que es sólido a temperatura ambiente y no genera problemas de olores ni de emisión de compuestos orgánicos volátiles (VOCs) en contraposición con el ácido metacrílico. El IA tiene, además, diferentes grupos funcionales en su estructura que lo hace muy versátil. El doble enlace del ácido itacónico puede ser susceptible de polimerizar vía polimerización por adición, principalmente por polimerización radical, para formar polímeros. Además, sus dos grupos carboxílicos pueden funcionalizarse con una gran cantidad de moléculas para obtener polímeros a medida. Una característica que no tiene el ácido metacrílico en comparación con el ácido itacónico, es la capacidad de formar polímeros mediante policondensación con dialcoholes.

Polimerización radical del ácido itacónico y sus derivados

Como se ha comentado anteriormente, el ácido itacónico se puede polimerizar utilizando iniciadores radicales convencionales para dar lugar al poli(ácido itacónico) (PIA). La síntesis del PIA puede realizarse en medio acuoso con iniciadores como los persulfatos.⁶⁸ No obstante, la reactividad del doble enlace es bastante baja respecto el ácido metacrílico.⁶⁹ Esto es debido principalmente a dos factores: 1) el radical del ácido itacónico se estabiliza por resonancia y da lugar a procesos de transferencia de cadena, es decir, que los radicales pueden consumirse en otros procesos, como la terminación, antes de continuar la propagación;^{68,70} 2) el impedimento estérico que provoca los dos grupos carboxílicos reduciendo la velocidad de propagación. Una desventaja respecto al ácido metacrílico es que se necesita añadir más del 1% molar de iniciador para obtener

buenas conversiones, esto hace que el peso molecular de los polímeros obtenidos sea más bajo.⁷¹

Sin embargo, y a pesar de los esfuerzos realizados para mejorar la polimerización del ácido itacónico, no fue hasta la implementación de las técnicas de polimerización radical controladas (CRP) cuando se produjo una gran mejora en el control de la estructura y el peso molecular de los polímeros del ácido itacónico, consigiéndose nuevas estructuras más complejas como por ejemplo copolímeros en bloque.⁷² Las técnicas de polimerización controlada más utilizadas para la síntesis de nuevos polímeros de ácido itacónico y sus derivados son las polimerizaciones radical por transferencia de átomo (ATRP) y la polimerización por trasferencia de cadena por adición-fragmentación reversible (RAFT).^{73,74}

Post funcionalización de polímeros por polimerización radical

El ácido itacónico se puede funcionalizar para obtener polímeros con funcionalidades y propiedades deseadas. Dados los distintos grupos funcionales que presenta, las posibilidades de incorporar nuevos grupos son muy diversas.

En primer lugar, el PIA es un poliácido y pueden realizarse reacciones de esterificación en los grupos ácidos. De esta manera, una vez obtenido el polímero, se le puede incorporar grupos funcionales con las propiedades que se deseen. El problema es la baja solubilidad del polímero PIA en disolventes orgánicos y la baja reactividad de sus ácidos, resultando muy complicado su post-funcionalización.⁷⁵

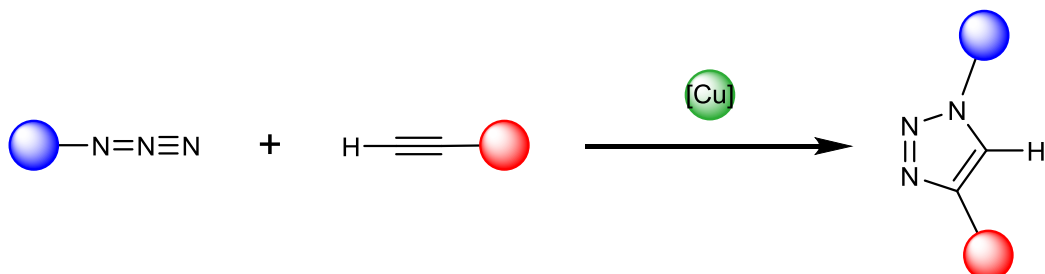
Para solventar este problema se puede realizar la esterificación directamente al monómero de ácido itacónico con la molécula objetivo mediante catálisis ácida, y posteriormente realizar la polimerización. Teniendo en cuenta los problemas que presenta el ácido itacónico en la polimerización, el grupo funcional no debe ser muy voluminoso, a fin de no impedir su polimerización. En algunos casos, la polimerización radical convencional de estos derivados del ácido itacónico se mejoraba visiblemente respecto a la polimerizan del IA.

Una estrategia muy interesante, desarrollada en esta tesis doctoral, es la funcionalización del ácido itacónico con alcohol propargílico. Este nuevo monómero polimeriza razonablemente bien mediante polimerización radical convencional dando lugar a un polímero soluble en disolventes orgánicos con grupos alquino como grupos laterales. Este tipo de grupo funcional nos permite llevar a cabo reacciones de química click de cicloadición azida-alquino catalizada con cobre (I) (CuAAC) e incorporar multitud

de funcionalidades y, por tanto, actividades o propiedades. En la década 1960, Huisgen ya aplicaba la reacción de cicloadición 1,3-dipolar para sintetizar compuestos heterocíclicos de cinco miembros en química orgánica. Los anillos de 1,2,3-triazol sintetizados mediante una cicloadición azida-alquino eran las reacciones más útiles. Sin embargo, este tipo de reacciones requerían altas temperaturas y tiempos de reacción largos, además de no tener una buena regioselectividad si no se utilizaban catalizadores.⁷⁶

A principios de los 2000, Sharpless acuñó el concepto de química click.⁷⁷ La química click es un conjunto de reacciones simples, eficientes y fiables que ocurren rápidamente y no producen subproductos. De todas las reacciones click, la cicloadición 1,3-dipolar es la más utilizada, especialmente, utilizando compuestos que contienen azidas y alquinos.

Un poco más tarde, tanto Sharpless⁷⁸ como Meldal,⁷⁹ independientemente, descubrieron una estrategia innovadora que utiliza iones de cobre (I) para realizar cicloadiciones 1,3-dipolar. El uso del catalizador de cobre permitió lograr una gran regioselectividad, además de aumentar exponencialmente la velocidad de reacción, y poder realizar las reacciones a temperatura ambiente. Las reacciones que se producían con azida y alquino en presencia de iones de cobre (I) se denominaron cicloadiciones azida-alquino catalizadas por cobre (I) (CuAAC, del inglés *copper catalyzed azide-alkyne cycloaddition*). Estas reacciones producen compuestos 1,2,3-triazol 1,4-disustituidos (ver Esquema 1).

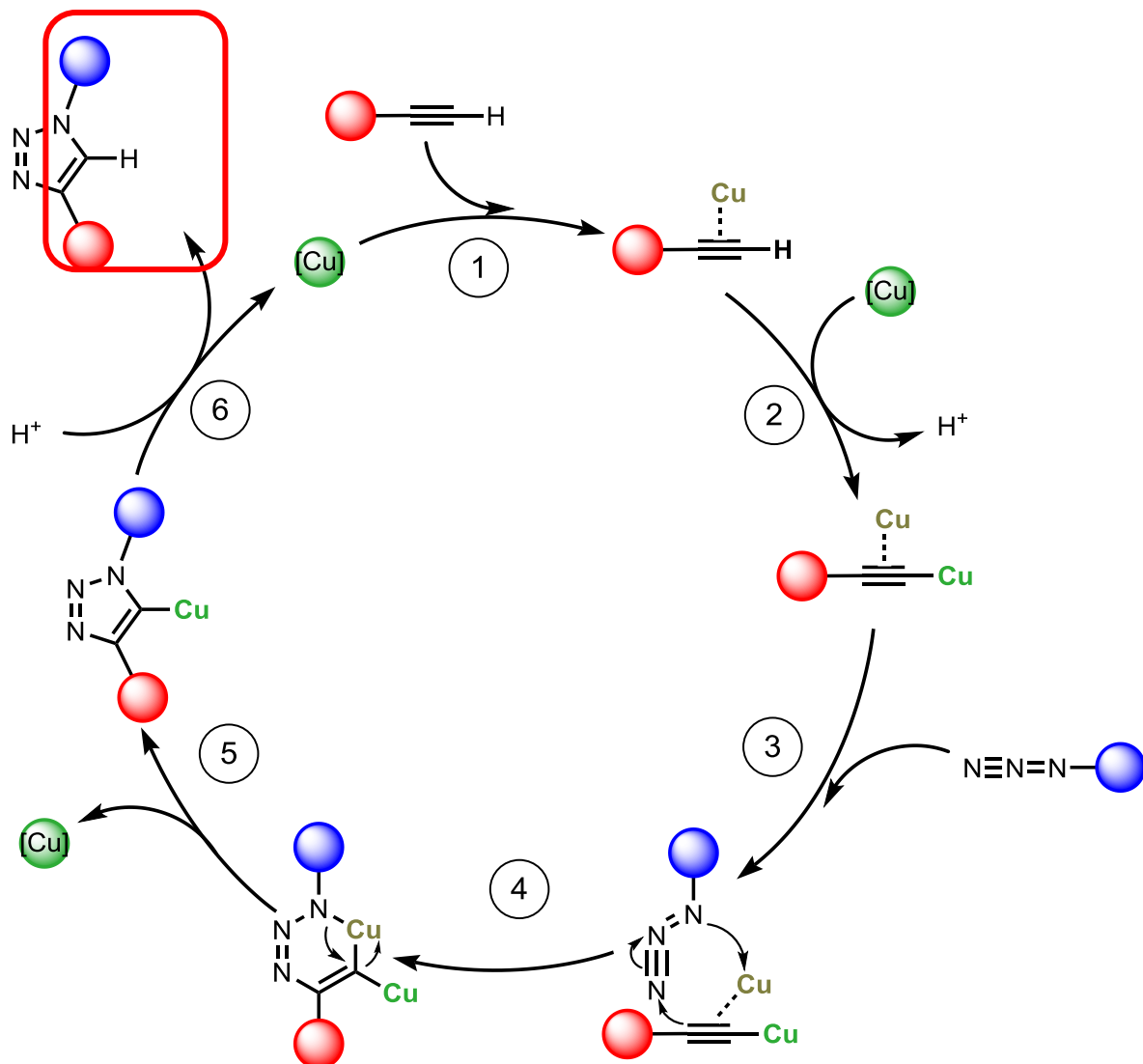


Esquema 1. Formación de un 1,2,3-triazol-1,4-disustituido utilizando una azida y un alquino en presencia de cobre.

Al mismo tiempo, Bertozzi^{80,81} desarrolló reacciones de click que podían funcionar dentro de los organismos vivos sin interferir con el funcionamiento químico de las células. Por estos descubrimientos, estos tres grandes científicos recibieron recientemente el Premio Nobel de Química 2022 “por el desarrollo de la química de click y la química bioortogonal”.⁸²

El mecanismo de reacción de la CuAAC fue inicialmente propuesto por Sharpless mediante la coordinación de un solo núcleo de cobre.⁷⁸ Sin embargo, estudios más recientes observaron un intermedio de reacción en el que intervienen dos núcleos de cobre como se puede ver en el Esquema 2.

La reacción comienza con la coordinación π del primer núcleo de cobre al alquino terminal (1). A continuación, se produce una desprotonación del alquino y se incorpora el segundo núcleo de cobre (2). La azida, junto con el complejo de cobre anterior, forman un ciclo de seis miembros (3-4). Posteriormente este anillo se transforma en un anillo de cinco miembros (5). Y finalmente el anillo se protona para formar el heterociclo de triazol (6).^{83,84} El mecanismo explica la gran regioselectividad que existe en este tipo de reacciones, en comparación de las reacciones no catalizadas.



Esquema 2. Mecanismo de reacción propuesto para la reacción CuAAC con un intermedio de reacción dinuclear de cobre.

Las principales ventajas de las reacciones CuAAC son su gran fiabilidad, su velocidad de reacción, permitiendo la síntesis de un gran abanico de compuestos de 1,2,3-triazol-1,4-disustituidos, gracias a su regioselectividad. Por otro lado, el cobre utilizado como catalizador es un metal tóxico para los seres vivos, lo que reduce algunos de sus usos y requiere de una purificación exhaustiva.⁸⁵ No obstante, en los últimos años se han logrado realizar reacciones CuAAC sin la necesidad de usar cobre como catalizador gracias a la utilización de anillos de ciclooctino tensionados.^{86,87}

Dada la gran versatilidad, las reacciones CuAAC tienen una gran aplicabilidad en las síntesis de compuesto orgánicos, como la síntesis de catenanos y rotaxanos,⁸⁸ agentes anticancerígenos,⁸⁹⁻⁹² agentes antimicrobianos,^{93,94} o agentes antivirales.⁹⁵ Además, se puede utilizar para sintetizar polímeros mediante polimerización click.^{96,97}

Polimerización por condensación del ácido itacónico

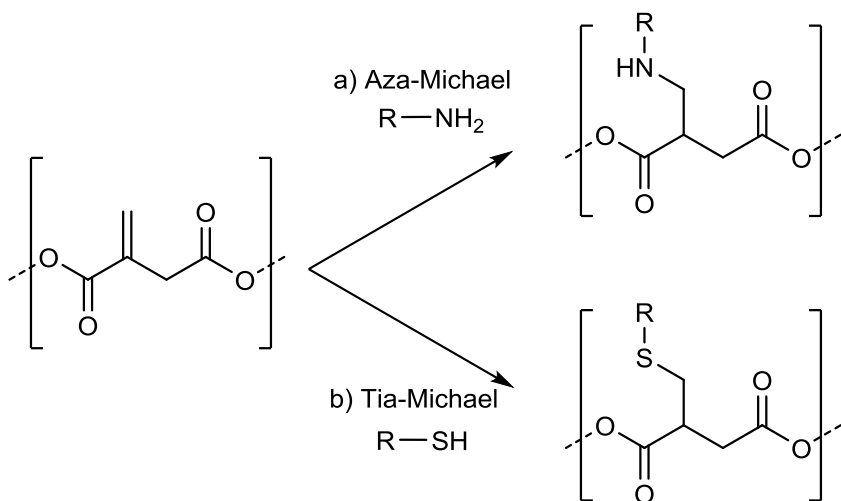
El ácido itacónico también tiene la capacidad de polimerizar mediante polimerización por condensación debido a los dos grupos carboxílicos. Además, se pueden utilizar en este tipo de condensación dialcoholes de origen natural y renovable, como 1,3-propanodiol, 1,4-butanodiol o el glicerol.⁹⁸ Aun siendo una vía prometedora de creación de nuevos polímeros, el ácido itacónico presenta inconvenientes debido a la diferente reactividad de los grupos carboxílicos y a las reacciones de isomerización o entrecruzamiento indeseadas por la presencia del doble enlace. A pesar de estos problemas, se han logrado sintetizar diversos sistemas poliméricos basados en ácido itacónico por policondensación.⁹⁹

Otra forma de obtener polímeros por policondensación, que se ha desarrollado en los últimos años, es mediante polimerización enzimática, utilizando la enzima lipasa B *Cándida antártica* (CALB).¹⁰⁰ Este método se puede considerar más sostenible para la síntesis de polímeros biobasados si se utilizan monómeros derivados de fuentes renovables. Estas enzimas permiten reducir la temperatura de reacción en la policondensación lo que evitaría problemas con el doble enlace del ácido itaconico.¹⁰¹

Post funcionalización de polímeros por condensación

Por otro lado, los polímeros obtenidos por policondensación también pueden ser modificados posteriormente, gracias al doble enlace presente en la estructura. Esto permite la realización de adiciones tipo-Michael. Estas reacciones consisten en el ataque de un nucleófilo a un compuesto carbonílico α,β -insaturado. Si el compuesto es nitrogenado obtendremos una aza-Michael y si el compuesto es tiolado se obtiene una

tia-Michael, como se puede ver en el Esquema 3. Mediante estas reacciones, y empleando compuestos difuncionalizados como diaminas o ditioles, se pueden producir entrecruzamiento de estos polímeros para la formación de sistemas entrecruzados o geles.



Esquema 3. Reactividad del polímero de ácido itacónico: a) aza-Michael y b) tia-Michael.

Potenciales aplicaciones de los polímeros basados en ácido itacónico.

Debido a su gran capacidad de funcionalización y su biodegradabilidad, los compuestos y polímeros derivados del ácido itacónico, se pueden utilizar en una gran cantidad de aplicaciones, ya sea como nuevos materiales o para sustituir a otros procedentes de fuentes fósiles. Así, se ha evaluado su empleo en las siguientes aplicaciones:

Industria médica: El ácido itacónico y sus derivados se pueden copolimerizar con otros componentes para formar materiales con grupos bioactivos que se pueden utilizar por ejemplo con agentes anticancerígenos¹⁰² o antimicrobianos para evitar o reducir infecciones bacterianas.¹⁰³

Industria del envasado de alimentos: Los derivados del ácido itacónico pueden ser utilizados en el envasado de alimentos principalmente por sus propiedades biodegradables.^{104,105} Pero adicionalmente se pueden funcionalizar con compuestos antimicrobianos para la formación de envases activos.⁷⁵

Industria textil: Se ha utilizado el ácido itacónico para reforzar fibras de algodón y mejorar sus propiedades, como por ejemplo evitar las arrugas en tejidos de algodón.¹⁰⁶

Industria cosmética: actualmente la empresa Itaconix[©] ya comercializa productos derivados del ácido itacónico para su utilización en cosmética para el cuidado de la piel o como desodorantes.

En muchas de estas aplicaciones, se plantea el uso de los polímeros derivados de ácido itacónico (sobre todo en el caso de los polímeros funcionalizados con grupos activos, tales como grupos antimicrobianos) como componentes minoritarios o aditivos, en materiales poliméricos comunes como termoplásticos biobasados y/o biodegradables tales como el PLA. De esta manera se reducen costes, ya que se añaden en pequeñas proporciones a material, manteniéndose las propiedades de estos termoplásticos, así como sus condiciones de procesado. En esta tesis doctoral se han empleado los polímeros antimicrobianos derivados de IA como componentes minoritarios en mezclas con PLA y PBAT, aportando de esta manera propiedades antimicrobianas, manteniendo su origen biobasado, su biodegradabilidad y sus propiedades físico-químicas. En el siguiente apartado se describen de qué manera se pueden incorporar los polímeros antimicrobianos como aditivos en las matrices poliméricas mencionadas y así obtener sistemas antimicrobianos biobasados y biodegradables.

1.1.3 Métodos de obtención de sistemas antimicrobianos biodegradables: Incorporación de polímeros antimicrobianos a matrices poliméricas biobasadas y biodegradables.

Los polímeros tienen la peculiaridad, debido a su estructura, de ser procesados fácilmente, pudiéndose crear diferentes estructuras y dispositivos con propiedades modulables según su uso requerido, desde envases de alimentos, dispositivos médicos avanzados, tejidos poliméricos, etc. Durante el procesado se pueden mezclar diferentes polímeros, además de incorporar plastificantes, cargas o aditivos, para mejorar las propiedades finales del material.

Existen varios métodos para el procesado de polímeros como la extrusión en fundido, inyección, moldeo por compresión o técnicas más novedosas como la impresión 3D o el electrohilado. En esta tesis doctoral, en concreto se han empleado como técnicas de procesado, la extrusión en fundido, el moldeo por compresión y el electrohilado, para el desarrollo tanto de films enfocados al envasado de alimentos, como de tejidos no tejidos para aplicaciones en regeneración tisular, en ambos casos se han llevado a cabo a partir de mezclas de biopolímeros con los polímeros antimicrobianos derivados de IA. A continuación, se detallan estas técnicas.

Procesado de polímeros por extrusión en fundido

El proceso de extrusión en fundido se lleva realizando desde 1930, para el procesado y conformado de los plásticos, siendo una de las técnicas más empleadas. Muchos de los productos plásticos actuales, films, láminas o tubos, se producen de esta manera.¹⁰⁷ En esta técnica, el polímero fundido a temperaturas por encima de la temperatura de transición vítrea o de la temperatura de fusión en polímeros semicristalinos, es forzado a pasar a través de un cabezal, por medio del empuje generado por la acción giratoria de un husillo que gira concéntricamente en una cámara a temperatura controlada. Para un correcto procesado de polímeros es necesario controlar 3 variables: la temperatura de trabajo, la velocidad de husillo y el tiempo de extrusión. Esta técnica nos permite por un lado, el mezclado de dos o más polímeros, así como la incorporación de plastificantes, cargas o fármacos, para dotarles de nuevas propiedades como, por ejemplo, propiedades antimicrobianas. De hecho, uno de los usos que recibe la extrusión de polímeros es la inclusión de fármacos para su liberación.¹⁰⁸

Para poder utilizar estos polímeros ya extruidos como materiales bioactivos para la industria médica o de envasado, es necesario proporcionarles una forma determinada para realizar correctamente sus funciones. Es por ello que se utiliza el moldeo por compresión de los materiales utilizando un molde como una de las técnicas más empleadas en la industria. De esta forma se pueden obtener láminas u otras morfologías que se adapten a las necesidades de la industria. Sin embargo, ambas técnicas de procesado, extrusión y compresión, tiene una gran desventaja, no se puede utilizar compuestos que degraden a la temperatura de trabajo. Por lo que es necesario el uso de otros procesos menos agresivos sobre todo si se quiere utilizar moléculas termolábiles, como es el caso de muchos agentes antimicrobianos.

Procesado de polímeros por electrohilado

El electrohilado ya se conocía desde el siglo XVII con los primeros experimentos donde se estudiaba cómo una gota de agua formaba una forma cónica en presencia de un campo eléctrico. Posteriormente, en el año 1969 Geoffrey Taylor describió el modelo matemático de ese cono, denominándolo cono de Taylor.¹⁰⁹ A pesar de ser una técnica muy interesante para la fabricación de fibras, no fue hasta la década de los 90 cuando se empezó a popularizar esta técnica, gracias al avance de los microscopios electrónicos para observar las fibras formadas de tamaño nano y micrométrico.

El electrohilado es una técnica que consiste en aplicar un fuerte campo eléctrico entre una punta donde se encuentra la disolución polimérica y un colector. La diferencia de potencial crea el cono de Taylor que permite el estiramiento y alargamiento de las gotas produciendo fibras y micro/nanofibras que finalmente se recogen en un colector (Figura 8). Estas fibras se les suele denominar tejido no tejido. Las condiciones de trabajo son más suaves comparadas con la técnica de extrusión, lo que permite la incorporación de moléculas o polímeros termolábiles.¹¹⁰

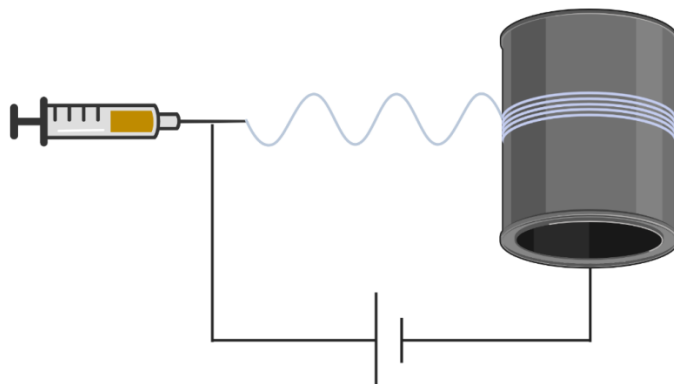


Figura 8. Diagrama esquemático del funcionamiento del aparato de electrohilado rotatorio utilizado en esta tesis doctoral.

Existen numerosos factores que influyen a la hora de fabricar las fibras, como la temperatura, la humedad, el voltaje e incluso la distancia de la boquilla a la zona de recogida de la muestra. Por otro lado, los polímeros deben tener unas características optimas, entre otras, un alto peso molecular, tener una viscosidad adecuada en disolución y utilizar disolventes adecuados para el proceso de electrohilado. Todo ello influye en las características morfológicas de las fibras como se puede ver en la tabla 1.¹¹¹

Variando esas condiciones podemos obtener fibras de diferente tamaño desde micrométrico hasta nanométrico, se pueden alinear o incluso fomentar la aparición de poros en la superficie de las fibras variando la humedad relativa. Además, esta técnica también permite la introducción de cargas y otros aditivos en las fibras para dotarlas de propiedades deseadas. Se pueden incorporar un gran número de moléculas, nanopartículas u otros polímeros que no se puedan hilar por sí mismos.¹¹²

Las fibras obtenidas por electrohilado se emplean en numerosos campos, especialmente en el campo de la biomedicina. Estas fibras pueden utilizarse como andamios para la regeneración y reparación de tejidos,¹¹³ y como apósticos para la curación de heridas,¹¹⁴ entre otros usos.

Tabla 1. Parámetros del electrohilado y su efecto en las fibras.

Parámetros	Característica morfológica afectada	Efecto
Voltaje	Diámetro	Al aumentar el voltaje disminuye el diámetro
Caudal de disolución	Diámetro y morfología	Afecta a la formación de fibras y al diámetro
Distancia del colector	Diámetro y morfología	Al aumentar la distancia disminuye el diámetro
Concentración y viscosidad	Formación de fibras	Si es alta: Puede bloquear la punta y causa defectos. Si es baja: Causa defectos
Conductividad de la disolución	Diámetro	Al aumentar disminuye el diámetro de fibra
Disolvente	Morfología de fibras	Debe disolver el polímero y relativamente volátil
Humedad y temperatura	Diámetro y morfología	Cambios en la morfología Creación de poros

1.1.4 Antecedentes e hipótesis

Esta tesis doctoral, enfocada en el desarrollo de sistemas poliméricos antimicrobianos, se enmarca dentro de una de las líneas de investigación del grupo de Ingeniería Macromolecular (MacroEng) del Instituto de Ciencia y Tecnología de Polímeros del CSIC (ICTP). Desde hace años el grupo se dedica al diseño, síntesis y desarrollo de sistemas polímeros antimicrobianos, así como al estudio de su estructura, propiedades y aplicaciones. El grupo de investigación ha desarrollado varios proyectos en esta temática financiados por organismos tanto públicos como privados y fruto de sus resultados ha publicado numerosos artículos de investigación, capítulos de libro, así como una patente. Cabe destacar que MacroEng es un grupo de prestigio internacional en el campo, colaborando con importantes grupos de investigación de todo el mundo. Ha publicado importantes artículos de revisión en prestigiosas revistas,¹¹⁵⁻¹²¹ uno de ellos en *Progress in Polymer Science* con más de 1000 citas, y ha editado un libro de la RSC titulado “Polymeric Materials with Antimicrobial Activity: From Synthesis to Applications”.

El grupo de investigación comenzó en la temática con el desarrollo de nanocomposites basados en nanopartículas de dióxido de titanio y polímeros tales como

el fluoruro de polivinilideno (PVDF), el polipropileno (PP), la policaprolactona (PCL) y el copolímero etileno alcohol vinílico (EVOH).^{122–128} Estos sistemas presentaban excelentes propiedades asociadas al dióxido de titanio nanométrico, con actividad fotocatalítica bajo irradiación ultravioleta (UV). Igualmente, en el grupo se trabajó en la síntesis de polímeros hidrófilos y superhidrófobos para la preparación de superficies con propiedades antiadherentes o “antifouling”, con el objetivo de evitar la adhesión y posterior colonización bacteriana.^{129–133} Principalmente se prepararon superficies donde se controló tanto la composición química, empleando polímeros derivados de etilenglicol y polímeros fluorados, como su estructuración, con el desarrollo de superficies micro y nanoestructuradas. A pesar de las buenas propiedades de las superficies “antifouling”, éstas no son eficientes a largo plazo, ya que terminan ensuciándose y siendo colonizadas finalmente por poblaciones microbianas. Con el objetivo de crear materiales con mayor eficiencia antimicrobiana, seguidamente la línea derivó en la preparación de polímeros con actividad biocida inherente, principalmente empleando polímeros catiónicos. En un primer lugar se emplearon polímeros basados en monómeros comerciales como el metacrilato de dimetilaminoetilo (DMAEMA)^{134,135} y posteriormente se diseñaron monómeros novedosos con grupos triazolio y tiazolio (derivado de la vitamina B1).^{39,42,136–143} Estos últimos polímeros funcionalizados con triazolio y tiazolio, y derivados principalmente de metacrilatos, aunque también de monómeros estirénicos, mostraron propiedades excelentes, siendo muy activos frente a bacterias Gram-positivas y Gram-negativas, incluidas bacterias resistentes, y frente a hongos. Se evaluaron otras propiedades importantes de cara a su aplicabilidad, como su citotoxicidad, y sus propiedades térmicas y estructurales, comprobándose además, su capacidad de impartir actividad antimicrobiana a materiales poliméricos (derivados del petróleo como poliestireno, poliacrilonitrilo y polimetacrilatos) cuando eran añadidos en bajas proporciones.^{144–150} El diseño de estos polímeros con grupos tiazolio y triazolio supuso para el grupo de investigación un gran impacto y un salto de calidad importante.

Sin embargo, dada las necesidades actuales en cuanto a sostenibilidad y cuidado del medio ambiente, se están buscando alternativas a los polímeros derivados del petróleo. Actualmente la investigación en compuestos de origen biológico está en pleno auge para el desarrollo de nuevos compuestos y polímeros más amigables con el medioambiente. Concretamente, polímeros biobasados como el poli(ácido láctico) (PLA) o el poli(ácido glicólico) (PGA), reducen la dependencia de los recursos fósiles y al mismo tiempo mejoran la huella de carbono del producto. Por ello, el siguiente reto del grupo de

investigación consistió en el desarrollo de polímeros antimicrobianos biobasados con el objetivo de afrontar los problemas medioambientales actuales y contribuir con soluciones a estas nuevas demandas. Así, el desarrollo de esta tesis doctoral ha supuesto un paso más en la línea de investigación, con el diseño y preparación de nuevos sistemas poliméricos antimicrobianos derivados de un monómero biobasado con gran potencial como es el ácido itacónico. Además, el origen biobasado de estos derivados poliméricos lleva asociado, en muchos casos, una mejora de otras propiedades tales como la biodegradabilidad y la biocompatibilidad. Los potenciales beneficios de estos desarrollos, así como los desafíos de la temática aseguran el fortalecimiento de esta línea de investigación en el grupo.

1.1.5 Referencias

- (1) Bennett, J. W.; Chung, K.-T. Alexander Fleming and the Discovery of Penicillin; 2001; pp 163–184.
- (2) Gaynes, R. The Discovery of Penicillin—New Insights After More Than 75 Years of Clinical Use - Volume 23, Number 5—May 2017 - Emerging Infectious Diseases Journal - CDC. *Emerg. Infect. Dis.* **2017**, 23 (5), 849–853.
- (3) Martin, M. J.; Thottathil, S. E.; Newman, T. B. Antibiotics Overuse in Animal Agriculture: A Call to Action for Health Care Providers. *Am. J. Public Health* **2015**, 105 (12), 2409–2410.
- (4) Murray, C. J. L.; Ikuta, K. S.; Sharara, F.; Swetschinski, L.; Robles Aguilar, G.; Gray, A.; Han, C.; Bisignano, C.; Rao, P.; Wool, E.; et al. Global Burden of Bacterial Antimicrobial Resistance in 2019: A Systematic Analysis. *Lancet* **2022**, 399 (10325), 629–655.
- (5) O'Neill, J. Tackling Drug-Resistant Infections Globally: Final Report and Recommendations. **2016**.
- (6) Kapoor, G.; Saigal, S.; Elongavan, A. Action and Resistance Mechanisms of Antibiotics: A Guide for Clinicians. *J. Anaesthesiol. Clin. Pharmacol.* **2017**, 33 (3), 300.
- (7) Konai, M. M.; Bhattacharjee, B.; Ghosh, S.; Haldar, J. Recent Progress in Polymer Research to Tackle Infections and Antimicrobial Resistance. *Biomacromolecules* **2018**, 19 (6), 1888–1917.
- (8) Rangel-Núñez, C.; Molina-Pinilla, I.; Ramírez-Trujillo, C.; Suárez-Cruz, A.; Martínez, S. B.; Bueno-Martínez, M. Tackling Antibiotic Resistance: Influence of Aliphatic Branches on Broad-Spectrum Antibacterial Polytriazoles against ESKAPE Group Pathogens. *Pharmaceutics* **2022**, 14 (11), 2518.
- (9) Alfei, S.; Schito, A. M. Positively Charged Polymers as Promising Devices against Multidrug Resistant Gram-Negative Bacteria: A Review. *Polymers* **2020**, 12 (5), 1195.
- (10) Konai, M. M.; Bhattacharjee, B.; Ghosh, S.; Haldar, J. Recent Progress in Polymer Research to Tackle Infections and Antimicrobial Resistance. *Biomacromolecules* **2018**, 19 (6), 1888–1917.
- (11) Ghosh, S.; Mukherjee, S.; Patra, D.; Haldar, J. Polymeric Biomaterials for Prevention and Therapeutic Intervention of Microbial Infections. *Biomacromolecules* **2022**, 23 (3), 592–608.
- (12) Jain, A.; Duvvuri, L. S.; Farah, S.; Beyth, N.; Domb, A. J.; Khan, W.; Jain, A.; Duvvuri, L. S.; Khan, W.; Farah, S.; et al. Antimicrobial Polymers. *Adv. Healthc. Mater.* **2014**, 3 (12), 1969–1985.
- (13) Siedenbiedel, F.; Tiller, J. C. Antimicrobial Polymers in Solution and on Surfaces: Overview and Functional Principles. *Polym. 2012, Vol. 4, Pages 46-71* **2012**, 4 (1), 46–71.
- (14) González-Henríquez, C. M.; Sarabia-Vallejos, M. A.; Hernandez, J. R. Antimicrobial Polymers for Additive Manufacturing. *Int. J. Mol. Sci.* **2019**, Vol. 20, Page 1210 **2019**, 20 (5), 1210.
- (15) Solomon, D. D.; Sherertz, R. J. Antibiotic Releasing Polymers. *J. Control. Release* **1987**, 6 (1), 343–352.
- (16) Yahyaoui, M.; Gordobil, O.; Herrera Díaz, R.; Abderrabba, M.; Labidi, J. Development of Novel Antimicrobial Films Based on Poly(Lactic Acid) and Essential Oils. *React. Funct. Polym.* **2016**, 109, 1–8.
- (17) Ribeiro-Santos, R.; Andrade, M.; Sanches-Silva, A. Application of Encapsulated Essential Oils as Antimicrobial Agents in Food Packaging. *Curr. Opin. Food Sci.* **2017**, 14, 78–84.
- (18) Carbone, M.; Donia, D. T.; Sabbatella, G.; Antiochia, R. Silver Nanoparticles in Polymeric Matrices for Fresh Food Packaging. *J. King Saud Univ. - Sci.* **2016**, 28 (4), 273–279.
- (19) Cano, A.; Cháfer, M.; Chiralt, A.; González-Martínez, C. Development and Characterization of Active Films Based on Starch-PVA, Containing Silver Nanoparticles. *Food Packag. Shelf Life* **2016**, 10, 16–24.
- (20) K., S. S.; Indumathi, M. P.; Rajarajeswari, G. R. Mahua Oil-Based Polyurethane/Chitosan/Nano ZnO Composite Films for Biodegradable Food Packaging Applications. *Int. J. Biol. Macromol.* **2019**, 124, 163–174.
- (21) Ren, J.; Wang, S.; Gao, C.; Chen, X.; Li, W.; Peng, F. TiO₂-Containing PVA/Xylan Composite Films with Enhanced Mechanical Properties, High Hydrophobicity and UV Shielding Performance. *Cellulose* **2015**, 22 (1), 593–602.
- (22) Ashfaq, A.; Khursheed, N.; Fatima, S.; Anjum, Z.; Younis, K. Application of Nanotechnology in Food

- Packaging: Pros and Cons. *J. Agric. Food Res.* **2022**, *7*, 100270.
- (23) Han, H.; Liu, C.; Zhu, J.; Li, F. X.; Wang, X. L.; Yu, J. Y.; Qin, X. H.; Wu, D. Q. Contact/Release Coordinated Antibacterial Cotton Fabrics Coated with N-Halamine and Cationic Antibacterial Agent for Durable Bacteria-Killing Application. *Int. J. Mol. Sci.* **2020**, *Vol. 21*, *Page 6531* **2020**, *21* (18), 6531.
- (24) Rong, F.; Tang, Y.; Wang, T.; Feng, T.; Song, J.; Li, P.; Huang, W. Nitric Oxide-Releasing Polymeric Materials for Antimicrobial Applications: A Review. *Antioxidants* **2019**, *Vol. 8*, *Page 556* **2019**, *8* (11), 556.
- (25) Lim, D. S. W.; Yuan, Y.; Zhang, Y. PH-Degradable Polymers as Impermanent Antimicrobial Agents for Environmental Sustainability. *ACS Appl. Bio Mater.* **2021**, *4* (2), 1544–1551.
- (26) Yuan, Y.; Lim, D. S. W.; Wu, H.; Lu, H.; Zheng, Y.; Wan, A. C. A.; Ying, J. Y.; Zhang, Y. PH-Degradable Imidazolium Oligomers as Antimicrobial Materials with Tuneable Loss of Activity. *Biomater. Sci.* **2019**, *7* (6), 2317–2325.
- (27) Luo, H.; Yin, X. Q.; Tan, P. F.; Gu, Z. P.; Liu, Z. M.; Tan, L. Polymeric Antibacterial Materials: Design, Platforms and Applications. *J. Mater. Chem. B* **2021**, *9* (12), 2802–2815.
- (28) Mukhopadhyay, S.; Bharath Prasad, A. S.; Mehta, C. H.; Nayak, U. Y. Antimicrobial Peptide Polymers: No Escape to ESKAPE Pathogens—a Review. *World J. Microbiol. Biotechnol.* **2020**, *36* (9), 1–14.
- (29) Roy, S.; Sarkhel, S.; Bisht, D.; Hanumantharao, S. N.; Rao, S.; Jaiswal, A. Antimicrobial Mechanisms of Biomaterials: From Macro to Nano. *Biomater. Sci.* **2022**, *10* (16), 4392–4423.
- (30) Pham, P.; Oliver, S.; Boyer, C. Design of Antimicrobial Polymers. *Macromol. Chem. Phys.* **2022**, *2200226*, 1–28.
- (31) Pankratova, G.; Hederstedt, L.; Gorton, L. Extracellular Electron Transfer Features of Gram-Positive Bacteria. *Anal. Chim. Acta* **2019**, *1076*, 32–47.
- (32) Timofeeva, L.; Kleshcheva, N. Antimicrobial Polymers: Mechanism of Action, Factors of Activity, and Applications. *Appl. Microbiol. Biotechnol.* **2011**, *89* (3), 475–492.
- (33) Broxton, P.; Woodcock, P. M.; Heatley, F.; Gilbert, P. Interaction of Some Polyhexamethylene Biguanides and Membrane Phospholipids in Escherichia Coli. *J. Appl. Bacteriol.* **1984**, *57* (1), 115–124.
- (34) Zheng, Z.; Xu, Q.; Guo, J.; Qin, J.; Mao, H.; Wang, B.; Yan, F. Structure-Antibacterial Activity Relationships of Imidazolium-Type Ionic Liquid Monomers, Poly(Ionic Liquids) and Poly(Ionic Liquid) Membranes: Effect of Alkyl Chain Length and Cations. *ACS Appl. Mater. Interfaces* **2016**, *8* (20), 12684–12692.
- (35) Chiloeches, A.; Echeverría, C.; Fernández-García, M.; Muñoz-Bonilla, A. Influence of Polymer Composition and Substrate on the Performance of Bioinspired Coatings with Antibacterial Activity. *Coatings* **2019**, *9* (11), 733.
- (36) Palermo, E. F.; Kuroda, K. Structural Determinants of Antimicrobial Activity in Polymers Which Mimic Host Defense Peptides. *Appl. Microbiol. Biotechnol.* **2010**, *87* (5), 1605–1615.
- (37) Xue, Y.; Xiao, H.; Zhang, Y. Antimicrobial Polymeric Materials with Quaternary Ammonium and Phosphonium Salts. *Int. J. Mol. Sci.* **2015**, *16* (2), 3626.
- (38) Arshad, M. F.; Alam, A.; Alshammari, A. A.; Alhazza, M. B.; Alzimam, I. M.; Alam, M. A.; Mustafa, G.; Ansari, M. S.; Alotaibi, A. M.; Alotaibi, A. A.; et al. Thiazole: A Versatile Standalone Moiety Contributing to the Development of Various Drugs and Biologically Active Agents. *Mol.* **2022**, *Vol. 27*, *Page 3994* **2022**, *27* (13), 3994.
- (39) Tejero, R.; López, D.; López-Fabal, F.; Gómez-Garcés, J. L.; Fernández-García, M. Antimicrobial Polymethacrylates Based on Quaternized 1,3-Thiazole and 1,2,3-Triazole Side-Chain Groups. *Polym. Chem.* **2015**, *6* (18), 3449–3459.
- (40) Müller, I. B.; Bergmann, B.; Groves, M. R.; Couto, I.; Amaral, L.; Begley, T. P.; Walter, R. D.; Wrenger, C. The Vitamin B1 Metabolism of *Staphylococcus Aureus* Is Controlled at Enzymatic and Transcriptional Levels. *PLoS One* **2009**, *4* (11), e7656.
- (41) Zhang, B. Comprehensive Review on the Anti-Bacterial Activity of 1,2,3-Triazole Hybrids. *Eur. J. Med. Chem.* **2019**, *168*, 357–372.

- (42) Cuervo-Rodríguez, R.; Muñoz-Bonilla, A.; Araujo, J.; Echeverría, C.; Fernández-García, M. Influence of Side Chain Structure on the Thermal and Antimicrobial Properties of Cationic Methacrylic Polymers. *Eur. Polym. J.* **2019**, *117*, 86–93.
- (43) Patel, J. N.; Dolia, M. B.; Patel, K. H.; Patel, R. M. Homopolymer of 4-Chloro-3-Methyl Phenyl Methacrylate and Its Copolymers with Butyl Methacrylate: Synthesis, Characterization, Reactivity Ratios and Antimicrobial Activity. *J. Polym. Res.* **2006**, *13* (3), 219–228.
- (44) Kuroda, K.; Degrado, W. F. Amphiphilic Polymethacrylate Derivatives as Antimicrobial Agents. **2005**.
- (45) Kenawy, E. R.; Worley, S. D.; Broughton, R. The Chemistry and Applications of Antimicrobial Polymers: A State-of-the-Art Review. *Biomacromolecules* **2007**, *8* (5), 1359–1384.
- (46) Kou, L.; Liang, J.; Ren, X.; Kocer, H. B.; Worley, S. D.; Tzou, Y. M.; Huang, T. S. Synthesis of a Water-Soluble Siloxane Copolymer and Its Application for Antimicrobial Coatings. *Ind. Eng. Chem. Res.* **2009**, *48* (14), 6521–6526.
- (47) Qu, H.-H.; Wang, C.; Guo, Y.-X.; Zhao, Z.-Y.; Qiao, L.; Yang, J.-B.; Wu, H.-X.; Li, Q.-S.; Dong, A. Electrospun N-Halamine/ZnO-Based Platform Eradicates Bacteria through Multimodal Antimicrobial Mechanism of Action. *Rare Met.* **2023**, *42* (1), 222–233.
- (48) Chien, H. W.; Chiu, T. H.; Lee, Y. L. Rapid Biocidal Activity of N-Halamine-Functionalized Polydopamine and Polyethylene Imine Coatings. *Langmuir* **2021**, *37* (26), 8037–8044.
- (49) Wang, F.; Huang, L.; Zhang, P.; Si, Y.; Yu, J.; Ding, B. Antibacterial N-Halamine Fibrous Materials. *Compos. Commun.* **2020**, *22*, 100487.
- (50) Huang, K. S.; Yang, C. H.; Huang, S. L.; Chen, C. Y.; Lu, Y. Y.; Lin, Y. S. Recent Advances in Antimicrobial Polymers: A Mini-Review. *Int. J. Mol. Sci.* **2016**, Vol. 17, Page 1578 **2016**, *17* (9), 1578.
- (51) Tiller, J. C.; Liao, C.-J.; Lewis, K.; Klibanov, A. M. Designing Surfaces That Kill Bacteria on Contact. *Proc. Natl. Acad. Sci.* **2001**, *98* (11), 5981–5985.
- (52) Ghosh, S.; Jolly, L.; Haldar, J. Polymeric Paint Coated Common-Touch Surfaces That Can Kill Bacteria, Fungi and Influenza Virus. *MRS Commun.* **2021**, *11* (5), 610–618.
- (53) Erkoc, P.; Ulucan-Karnak, F. Nanotechnology-Based Antimicrobial and Antiviral Surface Coating Strategies. *Prosthes.* **2021**, Vol. 3, Pages 25-52 **2021**, *3* (1), 25–52.
- (54) Rojo, L.; García-Fernández, L.; Aguilar, M. R.; Vázquez-Lasa, B. Antimicrobial Polymeric Biomaterials Based on Synthetic, Nanotechnology, and Biotechnological Approaches. *Curr. Opin. Biotechnol.* **2022**, *76*, 102752.
- (55) Huang, T.; Qian, Y.; Wei, J.; Zhou, C. Polymeric Antimicrobial Food Packaging and Its Applications. *Polym.* **2019**, Vol. 11, Page 560 **2019**, *11* (3), 560.
- (56) Díez-Pascual, A. M. Antimicrobial Polymer-Based Materials for Food Packaging Applications. *Polym.* **2020**, Vol. 12, Page 731 **2020**, *12* (4), 731.
- (57) Friné, V. C.; Hector, A. P.; Manuel, N. D. S.; Estrella, N. D.; Antonio, G. J. Development and Characterization of a Biodegradable PLA Food Packaging Hold Monoterpene–Cyclodextrin Complexes against Alternaria Alternata. *Polym.* **2019**, Vol. 11, Page 1720 **2019**, *11* (10), 1720.
- (58) Tripathi, S.; Mehrotra, G. K.; Dutta, P. K. Chitosan Based Antimicrobial Films for Food Packaging Applications. *E-Polymers* **2008**, *8* (1).
- (59) Morais, D. S.; Guedes, R. M.; Lopes, M. A. Antimicrobial Approaches for Textiles: From Research to Market. *Mater.* **2016**, Vol. 9, Page 498 **2016**, *9* (6), 498.
- (60) Palza, H. Antimicrobial Polymers with Metal Nanoparticles. *Int. J. Mol. Sci.* **2015**, Vol. 16, Pages 2099-2116 **2015**, *16* (1), 2099–2116.
- (61) Lin, J.; Qiu, S.; Lewis, K.; Klibanov, A. M. Mechanism of Bactericidal and Fungicidal Activities of Textiles Covalently Modified with Alkylated Polyethylenimine. *Biotechnol. Bioeng.* **2003**, *83* (2), 168–172.
- (62) Lu, G.; Wu, D.; Fu, R. Studies on the Synthesis and Antibacterial Activities of Polymeric Quaternary Ammonium Salts from Dimethylaminoethyl Methacrylate. *React. Funct. Polym.* **2007**, *67* (4), 355–366.
- (63) Zhang, Z.; Cheng, G.; Carr, L. R.; Vaisocherová, H.; Chen, S.; Jiang, S. The Hydrolysis of Cationic Polycarboxybetaine Esters to Zwitterionic Polycarboxybetaines with Controlled Properties.

- Biomaterials* **2008**, 29 (36), 4719–4725.
- (64) Lim, B. K. H.; Thian, E. S. Biodegradation of Polymers in Managing Plastic Waste — A Review. *Sci. Total Environ.* **2022**, 813, 151880.
- (65) Geyer, R.; Jambeck, J. R.; Law, K. L. Production, Use, and Fate of All Plastics Ever Made. *Sci. Adv.* **2017**, 3 (7).
- (66) Werpy, T.; Petersen, G. Top Value Added Chemicals from Biomass: Volume I -- Results of Screening for Potential Candidates from Sugars and Synthesis Gas. *Us Nrel* **2004**, Medium: ED; Size: 76 pp. pages.
- (67) Steiger, M. G.; Blumhoff, M. L.; Mattanovich, D.; Sauer, M.; Mira, N. P.; Superior, I.; Jarboe, L. R. Biochemistry of Microbial Itaconic Acid Production. **2013**.
- (68) Bednarz, S.; Wesołowska-Piętak, A.; Konefał, R.; Świergosz, T. Persulfate Initiated Free-Radical Polymerization of Itaconic Acid: Kinetics, End-Groups and Side Products. *Eur. Polym. J.* **2018**, 106, 63–71.
- (69) Marvel, C. S.; Shepherd, T. H. Polymerization Reactions of Itaconic Acid and Some of Its Derivatives. *J. Org. Chem.* **1959**, 24 (5), 599–605.
- (70) Barson, C. A. Chain Transfer. In *Comprehensive Polymer Science and Supplements*; Elsevier, 1989; pp 171–183.
- (71) Stawski, D.; Połowiński, S. Polymerization of Itaconic Acid. *Polimery* **2005**, 50 (2), 118–122.
- (72) Sollka, L.; Lienkamp, K.; Sollka, L.; Lienkamp, K. Progress in the Free and Controlled Radical Homo- and Co-Polymerization of Itaconic Acid Derivatives: Toward Functional Polymers with Controlled Molar Mass Distribution and Architecture. *Macromol. Rapid Commun.* **2021**, 42 (4), 2000546.
- (73) Hatton, F. L. Recent Advances in RAFT Polymerization of Monomers Derived from Renewable Resources. *Polym. Chem.* **2020**, 11 (2), 220–229.
- (74) Sollka, L.; Lienkamp, K. Progress in the Free and Controlled Radical Homo- and Co-Polymerization of Itaconic Acid Derivatives: Toward Functional Polymers with Controlled Molar Mass Distribution and Architecture. *Macromol. Rapid Commun.* **2021**, 42 (4), 2000546.
- (75) Cottet, C.; Salvay, A. G.; Peltzer, M. A.; Fernández-García, M. Incorporation of Poly(Itaconic Acid) with Quaternized Thiazole Groups on Gelatin-Based Films for Antimicrobial-Active Food Packaging. *Polymers* **2021**, 13 (2), 1–21.
- (76) Prof Rolf Huisgen, B. D. 1,3-Dipolar Cycloadditions. Past and Future. *Angew. Chemie Int. Ed. English* **1963**, 2 (10), 565–598.
- (77) Kolb, H. C.; Finn, M. G.; Sharpless, K. B. Click Chemistry: Diverse Chemical Function from a Few Good Reactions. *Angew. Chemie Int. Ed.* **2001**, 40 (11), 2004–2021.
- (78) Rostovtsev, V. V.; Green, L. G.; Fokin, V. V.; Sharpless, K. B. A Stepwise Huisgen Cycloaddition Process: Copper(I)-Catalyzed Regioselective “Ligation” of Azides and Terminal Alkynes. *Angew. Chemie Int. Ed.* **2002**, 41 (14), 2596–2599.
- (79) Tornøe, C. W.; Christensen, C.; Meldal, M. Peptidotriazoles on Solid Phase: [1,2,3]-Triazoles by Regiospecific Copper(I)-Catalyzed 1,3-Dipolar Cycloadditions of Terminal Alkynes to Azides. *J. Org. Chem.* **2002**, 67 (9), 3057–3064.
- (80) Agard, N. J.; Prescher, J. A.; Bertozzi, C. R. A Strain-Promoted [3 + 2] Azide-Alkyne Cycloaddition for Covalent Modification of Biomolecules in Living Systems. *J. Am. Chem. Soc.* **2004**, 126 (46), 15046–15047.
- (81) Agard, N. J.; Baskin, J. M.; Prescher, J. A.; Lo, A.; Bertozzi, C. R. A Comparative Study of Bioorthogonal Reactions with Azides. *ACS Chem. Biol.* **2006**, 1 (10), 644–648.
- (82) *The Nobel Prize in Chemistry 2022 - NobelPrize.org.* <https://www.nobelprize.org/prizes/chemistry/2022/summary/> (accessed 2023-01-18).
- (83) Özklıllç, Y.; Tüzün, N. S. A DFT Study on the Binuclear CuAAC Reaction: Mechanism in Light of New Experiments. *Organometallics* **2016**, 35 (16), 2589–2599.
- (84) Li, L.; Zhang, Z. Development and Applications of the Copper-Catalyzed Azide-Alkyne Cycloaddition (CuAAC) as a Bioorthogonal Reaction. *Mol. 2016, Vol. 21, Page 1393* **2016**, 21 (10), 1393.

- (85) Kaur, J.; Saxena, M.; Rishi, N. An Overview of Recent Advances in Biomedical Applications of Click Chemistry. *Bioconjug. Chem.* **2021**, 32 (8), 1455–1471.
- (86) Gori, A.; Sola, L.; Gagni, P.; Bruni, G.; Liprino, M.; Peri, C.; Colombo, G.; Cretich, M.; Chiari, M. Screening Complex Biological Samples with Peptide Microarrays: The Favorable Impact of Probe Orientation via Chemoselective Immobilization Strategies on Clickable Polymeric Coatings. *Bioconjug. Chem.* **2016**, 27 (11), 2669–2677.
- (87) Singh, S.; Dubinsky-Davidchik, I. S.; Kluger, R. Strain-Promoted Azide–Alkyne Cycloaddition for Protein–Protein Coupling in the Formation of a Bis-Hemoglobin as a Copper-Free Oxygen Carrier. *Org. Biomol. Chem.* **2016**, 14 (42), 10011–10017.
- (88) Hänni, K. D.; Leigh, D. A. The Application of CuAAC ‘Click’ Chemistry to Catenane and Rotaxane Synthesis. *Chem. Soc. Rev.* **2010**, 39 (4), 1240–1251.
- (89) Mandalapu, D.; Saini, K. S.; Gupta, S.; Sharma, V.; Yaseen Malik, M.; Chaturvedi, S.; Bala, V.; Hamidullah; Thakur, S.; Maikhuri, J. P.; et al. Synthesis and Biological Evaluation of Some Novel Triazole Hybrids of Curcumin Mimics and Their Selective Anticancer Activity against Breast and Prostate Cancer Cell Lines. *Bioorg. Med. Chem. Lett.* **2016**, 26 (17), 4223–4232.
- (90) Suzuki, T.; Kasuya, Y.; Itoh, Y.; Ota, Y.; Zhan, P.; Asamitsu, K.; Nakagawa, H.; Okamoto, T.; Miyata, N. Identification of Highly Selective and Potent Histone Deacetylase 3 Inhibitors Using Click Chemistry-Based Combinatorial Fragment Assembly. *PLoS One* **2013**, 8 (7), e68669.
- (91) Hao, S. Y.; Feng, S. L.; Wang, X. R.; Wang, Z.; Chen, S. W.; Hui, L. Novel Conjugates of Podophyllotoxin and Coumarin: Synthesis, Cytotoxicities, Cell Cycle Arrest, Binding CT DNA and Inhibition of Topo II β . *Bioorg. Med. Chem. Lett.* **2019**, 29 (16), 2129–2135.
- (92) Rayam, P.; Polkam, N.; Kuntala, N.; Banothu, V.; Anantara, H. S.; Perumal, Y.; Balasubramanian, S.; Anireddy, J. S. Design and Synthesis of Oxaprozin-1,3,4-Oxadiazole Hybrids as Potential Anticancer and Antibacterial Agents. *J. Heterocycl. Chem.* **2020**, 57 (3), 1071–1082.
- (93) Kant, R.; Kumar, D.; Agarwal, D.; Gupta, R. D.; Tilak, R.; Awasthi, S. K.; Agarwal, A. Synthesis of Newer 1,2,3-Triazole Linked Chalcone and Flavone Hybrid Compounds and Evaluation of Their Antimicrobial and Cytotoxic Activities. *Eur. J. Med. Chem.* **2016**, 113, 34–49.
- (94) Savanur, H. M.; Naik, K. N.; Ganapathi, S. M.; Kim, K. M.; Kalkhambkar, R. G. Click Chemistry Inspired Design, Synthesis and Molecular Docking Studies of Coumarin, Quinolinone Linked 1,2,3-Triazoles as Promising Anti-Microbial Agents. *ChemistrySelect* **2018**, 3 (19), 5296–5303.
- (95) Çapçı, A.; Lorion, M. M.; Mai, C.; Hahn, F.; Hodek, J.; Wangen, C.; Weber, J.; Marschall, M.; Ackermann, L.; Tsogoeva, S. B. (Iso)Quinoline–Artemisinin Hybrids Prepared through Click Chemistry: Highly Potent Agents against Viruses. *Chem. – A Eur. J.* **2020**, 26 (52), 12019–12026.
- (96) Qin, A.; Lam, J. W. Y.; Tang, B. Z. Click Polymerization. *Chem. Soc. Rev.* **2010**, 39 (7), 2522–2544.
- (97) Huang, D.; Qin, A.; Tang, B. Z. CHAPTER 2. Transition Metal-Catalyzed Click Polymerization; 2018; pp 36–85.
- (98) Dai, J.; Ma, S.; Wu, Y.; Han, L.; Zhang, L.; Zhu, J.; Liu, X. Polyesters Derived from Itaconic Acid for the Properties and Bio-Based Content Enhancement of Soybean Oil-Based Thermosets. *Green Chem.* **2015**, 17 (4), 2383–2392.
- (99) Schoon, I.; Kluge, M.; Eschig, S.; Robert, T. Catalyst Influence on Undesired Side Reactions in the Polycondensation of Fully Bio-Based Polyester Itaconates. *Polym. 2017, Vol. 9, Page 693* **2017**, 9 (12), 693.
- (100) Hevilla, V.; Sonseca, A.; Echeverría, C.; Muñoz-Bonilla, A.; Fernández-García, M. Enzymatic Synthesis of Polyesters and Their Bioapplications: Recent Advances and Perspectives. *Macromol. Biosci.* **2021**, 21 (10), 2100156.
- (101) Barrett, D. G.; Merkel, T. J.; Luft, J. C.; Yousaf, M. N. One-Step Syntheses of Photocurable Polyesters Based on a Renewable Resource. *Macromolecules* **2010**, 43 (23), 9660–9667.
- (102) Zhao, W.; Li, A.; Zhang, A.; Zheng, Y.; Liu, J. Recent Advances in Functional-Polymer-Decorated Transition-Metal Nanomaterials for Bioimaging and Cancer Therapy. *ChemMedChem* **2018**, 13 (20), 2134–2149.
- (103) Sakthivel, M.; Franklin, D. S.; Sudarsan, S.; Chitra, G.; Sridharan, T. B.; Guhanathan, S. Investigation on PH/Salt-Responsive Multifunctional Itaconic Acid Based Polymeric Biocompatible,

- Antimicrobial and Biodegradable Hydrogels. *React. Funct. Polym.* **2018**, *122*, 9–21.
- (104) Devi, N.; Singh, S.; Manickam, S.; Cruz-Martins, N.; Kumar, V.; Verma, R.; Kumar, D. Itaconic Acid and Its Applications for Textile, Pharma and Agro-Industrial Purposes. *Sustain.* **2022**, Vol. 14, Page 13777 **2022**, *14* (21), 13777.
- (105) Teleky, B. E.; Vodnar, D. C. Recent Advances in Biotechnological Itaconic Acid Production, and Application for a Sustainable Approach. *Polym.* **2021**, Vol. 13, Page 3574 **2021**, *13* (20), 3574.
- (106) Yang, C. Q.; Hu, C.; Lickfield, G. C. Crosslinking Cotton with Poly(Itaconic Acid) and in Situ Polymerization of Itaconic Acid: Fabric Mechanical Strength Retention. *J. Appl. Polym. Sci.* **2003**, *87* (12), 2023–2030.
- (107) Hyvärinen, M.; Jabeen, R.; Kärki, T. The Modelling of Extrusion Processes for Polymers—A Review. *Polym.* **2020**, Vol. 12, Page 1306 **2020**, *12* (6), 1306.
- (108) Ren, Y.; Mei, L.; Zhou, L.; Guo, G. Recent Perspectives in Hot Melt Extrusion-Based Polymeric Formulations for Drug Delivery: Applications and Innovations. *AAPS PharmSciTech* **2019**, *20* (3), 1–12.
- (109) Taylor, G. Disintegration of Water Drops in an Electric Field. *Proc. R. Soc. London. Ser. A. Math. Phys. Sci.* **1964**, *280* (1382), 383–397.
- (110) Sun, Y.; Li, Y.; Nan, S.; Zhang, L.; Huang, H.; Wang, J. Synthesis and Characterization of PH-Sensitive Poly(Itaconic Acid)–Poly(Ethylene Glycol)–Folate–Poly(l-Histidine) Micelles for Enhancing Tumor Therapy and Tunable Drug Release. *J. Colloid Interface Sci.* **2015**, *458*, 119–129.
- (111) Haider, A.; Haider, S.; Kang, I. K. A Comprehensive Review Summarizing the Effect of Electrospinning Parameters and Potential Applications of Nanofibers in Biomedical and Biotechnology. *Arab. J. Chem.* **2018**, *11* (8), 1165–1188.
- (112) Xue, J.; Wu, T.; Dai, Y.; Xia, Y. Electrospinning and Electrospun Nanofibers: Methods, Materials, and Applications. *Chem. Rev.* **2019**, *119* (8), 5298–5415.
- (113) Xu, H.; Li, H.; Ke, Q.; Chang, J. An Anisotropically and Heterogeneously Aligned Patterned Electrospun Scaffold with Tailored Mechanical Property and Improved Bioactivity for Vascular Tissue Engineering. *ACS Appl. Mater. Interfaces* **2015**, *7* (16), 8706–8718.
- (114) Dias, J. R.; Granja, P. L.; Bártolo, P. J. Advances in Electrospun Skin Substitutes. *Prog. Mater. Sci.* **2016**, *84*, 314–334.
- (115) Muñoz-Bonilla, A.; Fernández-García, M. The Roadmap of Antimicrobial Polymeric Materials in Macromolecular Nanotechnology. *Eur. Polym. J.* **2015**, *65*, 46–62.
- (116) Muñoz-Bonilla, A.; Fernández-García, M. Polymeric Materials with Antimicrobial Activity. *Prog. Polym. Sci.* **2012**, *37* (2), 281–339.
- (117) Álvarez-Paino, M.; Muñoz-Bonilla, A.; Fernández-García, M. Antimicrobial Polymers in the Nano-World. *Nanomater.* **2017**, Vol. 7, Page 48 **2017**, *7* (2), 48.
- (118) Muñoz-Bonilla, A.; Fernández-García, M. Poly(Ionic Liquid)s as Antimicrobial Materials. *Eur. Polym. J.* **2018**, *105*, 135–149.
- (119) Muñoz-Bonilla, A.; Echeverría, C.; Sonseca, Á.; Arrieta, M. P.; Fernández-García, M. Bio-Based Polymers with Antimicrobial Properties towards Sustainable Development. *Materials* **2019**, *12* (4), 641.
- (120) Yañez-Macías, R.; Muñoz-Bonilla, A.; De Jesús-Tellez, M. A.; Maldonado-Textile, H.; Guerrero-Sánchez, C.; Schubert, U. S.; Guerrero-Santos, R. Combinations of Antimicrobial Polymers with Nanomaterials and Bioactives to Improve Biocidal Therapies. *Polym.* **2019**, Vol. 11, Page 1789 **2019**, *11* (11), 1789.
- (121) Echeverría, C.; Torres, M. D. T.; Fernández-García, M.; de la Fuente-Núñez, C.; Muñoz-Bonilla, A. Physical Methods for Controlling Bacterial Colonization on Polymer Surfaces. *Biotechnol. Adv.* **2020**, *43*, 107586.
- (122) Kubacka, A.; Serrano, C.; Ferrer, M.; Lunsdorf, H.; Bielecki, P.; Cerrada, M. L.; Fernández-García, M.; Fernández-García, M. High-Performance Dual-Action Polymer-TiO₂ Nanocomposite Films via Melting Processing. *Nano Lett.* **2007**, *7* (8), 2529–2534.
- (123) Cerrada, M. L.; Serrano, C.; Sánchez-Chaves, M.; Fernández-Garcí, M.; Fernández-Martín, F.; De

- Andrés, A.; Riobóo, R. J. J.; Kubacka, A.; Ferrer, M.; Fernández-García, M. Self-Sterilized EVOH-TiO₂ Nanocomposites: Interface Effects on Biocidal Properties. *Adv. Funct. Mater.* **2008**, *18* (13), 1949–1960.
- (124) Serrano, C.; Cerrada, M. L.; Fernández-García, M.; Ressia, J.; Vallés, E. M. Rheological and Structural Details of Biocidal IPP-TiO₂ Nanocomposites. *Eur. Polym. J.* **2012**, *48* (3), 586–596.
- (125) Serrano, C.; Ressia, J. A.; Vallés, E. M.; Fernández-García, M.; Cerrada, M. L. Interfacial Agent Effect on Rheological Response and Crystallite Characteristics in Germicidal Polypropylene/Titanium Dioxide Nanocomposites. *Polym. Int.* **2012**, *61* (11), 1655–1665.
- (126) Christoforidis, K. C.; Kubacka, A.; Ferrer, M.; Cerrada, M. L.; Fernández-García, M.; Fernández-García, M. Role of TiO₂ Morphological Characteristics in EVOH–TiO₂ Nanocomposite Films: Self-Degradation and Self-Cleaning Properties. *RSC Adv.* **2013**, *3* (22), 8541–8550.
- (127) Muñoz-Bonilla, A.; Cerrada, M. L.; Fernández-García, M.; Kubacka, A.; Ferrer, M.; Fernández-García, M. Biodegradable Polycaprolactone-Titania Nanocomposites: Preparation, Characterization and Antimicrobial Properties. *Int. J. Mol. Sci.* **2013**, Vol. *14*, Pages 9249–9266 **2013**, *14* (5), 9249–9266.
- (128) Muñoz-Bonilla, A.; Kubacka, A.; Fernández-García, M.; Ferrer, M.; Fernández-García, M.; Cerrada, M. L. Visible and Ultraviolet Antibacterial Behavior in PVDF–TiO₂ Nanocomposite Films. *Eur. Polym. J.* **2015**, *71*, 412–422.
- (129) Muñoz-Bonilla, A.; Van Herk, A. M.; Heuts, J. P. A. Preparation of Hairy Particles and Antifouling Films Using Brush-Type Amphiphilic Block Copolymer Surfactants in Emulsion Polymerization. *Macromolecules* **2010**, *43* (6), 2721–2731.
- (130) Muñoz-Bonilla, A.; Van Herk, A. M.; Heuts, J. P. A. Adding Stimuli-Responsive Extensions to Antifouling Hairy Particles. *Polym. Chem.* **2010**, *1* (5), 624–627.
- (131) Muñoz-Bonilla, A.; Ali, S. I.; Del Campo, A.; Fernández-García, M.; Van Herk, A. M.; Heuts, J. P. A. Block Copolymer Surfactants in Emulsion Polymerization: Influence of the Miscibility of the Hydrophobic Block on Kinetics, Particle Morphology, and Film Formation. *Macromolecules* **2011**, *44* (11), 4282–4290.
- (132) De León, A. S.; Del Campo, A.; Fernández-García, M.; Rodríguez-Hernández, J.; Muñoz-Bonilla, A. Hierarchically Structured Multifunctional Porous Interfaces through Water Templatated Self-Assembly of Ternary Systems. *Langmuir* **2012**, *28* (25), 9778–9787.
- (133) De León, A. S.; Del Campo, A.; Cortajarena, A. L.; Fernández-García, M.; Muñoz-Bonilla, A.; Rodríguez-Hernández, J. Formation of Multigradient Porous Surfaces for Selective Bacterial Entrapment. *Biomacromolecules* **2014**, *15* (9), 3338–3348.
- (134) Álvarez-Paino, M.; Muñoz-Bonilla, A.; López-Fabal, F.; Gómez-Garcés, J. L.; Heuts, J. P.; Fernández-García, M. Effect of Glycounits on the Antimicrobial Properties and Toxicity Behavior of Polymers Based on Quaternized DMAEMA. *Biomacromolecules* **2015**, *16* (1), 295–303.
- (135) Álvarez-Paino, M.; Muñoz-Bonilla, A.; López-Fabal, F.; Gómez-Garcés, J. L.; Heuts, J. P. A.; Fernández-García, M. Functional Surfaces Obtained from Emulsion Polymerization Using Antimicrobial Glycosylated Block Copolymers as Surfactants. *Polym. Chem.* **2015**, *6* (34), 6171–6181.
- (136) Tejero, R.; López, D.; López-Fabal, F.; Gómez-Garcés, J. L.; Fernández-García, M. High Efficiency Antimicrobial Thiazolium and Triazolium Side-Chain Polymethacrylates Obtained by Controlled Alkylation of the Corresponding Azole Derivatives. *Biomacromolecules* **2015**, *16* (6), 1844–1854.
- (137) Tejero, R.; Gutiérrez, B.; López, D.; López-Fabal, F.; Gómez-Garcés, J. L.; Fernández-García, M. Copolymers of Acrylonitrile with Quaternizable Thiazole and Triazole Side-Chain Methacrylates as Potent Antimicrobial and Hemocompatible Systems. *Acta Biomater.* **2015**, *25*, 86–96.
- (138) Tejero, R.; López, D.; Fernández-García, M. Influence of Spacer Group on the Structure and Thermal Properties of Copolymers Based on Acrylonitrile and Methacrylic 1,3-Thiazole and 1,2,3-Triazole Derivatives. *Eur. Polym. J.* **2015**, *71*, 401–411.
- (139) Muñoz-Bonilla, A.; López, D.; Fernández-García, M. Providing Antibacterial Activity to Poly(2-Hydroxy Ethyl Methacrylate) by Copolymerization with a Methacrylic Thiazolium Derivative. *Int. J. Mol. Sci.* **2018**, Vol. *19*, Page 4120 **2018**, *19* (12), 4120.
- (140) Chiloeches, A.; Echeverría, C.; Cuervo-Rodríguez, R.; Plachà, D.; López-Fabal, F.; Fernández-

- García, M.; Muñoz-Bonilla, A. Adhesive Antibacterial Coatings Based on Copolymers Bearing Thiazolium Cationic Groups and Catechol Moieties as Robust Anchors. *Prog. Org. Coatings* **2019**, *136*, 105272.
- (141) Cuervo-Rodríguez, R.; Muñoz-Bonilla, A.; López-Fabal, F.; Fernández-García, M. Hemolytic and Antimicrobial Activities of a Series of Cationic Amphiphilic Copolymers Comprised of Same Centered Comonomers with Thiazole Moieties and Polyethylene Glycol Derivatives. *Polymers* **2020**, *12* (4), 972.
- (142) Plachá, D.; Muñoz-Bonilla, A.; Škrlová, K.; Echeverría, C.; Chiloeches, A.; Petr, M.; Lafdi, K.; Fernández-García, M. Antibacterial Character of Cationic Polymers Attached to Carbon-Based Nanomaterials. *Nanomaterials* **2020**, *10* (6), 1–14.
- (143) Cuervo-Rodríguez, R.; López-Fabal, F.; Muñoz-Bonilla, A.; Fernández-García, M. Antibacterial Polymers Based on Poly(2-Hydroxyethyl Methacrylate) and Thiazolium Groups with Hydrolytically Labile Linkages Leading to Inactive and Low Cytotoxic Compounds. *Mater. 2021, Vol. 14, Page 7477* **2021**, *14* (23), 7477.
- (144) Alvarez-Paino, M.; Juan-Rodríguez, R.; Cuervo-Rodríguez, R.; Tejero, R.; López, D.; López-Fabal, F.; Gómez-Garcés, J. L.; Muñoz-Bonilla, A.; Fernández-García, M. Antimicrobial Films Obtained from Latex Particles Functionalized with Quaternized Block Copolymers. *Colloids Surfaces B Biointerfaces* **2016**, *140*, 94–103.
- (145) Alvarez-Paino, M.; Bonilla, P.; Cuervo-Rodríguez, R.; López-Fabal, F.; Gómez-Garcés, J. L.; Muñoz-Bonilla, A.; Fernández-García, M. Antimicrobial Surfaces Obtained from Blends of Block Copolymers Synthesized by Simultaneous ATRP and Click Chemistry Reactions. *Eur. Polym. J.* **2017**, *93*, 53–62.
- (146) Cuervo-Rodríguez, R.; López-Fabal, F.; Gómez-Garcés, J. L.; Muñoz-Bonilla, A.; Fernández-García, M.; Cuervo-Rodríguez, R.; López-Fabal, F.; Gómez-Garcés, J. L.; Muñoz-Bonilla, A.; Fernández-García, M. Contact Active Antimicrobial Coatings Prepared by Polymer Blending. *Macromol. Biosci.* **2017**, *17* (11), 1700258.
- (147) Tejero, R.; Gutiérrez, B.; López, D.; López-Fabal, F.; Gómez-Garcés, J. L.; Muñoz-Bonilla, A.; Fernández-García, M. Tailoring Macromolecular Structure of Cationic Polymers towards Efficient Contact Active Antimicrobial Surfaces. *Polym. 2018, Vol. 10, Page 241* **2018**, *10* (3), 241.
- (148) Muñoz-Bonilla, A.; Cuervo-Rodríguez, R.; López-Fabal, F.; Gómez-Garcés, J. L.; Fernández-García, M. Antimicrobial Porous Surfaces Prepared by Breath Figures Approach. *Mater. (Basel, Switzerland)* **2018**, *11* (8).
- (149) del Campo, A.; Echeverría, C.; San Martín, M.; Cuervo-Rodríguez, R.; Fernández-García, M.; Muñoz-Bonilla, A.; Echeverría, C.; San Martin, M.; Fernández-García, M.; Muñoz-Bonilla, A.; et al. Porous Microstructured Surfaces with PH-Triggered Antibacterial Properties. *Macromol. Biosci.* **2019**, *19* (8), 1900127.
- (150) Muñoz-Bonilla, A.; Zagora, J.; Plachá, D.; Echeverría, C.; Chiloeches, A.; Fernández-García, M. Chemical Hydrogels Bearing Thiazolium Groups with a Broad Spectrum of Antimicrobial Behavior. *Polym. 2020, Vol. 12, Page 2853* **2020**, *12* (12), 2853.

1.2 Objetivos

Actualmente la investigación en compuestos de origen biológico está en pleno auge para el desarrollo de nuevos compuestos y polímeros, así como para poder sustituir los compuestos derivados del petróleo por otros más amigables con el medioambiente. El ácido itacónico es un candidato idóneo para este cometido.

Sin embargo, a pesar de las potenciales propiedades del ácido itacónico como precursor de polímeros biobasados, es necesario la continua investigación y desarrollo de nuevos sistemas basados en el ácido itacónico con el objetivo de consolidar y ampliar su potencial.

Esta tesis tiene como objetivo la creación de nuevos polímeros biodegradables con actividad antimicrobiana derivados del ácido itacónico para su uso como material biomédico, como por ejemplo en ingeniería tisular como componente de apósitos para la curación de heridas, así como en otras aplicaciones como el envasado de alimentos.

El trabajo se ha recogido en 5 artículos publicados en revistas científicas, los cuales se han desarrollado en 4 capítulos para una presentación clara de los resultados, incluyendo el capítulo 1 de introducción y el capítulo 4 de conclusiones. Los capítulos 2 y 3 se centran en los distintos sistemas poliméricos creados a partir del ácido itacónico:

En el **Capítulo 2** titulado “Polímeros biobasados derivados del ácido itacónico” se incluyen dos artículos:

- Biobased polymers derived from itaconic acid bearing clickable groups with potent antibacterial activity and negligible hemolytic activity, *Polymer Chemistry* 12(21), 3190-3200, 2021.
- Antibacterial and compostable polymers derived from biobased itaconic acid as environmentally friendly additives for biopolymers, *Polymer Testing* 109,107541, 2022.

Este capítulo tiene como objetivo el desarrollo de los polímeros y copolímeros derivados del ácido itacónico modificados con grupos propargilo que pueden modificarse posteriormente por química click para la incorporación de un grupo antimicrobiano. Se ha realizado la copolimerización con el monómero hidrófobo itaconato de dimetilo, para evaluar el carácter hidrófilo/hidrófobo de los polímeros, mientras que el grupo antimicrobiano introducido ha sido el grupo tiazolio. Además, otro de los objetivos de este capítulo es el estudio de sus propiedades térmicas, así como de su actividad

antimicrobiana y su biodegradación en condiciones de compostaje, para evaluar su potencial en las aplicaciones propuestas.

El **Capítulo 3** titulado “Fibras electrohiladas de PLA y PBAT con polímeros biobasados antimicrobianos” agrupa 3 publicaciones:

- Electrospun Polylactic Acid-Based Fibers Loaded with Multifunctional Antibacterial Biobased Polymers, ACS Applied Polymer Materials 4(9), 6543-6552, 2022.
- PLA and PBAT-Based Electrospun Fibers Functionalized with Antibacterial Bio-Based Polymers, Macromolecular Bioscience 23(1), 2200401, 2023
- Synergistic combination of antimicrobial peptides and cationic polyitaconates in multifunctional PLA fibers, ACS Applied Bio Materials, 2023, aceptado.

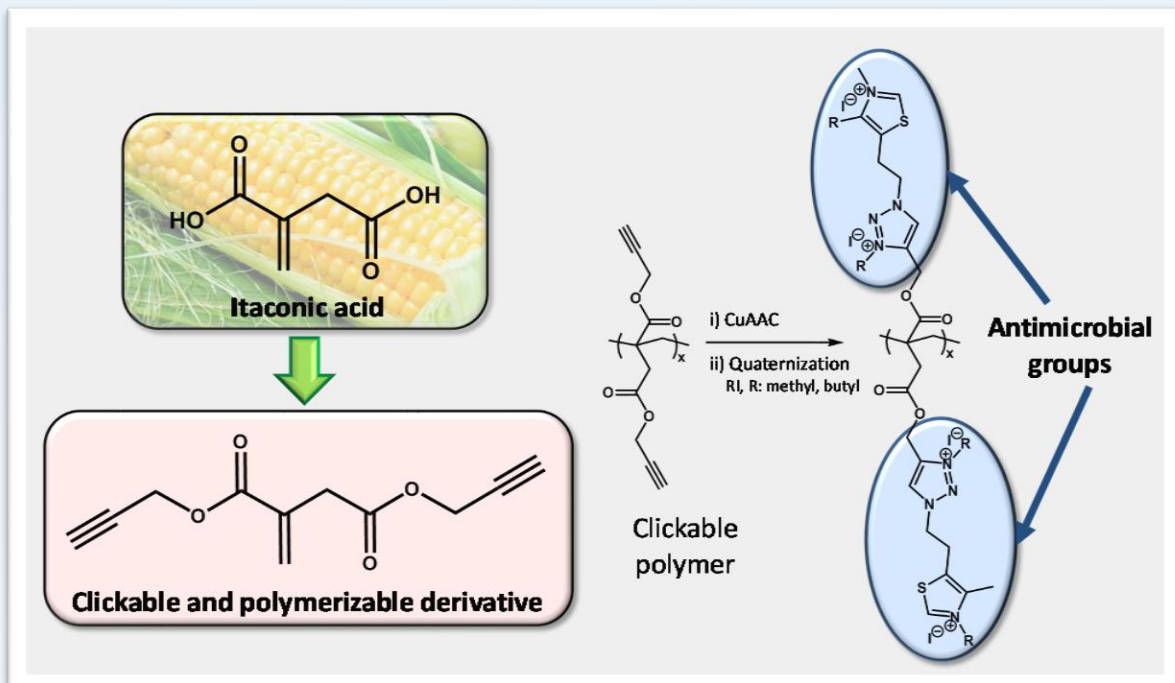
El objetivo principal de este capítulo es el uso de los polímeros biobasados con actividad antimicrobiana que presentaban mejores propiedades en el Capítulo 3, como componentes en tejidos no tejidos obtenidos mediante electrohilado. Igualmente, se desarrollan otros polímeros derivados del poli(itaconato) con grupos propargilo, combinando los grupos tiazolio/triazolio con grupos halamina y con péptidos antimicrobianos, con el objetivo de mejorar la actividad antimicrobiana de los polímeros y buscar posibles efectos sinérgicos. Todos los polímeros antimicrobianos desarrollados se incorporan a tejidos de fibras de PLA y PBAT, para dotar a estos tejidos de propiedades antimicrobianas manteniendo su biodegradabilidad. Uno de los objetivos buscados es la optimización del proceso de electrohilado para obtener fibras homogéneas y funcionalizadas con los polímeros antimicrobianos. Igualmente, este capítulo tiene como objetivo evaluar sus propiedades morfológicas, térmicas y antimicrobianas, así como su biodegradación y su biocompatibilidad mediante ensayos de viabilidad celular frente a fibroblastos humanos.

Capítulo 2

Polímeros biobasados derivados del ácido itacónico

2.1 Biobased polymers derived from itaconic acid bearing clickable groups with potent antibacterial activity and negligible hemolytic activity

2.2 Antibacterial and compostable polymers derived from biobased itaconic acid as environmentally friendly additives for biopolymers



2.1 Biobased polymers derived from itaconic acid bearing clickable groups with potent antibacterial activity and negligible hemolytic activity

Polymer Chemistry 2021, 12 (21), 3190–3200

Polymer Chemistry

PAPER

 Check for updates

Cite this: *Polym. Chem.*, 2021, **12**, 3190

Received 23rd January 2021,
Accepted 30th April 2021
DOI: 10.1039/d1py00098e
rsc.li/polymers



ROYAL SOCIETY
OF CHEMISTRY

[View Article Online](#)
[View Journal](#) | [View Issue](#)

Biobased polymers derived from itaconic acid bearing clickable groups with potent antibacterial activity and negligible hemolytic activity†

A. Chiloeches,^{a,b} A. Funes,^c R. Cuervo-Rodríguez,^c F. López-Fabal,^{d,e} M. Fernández-García,^{a,f} C. Echeverría  *^{a,f} and A. Muñoz-Bonilla  *^{a,f}

Herein, we report, for the first time, the synthesis of clickable polymers derived from biobased itaconic acid, which was then used for the preparation of novel cationic polymers with antibacterial properties and low hemotoxicity via click chemistry. Itaconic acid (IA) was subjected to chemical modification by incorporating clickable alkyne groups on the carboxylic acids. The resulting monomer with pendant alkyne groups was easily polymerized and copolymerized with dimethyl itaconate (DMI) by radical polymerization. The feed molar ratio of comonomers was varied to precisely tune the content of alkyne groups in the copolymers and the amphiphilic balance. Subsequently, an azide with a thiazole group, which is a component of the vitamin thiamine (B1), was attached onto the polymers by copper-catalyzed azide-alkyne cycloaddition (CuAAC) click chemistry leading to triazole linkages. *N*-Alkylation reactions of the thiazole and triazole groups with methyl and butyl iodides provide the corresponding itaconate derivatives with pendant azonium groups. The copolymers with variable cationic charge densities and hydrophobic/hydrophilic balances, depending on the comonomer feed ratio, display potent antibacterial activity against Gram-positive bacteria, whereas the activity was almost null against Gram-negative bacteria. Hemotoxicity assays demonstrated that the copolymers exhibited negligible hemolysis and excellent selectivity, more than 1000-fold, for Gram-positive bacteria over human red blood cells.

Introduction

In the last few years, antimicrobial peptides (AMPs) have inspired the synthesis of novel antimicrobial polymers with potent efficiency for the treatment of microbial infections also caused by antibiotic-resistant bacteria.^{1–3} These polymers are typically amphiphilic structures able to attach to negatively charged bacterial membranes with cationic hydrophilic segments, and, then, insert into them through the hydrophobic

parts disrupting the cytoplasmic membrane.^{3,4} This action is rapid and makes it relatively difficult for the bacteria to develop resistance. As an additional advantage, in the majority of the reported synthetic polymers, the problems associated with AMPs such as high cost and poor pharmacokinetic properties have been overcome. However, most synthetic antimicrobial polymers are based on non-degradable backbones,^{5–8} which limit their application in clinical uses as they can be accumulated in the body and exert long term toxicity. Biodegradability is also an important and desired property for many biomedical applications including bioresorbable stents and prostheses, food packaging and agricultural uses, which also contributes to sustainability by reducing the waste impact of fossil-based polymers. Although little research has been performed until now on the synthesis of biobased/biodegradable antimicrobial polymers,⁹ recently, a few examples have been reported that include functionalized polycarbonates^{10,11} polycaprolactone¹² and polyactides.¹³ Biobased polymers such as polyactides also possess properties such as biocompatibility, environmental safety and sustainability, which could be essential in biomedical devices, wound dressing, food packaging, textiles and cosmetic applications. Therefore, research on sustainable antimicrobial materials is

^a*Instituto de Ciencia y Tecnología de Polímeros (ICTP-CSIC), C/Juan de la Cierva 3, 28006 Madrid, Spain. E-mail: sbonilla@ictp.csic.es; cecheverria@ictp.csic.es*

^b*Universidad Nacional de Educación a Distancia (UNED), C/Bravo Murillo, 38, 28015 Madrid, Spain*

^c*Facultad de Ciencias Químicas, Universidad Complutense de Madrid, Avenida Complutense s/n, Ciudad Universitaria, 28040 Madrid, Spain*

^d*Hospital Universitario de Móstoles C/Dr. Luis Montes, s/n, 28935 Móstoles, Madrid, Spain*

^e*Facultad de Ciencias Experimentales, Universidad Francisco de Vitoria, Carretera Pozuelo a Majadahonda, Km 1.800, 28223 Madrid, Spain*

^f*Interdisciplinary Platform for Sustainable Plastics towards a Circular Economy-Spanish National Research Council (SusPlast-CSIC), Madrid, Spain*

† Electronic supplementary information (ESI) available. See DOI: 10.1039/d1py00098e

3190 | *Polym. Chem.*, 2021, **12**, 3190–3200

This journal is © The Royal Society of Chemistry 2021

2.1.1 Abstract

Herein, we report, for the first time, the synthesis of clickable polymers derived from biobased itaconic acid, which was then used for the preparation of novel cationic polymers with antibacterial properties and low hemotoxicity via *click chemistry*. Itaconic acid (IA) was subjected to chemical modification by incorporating clickable alkyne groups on the carboxylic acids. The resulting monomer with pendant alkyne groups was easily polymerized and copolymerized with dimethyl itaconate (DMI) by radical polymerization. The feed molar ratio of comonomers was varied to precisely tune the content of alkyne groups in the copolymers and the amphiphilic balance. Subsequently, an azide with a thiazole group, which is a component of the vitamin thiamine (B1), was attached onto the polymers by copper-catalyzed azide-alkyne cycloaddition (CuAAC) click chemistry leading to triazole linkages. *N*-Alkylation reactions of the thiazole and triazole groups with methyl and butyl iodides provide the corresponding itaconate derivatives with pendant azolium groups. The copolymers with variable cationic charge densities and hydrophobic/hydrophilic balances, depending on the comonomer feed ratio, display potent antibacterial activity against Gram-positive bacteria, whereas the activity was almost null against Gram-negative bacteria. Hemotoxicity assays demonstrated that the copolymers exhibited negligible hemolysis and excellent selectivity, more than 1000-fold, for Gram-positive bacteria over human red blood cells.

2.1.2 Introduction

In the last few years, antimicrobial peptides (AMPs) have inspired the synthesis of novel antimicrobial polymers with potent efficiency for the treatment of microbial infections also caused by antibiotic-resistant bacteria.¹⁻³ These polymers are typically amphiphilic structures able to attach to negatively charged bacterial membranes with cationic hydrophilic segments, and, then, insert into them through the hydrophobic parts disrupting the cytoplasmic membrane.^{3,4} This action is rapid and makes it relatively difficult for the bacteria to develop resistance. As an additional advantage, in the majority of the reported synthetic polymers, the problems associated with AMPs such as high cost and poor pharmacokinetic properties have been overcome. However, most synthetic antimicrobial polymers are based on non-degradable backbones,⁵⁻⁸ which limit their application in clinical uses as they can be accumulated in the body and exert long term toxicity. Biodegradability is also an important and desired property for many biomedical applications including bioresorbable stents and prostheses, food packaging and agricultural uses, which also contributes to sustainability by reducing the waste impact of fossil-based polymers. Although little research has been performed until now on the synthesis of biobased/biodegradable antimicrobial polymers,⁹ recently, a few examples have been reported that include functionalized polycarbonates^{10,11}, polycaprolactone¹² and polylactides.¹³ Biobased polymers such as polylactides also possess properties such as biocompatibility, environmental safety and sustainability, which could be essential in biomedical devices, wound dressing, food packaging, textiles and cosmetic applications. Therefore, research on sustainable antimicrobial materials is necessary and remains a challenge in the fields of polymer chemistry and materials science. On this basis, itaconic acid (IA) is a very promising biorenewable building block and one of the top chemicals obtained from biomass, whose annual production is estimated to be more than 80 kilotons.¹⁴ Itaconic acid is produced on a large scale by fermentation of biomass such as corn or rice, and also from lignocellulosic feedstocks.¹⁵ Due to the different functionalities of itaconic acid, polymeric derivatives can be synthesized either through radical polymerization^{16,17} of the itaconic acid via the α,β-unsaturated double bonds or through subjecting the double carboxylic groups to polycondensation.^{18,19} Thanks to these structural characteristics and its similarity to acrylic acid, IA and its derivatives such as dimethyl itaconate (DMI) have been extensively investigated as alternative monomers to prepare acrylic and methacrylic polymers. Also, the possibility of modifying the remaining functional groups via post polymerization reactions^{20,21} extends even more the potential

of developing new materials with tunable properties. Most of these modification reactions reported in the literature involve the double bond functionalities rather than the carboxylic acid groups.

Here, we proposed a new versatile method to modify the carboxylic acids of the itaconic acid monomer by incorporating pendant alkyne groups leading to clickable itaconic acid derivatives that can be polymerized via radical polymerization. This new approach can be used to further functionalize the IA-biobased polymers by copper-catalyzed azide-alkyne cycloaddition (CuAAC) click chemistry via triazole linkages. The facile and efficient reaction will allow the synthesis of new functional polymers. Specifically, we focused on incorporating antimicrobial azolium functionalities derived from vitamin thiamine (B1) to render biobased antimicrobial polymers.

2.1.3 Experimental Section

Materials

For the preparation of polymers, the following chemicals were obtained. 2-(4-Methylthiazol-5-yl)ethanol azide was synthesized as previously described.²² Itaconic acid (IA, ≥99%), propargyl alcohol (≥99%), 4-(dimethylamino)pyridine (DMAP, ≥99%), *N,N'*-dicyclohexylcarbodiimide (DCC, 99%), hydroquinone (99%), copper(I) chloride (CuCl, ≥99.995%), *N,N,N',N",N"*-pentamethyldiethylenetriamine (PMDETA, 99%), dimethyl itaconate (DMI, 99%), iodomethane (MeI, 99.5%), 1-iodobutane (BuI, 99%), neutral aluminum oxide, sodium bicarbonate (NaHCO₃, ≥99.7%), magnesium sulfate anhydrous (MgSO₄, ≥99.5%), ammonium persulfate (APS, 98%), anhydrous tetrahydrofuran (THF, 99.9%), and anhydrous *N,N*-dimethylformamide (DMF, 99.8%) were purchased from Sigma-Aldrich and used as received. The radical initiator 2,2'-azobisisobutyronitrile (AIBN, 98%) was purchased from Acros and was recrystallized twice from methanol. All the organic solvents were of AR grade, and tetrahydrofuran (THF), *N,N*-dimethylformamide (DMF), ethanol (EtOH), isopropyl alcohol (iPrOH), hexane and chloroform (CHCl₃) were obtained from Scharlau. Ethyl acetate (EtOAc) was obtained from Cor Química S.L., toluene from Merck and sulfuric acid (H₂SO₄) from Panreac. Deuterated chloroform (CDCl₃), water (D₂O) and dimethyl sulfoxide (DMSO-*d*₆) were acquired from Sigma-Aldrich. Cellulose dialysis membranes (CelluSep T1) were purchased from Membrane Filtration Products, Inc.

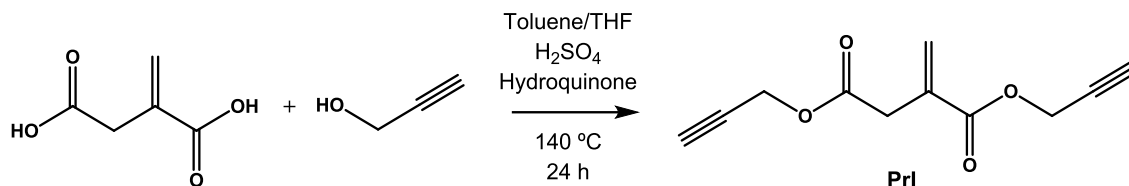
For the antibacterial assay, the following were obtained: sodium chloride solution (NaCl suitable for cell culture, BioXtra) and phosphate buffered saline powder (pH 7.4) were obtained from Sigma-Aldrich. BBL Mueller–Hinton broth used as a microbial growth medium was purchased from Becton, Dickinson and Company and 96 well microplates were purchased from BD Biosciences. Columbia agar (5% sheep blood) plates were obtained from BioMérieux. American Type Culture Collection (ATCC): *Pseudomonas aeruginosa* (*P. aeruginosa*, ATCC 27853), *Escherichia coli* (*E. coli*, ATCC 25922), *Staphylococcus epidermidis* (*S. epidermidis*, ATCC 12228) and *Staphylococcus aureus* (*S. aureus*, ATCC 29213), used as bacterial strains, were purchased from Oxoid.

Characterization

¹H and ¹³C NMR spectra were recorded on a Bruker Avance III HD-400AVIII spectrometer at room temperature using CDCl₃, DMSO-d₆ and D₂O as solvents (purchased from Sigma-Aldrich). Fourier transform infrared (FTIR) spectra were recorded on a PerkinElmer Spectrum Two instrument, equipped with an attenuated total reflection (ATR) module. Mass spectrometry (MS) analysis was performed for high resolution ESI measurements using an Agilent 6500 Series Accurate-Mass Q-TOF LC/MS System, equipped with an Agilent 1200 LC. Size exclusion chromatography (SEC) measurements were performed using a Waters Division Millipore system equipped with a Waters 2414 refractive index detector. DMF (Scharlau) stabilized with 0.1 M LiBr (Sigma Aldrich, >99.9%) was used as an eluent at a flow rate of 1 mL min⁻¹ at 50 °C. Calibration was made with poly(methyl methacrylate) standards (Polymer Laboratories LTD). Zeta potential measurements of the cationic copolymers in distilled water at 25 °C were performed with a Zetasizer Nano series ZS (Malvern Instruments Ltd) using the Smoluchowski equation.

Synthesis of di(prop-2-yn-1-yl) itaconate (Prl)

The monomer di(prop-2-yn-1-yl) itaconate bearing clickable alkyne groups was synthesized via the condensation reaction of itaconic acid with propargyl alcohol according to Scheme 1.



Scheme 1. Synthesis of di(prop-2-yn-1-yl) itaconate (Prl).

Briefly, itaconic acid (15.0 g, 115 mmol), propargyl alcohol (32.3 g, 576 mmol) and hydroquinone (1.26 g, 11.5 mmol) were placed in a three neck flask equipped with a Dean-Stark trap and the mixture was dissolved in THF (50 mL) at 60 °C. Then, toluene (250 mL) and H_2SO_4 (300 μL , 5.75 mmol) were added and the reaction mixture was heated under reflux for 24 h, during which period 4 mL of water was collected. After that, the solvents were partially removed under reduced pressure using a rotary evaporator, and the mixture was washed repeatedly with saturated NaHCO_3 aqueous solution. The organic extract was dried over anhydrous MgSO_4 and then filtered. The residual reaction mixture was finally purified by passing through a neutral alumina column using hexane : EtOAc (1 : 1) as a solvent. After solvent evaporation under reduced pressure, a yellow oil was obtained (22.998 g, 97% yield). HR-MS (ESI): m/z required for $\text{C}_{11}\text{H}_{10}\text{O}_4$, 206.05863; found, 206.05791.

$^1\text{H-NMR}$ (400MHz, CDCl_3), δ (ppm): 6.40 (d, 1H, $=\text{CH}_2$), 5.80 (d, 1H, $=\text{CH}_2$), 4.76 (d, 2H, $-\text{CH}_2\text{C}\equiv\text{CH}$), 4.70 (d, $J = 2.45$, 2H, $-\text{CH}_2\text{C}\equiv\text{CH}$), 3.40 (s, 2H, $-\text{CH}_2$), 2.48 (m, $J = 2.45$, 2H, $-\text{CH}_2\text{C}\equiv\text{CH}$).

$^{13}\text{C-NMR}$ (100MHz, CDCl_3), δ (ppm): 169.80 ($\text{C}=\text{O}$), 165.75 ($\text{C}=\text{O}$), 132.78 ($-\text{C}=\text{CH}_2$), 130.03 ($-\text{C}=\text{CH}_2$), 75.22 (2C, $-\text{CH}_2\text{C}\equiv\text{CH}$), 52.72 ($-\text{CH}_2\text{C}\equiv\text{CH}$), 52.56 ($-\text{CH}_2\text{C}\equiv\text{CH}$), 37.38 ($-\text{CH}_2$).

Synthesis of bis((1-(2-(4-methylthiazol-5-yl)ethyl)-1*H*-1,2,3-triazol-4-yl)methyl) itaconate (TTI)

The monomer TTI bearing thiazol and triazol moieties was synthesized by the alkyne-azide click cycloaddition reaction between the Prl monomer previously prepared and 2-(4-methylthiazol-5-yl)ethanol azide (see Scheme S1 in the ESI). In a typical experiment, Prl (0.612 g, 2.97 mmol), 2-(4-methylthiazol-5-yl)ethanol azide (1.025 g, 6.10 mmol), PMDETA (208 μL , 1 mmol) and CuCl (0.030 g, 0.30 mmol) were dissolved in 30 mL of CHCl_3 . The reaction mixture was stirred at room temperature for 24 h. Then, the reaction mixture was passed through a neutral alumina column to remove the copper compounds.

The monomer was purified by column chromatography using first hexane : EtOAc (from 1 : 1 to 1 : 3) as a solvent and then ethanol. Afterwards, the solvent was removed by rotary evaporation to obtain a yellow liquid (0.822 g, 51% yield).

¹H-NMR (400 MHz, CDCl₃), δ(ppm): 8.57 (s, 1H, *H*-thiazole), 8.56 (s, 1H, *H*-thiazole), 7.42 (s, 1H, *H*-triazole), 7.40 (s, 1H, *H*-triazole), 6.32 (s, 1H, =CH₂), 5.70 (s, 1H, =CH₂), 5.22 (s, 2H, O-CH₂-triazole), 5.15 (s, 2H, O-CH₂-triazole), 4.55 (t, *J* = 6.8, 4H, CH₂-N), 3.39 (t, *J* = 6.8, 4H, CH₂-thiazole), 3.32 (s, 2H, -CH₂-), 2.21 (s, 6H, CH₃-thiazole).

¹³C-NMR (100 MHz, CDCl₃), δ(ppm): 170.50 (C=O), 165.90 (C=O), 150.85 (2C, thiazole C-CH₃), 150.50 (2C, thiazole C-H), 142.77 (2C, triazole C_{quat}), 133.23 (-C=CH₂), 129.77 (-C=CH₂), 125.85 (2C, thiazole C_{quat}), 124.5 (triazole C-H), 124.4 (triazole C-H), 58.26 (O-CH₂-), 58.14 (O-CH₂-), 51.18 (2C, CH₂-N), 37.94 (-CH₂-), 27.45 (2C, -CH₂ thiazole), 14.71 (2C, CH₃-thiazole).

Synthesis of poly(di(prop-2-yn-1-yl) itaconate-co-dimethyl itaconate) copolymers (P100, P75, P50, P25, and P0)

A series of copolymers and homopolymers with different chemical compositions were prepared by conventional radical polymerization of PrI and DMI comonomers using different feed molar ratios (PrI/DMI = 100/0, 75/25, 50/50, 25/75 and 0/100), at a total concentration of 2 M in anhydrous DMF, at 70 °C. The copolymers were named P100, P75, P50, P25 and P0, for the feed molar ratios PrI/DMI = 100/0, 75/25, 50/50, 25/75 and 0/100, respectively. Briefly (e.g. for the sample PrI/DMI = 50/50, copolymer P50), both monomers, PrI (2.06 g, 10.0 mmol) and DMI (1.59 g, 10.0 mmol), at a total concentration of 2 M in anhydrous DMF, were added into a glass tube. Subsequently, the initiator AIBN (0.16 g, 1.0 mmol) was added and the mixture was deoxygenated by purging argon for 15 min. The polymerization reaction mixture was stirred at 70 °C for 24 h. The copolymer was isolated by precipitation in ethanol, yielding a white solid, which was collected and dried overnight under vacuum at room temperature (1.654 g, 45%).

Copolymer P50: **¹H-NMR (400 MHz, CDCl₃)**, δ(ppm): 4.67 (4H, -CH₂C≡CH), 3.58 (6H, O-CH₃), 2.49 (2H, -CH₂C≡CH), 1.99-1.00 (8H, CH₂-CO and -CH₂-chain).

Copolymer P50: **¹H-NMR (400 MHz, DMSO-d₆)**, δ(ppm): 4.67 (4H, -CH₂C≡CH), 3.58 (6H, O-CH₃ and 2H, -CH₂C≡CH), 3.00-1.50 (8H, -CH₂CO and CH₂-chain-).

Synthesis of poly(bis((1-(2-(4-methylthiazol-5-yl)ethyl)-1H-1,2,3-triazol-4-yl)methyl)itaconate-co-dimethyl itaconate), copolymers (P100T, P75T, P50T and P25T).

The incorporation of the thiazole and triazole moieties into the homopolymer (P100) and copolymers (P75, P50, and P25) was performed by Cu(I)-catalyzed azide-alkyne cycloaddition (CuAAC) click chemistry using 2-(4-methylthiazol-5-yl)ethanol azide. In a typical procedure, the copolymer (e.g. for the sample P50) (1.60 g, 8.8 meq. of alkyne groups), 2-(4-methylthiazol-5-yl)ethanol azide (1.51 g, 9.0 mmol), PMDETA (312 µL, 1.5 mmol) and CuCl (0.05 g, 0.5 mmol) were dissolved in 40 mL of CHCl₃. The mixture was stirred at room temperature for 24 h and then it was passed through a neutral alumina column. The resulting copolymer was isolated by precipitation in hexane, and the degree of modification was almost quantitative. The copolymers were named P100T, P75T, P50T, and P25T for the molar ratios TTI/DMI = 100/0, 75/25, 50/50 and 25/75, respectively.

Copolymer P50T: **¹H-NMR (400 MHz, CDCl₃)**, δ(ppm): 8.61 (2H, H-thiazole), 7.71 (2H, H-triazole), 5.15 (4H, O-CH₂-triazole), 4.62 (4H, CH₂-N), 3.64 (6H, O-CH₃) 3.45 (4H, CH₂-thiazole), 2.21 (6H, CH₃-thiazole), 2.00-1.00 (8H, CH₂-CO and -CH₂-chain).

Copolymer P50T: **¹H-NMR (400 MHz, DMSO-d₆)**, δ(ppm): 8.74 (2H, H-thiazole), 8.00 (2H, H-triazole), 5.01 (4H, O-CH₂-triazole), 4.52 (4H, CH₂-N), 3.50 (6H, O-CH₃) 3.26 (4H, CH₂-thiazole), 2.10 (6H, CH₃-thiazole), 3.00-1.50 (8H, CH₂CO and CH₂-chain-).

Quaternization reactions: Synthesis of cationic polymers (P100T-Q, P75T-Q, P50T-Q, and P25T-Q)

The homopolymer (P100T) and the copolymers (P75T, P50T and P25T) were modified by the *N*-alkylation reaction with either iodomethane (MeI) or 1-iodobutane (BuI) leading to the corresponding cationic polymers. A typical quaternization reaction with MeI is described below for the P50T copolymer as an example. The copolymer (1.50 g, 4.3 meq. of thiazole and 4.3 meq. of triazole groups) was dissolved in 25 mL of anhydrous DMF and then a large excess of MeI was added (2.7 mL, 43.0 mmol; the ratio of thiazole and triazole groups to alkyl iodide is ≈ 1 : 5). The mixture was deoxygenated with argon for 15 min, sealed, and then stirred at 70 °C for one week to achieve a high degree of modification. The resulting cationic copolymer was purified by precipitation in n-hexane followed by dialysis against distilled water and finally was isolated by freeze-drying. The degree of quaternization was almost quantitative. The copolymers quaternized with

methyl iodide were named P100T-Me, P75T-Me, P50T-Me, and P25T-Me and those quaternized with butyl iodide were named P100T-Bu, P75T-Bu, P50T-Bu, and P25T-Bu.

Homopolymer P100T-Me: **$^1\text{H-NMR}$ (400 MHz, D_2O)**, δ (ppm): 8.89 (2H, *H*-thiazole), 7.96 (2H, *H*-triazole), 5.44 (4H, O- CH_2 -triazole), 5.02 (4H, CH_2 -N), 4.37 (6H, N^+CH_3 triazole), 4.10 (6H, N^+CH_3 thiazole), 3.77 (4H, CH_2 thiazole), 2.51 (6H, CH_3 -thiazole).

Homopolymer P100T-Bu: **$^1\text{H-NMR}$ (400 MHz, D_2O)**, δ (ppm): 8.93 (2H, *H*-thiazole), 8.20 (2H, *H*-triazole), 5.46 (4H, O- CH_2 -triazole), 5.05 (4H, CH_2 -N), 4.65 (4H, N^+CH_2 triazole), 3.45 (4H, N^+CH_2 thiazole), 3.9-3.50 (4H, CH_2 -thiazole), 2.54 (6H, CH_3 -thiazole), 1.90 (8H, CH_2 - CH_2 - CH_3), 1.37 (8H, CH_2 - CH_2 - CH_3), 0.96 (12H, CH_2 - CH_2 - CH_3).

Copolymer P50T-Me: **$^1\text{H-NMR}$ (400 MHz, D_2O)**, δ (ppm): 8.92 (2H, *H*-thiazole), 8.07 (2H, *H*-triazole), 5.48 (4H, O- CH_2 -triazole), 5.05 (4H, CH_2 -N), 4.41 (6H, N^+CH_3 triazole), 4.13 (6H, N^+CH_3 thiazole), 3.80 (4H, CH_2 -thiazole), 3.68 (6H, - O-CH_3), 2.53 (6H, CH_3 -thiazole).

Copolymer P150T-Bu: **$^1\text{H-NMR}$ (400 MHz, D_2O)**, δ (ppm): 8.96 (2H, *H*-thiazole), 8.26 (2H, *H*-triazole), 5.47 (4H, O- CH_2 -triazole), 5.10 (4H, CH_2 -N), 4.68 (4H, N^+CH_2 triazole), 4.47 (4H, N^+CH_2 thiazole), 3.82 (4H, CH_2 -thiazole), 3.68 (6H, - O-CH_3), 2.54 (6H, CH_3 -thiazole), 1.93 (8H, CH_2 - CH_2 - CH_3), 1.40 (8H, CH_2 - CH_2 - CH_3), 0.95 (12H, CH_2 - CH_2 - CH_3).

Antibacterial assays

The antibacterial activities of the cationic polymers were tested following a standard broth dilution method according to the Clinical Laboratory Standards Institute (CLSI) to determine the minimum inhibition concentrations (MICs).²³ Bacterial cells were grown on 5% sheep blood Columbia agar plates for 24 h at 37 °C. Subsequently, the bacterial concentration was adjusted with saline to 10⁸ colony-forming units (CFU) mL⁻¹ (turbidity equivalent to ca. 0.5 McFarland turbidity standard). These suspensions were further diluted to 10⁶ CFU mL⁻¹ with fresh Mueller-Hinton broth. Stock solutions of the polymers at a concentration of 20 000 µg mL⁻¹ were prepared in the Mueller-Hinton broth medium using a minimum amount of DMSO (less than 6% v/v; higher DMSO content was found to be toxic for these bacterial strains^{22,24}). Then, 100 µL from each polymer solution were placed in the first column of a 96-well round-bottom microplate, and 50 µL of broth was added into the rest of the wells. From the first column, polymer solution (50 µL) was diluted by 2-fold serial dilutions in the rest of the wells, followed by the addition of 50 µL of the bacterial to yield a total volume of 100 µL and a bacterial concentration of 5 × 10⁵ CFU mL⁻¹. A positive control without the polymer and a negative control without bacteria

were also prepared. The plates were incubated at 37 °C for 24 h, and the MIC values were determined by checking the absence of bacterial growth visually. All the tests were performed in triplicate.

Hemotoxicity assays

Hemolysis studies were carried out as described previously.^{24,25} Fresh human blood was collected from healthy donors and used within the same day. Blood was drawn directly into the blood collecting tubes containing EDTA to prevent coagulation. The tubes were centrifuged at 3500 rpm for 20 min. Afterwards, the supernatant (plasma) and the buffy coat at the middle (white blood cells) were discarded and the red blood cells (RBCs) at the bottom were collected. The RBCs were washed with fresh sterile PBS and centrifuged three times. Subsequently, the RBCs were resuspended to a final concentration of 5% (v/v) in PBS. Polymer solutions were prepared in a mixture of PBS and a minimum amount of DMSO (up to 5% v/v, nontoxic under the experimental conditions used in this study) at a concentration of 40 000 µg mL⁻¹. Then, 100 µL of these polymer solutions were added in the first column of 96-well round-bottom microplates, while in the rest of the wells, 50 µL of PBS were added. Two-fold sequential dilutions of the polymer solutions were performed to obtain a series of concentrations, and finally, 150 µL of the RBC suspension were added to each well. Equally, Triton X-114 (1% v/v solution in PBS) was used as a positive control for 100% of hemolysis, whereas PBS was used as a negative control for 0% hemolysis. The microplates were incubated for 1 h at 37 °C. After this period, the plates were centrifuged at 1000 rpm for 10 min and the resulting supernatant in each well was transferred to a new 96-well microplate. Hemolysis was monitored by measuring the absorbance of the released hemoglobin at 550 nm using a microplate reader (Synergy HTX Multi-Mode Reader spectrophotometer, Bio-Tek). The percentage of hemolyzed erythrocytes was calculated according to the following equation:

$$\text{Hemolysis \%} = \frac{A_{\text{sample}} - A_{\text{negative control}}}{A_{\text{positive control}} - A_{\text{negative control}}} \times 100$$

An absolutely achromatic supernatant solution indicates no hemolysis ($A_{\text{negative control}}$) while a red solution indicates hemolysis ($A_{\text{positive control}}$). All experiments were performed in triplicate, and the data were expressed as mean ± SD (n = 3).

2.1.4 Results and discussion

Synthesis of antibacterial polymers derived from itaconic acid

Antimicrobial biobased polymers derived from itaconic acid were prepared following a novel strategy consisting of the incorporation of clickable alkyne groups into the structure, which enables the posterior inclusion of antimicrobial groups by click chemistry. For this purpose, three different synthetic approaches were proposed (Scheme S1 in the ESI and Scheme 2).

In the first approach, presented in Scheme S1A, we attempted the radical polymerization of IA through the α,β -unsaturated double bond using an APS initiator in aqueous media at 70 °C for 24 h. Subsequently, the obtained poly(itaconic acid) (PIA) was subjected to post-modification of the two carboxylic acid functionalities by the condensation reaction with propargyl alcohol, using EDC/NHS chemistry in aqueous media. However, this approach was discarded because, in addition to the problems associated with the polymerization of PIA such as low conversion and slow rate, the poly(itaconic acid) was insoluble in most organic solvents. Then, the incorporation of propargyl alcohol into the PIA led to a polymer insoluble in an aqueous reaction medium, which hindered the complete modification of PIA.

The second approach that we considered was the synthesis of a clickable monomer derived from IA, di(prop-2-yn-1-yl) itaconate (Prl) (see the experimental section and Scheme S1B). In this approach, the solubility issues were solved as the IA monomer has a higher solubility than PIA. The Prl monomer was successfully synthesized by the reaction between IA and propargyl alcohol in a mixture of toluene/THF and H₂SO₄, reaching a yield of 97%. Fig. 1A shows the ¹H-NMR spectrum of the obtained Prl monomer, which confirms the complete functionalization of the carboxylic acid groups and the presence of the vinyl signals at 6.40 and 5.80 ppm. The ¹³C-NMR spectrum displayed in Fig. S1A in the ESI also corroborated the chemical structure of the Prl monomer. The second step of this approach consisted in the incorporation of thiazole groups by Cu(I)-catalyzed azide-alkyne cycloaddition (CuAAC) click chemistry between the alkyne groups of Prl and 2-(4-methylthiazol-5-yl)ethanol azide forming a 1,2,3-triazole group, which is also susceptible to quaternization. Likewise, ¹H-NMR (Fig. 1B) and ¹³C-NMR spectra show typical peaks of the introduced functional groups, confirming the success of the reaction and the formation of the monomer derivative with thiazole and

triazole groups in its structure (TTI). See the ESI, Fig. S1B for the ^{13}C NMR spectrum of this monomer.

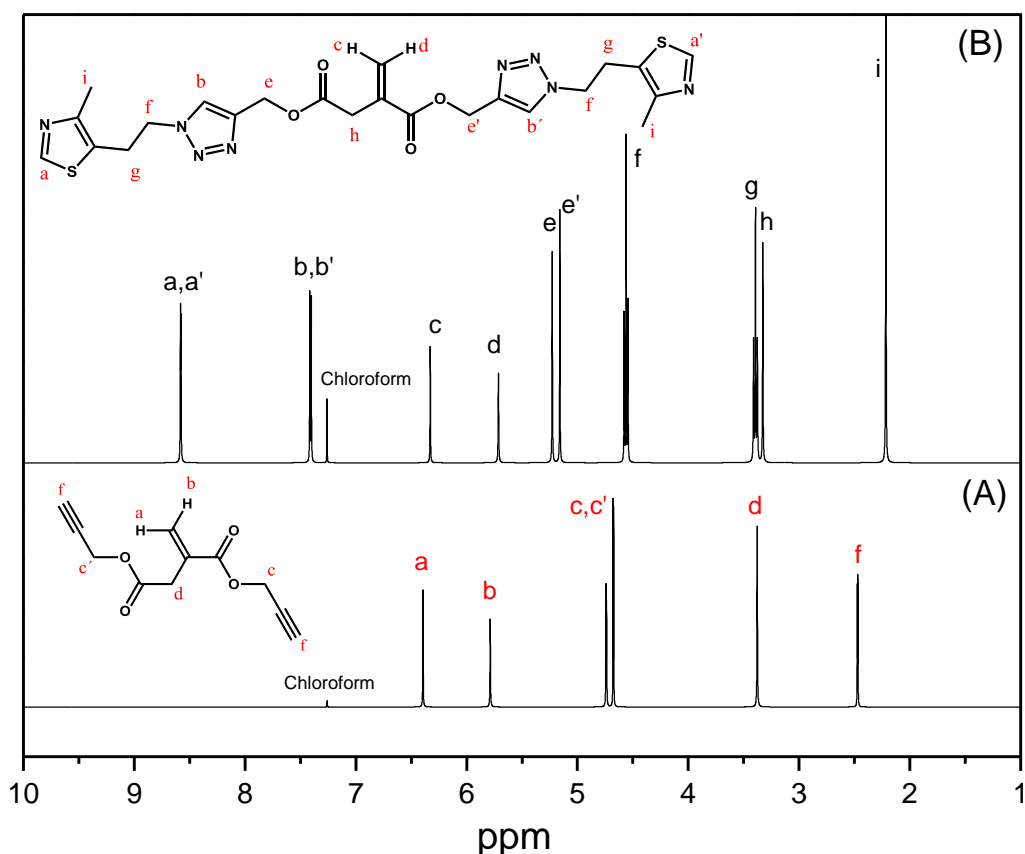
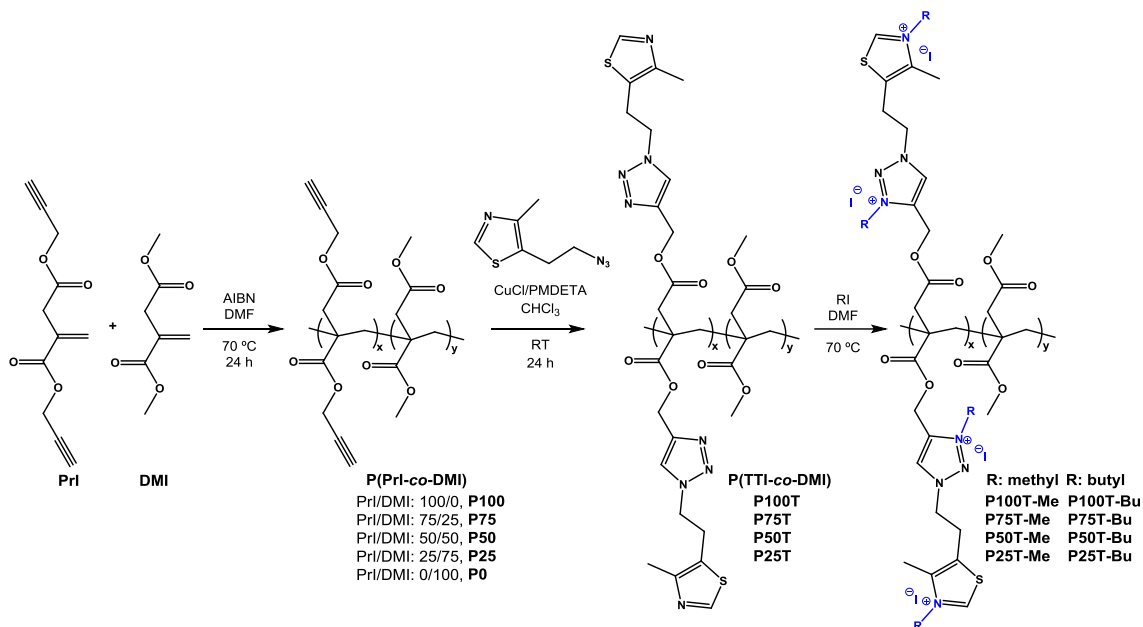


Figure 1. ^1H -NMR spectra of (A) clickable monomer PrI and (B) monomer derivative TTI with thiazole and triazole groups in deuterated chloroform.

In spite of the satisfactory synthesis of the biobased monomer TTI, this monomer did not easily polymerize or copolymerize with a comonomer such as dimethyl itaconate (DMI). We tried different polymerization conditions, both in bulk and in DMF solution. However, after 48 h of reaction, we were not able to obtain any polymer under all conditions tested, probably due to high steric hindrance among other reasons.

Then, a third approach was proposed (Scheme 2), the development of a clickable polymer derived from itaconic acid instead of using a clickable monomer. In this strategy, the clickable monomer PrI was successfully radical homopolymerized and copolymerized with dimethyl itaconate in DMF solution, at a total monomer concentration of 2 M, at 70 °C, with AIBN as a radical initiator. Therefore, homopolymers and a series of copolymers with different chemical compositions were obtained using different feed molar ratios (PrI/DMI = 100/0, 75/25, 50/50, 25/75 and 0/100).



Scheme 2. Synthesis of the antibacterial cationic copolymers derived from itaconic acid.

Fig. 2 and 3 show the FTIR and ¹H-NMR spectra, respectively, of the clickable copolymer P(PrI-co-DMI) for a feed chemical composition of PrI/DMI = 50/50 (named P50). In the FTIR spectrum, the characteristic peak of the alkyne C-H stretching band at 3283 cm⁻¹ and the bands assigned to the C≡C bond at 2128 cm⁻¹ and the C≡C-H bond at 642 cm⁻¹, clearly demonstrate the successful synthesis of the alkyne-functionalized polymers. Likewise, in the ¹H-NMR spectrum (Fig. 3A), the terminal methyne proton of the alkyne groups appears at 3.58 ppm and the rest of the signals consistent with the chemical structure of the copolymer. The chemical compositions of the obtained polymers, thus the molar content of PrI in the copolymer, were calculated by integration of the ¹H NMR spectral signals at 3.50 ppm (6H, O-CH₃ from DMI) compared to the signal at 4.67 ppm (4H) from PrI. Table 1 summarizes the molecular characteristics of the synthesized copolymers and homopolymers including the obtained chemical compositions. The molar ratios of the comonomers in the copolymers were found to be very similar to the feed molar ratios, and therefore, polymers will be referred to by their feed compositions to maintain uniformity. This fact is important because the copolymer composition can be easily modulated by varying the comonomer feed ratios.

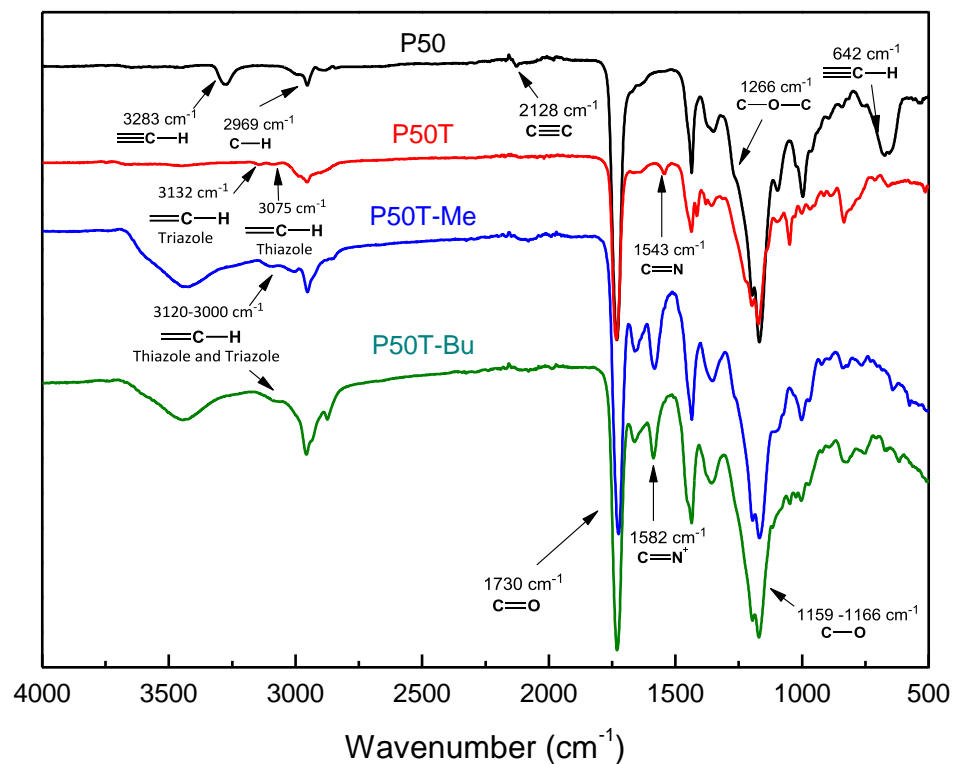


Figure 2. FTIR spectra of the copolymers P50, P50T, P50T-Me and P50T-Bu.

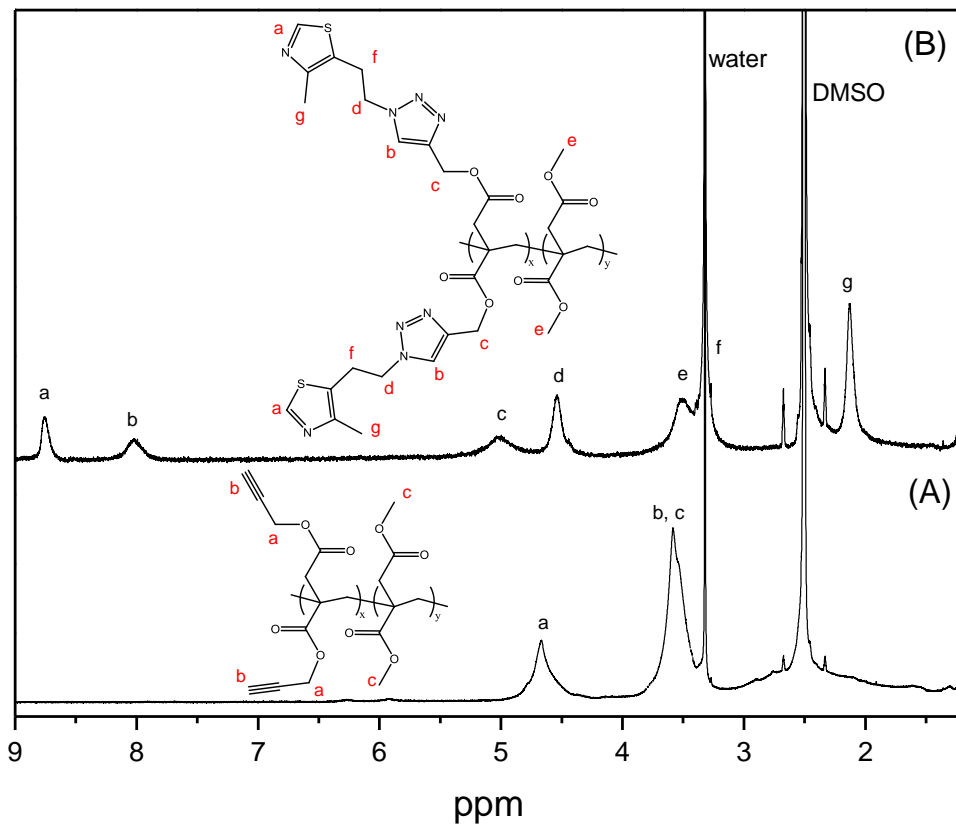


Figure 3. ^1H NMR spectra of the copolymers (A) P50 and (B) P50T in $\text{DMSO}-\text{d}_6$.

Table 1. Molecular characteristics of the P(PrI-co-DMI) polymers synthesized with different molar feed ratios [PrI]/[DMI], final chemical compositions (polymer ratio [PrI]/[DMI]), number average molecular weights (\bar{M}_n) and molecular weight dispersity (D) determined by SEC in DMF as an eluent. \bar{M}_n and D values of the polymers after click reactions leading to P(TTI-co-DMI) are also included.

Sample	Feed ratio	Polymer ratio	\bar{M}_n	D	Sample	\bar{M}_n ^b	D ^b
P(PrI-co-DMI)	[PrI]/[DMI]	[PrI]/[DMI] ^a	(g mol ⁻¹)		P(TTI-co-DMI)	(g mol ⁻¹)	
P100	100.0/0	100.0/0	6,700	1.58	P100T	7,100	1.59
P75	75.0/25.0	72.5/27.5	8,100	1.35	P75T	11,100	1.27
P50	50.0/50.0	50.1/49.9	7,500	1.31	P50T	11,700	1.25
P25	25.0/75.0	23.1/76.9	6,300	1.36	P25T	6,800	1.49
P0	0/100.0	0/100.0	4,800	1.27	P0	-	-

^a Polymer ratio [PrI]/[DMI] was determined by 1H-NMR.

^b \bar{M}_n and D values of the polymers after click reactions leading to P(TTI-co-DMI) polymers.

The molecular weights of the polymers were determined using SEC (Table 1) and were found to be low for all polymers, with values in the range of $\bar{M}_n = 4800\text{-}8100 \text{ g mol}^{-1}$, presenting low molecular weight dispersity (D) (1.58-1.27).

Once clickable polymers were synthesized with different contents of alkyne groups, the next step consists in the CuAAC click chemistry with 2-(4-methylthiazol-5-yl)ethanol azide, which led to polymers with thiazole and 1,2,3-triazole groups, P(TTI-co-DMI). The post-polymerization reaction was carried out under mild conditions and the degree of modification was almost quantitative. After the click reaction, the molecular weights of the polymers detected by SEC increased as a result of the incorporation of the azide molecules (Table 1), while the polydispersity indexes practically did not change. Equally, the new thiazole and triazole groups attached to the polymer structures were detected by FTIR. Fig. 2 shows the FTIR spectrum of P50T. The signals at 3132 and 3075 cm⁻¹ corresponding to the =C-H stretching vibrations of the triazole and thiazole groups, the signal at 1543 cm⁻¹ attributed to the C=N bond of thiazole, and the absence of the band

associated with the C≡C bond clearly indicate the successful coupling. The NMR spectra also confirm the completion of the click reaction and the formation of the P(TTI-co-DMI) copolymers. All the signals of the ¹H NMR spectra were consistent with the expected structures. The ¹H NMR spectrum of P50T displayed in Fig. 3B, as an example, shows the characteristic peaks at 8.74 ppm and 8.00, corresponding to the thiazole and triazole protons, respectively, concomitant with the disappearance of propargyl methylene signal at 4.67 ppm.

The last step of the synthesis procedure consists in the incorporation of permanent positive charges into the polymers to provide them with antibacterial activities. Both the pendant nucleophilic azole groups, triazole and thiazole, can be modified using very reactive alkylating reagents such as alkyl iodides. In this study, two alkylating agents with different chain lengths were used, methyl and butyl iodide, to tune the final hydrophobic/hydrophilic balance of the copolymer. This hydrophobic/hydrophilic balance is well known to have a strong influence on the antimicrobial activity and toxicity of the resulting polymers,^{2,26-28} and, in this work, it was also controlled by the content of the hydrophobic comonomer DMI. The synthesized P(TTI-co-DMI) (P100T, P75T, P50T and P25T) copolymers were reacted with a large excess of either methyl iodide or butyl iodide in DMF at 70 °C under an argon atmosphere. The reaction was performed for one week to ensure quantitative modification, which was confirmed by NMR and FTIR spectroscopy. Fig. 2 shows the comparison of the FTIR spectra of the quaternized copolymers with either methyl or butyl iodide of the samples with a molar ratio [PrI]/[DMI] = 50 (P50T-Me and P50T-Bu, respectively) with their unquaternized copolymer precursor (P50T). In both cases, the band at 1543 cm⁻¹ assigned to the $\nu(C=N)$ disappears and a new band corresponding to the $\nu(C=N)^+$ clearly emerges due to the formed thiazolium and triazolium groups, after the quaternization reactions. Similarly, the ¹H NMR spectrum demonstrates the success of the quaternization reaction and almost quantitative modifications of the thiazole and triazole groups (Fig. 4). The two peaks assigned to the aromatic protons of the 1,2,3-thiazole (~8.6 ppm) and 1,3-triazole (8.0-7.6 ppm) rings shift to lower field regions (~8.90 and ~8.3-8.0 ppm, respectively) as a result of the quaternization reaction due to the higher polarity resulting from the formation of azonium groups. Fig. S2, ESI, displays the ¹H-NMR spectrum of P50T-Me in DMSO-d₆, which supports the signal assignments. Likewise, Figs. S3 and S4 in the ESI display the COSY-NMR spectra of the P50T-Me and P50T-Bu copolymers, which were also obtained to support the signal assignments in the ¹H-NMR spectra of the H_f and H_g protons at 3.80 ppm (4H, CH₂-).

thiazole) and 3.68 ppm (6H, -O-CH₃), respectively. These assignments were verified through the analysis of the COSY-NMR spectra based on the correlation of the H_f protons with the H_d protons.

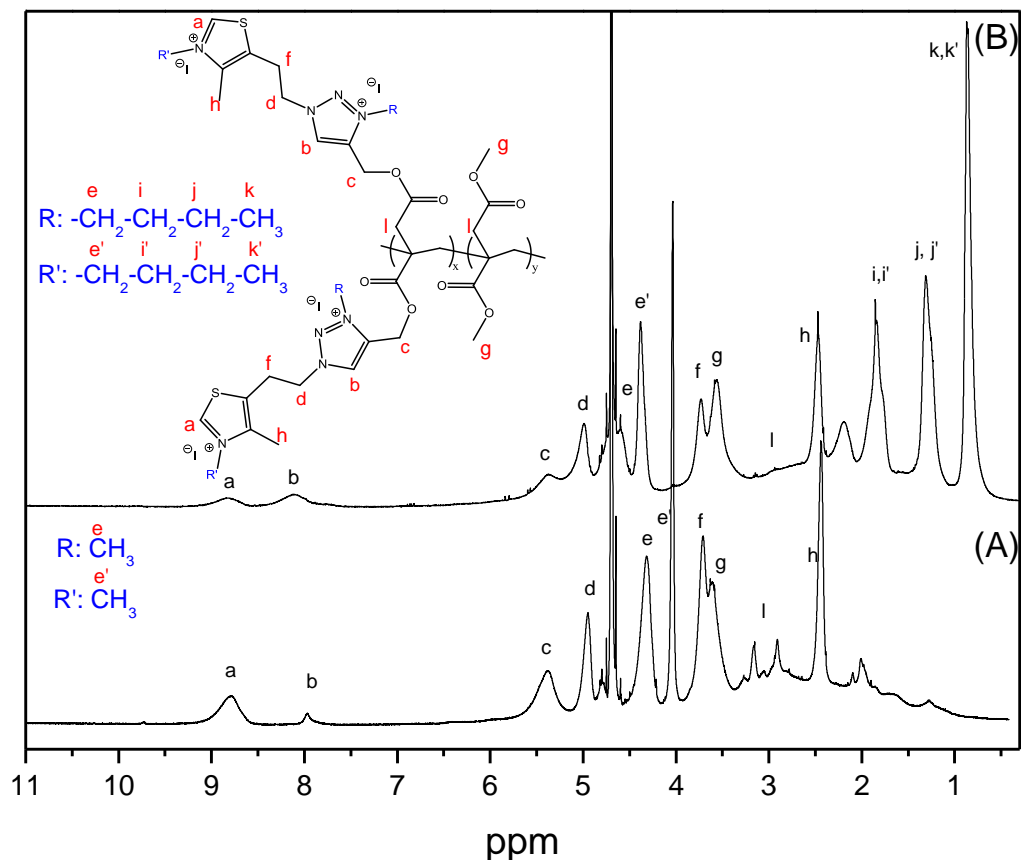


Figure 4. $^1\text{H-NMR}$ spectra in deuterated water of the copolymers (A) P75T-Me and (B) P75T-Bu.

For the estimation of the positive charge density of the synthesized copolymers, zeta potential measurements were performed in distilled water. Table 2 shows the zeta potential values (ζ) obtained for all the synthesized copolymers. As confirmed by NMR and FTIR studies, the quaternization reactions result in cationic copolymers with high positive ζ values, around +50 mV for both methylated and butylated copolymers. Only the copolymers with a low content of cationic units, P50T-Me and P25T-Me, present reduced charge density.

Table 2. Zeta potential values (ζ) obtained for all the synthesized cationic copolymers.

ζ (mV)				ζ (mV)			
P100T-Me	P75T-Me	P50T-Me	P25T-Me	P100T-Bu	P75T-Bu	P50T-Bu	P25T-Bu
56 ± 1	49 ± 3	38 ± 2	40 ± 3	48 ± 1	48 ± 2	49 ± 2	51 ± 2

Antibacterial activities of cationic polymers.

The antibacterial efficiency of the obtained cationic polymers derived from biobased itaconic acid was evaluated for both Gram-negative (*P. aeruginosa* and *E. coli*) and Gram-positive (*S. epidermidis* and *S. aureus*) opportunistic bacteria. The minimum inhibitory concentration (MIC) of the polymer derivatives, which is the lowest concentration of a polymer needed to prevent the visible growth of bacteria, was measured by the CLSI microbroth dilution reference method²³ against the different bacterial strains. The MIC values determined for all the polymers tested are summarized in Table 3.

Table 3. Antibacterial and hemolytic activities of the resulting cationic polymers derived from itaconic acid.

Copolymer	MIC ($\mu\text{g mL}^{-1}$)				HC_{50} ($\mu\text{g mL}^{-1}$)	$\text{HC}_{50}/\text{MIC}^*$
	<i>E. coli</i>	<i>P. aeruginosa</i>	<i>S. epidermidis</i>	<i>S. aureus</i>		
P100T-Me	>10000	10000	31	10	>10000	>1000
P75T-Me	10000	10000	31	10	>10000	>1000
P50T-Me	>10000	10000	312	312	>10000	>32
P25T-Me	>10000	10000	312	312	>10000	>32
P100T-Bu	>10000	5000	8	10	>10000	>1000
P75T-Bu	5000	5000	8	10	>10000	>1000
P50T-Bu	5000	10000	16	10	>10000	>1000
P25T-Bu	>10000	10000	31	10	>10000	>1000

*Calculated based on the MIC values of *S. aureus*.

Remarkably, huge differences in the activities of the polymers against Gram-positive and Gram-negative bacteria are clearly appreciated. Whereas the biobased cationic polymers present excellent activity against Gram-positive bacteria, they are totally inefficient

against Gram-negative bacteria. Typically, Gram-negative bacteria are found to be less susceptible to cationic polymers than Gram-positive due to the additional outer membrane that provides a tough barrier to be overcome.²⁹ The nature of the membrane also varies; in Gram-negative bacteria, the membranes are made of two negative phospholipidic membranes and lipopolysaccharides within the outer bilayer, while Gram-positive bacteria have thick cell walls, which consist of a large multilayer region of peptidoglycan with wall teichoic acid and lipoteichoic acid. Although this better behavior against Gram-positive bacteria was also revealed in our previous investigations with cationic methacrylic polymers bearing thiazole and triazole groups, such polymers also presented significant activity against Gram-negative bacteria.^{22,25,30} In the current work, the polymers derived from IA present four positive charges per monomeric unit, thus, a very high positive charge. In this case, with a high charge density, even when high content of the hydrophobic monomer DMI is used, the activity is almost nullified against Gram-negative bacteria. It seems that an excessive positive charge is detrimental to the disruptive action of polymers on Gram-negative bacterial membranes. On the other hand, against Gram-positive cells, the polymers were able to completely inhibit the bacterial growth at a low concentration, with MIC values that depend on the chemical composition, $[TTI]/[DMI]$ ratio, and the length of the alkyl group. The activity was increased as the content of the active TTI units augments in the copolymers. The butylated polymers with the highest contents of TTI, P100T-Bu and P75T-Bu, have a MIC value as low as $8 \mu\text{g mL}^{-1}$. When the influence of the length of the alkyl group on activity is compared, the copolymers quaternized with butyl iodide exhibit the lowest MIC values, which indicates that longer hydrophobic alkyl chains impart stronger antibacterial activity, as previously discussed in the literature.^{4,6} Then, it appears that increasing the hydrophobicity of the alkylating chains in the antimicrobial polymers enhances their activity, whereas the incorporation of the hydrophobic comonomer DMI into the copolymer structure not only did not improve the antibacterial potential, but also decrease the activity. Apparently, the activity against Gram-positive bacteria strongly depends on the cationic charge in the polymers, which is diluted by incorporating the DMI units. In fact, the copolymers with higher content of DMI units exhibited lower charge density as determined by Zeta potential measurements. Then, modifying the hydrophobic/hydrophilic balance by varying the length of the alkylating agent seems to be an effective way to improve the activity, as the density of cationic charge is maintained by increasing the hydrophobicity.

Hemotoxicity of cationic polymers

To evaluate the toxicity of the cationic polymers derived from itaconic acid, the hemolysis test was performed on human eukaryotic cells. In this study, the hemoglobin released from the human red blood cells (RBCs) was measured after one hour of incubation with each of the polymers at various concentrations. The hemolysis percentage as a function of the polymer concentration is shown in Fig. 5. The HC_{50} values, summarized in Table 3, refer to the polymer concentration that triggers 50% lysis of RBCs^{31,32} and the selectivity values for bacterial cells over mammalian cells that were estimated by the ratio of HC_{50} to MIC values for *S. aureus* ATCC 29213. Nevertheless, the high selectivity can also be applied to *S. epidermidis* bacteria.

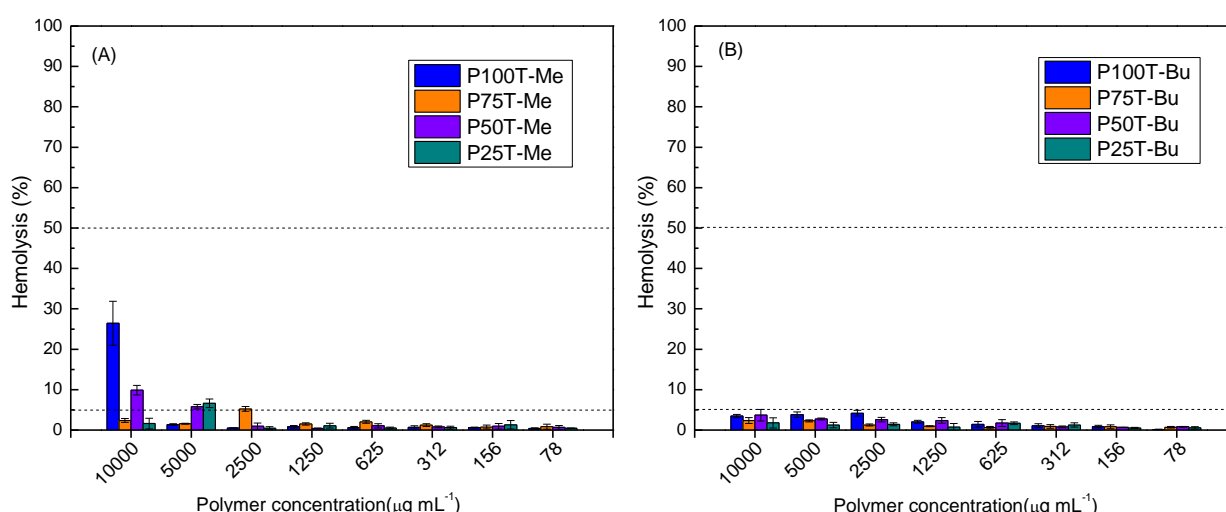


Figure 5. Hemolytic activity of the copolymers quaternized with either (A) methyl iodide or (B) butyl iodide.

As shown in Fig. 5, all the copolymers exhibit very low hemolysis, with hemolysis percentages well below 50% for the highest concentration tested, $10\,000\,\mu\text{g mL}^{-1}$. In fact, most of them present values even below 5%, in particular copolymers quaternized with butyl iodide. With regard to selectivity against bacteria over red blood cells, calculated by the ratio of HC_{50} and MIC values (Table 3; herein, the MIC values against *S. aureus* were used), all the itaconic acid derivatives demonstrate excellent selectivity values, with most copolymers showing more than 1000-fold selectivity toward bacteria over RBCs. This series of copolymers derived from biobased itaconic acid are promising antibacterial polymers as they exhibit excellent activity against Gram-positive bacteria and negligible hemolysis. It is well established that the hydrophobic/hydrophilic balance of polymers plays a crucial role in the selective attachment to a bacterial cell membrane.³³⁻³⁵ Typically,

polymers with high hydrophobicity show high hemolysis activity due to the strong interaction with the mammalian cell membrane.³⁶ The polymers developed in the current work are very hydrophilic with high charge density, demonstrating null toxicity while maintaining the antibacterial activity.

2.1.5 Conclusions

We described a facile approach to functionalize biobased polymers derived from itaconic acid. Using this strategy we successfully developed potent and highly selective antibacterial polymers containing azonium groups. This strategy consists in the modification of the carboxylic groups of poly(itaconic acid) by incorporating alkyne clickable groups, which can be further functionalized through the CuAAC click reaction. Then, click chemistry allows the coupling of 1,3-thiazole groups, a component of vitamin B1, concomitantly with the formation of 1,2,3-triazole linkages under mild conditions, reaching almost the quantitative degree of modification. The *N*-alkylation reaction of the azole groups provides cationic azonium groups to the polymers with consequent potent antibacterial activity against Gram-positive bacteria and very low toxicities against human red blood cells. Although the copolymers were not active against Gram-negative bacteria, the approach reported herein provides the basis to develop polymers with a broad spectrum of antibacterial activity in the future. Biobased polymers functionalized with clickable alkyne groups could be easily post modified by attachment of a variety of antimicrobial components, extending the activity to other microbial strains.

2.1.6 Acknowledgments

This work was funded by the MICINN (PID2019-104600RB-I00), the Agencia Estatal de Investigación (AEI, Spain) and Fondo Europeo de Desarrollo Regional (FEDER, EU). A. Chiloeches acknowledges MICIU for his FPU fellowship FPU18/01776.

2.1.7 References

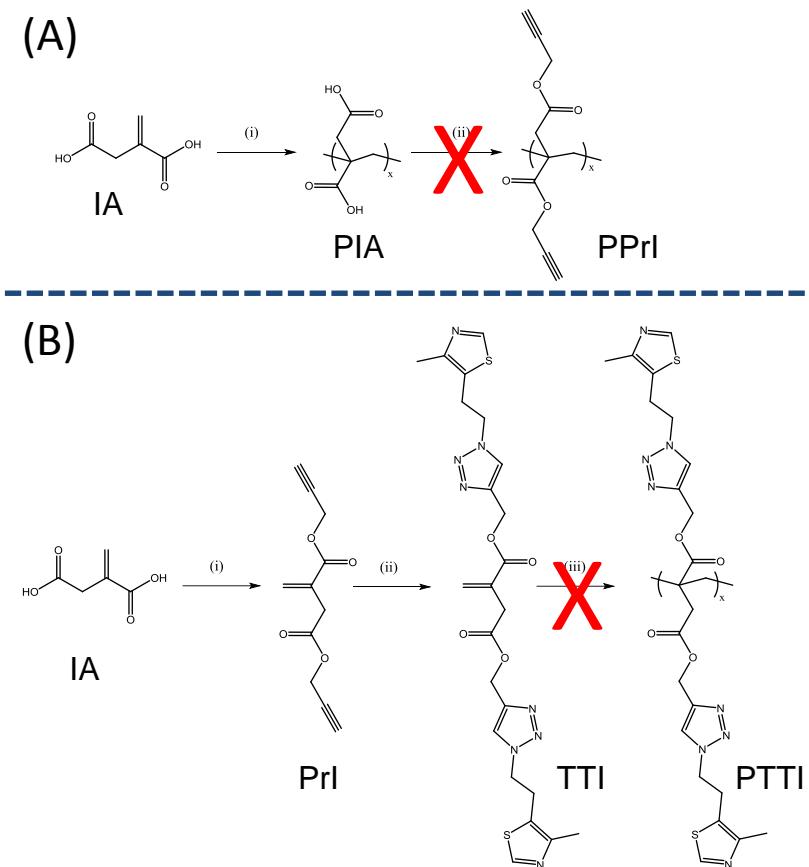
- (1) Al-Ahmad, A.; Laird, D.; Zou, P.; Tomakidi, P.; Steinberg, T.; Lienkamp, K. Nature-Inspired Antimicrobial Polymers - Assessment of Their Potential for Biomedical Applications. *PLoS One* **2013**, 8 (9).
- (2) Takahashi, H.; Caputo, G. A.; Vemparala, S.; Kuroda, K. Synthetic Random Copolymers as a Molecular Platform to Mimic Host-Defense Antimicrobial Peptides. *Bioconjug. Chem.* **2017**, 28 (5), 1340–1350.
- (3) Konai, M. M.; Bhattacharjee, B.; Ghosh, S.; Haldar, J. Recent Progress in Polymer Research to Tackle Infections and Antimicrobial Resistance. *Biomacromolecules* **2018**, 19 (6), 1888–1917.
- (4) Muñoz-Bonilla, A.; Fernández-García, M. Polymeric Materials with Antimicrobial Activity. *Prog. Polym. Sci.* **2012**, 37 (2), 281–339.
- (5) Nimmagadda, A.; Liu, X.; Teng, P.; Su, M.; Li, Y.; Qiao, Q.; Khadka, N. K.; Sun, X.; Pan, J.; Xu, H.; Li, Q.; Cai, J. Polycarbonates with Potent and Selective Antimicrobial Activity toward Gram-Positive Bacteria. *Biomacromolecules* **2017**, 18 (1), 87–95.
- (6) Sovadinova, I.; Palermo, E. F.; Urban, M.; Mpiga, P.; Caputo, G. A.; Kuroda, K. Activity and Mechanism of Antimicrobial Peptide-Mimetic Amphiphilic Polymethacrylate Derivatives. *Polymers* **2011**, 3 (3), 1512–1532.
- (7) Tew, G. N.; Scott, R. W.; Klein, M. L.; DeGrado, W. F. De Novo Design of Antimicrobial Polymers, Foldamers, and Small Molecules: From Discovery to Practical Applications. *Acc. Chem. Res.* **2010**, 43 (1), 30–39.
- (8) Laroque, S.; Reifarth, M.; Sperling, M.; Kersting, S.; Klöpzig, S.; Budach, P.; Storsberg, J.; Hartlieb, M. Impact of Multivalence and Self-Assembly in the Design of Polymeric Antimicrobial Peptide Mimics. *ACS Appl. Mater. Interfaces* **2020**, 12 (27), 30052–30065.
- (9) Muñoz-Bonilla, A.; Echeverria, C.; Sonseca, Á.; Arrieta, M. P.; Fernández-García, M. Bio-Based Polymers with Antimicrobial Properties towards Sustainable Development. *Materials* **2019**, 12 (4), 641.
- (10) Chin, W.; Zhong, G.; Pu, Q.; Yang, C.; Lou, W.; De Sessions, P. F.; Periaswamy, B.; Lee, A.; Liang, Z. C.; Ding, X.; Gao, S.; Chu, C. W.; Bianco, S.; Bao, C.; Tong, Y. W.; Fan, W.; Wu, M.; Hedrick, J. L.; Yang, Y. Y. A Macromolecular Approach to Eradicate Multidrug Resistant Bacterial Infections While Mitigating Drug Resistance Onset. *Nat. Commun.* **2018**, 9 (1), 917.
- (11) Chin, W.; Yang, C.; Ng, V. W. L.; Huang, Y.; Cheng, J.; Tong, Y. W.; Coady, D. J.; Fan, W.; Hedrick, J. L.; Yang, Y. Y. Biodegradable Broad-Spectrum Antimicrobial Polycarbonates: Investigating the Role of Chemical Structure on Activity and Selectivity. *Macromolecules* **2013**, 46 (22), 8797–8807.
- (12) Xu, Y.; Zhang, K.; Reghu, S.; Lin, Y.; Chan-Park, M. B.; Liu, X. W. Synthesis of Antibacterial Glycosylated Polycaprolactones Bearing Imidazoliums with Reduced Hemolytic Activity. *Biomacromolecules* **2019**, 20 (2), 949–958.
- (13) Kalekar, P. P.; Geng, Z.; Finn, M. G.; Collard, D. M. Azide-Substituted Polylactide: A Biodegradable Substrate for Antimicrobial Materials via Click Chemistry Attachment of Quaternary Ammonium Groups. *Biomacromolecules* **2019**, 20 (9), 3366–3374.
- (14) Magalhães Jr, A. I.; de Carvalho, J. C.; Medina, J. D. C.; Soccol, C. R. Downstream Process Development in Biotechnological Itaconic Acid Manufacturing. *Appl. Microbiol. Biotechnol.* **2017**, 101 (1), 1–12.
- (15) Cunha da Cruz, J.; Machado de Castro, A.; Camporese Sérvulo, E. F. World Market and Biotechnological Production of Itaconic Acid. *3 Biotech* **2018**, 8 (3), 138.
- (16) Bednarz, S.; Wesołowska-Piętak, A.; Konefał, R.; Świergosz, T. Persulfate Initiated Free-Radical Polymerization of Itaconic Acid: Kinetics, End-Groups and Side Products. *Eur. Polym. J.* **2018**, 106, 63–71.

- (17) Satoh, K.; Lee, D. H.; Nagai, K.; Kamigaito, M. Precision Synthesis of Bio-Based Acrylic Thermoplastic Elastomer by RAFT Polymerization of Itaconic Acid Derivatives. *Macromol. Rapid Commun.* **2014**, 35 (2), 161–167.
- (18) Robert, T.; Friebel, S. Itaconic Acid – a Versatile Building Block for Renewable Polyesters with Enhanced Functionality. *Green Chem.* **2016**, 18 (10), 2922–2934.
- (19) Noordzij, G. J.; Van Den Boomen, Y. J. G.; Gilbert, C.; Van Elk, D. J. P.; Roy, M.; Wilsens, C. H. R. M.; Rastogi, S. The Aza-Michael Reaction: Towards Semi-Crystalline Polymers from Renewable Itaconic Acid and Diamines. *Polym. Chem.* **2019**, 10 (29), 4049–4058.
- (20) Lv, A.; Li, Z. L.; Du, F. S.; Li, Z. C. Synthesis, Functionalization, and Controlled Degradation of High Molecular Weight Polyester from Itaconic Acid via ADMET Polymerization. *Macromolecules* **2014**, 47 (22), 7707–7716.
- (21) Chanda, S.; Ramakrishnan, S. Poly(Alkylene Itaconate)s - An Interesting Class of Polyesters with Periodically Located Exo-Chain Double Bonds Susceptible to Michael Addition. *Polym. Chem.* **2015**, 6 (11), 2108–2114.
- (22) Tejero, R.; López, D.; López-Fabal, F.; Gómez-Garcés, J. L.; Fernández-García, M. Antimicrobial Polymethacrylates Based on Quaternized 1,3-Thiazole and 1,2,3-Triazole Side-Chain Groups. *Polym. Chem.* **2015**, 6 (18), 3449–3459.
- (23) CLSI, Methods for Dilution Antimicrobial Susceptibility Tests for Bacteria That Grow Aerobically, Approved Standard-Ninth Edition, CLSI Document M07-A9, Clinical and Laboratory Standards Institute; Clinical and Laboratory Standards Institute: Wayne, PA, **2012**.
- (24) Álvarez-Paino, M.; Muñoz-Bonilla, A.; López-Fabal, F.; Gómez-Garcés, J. L.; Heuts, J. P.; Fernández-García, M. Effect of Glycounits on the Antimicrobial Properties and Toxicity Behavior of Polymers Based on Quaternized DMAEMA. *Biomacromolecules* **2015**, 16 (1), 295–303.
- (25) Cuervo-Rodríguez, R.; Muñoz-Bonilla, A.; López-Fabal, F.; Fernández-García, M. Hemolytic and Antimicrobial Activities of a Series of Cationic Amphiphilic Copolymers Comprised of Same Centered Comonomers with Thiazole Moieties and Polyethylene Glycol Derivatives. *Polymers* **2020**, 12 (4), 972.
- (26) Palermo, E. F.; Sovadinova, I.; Kuroda, K. Structural Determinants of Antimicrobial Activity and Biocompatibility in Membrane-Disrupting Methacrylamide Random Copolymers. *Biomacromolecules* **2009**, 10 (11), 3098–3107.
- (27) Ergene, C.; Yasuhara, K.; Palermo, E. F. Biomimetic Antimicrobial Polymers: Recent Advances in Molecular Design. *Polym. Chem.* **2018**, 9 (18), 2407–2427.
- (28) Palermo, E. F.; Lienkamp, K.; Gillies, E. R.; Ragogna, P. J. Antibacterial Activity of Polymers: Discussions on the Nature of Amphiphilic Balance. *Angew. Chemie - Int. Ed.* **2019**, 58 (12), 3690–3693.
- (29) Lienkamp, K.; Kumar, K.-N.; Som, A.; Nüsslein, K.; Tew, G. N. “Doubly Selective” Antimicrobial Polymers: How Do They Differentiate between Bacteria? *Chem. - A Eur. J.* **2009**, 15 (43), 11710–11714.
- (30) Chiloeches, A.; Echeverría, C.; Cuervo-Rodríguez, R.; Plachà, D.; López-Fabal, F.; Fernández-García, M.; Muñoz-Bonilla, A. Adhesive Antibacterial Coatings Based on Copolymers Bearing Thiazolium Cationic Groups and Catechol Moieties as Robust Anchors. *Prog. Org. Coatings* **2019**, 136, 105272.
- (31) Krumm, C.; Harmuth, S.; Hijazi, M.; Neugebauer, B.; Kampmann, A. L.; Geltenpoth, H.; Sickmann, A.; Tiller, J. C. Antimicrobial Poly(2-Methyloxazoline)s with Bioswitchable Activity through Satellite Group Modification. *Angew. Chemie - Int. Ed.* **2014**, 53 (15), 3830–3834.
- (32) Lienkamp, K.; Tew, G. N. Synthetic Mimics of Antimicrobial Peptides-a Versatile Ring-Opening Metathesis Polymerization Based Platform for the Synthesis of Selective Antibacterial and Cell-Penetrating Polymers. *Chem. - A Eur. J.* **2009**, 15 (44), 11784–11800.

- (33) Singh, M.; Singh, A.; Kundu, S.; Bansal, S.; Bajaj, A. Deciphering the Role of Charge, Hydration, and Hydrophobicity for Cytotoxic Activities and Membrane Interactions of Bile Acid Based Facial Amphiphiles. *Biochim. Biophys. Acta - Biomembr.* **2013**, 1828 (8), 1926–1937.
- (34) Rahman, M. A.; Bam, M.; Luat, E.; Jui, M. S.; Ganewatta, M. S.; Shokfai, T.; Nagarkatti, M.; Decho, A. W.; Tang, C. Macromolecular-Clustered Facial Amphiphilic Antimicrobials. *Nat. Commun.* **2018**, 9 (1), 5231.
- (35) Zhu, Z.; Jeong, G.; Kim, S. J.; Gadwal, I.; Choe, Y.; Bang, J.; Oh, M. K.; Khan, A.; Rao, J. Balancing Antimicrobial Performance with Hemocompatibility in Amphiphilic Homopolymers. *J. Polym. Sci. Part A Polym. Chem.* **2018**, 56 (21), 2391–2396.
- (36) Venkataraman, S.; Zhang, Y.; Liu, L.; Yang, Y. Y. Design, Syntheses and Evaluation of Hemocompatible PEGylated-Antimicrobial Polymers with Well-Controlled Molecular Structures. *Biomaterials* **2010**, 31 (7), 1751–1756.

2.1.8 Supporting Information

Biobased Polymers Derived from Itaconic Acid bearing clickable groups with Potent Antibacterial Activity and Negligible Hemolytic Activity



Scheme S1. Failed approaches 1 (A) and 2 (B) used to synthesize polymers derived from itaconic acid with thiazole and triazole groups.

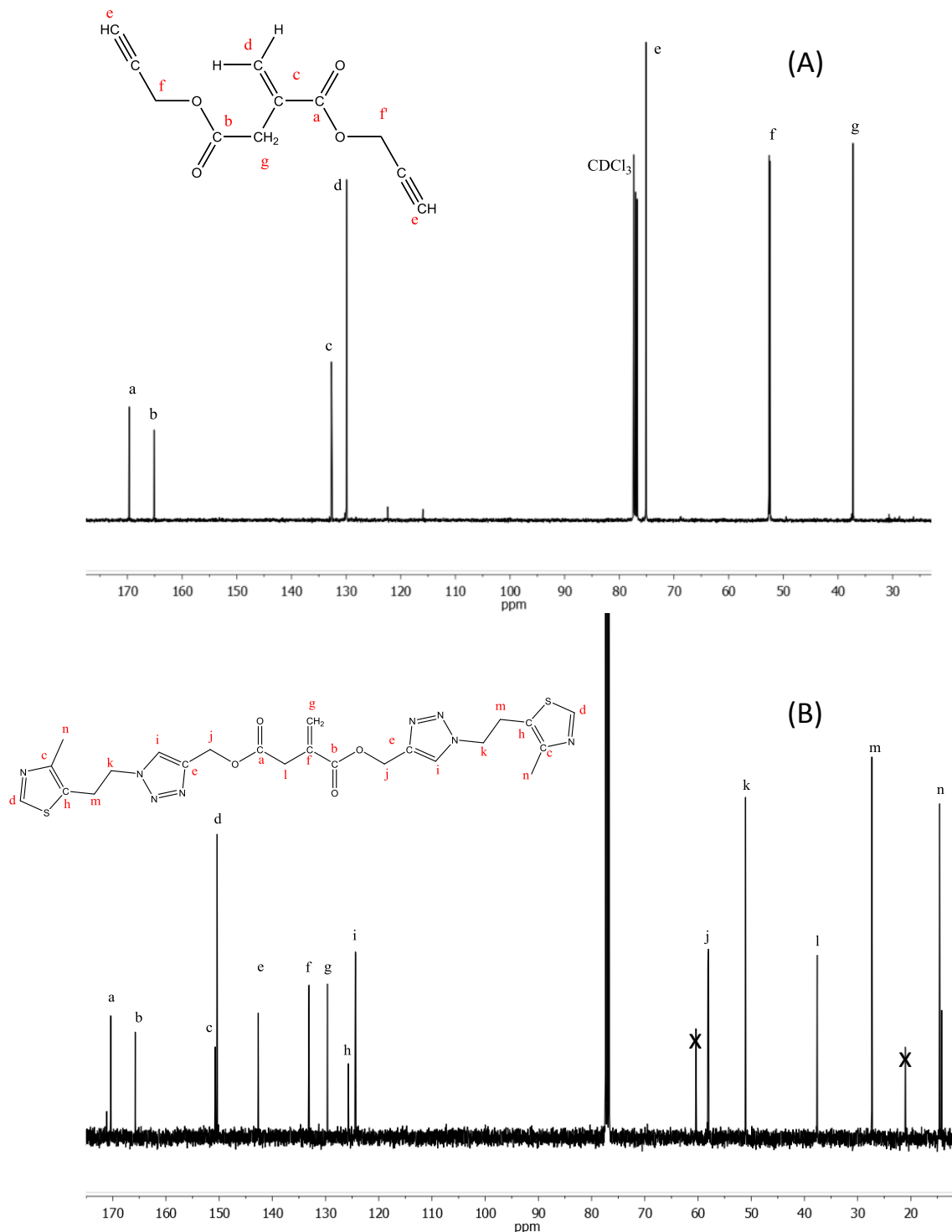


Figure S1. ^{13}C -NMR spectra of (A) clickable monomer PrI and (B) monomer derivative TTI with thiazole and triazole groups in deuterated chloroform.

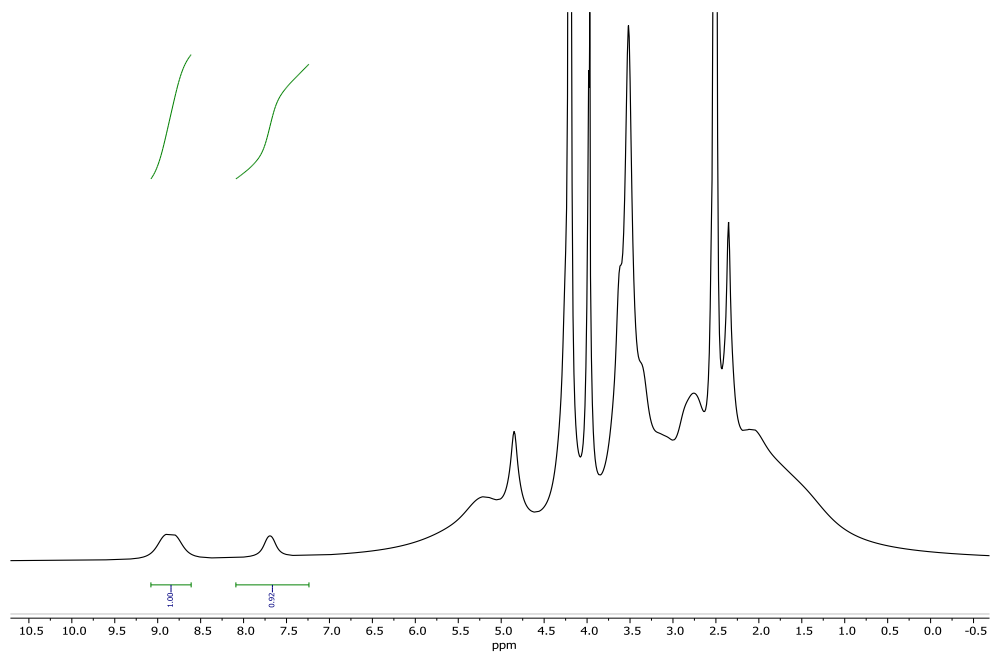


Figure S2. Copolymer P50T-Me. $^1\text{H-NMR}$ (400 MHz, DMSO-d_6), δ (ppm): 8.82 (2H, H-thiazole), 7.66 (2H, H-triazole), 5.24 (4H, O- CH_2 -triazole), 4.85 (4H, CH_2 -N), 4.15 (6H, N^+CH_3 triazole), 3.97 (6H, N^+CH_3 thiazole), 3.50 (4H, CH_2 -thiazole and 6H, -O- CH_3), 2.33 (6H, CH_3 -thiazole).

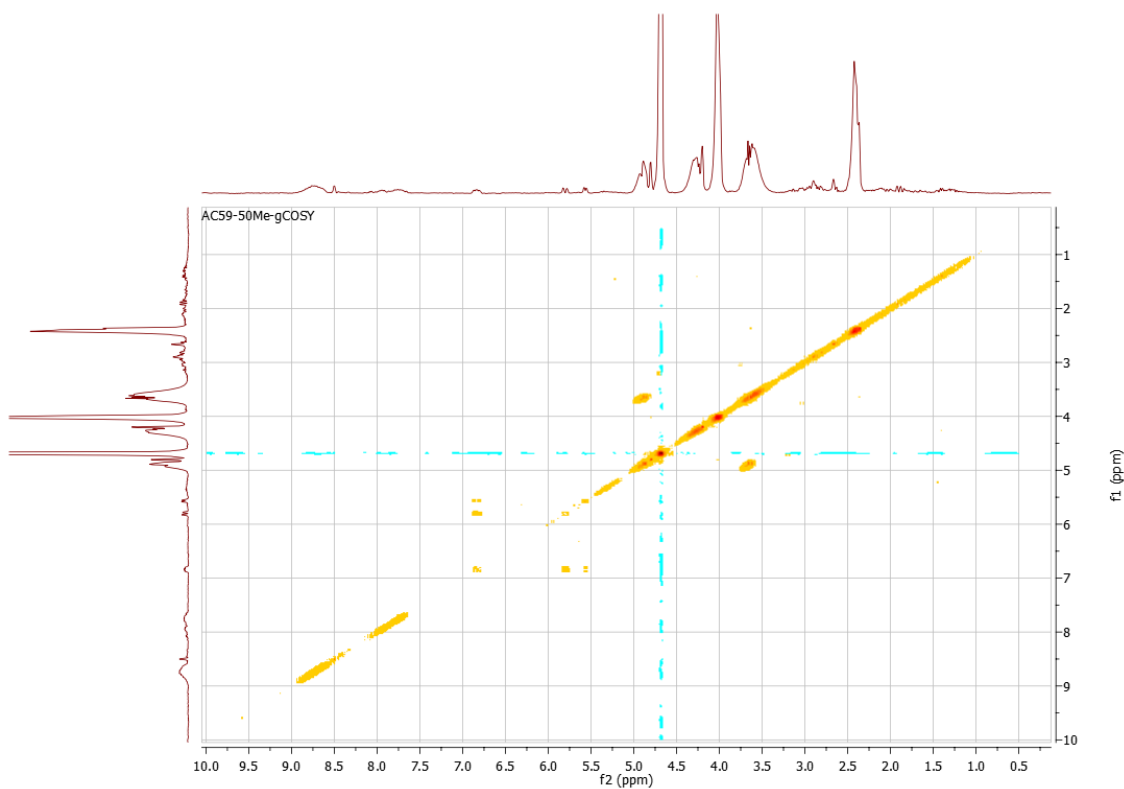


Figure S3. COSY-NMR spectrum in deuterated water of P50T-Me copolymer.

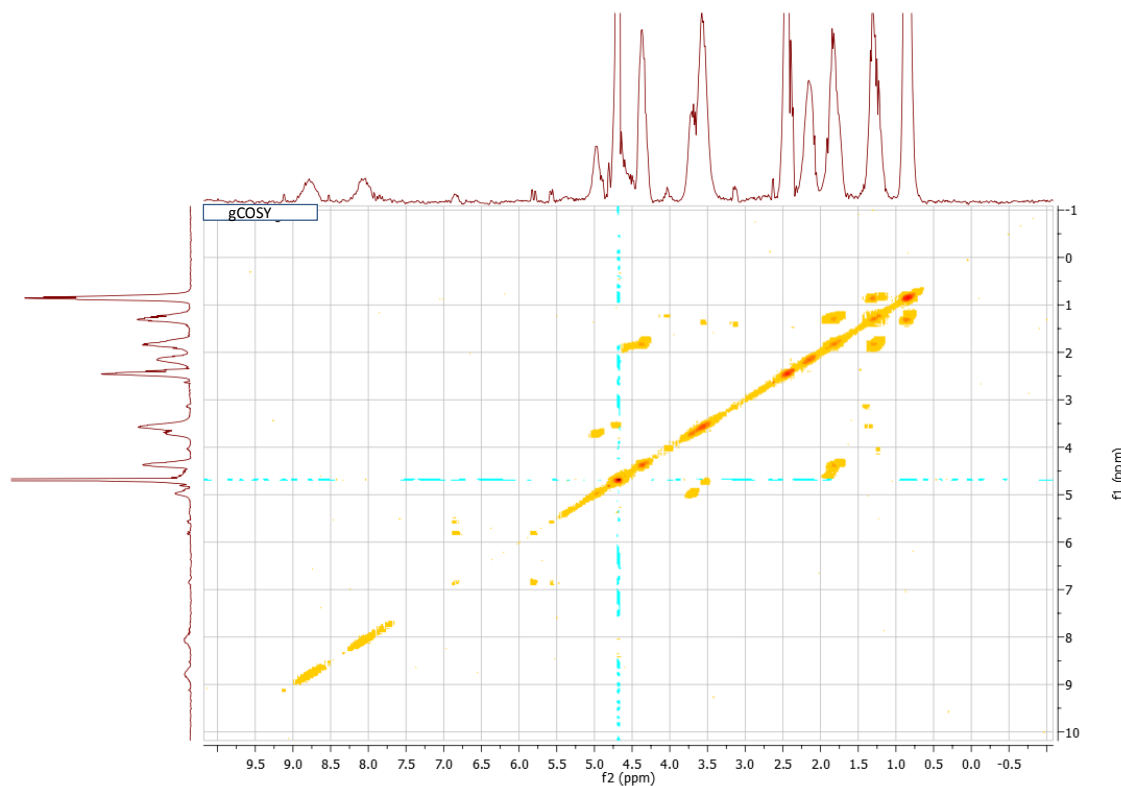


Figure S4. COSY-NMR spectrum in deuterated water of P50T-Bu copolymer.

2.2 Antibacterial and compostable polymers derived from biobased itaconic acid as environmentally friendly additives for biopolymer

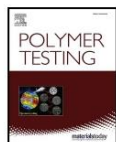
Polymer Testing 2022, 109, 107541

Polymer Testing 109 (2022) 107541

Contents lists available at ScienceDirect

Polymer Testing

journal homepage: www.elsevier.com/locate/polytest



Antibacterial and compostable polymers derived from biobased itaconic acid as environmentally friendly additives for biopolymers

A. Chiloeches ^{a,b}, R. Cuervo-Rodríguez ^c, F. López-Fabal ^d, M. Fernández-García ^{a,e}, C. Echeverría ^{a,e,**}, A. Muñoz-Bonilla ^{a,e,*}

^a Instituto de Ciencia y Tecnología de Polímeros (ICTP-CSIC), C/Juan de la Cierva 3, 28006, Madrid, Spain
^b Universidad Nacional de Educación a Distancia (UNED), C/ Bravo Murillo 38, 28015, Madrid, Spain
^c Facultad de Ciencias Químicas, Universidad Complutense de Madrid, Avenida Complutense s/n, Ciudad Universitaria, 28040, Madrid, Spain
^d Hospital Universitario de Móstoles, C/ Dr. Luis Montes s/n, 28935 Móstoles, Madrid, Spain
^e Interdisciplinary Platform for Sustainable Plastics towards a Circular Economy-Spanish National Research Council (SusPlast-CSIC), Madrid, Spain

ARTICLE INFO

Keywords:
 Biodegradable
 Antibacterial polymers
 Itaconate
 PBAT
 Blends
 Thermal properties

ABSTRACT

In this work, a series of antibacterial cationic copolymers derived from bio-sourced itaconic acid was studied as potential biobased active components in biodegradable formulations based on poly(butylene adipate-co-terephthalate) (PBAT) for packaging applications. These copolymers were first characterized by testing their antimicrobial activity against resistant bacterial strains, their biodegradability in compost conditions, and their thermal properties by differential scanning calorimetry (DSC) and thermogravimetric analysis (TGA). The antibacterial properties showed potent activity against Methicillin-resistant *Staphylococcus aureus* (MRSA), with MIC values as low as 78 µg mL⁻¹. Related to their biodegradability, the cationic polymers biodegraded fast under compost conditions and even a priming effect was observed in the compost. Thermal properties, characterized by DSC and TGA, showed that the copolymers thermally degraded at temperature relatively low; nevertheless, they are able to be processed at temperatures up to ~150 °C. Subsequently, these antibacterial polymers were successfully blended as minor active component (10 wt%) with PBAT by melt-extrusion and press-compression molding. The resulting biopolymeric films exhibit potent antibacterial activity, which confirm that the cationic polymers incorporated as active component are able to perverse this activity after the processing and impart antibacterial properties to PBAT bioplastic. Therefore, these antibacterial biobased polymers derived from itaconic acid seem to be good candidates for applications related to active food packaging or even for biomedical devices.

1. Introduction

Fossil-based plastics are present in almost every aspects of human life; around 8.3 billion tons of plastic have been manufactured since 1950, and production continues to grow [1]. However, in recent years, the negative impact of plastics on the environment has begun to be clear [2], and the reduction of their consumption is urgent for a sustainable development. In this sense, substitution or partial replacement of fossil-based plastics by degradable and renewable polymers has been explored as sustainable alternative, at least for some applications [3,4]. In fact, biobased and biodegradable polymers production capacity is estimated to grow from around 2.11 million tons in 2018 to 2.62 million tons in 2023 [5]. Starch, cellulose, and soy protein, as well as, synthetic polylactic acid (PLA) and polyhydroxyalcanoates (PHAs) are the most important biodegradable polymers derived from renewable resources; whereas poly(butylene adipate-co-terephthalate) (PBAT) based on fossil resources is considered nowadays one of the most promising biodegradable polymers in a wide range of applications due to its excellent properties like high ductility and low modulus of elasticity [6]. Biodegradable polymers have acquired particular importance in food packaging applications as packaging waste represents a significant part of solid waste with a negative impact on the environment. In packaging materials, in addition to biodegradability, other properties are especially desired including antioxidant and antimicrobial properties [7].

* Corresponding author. Instituto de Ciencia y Tecnología de Polímeros (ICTP-CSIC), C/Juan de la Cierva 3, 28006, Madrid, Spain.
 ** Corresponding author. Instituto de Ciencia y Tecnología de Polímeros (ICTP-CSIC), C/Juan de la Cierva 3, 28006, Madrid Spain.
 E-mail address: sbonilla@ictp.csic.es (A. Muñoz-Bonilla).

<https://doi.org/10.1016/j.polytesting.2022.107541>
 Received 20 December 2021; Received in revised form 2 March 2022; Accepted 9 March 2022
 Available online 10 March 2022
 0142-9418/© 2022 The Authors. Published by Elsevier Ltd. This is an open access article under the CC BY-NC-ND license
<http://creativecommons.org/licenses/by-nc-nd/4.0/>.

2.2.1 Abstract

In this work, a series of antibacterial cationic copolymers derived from bio-sourced itaconic acid was studied as potential biobased active components in biodegradable formulations based on poly(butylene adipate-co-terephthalate) (PBAT) for packaging applications. These copolymers were first characterized by testing their antimicrobial activity against resistant bacterial strains, their biodegradability in compost conditions, and their thermal properties by differential scanning calorimetry (DSC) and thermogravimetric analysis (TGA). The antibacterial properties showed potent activity against Methicillin-resistant *Staphylococcus aureus* (MRSA), with MIC values as low as $78 \mu\text{g}\cdot\text{mL}^{-1}$. Related to their biodegradability, the cationic polymers biodegraded fast under compost conditions and even a priming effect was observed in the compost. Thermal properties, characterized by DSC and TGA, showed that the copolymers thermally degraded at temperature relatively low; nevertheless, they are able to be processed at temperatures up to $\sim 150^\circ\text{C}$. Subsequently, these antibacterial polymers were successfully blended as minor active component (10 wt%) with PBAT by melt-extrusion and press-compression molding. The resulting biopolymeric films exhibit potent antibacterial activity, which confirm that the cationic polymers incorporated as active component are able to preserve this activity after the processing and impart antibacterial properties to PBAT bioplastic. Therefore, these antibacterial biobased polymers derived from itaconic acid seem to be good candidates for applications related to active food packaging or even for biomedical devices.

Keywords: biodegradable; antibacterial polymers; itaconate; PBAT, blends; thermal properties.

2.2.2 Introduction

Fossil-based plastics are present in almost every aspects of human life; around 8.3 billion tons of plastic have been manufactured since 1950, and production continues to grow.¹ However, in recent years, the negative impact of plastics on the environment has begun to be clear,² and the reduction of their consumption is urgent for a sustainable development. In this sense, substitution or partial replacement of fossil-based plastics by degradable and renewable polymers has been explored as sustainable alternative, at least for some applications.^{3,4} In fact, biobased and biodegradable polymers production capacity is estimated to grow from around 2.11 million tons in 2018 to 2.62 million tons in 2023.⁵ Starch, cellulose, and soy protein, as well as, synthetic polylactic acid (PLA) and polyhydroxyalkanoates (PHAs) are the most important biodegradable polymers derived from renewable resources; whereas poly(butylene adipate-co-terephthalate) (PBAT) based on fossil resources is considered nowadays one of the most promising biodegradable polymers in a wide range of applications due to its excellent properties like high ductility and low modulus of elasticity.⁶

Biodegradable polymers have acquired particular importance in food packaging applications as packaging waste represents a significant part of solid waste with a negative impact on the environment. In packaging materials, in addition to biodegradability, other properties are especially desired including antioxidant and antimicrobial properties.⁷ Typically, antimicrobial agents such as antibiotics, silver compounds, essential oils, and antimicrobial polymers are incorporated at low percentages into the biopolymeric materials to provide such antimicrobial activity.⁸⁻¹⁰ Of all, antimicrobial polymers exhibit some important advantages, such as thermal and chemical stability and low tendency to diffuse, compared to low molecular weight components, providing long-term activity. Additionally, antimicrobial polymers hardly generate bacterial resistance and nowadays are considered a promising alternative to tackle antibiotic resistant infections, which is one of the biggest threats to global health and food security.¹¹⁻¹⁴ However, most of the reported antimicrobial polymers are derived from petroleum-sources,¹⁵⁻¹⁷ which can be a limitation in their use as additive or component in biodegradable formulation for food packaging. In recent years, research on biodegradable antimicrobial polymers is emerging as fruitful area that opens up new opportunities for a sustainable and safety development.^{9,18-22} Our group has recently published the synthesis of new antibacterial biobased polymers derived from itaconic acid (IA),^{23,24} which is a biorenewable resource obtained by fermentation of biomass.^{25,26} The

antimicrobial biopolymers bearing cationic azolium groups derived from vitamin thiamine (B1) demonstrate excellent antibacterial activity against Gram-positive bacteria and negligible toxicity to human cells.²³ Herein, we further investigate these biobased antibacterial polymers as active component/additive in biopolymeric formulation for potential application in food packaging. Firstly, the antimicrobial efficiency of the polymers was tested against resistant pathogens. Then, their biodegradation behavior under compost conditions was studied in order to primary evaluate their applicability as biodegradable component and ensure the complete biodegradation of the final material. The thermal properties of these antibacterial polymers are also crucial parameters to be studied because the active polymers need to withstand thermal processing to maintain bioactivity.²⁷ In this work, biopolymeric blends based on PBAT containing this antimicrobial biobased polymer as minor component were performed by hot melt extrusion process, and characterized to assess the effect of such antimicrobial biobased polymers on the final properties of the films.

2.2.3 Experimental part

Materials

Microcrystalline cellulose Avicel PH-101 was obtained from *Sigma-Aldrich* (St. Louis, MO, USA) and poly(butylene adipate-co-terephthalate) (PBAT ecoflex® F. Blend C1200) was purchased from BASF (Ludwigshafen, Germany). For biological studies, sodium chloride solution (NaCl suitable for cell culture, BioXtra) and phosphate buffered saline (PBS, pH 7.4) were obtained from *Sigma-Aldrich* (St. Louis, MO, USA). Growth medium, BBL Mueller–Hinton broth, was purchased from *Becton Dickinson Company* (Madrid, Spain) and Columbia agar (5% sheep blood) plates from *Thermo Scientific* (Madrid, Spain). *Staphylococcus aureus* resistant to methicillin and oxacillin (*S. aureus*, ATCC 43300) used as bacterial strain was purchased from *Oxoid, Thermo Fisher Scientific* (Madrid, Spain).

Synthesis of biobased antimicrobial polymers derived from itaconic acid

The series of antibacterial homopolymer and copolymers derived from itaconic acid, poly(bis((1-(2-(4-methylthiazol-5-yl)ethyl)-1H-1,2,3-triazol-4-yl)methyl) itaconate-co-dimethyl itaconate) quaternized with methyl iodide, P(TTI-co-DMI)-Me, were synthesized according to the procedure previously described by our group.²³ Briefly, IA was chemically modified by incorporating clickable alkyne groups on the carboxylic acids. Then, the

resulting monomer (PrI) with pendant alkyne groups was polymerized and copolymerized with dimethyl itaconate (DMI) by radical polymerization, leading clickable polymers derived from itaconic acid P(PrI-co-DMI). The feed molar ratio of comonomers was varied to precisely tune the content of alkyne groups. The polymers were named as P100, P75, P50, P25 and PDMI for [PrI]/[DMI] molar ratio of 100/0, 75/25, 50/50, 25/75 and 0/100, respectively. These copolymers with alkyne pendant groups can be ideal platforms to obtain a variety of biobased polymers with broaden physico-chemical properties and functionalities, due to high tolerance of azide-alkyne coupling reactions to a wide variety of functional groups. Herein, a thiazole group (a component of the vitamin thiamine B1) was incorporated onto the polymers by copper-catalyzed azide-alkyne cycloaddition (CuAAC) click chemistry also leading to triazole linkages. The resulting P(TTI-co-DMI) polymers were named as P100T, P75T, P50T and P25T and PDMI. N-alkylating reactions of the thiazole and triazole groups with methyl iodide provide the corresponding itaconate derivatives with pendant azolium groups, P(TTI-co-DMI)-Me (P100T-Me, P75T-Me, P50T-Me and P25T-Me). Copolymers were designed with tunable amphiphilicity, having variable molar ratio of hydrophobic units of DMI and cationic itaconate comonomers with pendent azolium groups derived from vitamin thiamine (TTI) (see Fig. 1).

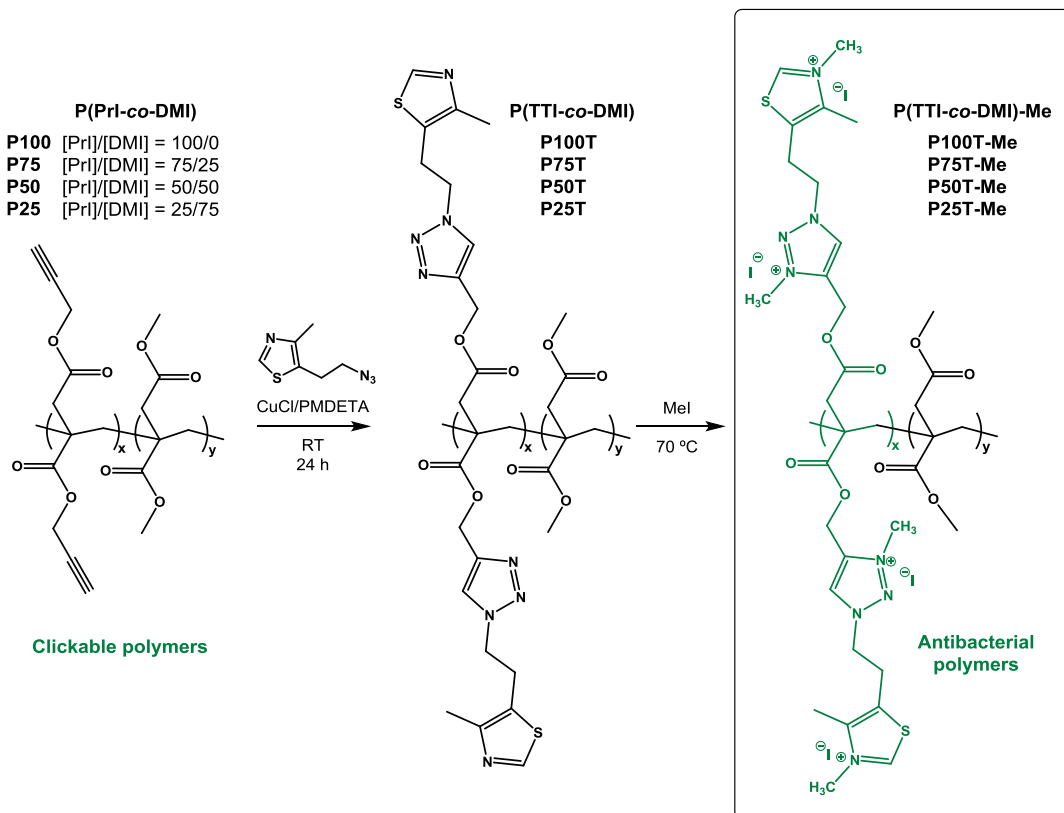


Figure 1. Chemical structure of the antibacterial copolymers derived from itaconic acid used in this study.

Processing of the biopolymeric blends

The processing of the biopolymeric blends and film preparation were performed as illustrated in Fig. 2. Biopolymeric blends based on PBAT and the homopolymer poly(bis((1-(2-(4-methylthiazol-5-yl)ethyl)-1H-1,2,3-triazol-4-yl)methyl) quaternized with methyl iodide (named as P100T-Me) were prepared by melt extrusion in an extruder equipped with twin conical co-rotating screws (MiniLab Haake Rheomex CTW5, Thermo Scientific, Waltham, MA, USA) and a capacity of 7 cm³. PBAT and P100T-Me were mixed together at a 90:10 ratio to obtain the blend PBAT/P100T-Me. Briefly, 6.3 g of PBAT and 0.7 g of P100T-Me were mixed and blended in the extruder at a screw speed of 100 rpm for 5 min at 150 °C. Prior to processing, all the materials were dried in an oven at 40 °C under vacuum for 24 h. Subsequently, the extruded samples were compressed into films of about 200 µm using a Collin P200P press (Ebersberg, Germany) at 150 °C and 50 bars.

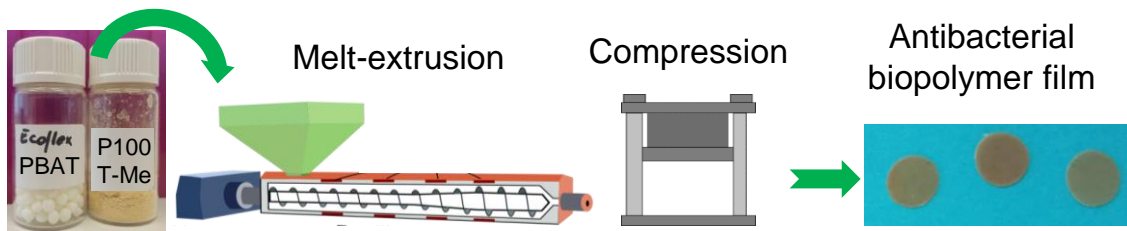


Figure 2. Scheme of the used methodology to obtain antibacterial and compostable biopolymer films.

Antibacterial assays

Minimum inhibition concentration (MIC) of cationic polymers

The antibacterial activity of the cationic polymers was tested against an antibiotic resistant bacterial strain, *Staphylococcus aureus* resistant to methicillin and oxacillin (*S. aureus*, ATCC 43300), MRSA. The minimum inhibition concentration (MIC) values were determined following a standard broth dilution method according to the Clinical Laboratory Standards Institute (CLSI).²⁸ Bacterial cells were culture on a 5% sheep blood Columbia agar plate during 24 h at 37 °C. From this plate, a bacterial suspension was prepared in saline solution with a concentration of ~10⁸ colony-forming units (CFU) mL⁻¹ (turbidity equivalent to ca. 0.5 McFarland turbidity standard). Subsequently, the suspension was diluted with fresh Mueller-Hinton broth to ~10⁶ CFU mL⁻¹. The bacterial suspension was, then, mixed with different concentrations of freshly prepared polymer solutions by serial dilutions in a 96-well plate. Briefly, polymer solutions at a concentration

of 5000 µg mL⁻¹ were prepared in Mueller-Hinton broth medium using a minimum amount of DMSO (less than 6% v/v, higher DMSO content demonstrated to be toxic for these bacterial strains).^{29,30} Subsequently, 100 µL from each polymer solution were added in the first column of a 96-well microplate, while 50 µL of fresh broth was added into the rest of the wells. Serial dilutions were performed from the first column, followed by the addition of 50 µL of the bacterial suspension to yield a total volume of 100 µL in each well and a bacterial concentration of ~5×10⁵ CFU mL⁻¹. The microplates were kept in an incubator at 37 °C during 24 h under constant shaking of 100 rpm. The MIC values were taken as the concentration of the polymer at which no microbial growth was visually observed. Positive controls without polymer and negative controls without bacteria were also performed. All the tests were run in triplicate.

Antibacterial Assessment of Biopolymer Films

Antibacterial test of the prepared biopolymer film based on PBAT/P100T-Me blend (90/10) was performed following the E2149-13a standard method from the American Society for Testing and Materials (ASTM),³¹ which is a standardized method to evaluate the antimicrobial activity of material surfaces. *Staphylococcus aureus* resistant to methicillin and oxacillin (*S. aureus*, ATCC 43300) was used as bacterial strain. In this analysis, bacterial suspension was prepared as described above but in PBS at a concentration of ~10⁶ CFU mL⁻¹. Polymer films were cut into round pieces of 6 mm diameter and ~5 mg weight. Each sample was placed in a sterile falcon tube containing 1 mL of the bacterial suspension inoculum and 9 mL of PBS to obtain a working concentration of ~10⁵ CFU mL⁻¹. Control experiments were also performed on PBAT films (without the cationic polymer) and also blank experiments with only the inoculum in the absence of film. Subsequently, the suspensions were shaken at 120 rpm for 24 h at 37 °C. After this period, 1 mL of each solution was taken and 1:10 serially diluted. Subsequently, 1 mL of the dilutions was placed on 5% sheep blood Columbia agar plates and incubated for 24 h at 37 °C. Then, the number of bacteria in each sample was determined by the plate counting method. The measurements were made at least in triplicate.

Biodegradation test

Biodegradation test was performed following a standard method for determining aerobic biodegradation of polymeric materials in soil, developed by American Society for Testing & Materials (ASTM D-5988-18).³² This method determines under laboratory conditions

the degree and rate of biodegradation of plastics in contact with soil, measuring the carbon dioxide evolved by the microorganisms as a function of time. The soil used in the test was composed of: water (12.8%), sand (21.3%), compost (64%), and yeast extract (1.9%), which was employed as biostimulation agent. For each sample, 500 mg of polymeric sample were mixed with 200 g of prepared soil in 1000 mL hermetically-sealed glass jar. Blank jars (without polymer) and with reference material jars (microcrystalline cellulose) were also prepared. To maintain moisture content constant, a beaker with 50 mL of water was placed in each jar. Then, a 50 mL beaker filled with 30 mL of 0.5 M KOH, as a CO₂ trapping solution, was also placed in each jar. The amount of CO₂ produced during biodegradation was measured by titration of the KOH solution with 0.25 M HCl and phenolphthalein as indicator. The measurement was conducted periodically and after each titration, KOH solution was replaced with a fresh solution. Each measurement was repeated at least three times. The net CO₂ generated from the analyzed polymers was calculated by subtracting the amount of CO₂ produced in the blank soil to the amount of CO₂ produced in each jars containing the polymers at this time. The biodegradation percentages were, then, estimated from the ratio between the cumulative amount of CO₂ produced and the theoretical CO₂ production calculated on the basis of the cationic copolymers carbon content following the next Equation (1):

$$\text{Biodegradation \%} = \frac{\sum \text{CO}_2P - \sum \text{CO}_2B}{\text{CO}_2 \text{ theoretical}} \times 100 \quad (1)$$

where $\sum \text{CO}_2P$ is the cumulative CO₂ produced (mg) in the polymer jars and $\sum \text{CO}_2B$ is the cumulative CO₂ produced (mg) in the blank jar. The CO₂ produced either in the polymer jars (CO₂P) or in the blank jar (CO₂B) at each period are obtained from Equation (2):

$$\text{CO}_2P \text{ or } \text{CO}_2B = (M_{KOH}V_{KOH} - M_{HCl}V_{HCl}) \times 44/1000 \quad (2)$$

where M_{KOH} is the concentration of the KOH absorption solution (mol/L); V_{KOH} is the volume of KOH of the absorption solution; M_{HCl} is the concentration of HCl solution used to titrate the KOH solution (mol/L); V_{HCl} is the volume of HCl solution consumed in the titration of KOH solution (mL).

The theoretical amount of CO₂ that can be produced is calculated by assuming that all the carbons of the tested polymer are transformed into CO₂, then, the mg of CO₂ theoretical is determined from Equation (3):

$$mg\ of\ CO_2\ theoretical = \frac{44 \times Y}{12} \quad (3)$$

where Y is the net total theoretical carbon (C) charged to each jars (mg).

Thermal Characterization

The thermal behavior of the cationic copolymers and of the blend films PBAT/P100T-Me was studied by differential scanning calorimetry (DSC). The measurements were performed on a TA Q2000 instrument (TA Instruments, US) under dry nitrogen ($50\text{ cm}^3\cdot\text{min}^{-1}$). The samples were equilibrated at $-60\text{ }^\circ\text{C}$ and heated to $140\text{ }^\circ\text{C}$ at $10\text{ }^\circ\text{C}/\text{min}$. Then, the samples were cooled to $-60\text{ }^\circ\text{C}$ and finally a second heating scan from $-60\text{ }^\circ\text{C}$ to $140\text{ }^\circ\text{C}$ was performed at the same rate. The glass transition temperatures (T_g) of the copolymers were obtained from the second heating scan. Thermogravimetric analysis (TGA) of samples was performed on a TGA Q500 thermal analyzer (TA Instruments, US) under air atmosphere ($50\text{ cm}^3\cdot\text{min}^{-1}$), at a heating rate of $10\text{ }^\circ\text{C}\cdot\text{min}^{-1}$ from 40 to $800\text{ }^\circ\text{C}$. Temperatures at the maximum degradation rate (T_{max}) were calculated from the first derivative of the TGA curves (DTG).

Scanning Electron Microscopy

Scanning electron microscopy (SEM) images of the surface of the biopolymer film based on PBAT/P100T-Me blend (90/10) in comparison with PBAT film were taken using a Philips XL30 (The Netherlands) with an acceleration voltage of 25 kV . The films were coated with gold prior to scanning. The motivation for performing the SEM analysis on the surface of the film rather than on the cross section was because the bacteria would be in direct contact with the surface.

2.2.4 Results and discussion

Characterization of biobased copolymers derived from itaconic acid

This copolymer series demonstrated excellent activity against Gram-positive bacteria and negligible hemotoxicity, presenting more than 1000-fold selectivity for Gram-positive bacteria over human red blood cells.²³ In the current work, we examine the antibacterial activity of these cationic copolymers against an antibiotic resistant Gram-positive bacterial strain, *Staphylococcus aureus* resistant to methicillin and oxacillin (*S. aureus*, ATCC 43300). Table 1 summarizes the MIC values obtained for the cationic polymers P(TTI-co-DMI)-Me named as P100T-Me, P75T-Me, P50T-Me and P25T-Me.

Table 1. Minimum inhibition concentration (MIC) values of the cationic polymers P(TTI-co-DMI)-Me against MRSA.

Polymer	[TTI]/[DMI] ratio	MIC ($\mu\text{g mL}^{-1}$)
P100T-Me	100/0	78
P75T-Me	75/25	78
P50T-Me	50/50	78
P25T-Me	25/75	312

Remarkably, most of the cationic copolymers tested in this study were able to completely inhibit the growth of the antibiotic resistant *S. aureus* in the micromolar concentration range, with MIC values of $78 \mu\text{g mL}^{-1}$. Only the copolymer with low content of the cationic units, P25T-Me, showed moderate activity. In our previous studies, these copolymers were tested against Gram-positive *Staphylococcus aureus* (*S. aureus*, ATCC 29213), which is a standard quality-control strain in laboratory testing, sensitive to a large variety of antimicrobials, including methicillin and oxacillin. The MIC values found against this susceptible strain were smaller than those found here against the antibiotic resistant strain, with values as low as $10 \mu\text{g mL}^{-1}$ for the copolymers with high content of cationic units, P100T-Me and P75T-Me.²³ Although the copolymers presented a MIC slightly higher against the resistant strain, they were greatly effective at inhibiting bacterial growth at low concentration in comparison with other antimicrobial cationic polymers tested in literature.³³ Previous reports on quarternized polymers based on biodegradable poly(L-lactic acid) (PLLA) showed MIC values of $14\text{-}520 \mu\text{g mL}^{-1}$ against MRSAs.³⁴ Biodegradable antimicrobial cationic polycarbonates have been also tested against MRSA strains with MIC values ranged $2000\text{-}8000 \mu\text{g L}^{-1}$,³⁵ while more recently biodegradable cationic polyaspartamide derivatives exhibited MIC values in the range of $20\text{-}70 \mu\text{g mL}^{-1}$.³⁶ Therefore, this strong antibacterial activity together with their low toxicity, make these copolymers good candidates as biocompatible antimicrobial agents in biobased polymeric materials.

Biodegradability is also an important property to be studied in polymers used in areas such as food packaging and agriculture. However, biodegradability studies of polyitaconates produced by radical polymerization are currently scarce in scientific literature. Itaconix LLC company commercializes polyitaconic acid readily biodegradable

in aqueous medium as tested following methods based on biological oxygen demand (BOD) and OECD 301A Biodegradation Test.^{37,38} Hence, the biodegradability of the synthesized cationic polymers and the precursor clickable polymers was evaluated under compost conditions, following the standard method for determining aerobic degradation of plastic in soil, D5988-18. This analysis acquires great importance, for instance, in the development of materials for compostable packaging at an industrial composting plant. Under aerobic conditions, polymer degradation produces CO₂, H₂O and cellular biomass of microorganisms.³⁹ In this method, the degree of degradability was assessed by measuring the CO₂ evolved by microorganisms as function of time by applying Equations (1)-(3). The temperature was selected at 58 °C (typically used in industrial composting), at which the development of thermophilic microorganisms with higher degradation activity is preferential and the degradation rate is higher.⁴⁰ Fig. 3 shows biodegradation curves for the cationic copolymers with outstanding antibacterial properties (P100T-Me, P75T-Me, P50T-Me), and for PDMI and P100 clickable polymeric precursor, in comparison with microcrystalline cellulose used as a positive degradation standard.

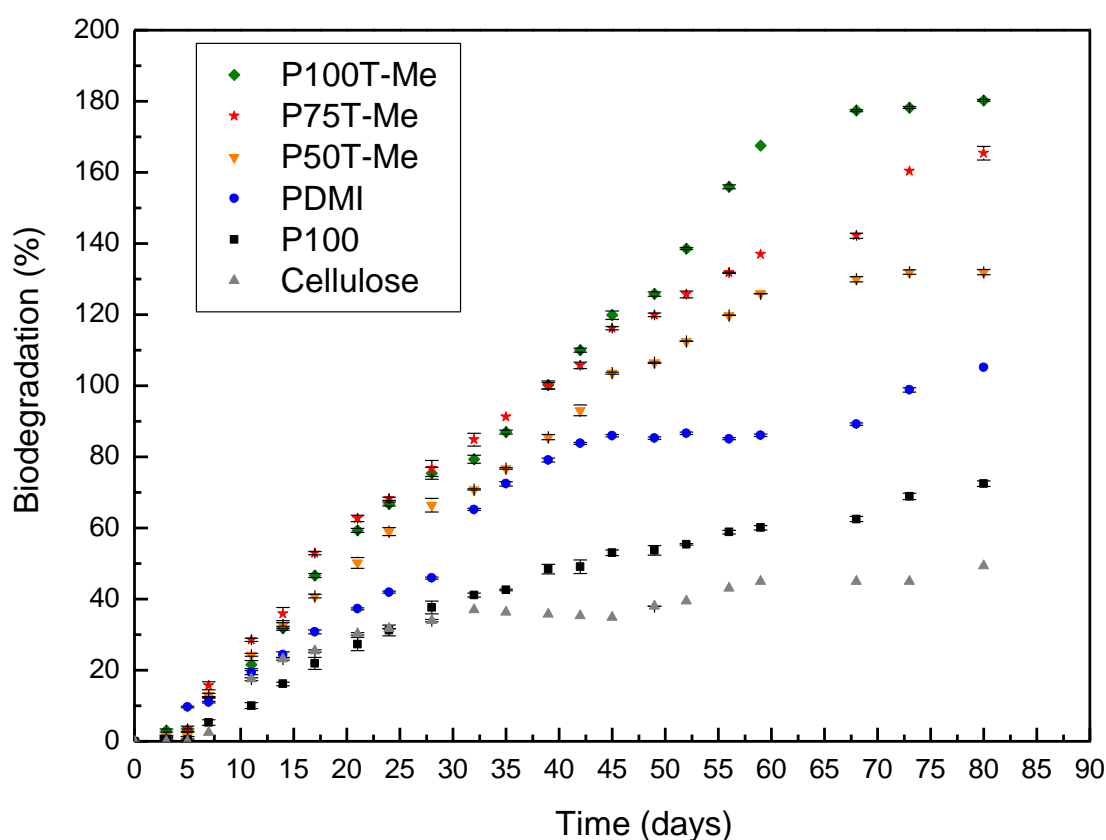


Figure 3. Biodegradation curves of the polymers derived from itaconic acid in comparison with microcrystalline cellulose sample.

It is clear that all the itaconate polymers were degraded faster than cellulose, particularly the cationic copolymers. As the content of the cationic comonomer augments in the copolymers, from PDMI to P100T-Me, the degradation rate accordingly increases. The reason of this behavior could be due to the water solubility of the cationic polymers, which may favor the degradation of the polymers. In fact, these cationic polymers reach percentage of biodegradation greater than 100%. This behavior has been previously observed in other systems and is known as priming, which occurs when the compost in the container with the samples produces more CO₂ than the compost in the blank container.⁴¹⁻⁴⁵ Thus, the produced CO₂ does not come exclusively from the polymer samples. Although the mechanism of this priming effect is not completely understood, could be associated to a stimulation of the organic matter mineralization, which is measured as released CO₂ and N mineralization.⁴⁶ The microorganisms could degrade the organic matter present in the compost by using as source of energy the carbon obtained from the degradation of the polymers. This effect has been observed in readily degradable polymers, polymers containing nitrogen and glucose.^{45,47-49} Indeed, composting is considered a biodegradation process, which is useful for waste disposal but also to supply organic material to soil. So, this priming effect observed in this work is indicative of the great susceptibility to biodegradation of these biobased polymers derived from itaconic acid. It is worthy to remark that these cationic polymers with demonstrated antibacterial character are able to biodegrade relatively fast under compost conditions, without apparently any retardation period associated. Previous studies performed on the biodegradation of polymers containing antibacterial agents such as silver particles, cinnamaldehyde or cationic components, showed that the antibacterial activity of the polymers did not prevent their biodegradation, although in some cases a retardation step was observed.^{8,10,47} The degradation of polymers involves enzymatic mechanisms, which depend on the polymer and other factors.^{39,50} Specific enzymes excreted by microorganisms such as bacteria and fungi alter the chemical and physical properties of polymers and fragment the polymer chains by bond cleavage. This is followed by the assimilation of the small residual molecules by the microorganisms and the mineralization of the metabolites producing CO₂ and H₂O. From this study, it seems that the effect that these polymers can have on the viability of the microorganisms and the excretion of enzyme is negligible, thus the secreted enzymes present in compost are able to degrade the cationic polymers very fast. On the other hand, the precursor clickable polymer P100 shows a degradation curve more similar to the cellulose profile, although the degradation

rate is slight faster. Therefore, from this study we can confirm the biodegradability of the obtained polymers derived from itaconic acid, showing that the modification of the PIA polymers does not hinder their readily biodegradability as demonstrated by Itaconix LLC company. Nevertheless, more studies are needed to evaluate the possible mechanisms of degradation.

The thermal properties of the cationic copolymers and their precursors were also investigated to evaluate the thermal behavior of these copolymers as potential biobased additives or components in biopolymeric blends. Table 2 summarizes the glass transition temperatures (T_g) of all copolymers, determined by DSC at the second heating scan. Additionally, the PDMI homopolymer was synthesized and analyzed in this study, which obtained T_g value around 95 °C matches well with those reported in other studies.²³ The incorporation of PrI clickable units leads to a decrease in the T_g values from 95 °C to 82 °C, for the P(PrI-co-DMI) copolymers, while the homopolymer P100 (100% of PrI units) exhibits a T_g as low as 65 °C. The further attachment of the pendant azoles groups by click reaction and the formation of TTI units in the copolymers decrease even more the T_g values, probably due to the flexibility of the incorporated long side chain. This decrease is more pronounced for the polymers with higher content of TTI units, P100T and P75T samples, with T_g values of 38 °C and 70 °C, respectively (see Fig. 4 as an example). Finally, the *N*-alkylating reaction provides positive charge to the polymers leading to a significant augment of the T_g values.⁵¹ This strong increase of T_g in cationic polymers such as poly(meth)acrylates or polyphosphates is typically associated to the electrostatic interactions that decrease the chain mobility.^{52,53} Thus, the resulting P(TTI-co-DMI)-Me cationic copolymers present a glassy character, with T_g higher than 100 °C except for the copolymer with the lowest content of the cationic units, P25T-Me, which practically has similar value as PDMI. Additionally, no melting transitions were observed in none of the polymers, thus, all the cationic polymers and precursors can be considered as amorphous materials.

Then, TGA analysis was carried out to evaluate the thermal stability and thermal resistance of these materials. The obtained parameters in air atmosphere, such as thermal decomposition temperature at 5% weight loss (T_{d5}), temperatures of the maximum rate of weight loss for each step (T_{dmax1} , T_{dmax2} , T_{dmax3} and T_{dmax4}) and residue percentage at 800 °C, are summarized in Table 2.

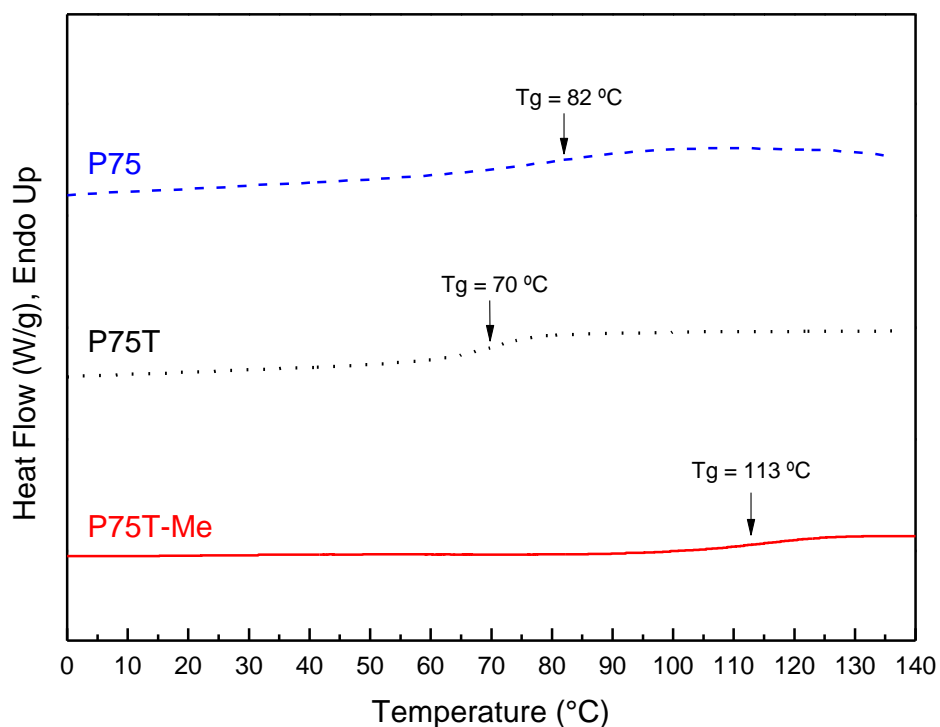


Figure 4. DSC curves for the copolymer family P75, P75T and P75T-Me.

Table 2. Thermal properties of the cationic polymers obtained by TGA and DSC.

Polymer	T _g (°C)	T _{d5} (°C)	T _{dmax1} (°C)	T _{dmax2} (°C)	T _{dmax3} (°C)	T _{dmax4} (°C)	Residue (%)
P100	65	284	332	432	-	-	30
P75	82	305	330	418	-	-	27
P50	82	300	327	394	-	-	23
P25	82	290	333	372	-	-	18
PDMI	95	283	310	343	-	-	2
P100T	38	240	272	376	430	-	24
P75T	70	247	275	381	440	-	23
P50T	82	237	270	390	426	-	19
P25T	80	244	277	386	430	-	22
P100T-Me	112	177	183	224	316	440	16
P75T-Me	113	170	171	229	303	436	16
P50T-Me	107	173	179	213	297	436	19
P25T-Me	95	182	160	200	310	432	18

It is clear from the analysis that the precursor polymers with clickable groups (P100, P75, P50 and P25) are the most stable series, with T_{d5} of around 300 °C. The copolymers present two main degradation steps, in which T_{dmax} values increase with respect to that of PDMI. The residue percentage at 800 °C increases as the content of clickable monomer augments in the copolymer. The incorporation of the azol groups, leading to the polymers P100T, P75T, P50T and P25T, drastically decreases the decomposition temperatures. Likewise, an additional degradation step was visible in the copolymers. This decrease in the T_{d5} is even more pronounced for the cationic polymers obtained by further alkylation reaction, P100T-Me, P75T-Me, P50T-Me and P25T-Me. In this series of polymers several degradation steps occurred. Fig. 5 shows, as an example, the TGA thermograms and derivative TGA curves (DTGA) of the copolymer family P50, P50T and P50T-Me.

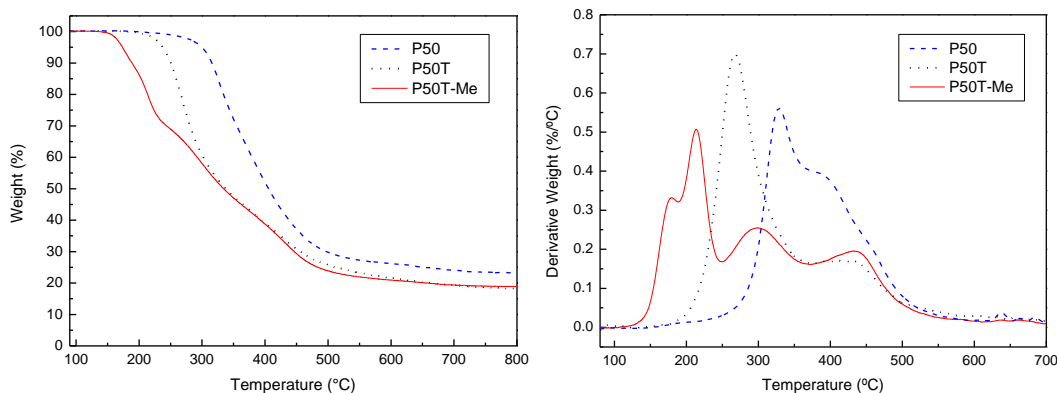


Figure 5. TGA and DTGA curves for the copolymer family P50, P50T and P50T-Me.

In the TGA graphs, all the cationic polymers presented similar degradation profiles consisting on four main degradation steps. The processes at relative low temperatures could be associated to the side chain of the cationic units, the cleavage of different chemical bonds and the volatilization of compounds. The following degradation stage at temperature range between 300 and 350 °C might be due to the cleavage of other pendant groups of the monomeric units, as well as to random scission of chemical bonds and depolymerization of chain-end unsaturated polymers, as typically found for PDMI and other itaconate derivatives. The last degradation stage at around ~430 °C could be related also to depolymerization processes of the pyrolyzed materials.⁵⁴ From these results, it is evident that all the antibacterial cationic copolymers start to degrade at temperatures below 200 °C, therefore, they can be considered as materials with a moderate thermal resistance, able to be processing at temperatures up to ~150 °C. Accordingly, these antibacterial polymers could be included as additive or minor component in formulations

of biobased/biodegradable polymers of low processing temperatures, such as poly(butylene adipate-co-terephthalate) (PBAT), poly(butylene-succinate-co-adipate) (PBSA) and starch-based biodegradable plastic resin, among others, although other processing parameters must be taken into consideration, including processing time, extruder screw speed in melt extrusion, etc.

Characterizations of biopolymeric blends based on PBAT

As a proof of concept, a biopolymeric blend of PBAT/P100T-Me (10/90) was prepared by melt extrusion process and subsequently films were obtained by compression molding at 150 °C. Fig. 1 shows the process carried out to obtain the biopolymer film containing PBAT (90 wt%) and the antibacterial biobased polymer P100T-Me (10 wt%).

Thermal characterization of the obtained blend films was performed, first by TGA. Fig. 6a displays the thermograms of the PBAT/P100T-Me blend film in comparison with a PBAT film obtained in the same processing conditions. A first degradation step associated with the cationic polymer P100T-Me is clearly observed together with degradations processes assigned to the PBAT. The weight loss of the first stage corresponding to P100T-Me was about ~10 wt%, percentage that fits well with the initial formulation. Then, the thermal properties were studied by DSC. Fig. 6b displays the second heating scan for the PBAT film and PBAT/P100T-Me blend film. In both films, it is clearly observed the glass transition and melting process of PBAT, with a glass transition temperature (T_g) and a melting temperature (T_m) values of -29 °C and 127 °C, respectively. The T_g associated with the antimicrobial polymer P100T-Me is not appreciated as overlaps with the melting of PBAT. Remarkably, incorporation of the antimicrobial polymer P100T-Me in a 10 wt% did not affect the thermal behavior of PBAT.

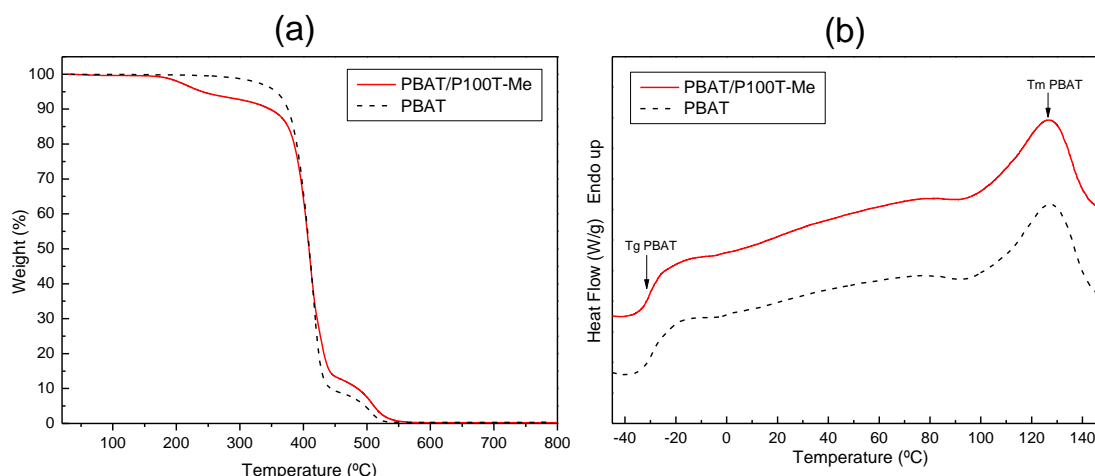


Fig. 6. a) TGA and b) DSC curves of PBAT and PBAT/P100T-Me films.

The surface of the prepared film that will be in direct contact with bacteria was analyzed by SEM in comparison with PBAT films obtained using similar processing conditions (see Fig. 7). In contrast to the PBAT films (Fig. 7a and b), the micrographs of the blend (Fig. 7c and d) reveal a textured patterned with a homogeneous dispersion of particles embedded on the film surfaces, which can be associated to the minor component P100T-Me. This functionalization of the surface with the cationic component would provide antibacterial properties to the films.

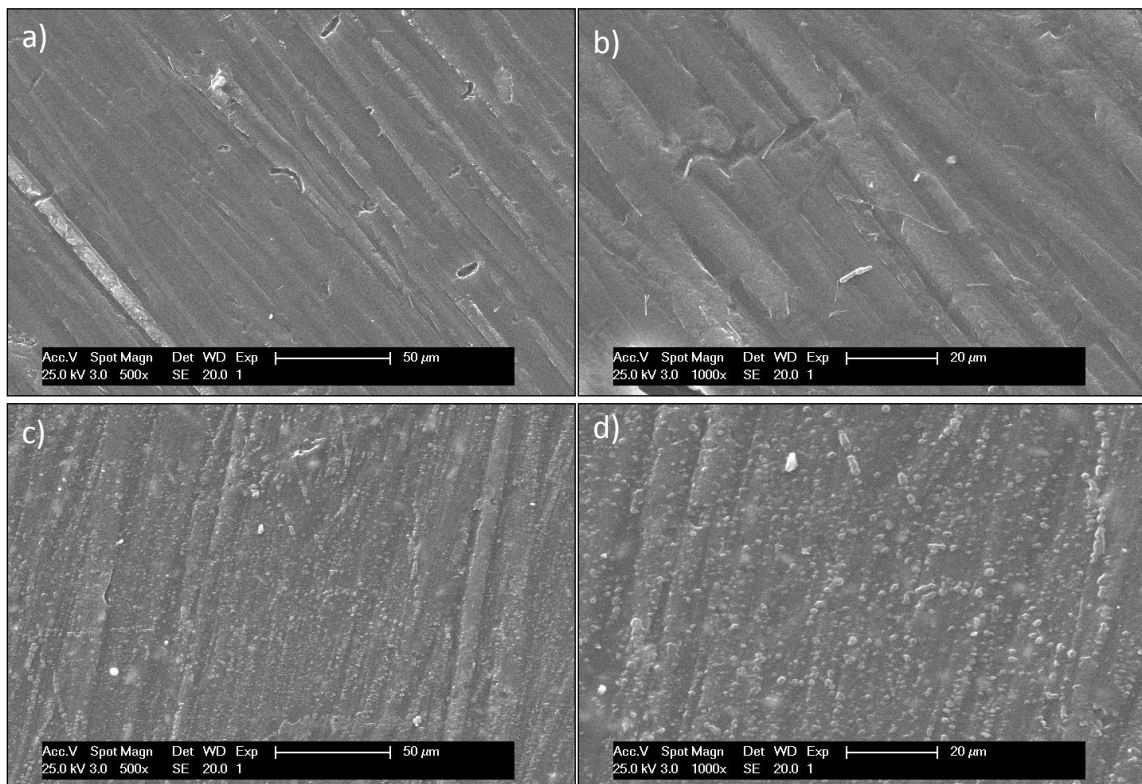


Figure 7. SEM micrographs of a) and b) PBAT film surface; c) and d) PBAT/P100T-Me film surface.

Subsequently, this film based on PBAT/P100T-Me blend (90/10) was cut into round pieces of 6 mm diameter (surface area of 0.56 cm^2) and ~5 mg weight (which means 0.5 mg of P100T-Me) to perform the antibacterial test against MRSA bacteria following the E2149-13a standard method.³¹ Fig. 8 shows the images of agar plates after spreading 1 mL of inoculum ($\sim 10^5 \text{ CFU mL}^{-1}$) in previous contact with PBAT film (control experiment) and with PBAT/P100T-Me film, and incubation.

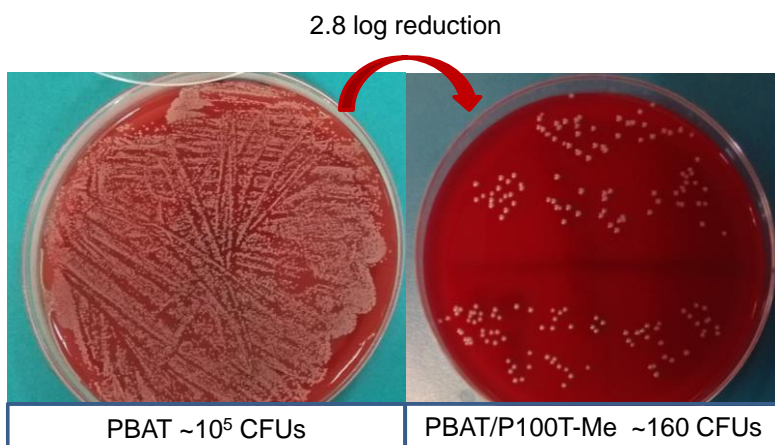


Figure 8. Pictures of the agar plates of MRSA after spreading 1 mL of inoculum in previous contact with PBAT film (left) and with PBAT/P100T-Me film (right), and incubation.

It is appreciated that the presence of the antimicrobial polymer in the film reduces bacterial counts, 2.8 log CFUs reduction is observed, which mean, that this PBAT/P100T-Me based film containing 0.9 mg cm⁻² of the antibacterial P100T-Me was able to reduce 5 log CFU cm⁻² of MRSA after 24 h of contact time, values similar to that found for other biopolymeric materials with antimicrobial agents reported in literature.^{8,55,56} These results show the potential to incorporate antibacterial biobased polymers directly into biopolymer materials to make antibacterial films in one step.

2.2.5 Conclusions

The developed cationic polymers derived from itaconic acid have demonstrated to be both effective against methicillin resistant bacteria and compostable. This antibacterial character of the copolymers did not compromise the biodegradation of the polymers in aerobic composting conditions, where a priming effect is clearly appreciated. The cationic copolymers degrade faster as the cationic unit content in the copolymers increases. The water solubility of the copolymers probably favors their degradability. To the best of our knowledge, this is the first work studying the compostability of biobased polymers with inherent antimicrobial activity. The thermal properties of the synthesized copolymers were evaluated by DSC and TGA. The incorporation of cationic azonium groups increases the T_g of the copolymers whereas drastically decreases the decomposition temperatures. Nevertheless, the copolymers can be processed at temperatures below ~150 °C, and served as a potential antimicrobial component of relative low processing temperatures biopolymeric materials. As proof of concept, the cationic copolymer with the highest TTI units was incorporated into biodegradable PBAT bioplastic, and the resulting

biocomposite film demonstrated strong antibacterial activity, achieving a 5 log reduction of antibiotic resistant bacterial strain.

2.2.6 Acknowledgments

This work was funded by the MICINN (PID2019-104600RB-I00), the Agencia Estatal de Investigación (AEI, Spain) and Fondo Europeo de Desarrollo Regional (FEDER, EU) and by CSIC (LINKA20364). A. Chiloeches acknowledges MICIU for his FPU fellowship FPU18/01776.

2.2.7 References

- (1) Walker, S.; Rothman, R. Life Cycle Assessment of Bio-Based and Fossil-Based Plastic: A Review. *J. Clean. Prod.* **2020**, 261, 121158.
- (2) Schmidt, C.; Krauth, T.; Wagner, S. Export of Plastic Debris by Rivers into the Sea. *Environ. Sci. Technol.* **2017**, 51 (21), 12246–12253.
- (3) Karan, H.; Funk, C.; Grabert, M.; Oey, M.; Hankamer, B. Green Bioplastics as Part of a Circular Bioeconomy. *Trends Plant Sci.* **2019**, 24 (3), 237–249.
- (4) RameshKumar, S.; Shaiju, P.; O'Connor, K. E.; Babu, R. Bio-Based and Biodegradable Polymers - State-of-the-Art, Challenges and Emerging Trends. *Curr. Opin. Green Sustain. Chem.* **2020**, 21, 75–81.
- (5) Bioplastics market data. https://www.european-bioplastics.org/wp-content/uploads/2016/02/Report_Bioplastics-Market-Data_2018.pdf.
- (6) Jian, J.; Xiangbin, Z.; Xianbo, H. An Overview on Synthesis, Properties and Applications of Poly(Butylene-Adipate-Co-Terephthalate)-PBAT. *Adv. Ind. Eng. Polym. Res.* **2020**, 3 (1), 19–26.
- (7) Malhotra, B.; Keshwani, A.; Kharkwal, H. Antimicrobial Food Packaging: Potential and Pitfalls. *Front. Microbiol.* **2015**, 6 (JUN), 611.
- (8) Wang, H.; Wei, D.; Zheng, A.; Xiao, H. Soil Burial Biodegradation of Antimicrobial Biodegradable PBAT Films. *Polym. Degrad. Stab.* **2015**, 116, 14–22.
- (9) Muñoz-Bonilla, A.; Echeverria, C.; Sonseca, Á.; Arrieta, M. P.; Fernández-García, M. Bio-Based Polymers with Antimicrobial Properties towards Sustainable Development. *Materials* **2019**, 12 (4), 641.
- (10) Wattanawong, N.; Aht-Ong, D. Antibacterial Activity, Thermal Behavior, Mechanical Properties and Biodegradability of Silver Zeolite/Poly(Butylene Succinate) Composite Films. *Polym. Degrad. Stab.* **2021**, 183, 109459.
- (11) Sugden, R.; Kelly, R.; Davies, S. Combatting Antimicrobial Resistance Globally. *Nat. Microbiol.* **2016**, 1 (10), 16187.
- (12) Piddock, L. J. V. V. The Crisis of No New Antibiotics-What Is the Way Forward? *Lancet Infect. Dis.* **2012**, 12 (3), 249–253.
- (13) Malheiro, J.; Simões, M. Antimicrobial Resistance of Biofilms in Medical Devices, Biofilms and Implantable Medical Devices. *Infect. Control* **2017**, 97–113.
- (14) Willyard, C. The Drug-Resistant Bacteria That Pose the Greatest Health Threats. *Nature* **2017**, 543, 7643.
- (15) Konai, M. M.; Bhattacharjee, B.; Ghosh, S.; Haldar, J. Recent Progress in Polymer Research to Tackle Infections and Antimicrobial Resistance. *Biomacromolecules* **2018**, 19 (6), 1888–1917.
- (16) Muñoz-Bonilla, A.; Fernández-García, M. Polymeric Materials with Antimicrobial Activity. *Prog. Polym. Sci.* **2012**, 37 (2), 281–339.
- (17) Ergene, C.; Yasuhara, K.; Palermo, E. F. Biomimetic Antimicrobial Polymers: Recent Advances in Molecular Design. *Polym. Chem.* **2018**, 9 (18), 2407–2427.
- (18) Arza, C. R.; Ilk, S.; Demircan, D.; Zhang, B. New Biobased Non-Ionic Hyperbranched Polymers as Environmentally Friendly Antibacterial Additives for Biopolymers. *Green Chem.* **2018**, 20 (6), 1238–1249.
- (19) Kalekar, P. P.; Geng, Z.; Finn, M. G.; Collard, D. M. Azide-Substituted Polylactide: A Biodegradable Substrate for Antimicrobial Materials via Click Chemistry Attachment of Quaternary Ammonium Groups. *Biomacromolecules* **2019**, 20 (9), 3366–3374.

- (20) Nimmagadda, A.; Liu, X.; Teng, P.; Su, M.; Li, Y.; Qiao, Q.; Khadka, N. K.; Sun, X.; Pan, J.; Xu, H.; Li, Q.; Cai, J. Polycarbonates with Potent and Selective Antimicrobial Activity toward Gram-Positive Bacteria. *Biomacromolecules* **2017**, 18 (1), 87–95.
- (21) Chin, W.; Zhong, G.; Pu, Q.; Yang, C.; Lou, W.; De Sessions, P. F.; Periaswamy, B.; Lee, A.; Liang, Z. C.; Ding, X.; Gao, S.; Chu, C. W.; Bianco, S.; Bao, C.; Tong, Y. W.; Fan, W.; Wu, M.; Hedrick, J. L.; Yang, Y. Y. A Macromolecular Approach to Eradicate Multidrug Resistant Bacterial Infections While Mitigating Drug Resistance Onset. *Nat. Commun.* **2018**, 9 (1), 917.
- (22) Smith, C. A.; Cataldo, V. A.; Dimke, T.; Stephan, I.; Guterman, R. Antibacterial and Degradable Thioimidazolium Poly(Ionic Liquid). *ACS Sustain. Chem. Eng.* **2020**, 8 (22), 8419–8424.
- (23) Chiloeches, A.; Funes, A.; Cuervo-Rodríguez, R.; López-Fabal, F.; Fernández-García, M.; Echeverría, C.; Muñoz-Bonilla, A. Biobased Polymers Derived from Itaconic Acid Bearing Clickable Groups with Potent Antibacterial Activity and Negligible Hemolytic Activity. *Polym. Chem.* **2021**, 12 (21), 3190–3200.
- (24) Cottet, C.; Salvay, A. G.; Peltzer, M. A.; Fernández-García, M. Incorporation of Poly(Itaconic Acid) with Quaternized Thiazole Groups on Gelatin-Based Films for Antimicrobial-Active Food Packaging. *Polymers* **2021**, 13 (2), 1–21.
- (25) Jr, A. I. M.; de Carvalho, J. C.; Medina, J. D. C.; Soccol, C. R.; Magalhães Jr, A. I.; de Carvalho, J. C.; Medina, J. D. C.; Soccol, C. R. Downstream Process Development in Biotechnological Itaconic Acid Manufacturing. *Appl. Microbiol. Biotechnol.* **2017**, 101 (1), 1–12.
- (26) Cunha da Cruz, J.; Machado de Castro, A.; Camporese Sérvulo, E. F.; da Cruz, J. C.; de Castro, A. M.; Sérvulo, E. F. C. World Market and Biotechnological Production of Itaconic Acid. *3 Biotech* **2018**, 8 (3), 138.
- (27) Simões, M. F.; Pinto, R. M. A. A.; Simões, S. Hot-Melt Extrusion in the Pharmaceutical Industry: Toward Filing a New Drug Application. *Drug Discov. Today* **2019**, 24 (9), 1749–1768.
- (28) CLSI, Methods for Dilution Antimicrobial Susceptibility Tests for Bacteria That Grow Aerobically, Approved Standard-Ninth Edition, CLSI Document M07-A9; Clinical and Laboratory Standards Institute: Wayne, PA, **2012**.
- (29) Tejero, R.; López, D.; López-Fabal, F.; Gómez-Garcés, J. L.; Fernández-García, M. Antimicrobial Polymethacrylates Based on Quaternized 1,3-Thiazole and 1,2,3-Triazole Side-Chain Groups. *Polym. Chem.* **2015**, 6 (18), 3449–3459.
- (30) Álvarez-Paino, M.; Muñoz-Bonilla, A.; López-Fabal, F.; Gómez-Garcés, J. L.; Heuts, J. P.; Fernández-García, M. Effect of Glycounits on the Antimicrobial Properties and Toxicity Behavior of Polymers Based on Quaternized DMAEMA. *Biomacromolecules* **2015**, 16 (1), 295–303.
- (31) ASTM E2149-13a, Standard Test Method for Determining the Antimicrobial Activity of Antimicrobial Agents Under Dynamic Contact Conditions; ASTM International: West Conshohocken, PA, **2013**.
- (32) ASTM D5988, Standard Test Method for Determining Aerobic Biodegradation of Plastic Materials in Soil; ASTM International: West Conshohocken, PA, **2018**.
- (33) Kanth, S.; Nagaraja, A.; Puttaiahgowda, Y. M. Polymeric Approach to Combat Drug-Resistant Methicillin-Resistant Staphylococcus Aureus. *J. Mater. Sci.* **2021**, 56 (12), 7265–7285.
- (34) Li, Z.; Chee, P. L.; Owh, C.; Lakshminarayanan, R.; Loh, X. J. Safe and Efficient Membrane Permeabilizing Polymers Based on PLLA for Antibacterial Applications. *RSC Adv.* **2016**, 6 (34), 28947–28955.
- (35) Cheng, J.; Chin, W.; Dong, H.; Xu, L.; Zhong, G.; Huang, Y.; Li, L.; Xu, K.; Wu, M.; Hedrick, J. L.; Yang, Y. Y.; Fan, W. Biodegradable Antimicrobial Polycarbonates with In Vivo Efficacy against Multidrug-Resistant MRSA Systemic Infection. *Adv. Healthc. Mater.* **2015**, 4 (14), 2128–2136.
- (36) Yan, S.; Chen, S.; Gou, X.; Yang, J.; An, J.; Jin, X.; Yang, Y.; Chen, L.; Gao, H. Biodegradable Supramolecular Materials Based on Cationic Polyaspartamides and Pillar[5]Arene for Targeting

- Gram-Positive Bacteria and Mitigating Antimicrobial Resistance. *Adv. Funct. Mater.* **2019**, 29 (38), 1904683.
- (37) Hughes, K. A.; Swift, G. Process for Polymerization of Itaconic Acid. US5223592A, June 29, **1993**.
- (38) Rice, E. W. W.; Baird, R. B. B.; Eaton, A. D. D. Standar Methods for the Examination of Water and Wastewater, sixteenth.; **1985**.
- (39) Pathak, V. M.; Navneet. Review on the Current Status of Polymer Degradation: A Microbial Approach. *Bioresour. Bioprocess.* **2017**, 4 (1), 1–31.
- (40) da Silva, S. A.; Hinkel, E. W.; Lisboa, T. C.; Selistre, V. V.; da Silva, A. J.; da Silva, L. O. F.; Faccin, D. J. L.; Cardozo, N. S. M. A Biostimulation-Based Accelerated Method for Evaluating the Biodegradability of Polymers. *Polym. Test.* **2020**, 91, 106732.
- (41) Kuzyakov, Y.; Friedel, J. K.; Stahr, K. Review of Mechanisms and Quantification of Priming Effects. *Soil Biol. Biochem.* **2000**, 32 (11–12), 1485–1498.
- (42) Kuzyakov, Y. Priming Effects: Interactions between Living and Dead Organic Matter. *Soil Biol. Biochem.* **2010**, 42 (9), 1363–1371.
- (43) Fontaine, S.; Mariotti, A.; Abbadie, L. The Priming Effect of Organic Matter: A Question of Microbial Competition? *Soil Biol. Biochem.* **2003**, 35 (6), 837–843.
- (44) Benyathiar, P.; Selke, S.; Auras, R. The Effect of Gamma and Electron Beam Irradiation on the Biodegradability of PLA Films. *J. Polym. Environ.* **2016**, 24 (3), 230–240.
- (45) Bher, A.; Unalan, I. U.; Auras, R.; Rubino, M.; Schvezov, C. E. Graphene Modifies the Biodegradation of Poly(Lactic Acid)-Thermoplastic Cassava Starch Reactive Blend Films. *Polym. Degrad. Stab.* **2019**, 164, 187–197.
- (46) Blagodatskaya, E.; Kuzyakov, Y. Mechanisms of Real and Apparent Priming Effects and Their Dependence on Soil Microbial Biomass and Community Structure: Critical Review. *Biol. Fertil. Soils* **2008**, 45 (2), 115–131.
- (47) Balaguer, M. P.; Villanova, J.; Cesar, G.; Gavara, R.; Hernandez-Munoz, P. Compostable Properties of Antimicrobial Bioplastics Based on Cinnamaldehyde Cross-Linked Gliadins. *Chem. Eng. J.* **2015**, 262, 447–455.
- (48) Plackett, D. V.; Holm, V. K.; Johansen, P.; Ndoni, S.; Nielsen, P. V.; Sipilainen-Malm, T.; Södergård, A.; Verstichel, S. Characterization of L-Polylactide and L-Polylactide-Polycaprolactone Co-Polymer Films for Use in Cheese-Packaging Applications. *Packag. Technol. Sci.* **2006**, 19 (1), 1–24.
- (49) Cano, A. I.; Cháfer, M.; Chiralt, A.; González-Martínez, C. Biodegradation Behavior of Starch-PVA Films as Affected by the Incorporation of Different Antimicrobials. *Polym. Degrad. Stab.* **2016**, 132, 11–20.
- (50) Kliem, S.; Kreutzbruck, M.; Bonten, C. Review on the Biological Degradation of Polymers in Various Environments. *Materials* **2020**, 13 (20), 4586.
- (51) Tejero, R.; Gutiérrez, B.; López, D.; López-Fabal, F.; Gómez-Garcés, J. L.; Muñoz-Bonilla, A.; Fernández-García, M. Tailoring Macromolecular Structure of Cationic Polymers towards Efficient Contact Active Antimicrobial Surfaces. *Polymers* **2018**, 10 (3), 241.
- (52) Cuervo-Rodríguez, R.; Muñoz-Bonilla, A.; Araujo, J.; Echeverría, C.; Fernández-García, M. Influence of Side Chain Structure on the Thermal and Antimicrobial Properties of Cationic Methacrylic Polymers. *Eur. Polym. J.* **2019**, 117, 86–93.
- (53) Tsutsi, T.; Sato, T.; Tanaka, T. Glass Transition in Aliphatic Lonenes. *Polym. J.* **1973**, 5 (3), 332–334.
- (54) Bonardd, S.; Alegria, A.; Saldias, C.; Leiva, A.; Kortaberria, G. Polyitaconates: A New Family of “All-Polymer” Dielectrics. *ACS Appl. Mater. Interfaces* **2018**, 10 (44), 38476–38492.

- (55) Aytac, Z.; Huang, R.; Vaze, N.; Xu, T.; Eitzer, B. D.; Krol, W.; MacQueen, L. A.; Chang, H.; Bousfield, D. W.; Chan-Park, M. B.; Ng, K. W.; Parker, K. K.; White, J. C.; Demokritou, P. Development of Biodegradable and Antimicrobial Electrospun Zein Fibers for Food Packaging. *ACS Sustain. Chem. Eng.* **2020**, 8 (40), 15354–15365.
- (56) Fu, Y.; Dudley, E. G. Antimicrobial-Coated Films as Food Packaging: A Review. *Compr. Rev. Food Sci. Food Saf.* **2021**, 20 (4), 3404–3437.

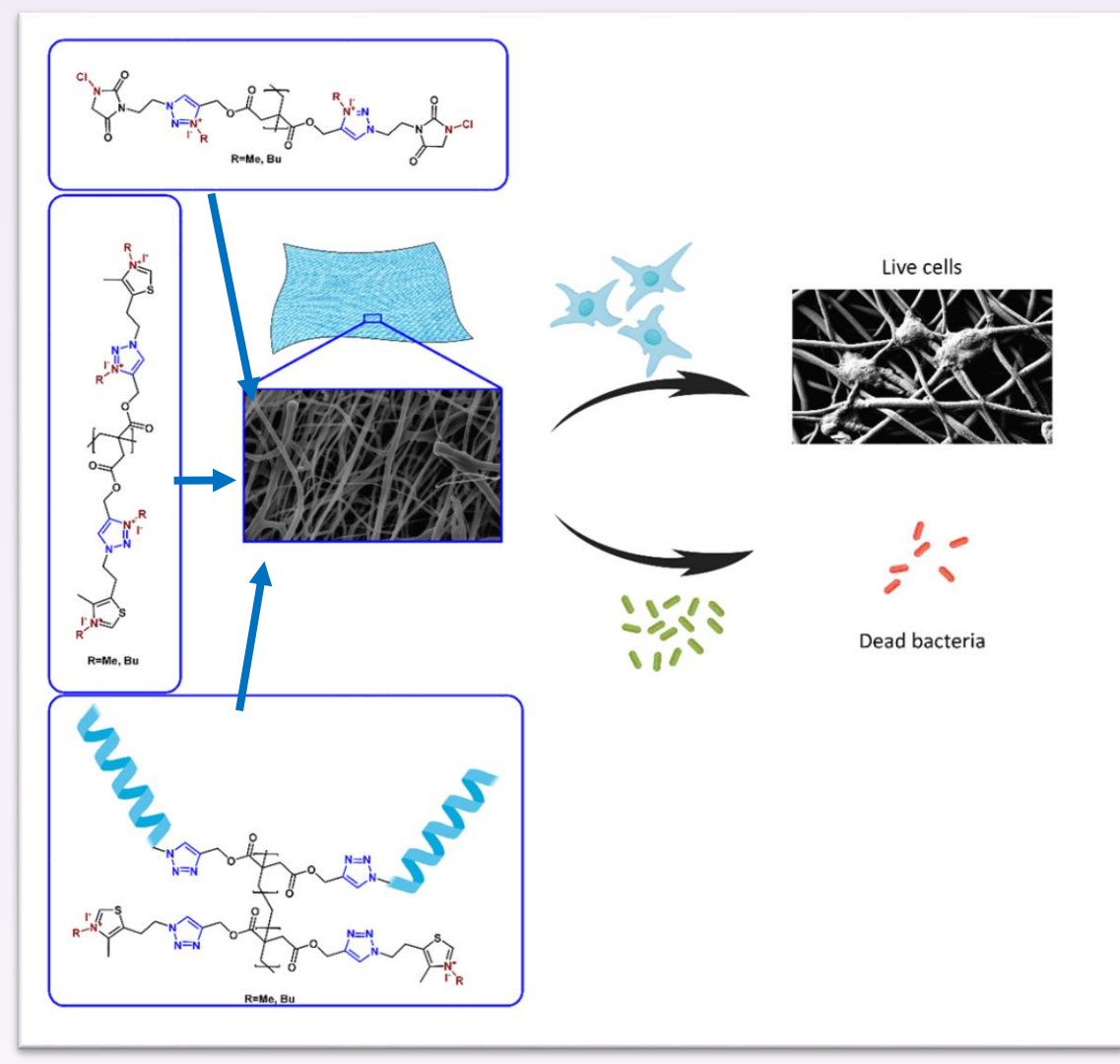
Capítulo 3

Fibras electrohiladas de PLA y PBAT con polímeros biobasados antimicrobianos

3.1 PLA and PBAT-based electrospun fibers functionalized with antibacterial bio-based polymers

3.2 Electrospun polylactic acid-based fibers loaded with multifunctional antibacterial biobased polymers

3.3 Synergistic combination of antimicrobial peptides and cationic polyitaconates in multifunctional PLA fibers



3.1 PLA and PBAT-Based Electrospun Fibers Functionalized with Antibacterial Bio-Based Polymers

Macromolecular Bioscience 2022, 2200401

RESEARCH ARTICLE



10165195; 0. Downloaded from https://onlinelibrary.wiley.com/doi/10.1002/mabi.202200401 by Csic Organicas Central On (Oficina Mayo) [UCL] Wiley Online Library on [12/12/2022]. See the Terms and Conditions (https://onlinelibrary.wiley.com/terms-and-conditions) on Wiley Online Library for rules of use. OA articles are governed by the applicable Creative Commons License.

PLA and PBAT-Based Electrospun Fibers Functionalized with Antibacterial Bio-Based Polymers

A. Chiloeches, R. Fernández-García, M. Fernández-García, A. Mariano, I. Bigioni,
A. Scotto d'Abusco,* C. Echeverría,* and A. Muñoz-Bonilla*

Antimicrobial fibers based on biodegradable polymers, poly(lactic acid) (PLA), and poly(butylene adipate-co-terephthalate) (PBAT) are prepared by electrospinning. For this purpose, a biodegradable/bio-based polyitaconate containing azoles groups (PTT) is incorporated at 10 wt.% into the electrospinning formulations. The resulting fibers functionalized with azole moieties are uniform and free of beads. Then, the accessible azole groups are subjected to *N*-alkylation, treatment that provides cationic azonium groups with antibacterial activity at the surface of fibers. The positive charge density, roughness, and wettability of the cationic fibers are evaluated and compared with flat films. It is confirmed that these parameters exert an important effect on the antimicrobial properties, as well as the length of the alkylating agent and the hydrophobicity of the matrix. The quaternized PLA/PTT fibers exhibit the highest efficiency against the tested bacteria, yielding a 4-Log reduction against *S. aureus* and 1.7-Log against MRSA. Then, biocompatibility and bioactivity of the fibers are evaluated in terms of adhesion, morphology and viability of fibroblasts. The results show no cytotoxic effect of the samples, however, a cytostatic effect is appreciated, which is ascribed to the strong electrostatic interactions between the positive charge at the fiber surface and the negative charge of the cell membranes.

1. Introduction

Polymeric fibers produced by electrospinning have been extensively studied in the past years for biomedical applications such as artificial vessels, scaffolds, and fibrous wound dressings and matrices because they present several advantages over traditional

products.^[1–3] Electrospinning is a very versatile technique that fabricates fiber with nano- to micrometer range diameters and controlled surface morphology, leading mats with unique characteristics: i) high specific surface area, ii) porous structure, which allows desired permeability and exudation, and iii) structure similar to an extracellular matrix that favors the cell attachment and proliferation. Besides, electrospinning allows the incorporation of additional functionalities into fibers, such as bioactive components, growth factors, or antimicrobial compounds that would improve the performance of these materials in biomedical applications such as wound dressing uses. In fact, wound infection is one of the major risk factors for wound healing failure, and complications in chronic wounds. Also, microbial contamination of implants, vessels, meshes of other devices provokes devastating infections, sepsis and often requires prompt removal of the devices. The incorporation of antimicrobial agents into biomaterials could help to combat these problems.^[4–9] In the design of

such products for clinical applications, biodegradable and biocompatible polymers, including poly(lactic acid) (PLA), polycaprolactone (PCL), poly(glycolic acid) (PGA), or poly(butylene adipate-co-terephthalate) (PBAT), are gaining increased importance as they metabolize in human body into biocompatible degradation products, and second surgery for removal is unnecessary.^[10,11]

A. Chiloeches, M. Fernández-García, C. Echeverría, A. Muñoz-Bonilla
Instituto de Ciencia y Tecnología de Polímeros (ICTP-CSIC)
C/ Juan de la Cierva 3, Madrid 28006, Spain
E-mail: cecheverria@ictp.csic.es; sbonilla@ictp.csic.es

The ORCID identification number(s) for the author(s) of this article can be found under <https://doi.org/10.1002/mabi.202200401>
© 2022 The Authors. *Macromolecular Bioscience* published by Wiley-VCH GmbH. This is an open access article under the terms of the Creative Commons Attribution License, which permits use, distribution and reproduction in any medium, provided the original work is properly cited.

DOI: 10.1002/mabi.202200401

A. Chiloeches
Escuela Internacional de Doctorado de la Universidad Nacional de Educación a Distancia (UNED)
C/ Bravo Murillo, 38, Madrid 28015, Spain
R. Fernández-García
Hospital Universitario de Móstoles C/ Dr. Luis Montes s/n, Móstoles, Madrid 28935, Spain
M. Fernández-García, C. Echeverría, A. Muñoz-Bonilla
Interdisciplinary Platform for Sustainable Plastics towards a Circular Economy-Spanish National Research Council (SusPlast-CSIC)
Madrid Spain
A. Mariano, I. Bigioni, A. Scotto d'Abusco
Department of Biochemical Sciences
Sapienza University of Rome
P.R. Moro, 5, Rome 00185, Italy
E-mail: anna.scottodabusco@uniroma1.it

3.1.1 Abstract

Antimicrobial fibers based on biodegradable polymers, poly(lactic acid) (PLA), and poly(butylene adipate-co-terephthalate) (PBAT) are prepared by electrospinning. For this purpose, a biodegradable/bio-based polyitaconate containing azoles groups (PTTI) (PTTI, previously named P100T) is incorporated at 10 wt % into the electrospinning formulations. The resulting fibers functionalized with azole moieties are uniform and free of beads. Then, the accessible azole groups are subjected to N-alkylation, treatment that provides cationic azolium groups with antibacterial activity at the surface of fibers. The positive charge density, roughness, and wettability of the cationic fibers are evaluated and compared with flat films. It is confirmed that these parameters exert an important effect on the antimicrobial properties, as well as the length of the alkylating agent and the hydrophobicity of the matrix. The quaternized PLA/PTTI fibers exhibit the highest efficiency against the tested bacteria, yielding a 4-Log reduction against *S. aureus* and 1.7-Log against MRSA. Then, biocompatibility and bioactivity of the fibers are evaluated in terms of adhesion, morphology and viability of fibroblasts. The results show no cytotoxic effect of the samples; however, a cytostatic effect is appreciated, which is ascribed to the strong electrostatic interactions between the positive charge at the fiber surface and the negative charge of the cell membranes.

3.1.2 Introduction

Polymeric fibers produced by electrospinning have been extensively studied in the past years for biomedical applications such as artificial vessels, scaffolds, and fibrous wound dressings and matrices because they present several advantages over traditional products.¹⁻³ Electrospinning is a very versatile technique that fabricates fiber with nano-to micrometer range diameters and controlled surface morphology, leading mats with unique characteristics: i) high specific surface area, ii) porous structure, which allows desired permeability and exudation, and iii) structure similar to an extracellular matrix that favors the cell attachment and proliferation. Besides, electrospinning allows the incorporation of additional functionalities into fibers, such as bioactive components, growth factors, or antimicrobial compounds that would improve the performance of these materials in biomedical applications such as wound dressing uses. In fact, wound infection is one of the major risk factors for wound healing failure, and complications in chronic wounds. Also, microbial contamination of implants, vessels, meshes of other devices provokes devastating infections, sepsis and often requires prompt removal of the devices. The incorporation of antimicrobial agents into biomaterials could help to combat these problems.⁴⁻⁹ In the design of such products for clinical applications, biodegradable and biocompatible polymers, including polylactic acid (PLA), polycaprolactone (PCL), poly(glycolic acid) (PGA), or poly(butylene adipate-co-terephthalate) (PBAT), are gaining increased importance as they metabolize in human body into biocompatible degradation products, and second surgery for removal is unnecessary.^{10,11}

Among all, PLA is one of the most widely used biopolymers due to its processing properties, full biodegradability, biocompatibility, and because it is approved for clinical use.¹² Although PLA has favorable mechanical properties, neat PLA exhibits brittleness with poor impact. PBAT, a biodegradable aliphatic-aromatic copolyester, is more flexible and has high elongation at break; however, has low tensile modulus. Both polymers have been also blended together to develop materials with enhanced mechanical properties.^{13,14} PBAT, as PLA, is biocompatible but has been scarcely studied as a biomaterial for medical applications. Anyhow, PLA and PBAT have hydrophobic nature, lack of cell recognition signals, and their cell adhesion, proliferation and differentiation properties are poor.^{12,15-17} Incorporation of bioactive compounds, such as hydroxyapatite, heparin and hyaluronic acid, inside the polymer matrix or at the surface of the materials are a promising strategy to improve hydrophilicity and biocompatibility.^{18,19} However, other bioactive compounds, such as antimicrobial agents, could compromise the

biocompatibility and biodegradability. Traditionally, quaternary ammonium salts, phosphonium salts, metal ions, and antibiotics are employed to impart antimicrobial activity to materials;²⁰⁻²² however, their use is normally accompanied by residual toxicity or a rapid increase in bacterial resistance. Antimicrobial polymers offer some important advantages, such as thermal and chemical stability, long-term activity, and lower level of bacterial resistance.^{23,24} Nevertheless, most of the reported antimicrobial polymers are derived from petroleum-sources, which jeopardize the biodegradability of the final material and might also affect the biocompatibility.

In this work, an antibacterial bio-based and biodegradable polymer derived from itaconic acid was employed to impart antibacterial character to PLA and PBAT fiber mats obtained by electrospinning. In addition, for comparative purpose, this antibacterial polymer was incorporated into flat PBAT-based films prepared by melt-extrusion and compression molding. Then, we studied the interactions between these functionalized materials with bacteria and eukaryotic fibroblast cells to determine their antimicrobial efficacy, bioactivity and safety for biomedical applications.

3.1.3 Results and discussion

Preparation of antimicrobial electrospun fibers based on PLA/PTTI and PBAT/PTTI.

The bio-based antimicrobial polymers, poly(bis((1-(2-(4-methylthiazol-5-yl)ethyl)-1H-1,2,3-triazol-4-yl)methyl) itaconate) quaternized with methyl and butyl iodide, PTTI-Me and PTTI-Bu, respectively, previously developed by our group were initially employed to impart antibacterial activity to PLA and PBAT electrospun fibers (Figure 1).

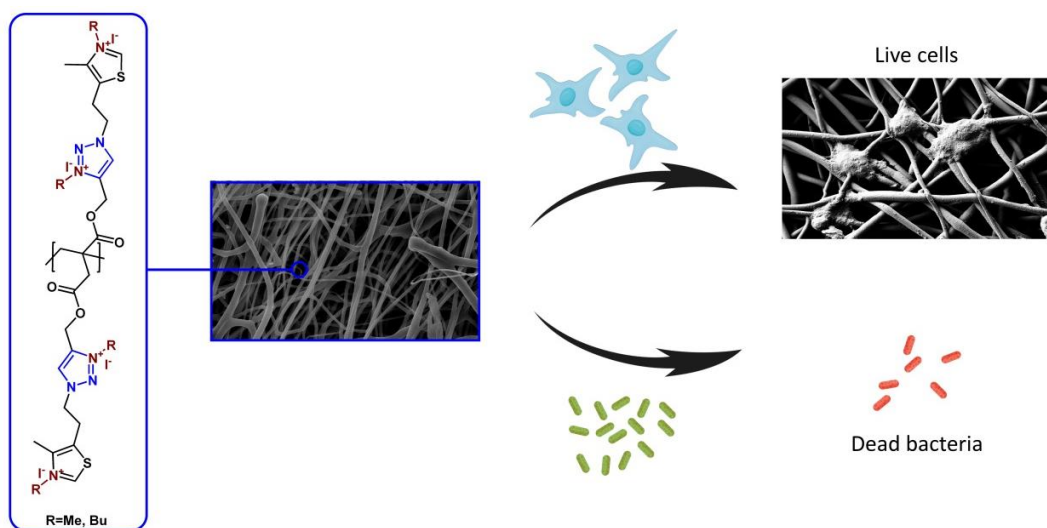


Figure 1. Schematic representation of functionalized polymeric fibers with PTTI-Me and PTTI-Bu derivatives and their interactions with cells and bacteria.

However, the antibacterial polymers PTTI-Me and PTTI-Bu containing cationic groups were not soluble in the solvent mixture compatible with PLA and PBAT employed in the electrospinning process. Therefore, to avoid heterogeneity and aggregation problems, we used the antibacterial precursor PTTI polymer, which is neutrally charged and soluble in the electrospinning solution. Thus, this polymer was incorporated into the CHCl₃/DMF (9:1) solvent mixture at 10 wt % together with 90 wt % of PLA or PBAT, at a total polymer concentration of 20 wt %. Subsequently, from these solutions, PLA or PBAT-based fibers loaded with the PTTI polymer bearing triazole groups were successfully obtained by electrospinning. Likewise, PLA and PBAT fibers were also prepared under similar conditions and used for comparison purpose. Figure 2 displays scanning electron microscopy (SEM) images of all prepared fibers. We can appreciate that the incorporation of the PTTI polymer reduces the diameter of the obtained fibers in both cases, PLA and PBAT-based fibers. While the average diameter of electrospun PLA fibers was $4 \pm 1 \mu\text{m}$, the PLA/PTTI fibers present a value of $3.5 \pm 1.2 \mu\text{m}$. Similarly, the average diameter diminishes from $3 \pm 1 \mu\text{m}$ for PBAT fibers to $2.1 \pm 0.6 \mu\text{m}$ for PBAT/PTTI fibers. The addition of this cationic polymer into the electrospinning solutions may modify characteristics such as viscosity, density, conductivity solution, and factors that affect the final fiber diameter.²⁵ Although the homogeneity is somehow reduced with the incorporation of the PTTI polymers, bead-free and uniform fibers with smooth surfaces were obtained (see insets of figures for higher magnification images).

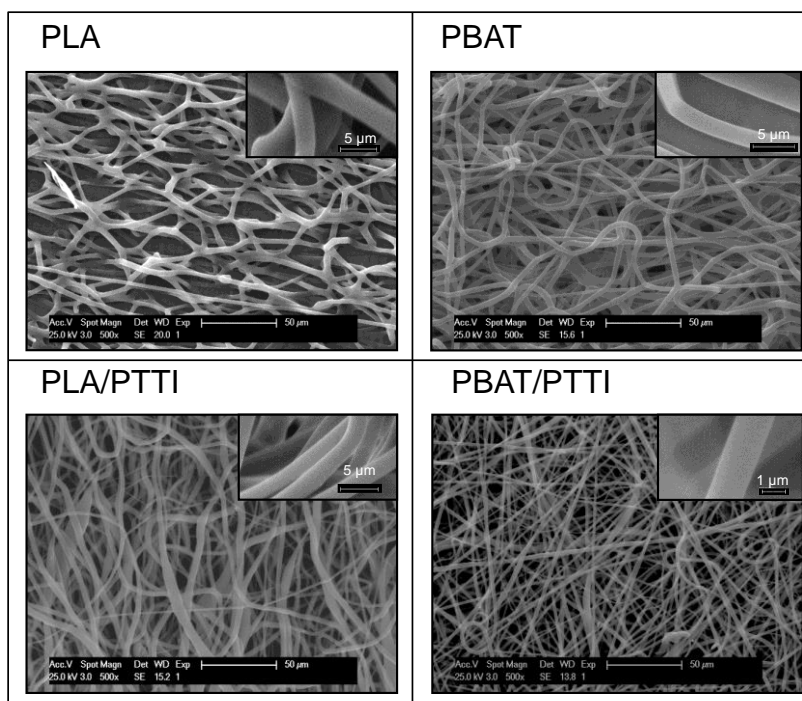


Figure 2. SEM images of PLA, PBAT, PLA/PTTI and PBAT/PTTI electrospun fibers.

Fourier transform infrared (FTIR) spectroscopy was employed to confirm that the polymers did not undergo any degradation during the electrospinning process. FTIR spectra displayed in Figure S1 (Supporting Information) show that PLA and PBAT-based fibers exhibit the band characteristics of such polymers without any evidence of degradation. PLA/PTTI and PBAT/PTTI have almost identical spectra, and new bands associated to PTTI polymers were not visible due to the low content of this polymer and overlapping of the signal. To confirm the presence of PTTI in the fibers, extractions with DMSO-d₆ were performed and analyzed by ¹H-nuclear magnetic resonance (NMR) spectroscopy. Figure S2 (Supporting Information) shows the ¹H-NMR spectrum of PTTI polymer and the signal assignment, demonstrating the stability of the polymer throughout the electrospinning process.

The PBAT and PLA-based fibers loaded with PTTI polymer precursor were subsequently surface functionalized to provide antimicrobial activity. *N*-alkylation reaction of the triazole and thiazole groups available at the surface was carried out with iodomethane or iodobutane to afford the corresponding cationic azolium groups (PLA/PTTI-Me, PLA/PTTI-Bu, PBAT/PTTI-Me, and PBAT/PTTI-Bu). These positively charged chains are responsible of the antimicrobial character as they can interact with the negatively charged membrane causing cell leakage and eventually bacterial death.^{26,27} The success of the quaternization reaction at the surface of the fibers was confirmed by ¹H-NMR spectroscopy of the quaternized PTTI extracted in DMSO-d₆ (Figure S2, Supporting information), in which the peaks associated to azolium groups (~10.08 and ~9.20 ppm) can be observed. Positive charge density of the surface has a large influence on the killing efficiency charge densities of greater than $1\text{-}5 \times 10^{15}$ are typically needed for a good activity;^{28,29} therefore, these positive charges were quantified by measuring the accessible cationic units able to selectively bind anionic fluorescein molecules. The fluorescein adsorbed on the surface was subsequently desorbed with cetyltrimethylammonium bromide (CTAB) and quantified by UV-vis spectroscopy. Table 1 summarizes the charge density obtained at the surface of PLA and PBAT-based fibers after *N*-alkylation reaction with two different alkylating agents. The estimated charge density at the surface of fibers was found to be $\sim 10^{14}\text{-}10^{15}\text{ N}^+ \text{ cm}^{-2}$, values near to other contact-active antibacterial surfaces.³⁰ Remarkably, the fibers quaternized with iodomethane exhibit values higher than $10^{15}\text{ N}^+ \text{ cm}^{-2}$, thus, sufficient charge to disrupt the bacterial cell wall and hence high antibacterial activity. It is clearly appreciated that charge density lowered drastically when the quaternization reaction was performed with

iodobutane, which is consistent with the general trend observed that the degree of quaternization decreases with increasing size of the alkylating agent due to steric effect.³¹

The roughness of the obtained fiber mats was also measured as a key parameter influencing the bioactivity of the material surface. Figure 3 displays the surface roughness, R_a , of the mats and its correlation with the fiber diameter.

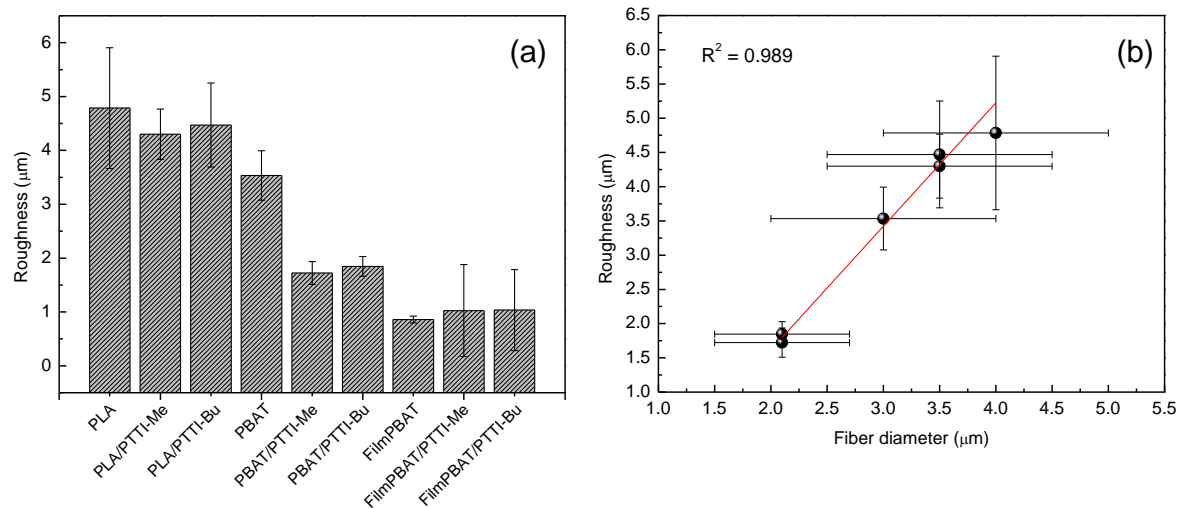


Figure 3. a) Roughness R_a of the obtained fiber mats and films and b) roughness values compared to the fiber diameter (the red line is a linear trend line with corresponding R^2 value).

The roughness of the fiber mats loaded with the polyitaconate antimicrobial polymers (PTT1-Me and PTT1-Bu) is lower than that of neat PLA and PBAT fibers. As previously reported and clearly observed in Figure 3b, the surface roughness measured in electrospun fibers was found to augment with the diameter of the constituent fibers.³² As expected, no differences were found between methylated and butylated samples, because the fibers were subjected to surface modification by *N*-alkylation reaction in a post-electrospinning reaction, and the fiber diameter did not vary. Surface roughness also plays an important role in the wettability of a surface, which will affect the contact and interactions between surface and biological environment.³³ Then, water contact angles were measured to assess the surface wettability of the obtained fiber mats and films. Figure 4 collects the obtained contact angle values for all the tested materials. It is clearly seen that electrospun fibers exhibited very high water contact angles due to the surface roughness, as previously reported.^{34,35} Slight differences in the contact angle values can be observed between PLA- and PBAT-based fibers due to the smaller diameters found for PBAT-based fibers and also due to the higher hydrophobicity of PBAT in comparison with PLA. The decrease in the fiber diameters causes an increase in contact angle because the topography influences air entrapment between the fiber interfaces and

hence modifies the liquid-solid interface.³⁴ As expected, PBAT films with smooth surfaces exhibit much lower contact angle values than fiber mats. However, the differences found between functionalized surfaces with polyitaconate derivatives and non-functionalized samples were not significant, suggesting that the predominant factors affecting wettability are the topography and surface roughness as observed in other studies.³⁵

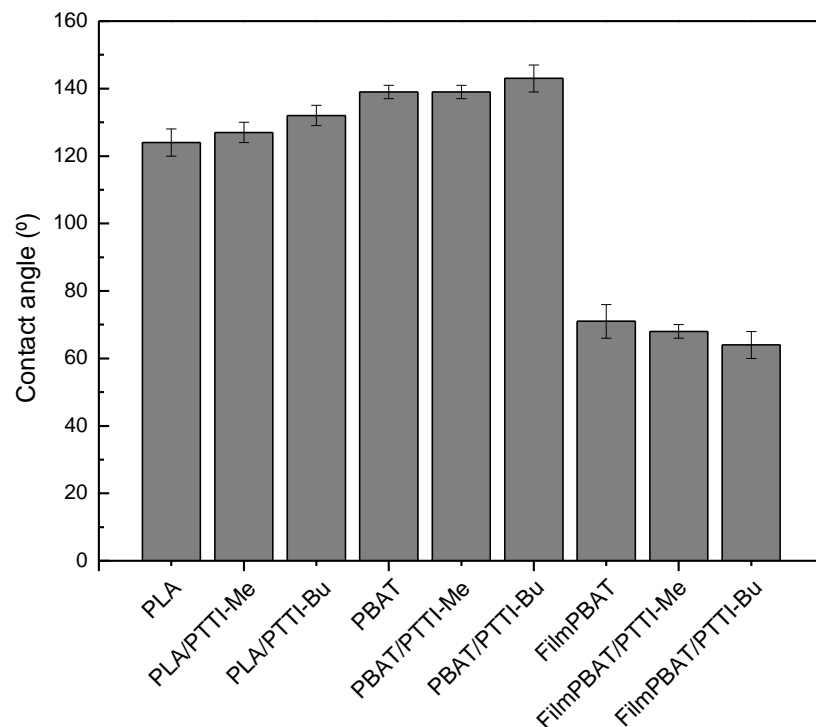


Figure 4. Contact angle measurements of the obtained fiber mats and films.

Preparation of antimicrobial films based on PBAT/PTTI.

Subsequently, biodegradable antimicrobial films were prepared through the incorporation of the polyitaconate derivatives into the biopolymers, by melt extrusion followed by compression molding. However, these polyitaconate derivatives exhibit moderate thermal resistance with degradation temperatures below 200 °C.³⁶ For this reason, these antimicrobial polymers can be only used in processing treatments up to ~150 °C. Accordingly, in this work, PTTI-Me and PTTI-Bu antibacterial polymers were only incorporated in PBAT films, a biodegradable polymer of low processing temperature, whereas PLA films could not perform due to its processing temperature ~200 °C. Thus, PTTI-Me and PTTI-Bu (10 wt %) were directly extruded together with PBAT pellets and then films were obtained via compression molding. The films obtained were labeled as FilmPBAT/PTT1-Me and FilmPBAT/PTT1-Bu. The FTIR spectra of the resulting films confirmed that the polymers did not suffer any appreciable degradation process during

extrusion and compression molding (see Figure S3, Supporting Information). Subsequently, the number of cationic groups accessible at the surface of the films, which are responsible of the antimicrobial character, was estimated from the titration method using fluorescein as described above. In this case, similar charge density was obtained from films functionalized with methylated PTTI-Me and butylated PTTI-Bu, 9×10^{14} and $8 \times 10^{14} \text{ N}^+ \text{ cm}^{-2}$, respectively, because the polyitaconate were previously and almost completely quaternized before the blend extrusion process with PBAT. Remarkably, in these films containing the cationic polymers with high number of positive charge, the surface charge is much lower than that obtained in the PLA/PTTI-Me fibers, in which, in principle, only the thiazole and triazole groups available at the surface were quaternized. This can be explained by the large surface area of the fiber mats in comparison with the films. Besides and as expected, the roughness of these films is much lower than the value obtained for the fibers (see Figure 3).

Antibacterial efficacy

In previous works, our group has demonstrated the antimicrobial effectiveness of the cationic polymers PTTI-Me and PTTI-Bu against Gram-positive bacteria.³⁷ Besides, the polymer quaternized with butyl iodide showed higher inhibitory activity because longer hydrophobic alkyl chains provides stronger antibacterial activity as generally improves the insertion into and disruption of the bacterial membrane, which is in agreement with previous reports.³⁸ In this work, the antibacterial activity of PLA and PBAT-based fiber mats and PBAT films loaded with 10 wt % of PTTI-Me and PTTI-Bu was evaluated against Gram-positive, *S. aureus* and *Methicillin-Resistant S. aureus* and Gram-negative, *P. aeruginosa* bacteria. In the antibacterial test, fiber mats and films of $1 \times 1 \text{ cm}^2$ were inoculated in 10 mL of bacterial suspension ($10^5 \text{ CFUs mL}^{-1}$). Controls of PLA and PBAT fibers and PBAT film alone, and an inoculum without fibers were also tested. After 24 h of incubation, the percentage of bacterial viable count reduction related to controls upon contact with antibacterial fibers and films were determined and summarized in Table 1. The results clearly indicate, as expected, that all tested samples are more effective against Gram-positive bacteria, *S. aureus*, and MRSA. It was also appreciated a correlation between surface charge and antibacterial activity.

Table 1. Antibacterial activity expressed as percentage of bacterial reduction (%) and Log reduction (Log) of tested fibers and films against, *S. aureus*, MRSA and *P. aeruginosa*. Surface charge of tested fibers and films expressed as $N^+ cm^{-2}$.

Sample	<i>S. aureus</i>		MRSA		<i>P. aeruginosa</i>		Surface charge
	%	Log	%	Log	%	Log	$N^+ cm^{-2}$
PLA/PTTI-Me	99.99	4	98.1	1.7	38	0.2	$6 \cdot 10^{15}$
PLA/PTTI-Bu	41.0	0.26	-	-	-	-	$4 \cdot 10^{14}$
PBAT/PTTI-Me	82.9	0.76	99.93	3.2	-	-	$3 \cdot 10^{15}$
PBAT/PTTI-Bu	69.6	0.52	92.8	1.1	-	-	$3 \cdot 10^{14}$
FilmPBAT/PTTI-Me	92.3	1.11	74.8	0.6	50	0.3	$9 \cdot 10^{14}$
FilmPBAT/PTTI-Bu	99.7	2.46	99.4	2.2	58	0.4	$8 \cdot 10^{14}$

In fiber mats, the samples quaternized with iodobutane, PLA/PTTI-Bu, and PBAT/PTTI-Bu, exhibit significantly much less activity, with lower bacterial reduction, than the fibers quaternized with iodomethane, which present higher number of positive charges at their surface, with values above $1 \times 10^{15} N^+ cm^{-2}$. As proposed before, the *N*-alkylation reaction with long chain lengths provokes a significant drop in conversion, and then, in the surface charge due to steric effect. It has to be mentioned that butylated and methylated fibers had similar roughness values, then, this factor would not contribute to this difference found in the antibacterial activity. Remarkably, the PLA/PTTI-Me fibers yield a 4-Log reduction after 24 h of contact against *S. aureus*, 1.7-Log reduction against MRSA, and 0.21 against *P. aeruginosa*. When comparing PLA and PBAT-based fibers, PLA based fibers with higher surface charge and also higher roughness were found to kill significantly more bacteria than the corresponding PBAT-based fibers. This can be attributed to the higher hydrophobicity thus, lower water wettability of PBAT, which could affect the *N*-alkylation reaction and also to the contact between bacteria and surface material.

Concerning the results of the PBAT-based films, in contrast to the fiber mats, the sample contained the butylated polymer (FilmPBAT/PTTI-Bu) exhibits higher antibacterial activity than the methylated polymer (FilmPBAT/PTTI-Me) against all tested microorganisms. This finding can be explained on the basis of the similar surface charge density achieved in both mats, in which the difference between them lies in the length of the alkylating chain. In this case, almost completely quaternized polymers, with similar number of cationic groups, were incorporated directly to the PBAT matrix, then; the length of the

hydrophobic alkylating chain (butyl or methyl) is the key factor affecting the antimicrobial activity. The hydrophilic/hydrophobic character is crucial in the design of antimicrobial polymeric materials, as cationic charge may bind to the bacterial membrane through electrostatic attraction while hydrophobic part is needed to insert into the inner hydrophobic core of the membrane.³⁹

Cells viability and cells grow on fibers and films surfaces

Subsequently, we analyzed the biocompatibility and bioactivity of the antimicrobial fibers and films, in terms of adhesion, morphology and viability of fibroblasts. Fibroblasts viability onto these fiber mats and films based on PLA and PBAT was assessed by MTS-based colorimetric assay at 24 h. We analyzed both, the cells adhered onto the samples and the cells not adhered and remained in the bottom of the wells. Figure 5 shows the cell viability of cells adsorbed and cells remained into cell culture plate in comparison with cells seeded in 96-well cell culture plates considered as negative control (100% viability). The sum of both measurements shows that the antimicrobial fiber mats and films are not toxic against human fibroblasts and not detrimental for cell viability, with a viability percentage close to 100%.

When focusing on the cells adsorbed onto the surface of PBAT and PLA-based samples, several parameters, such as roughness, hydrophilicity, surface charge, and influence cell-material interaction. Figure 5 clearly shows that PLA fibers are able to attach more fibroblasts (absorbance of 3-(4,5-dimethylthiazol-2-yl)-5-(3-carboxymethoxyphenyl)2-(4-sulfophenyl)-2H-tetrazolium, MTS) than PBAT fibers, because the higher hydrophobicity of PBAT would suppress the adhesion of fibroblasts, thereby inhibiting their growth.

Roughness of PBAT-based fibers is also lower than that found for PLA fibers, which also could have a negative effect on the cell adhesion. This effect is even more evident in FilmPBAT sample, with lower roughness. Another interesting finding is the effect of the surface charge density on cell growth. When PLA/PTTI-Me and PLA/PTTI-Bu fibers, with similar R_a values, were compared, a significant difference in cell adhesion is appreciated, which can be associated to the surface charge.

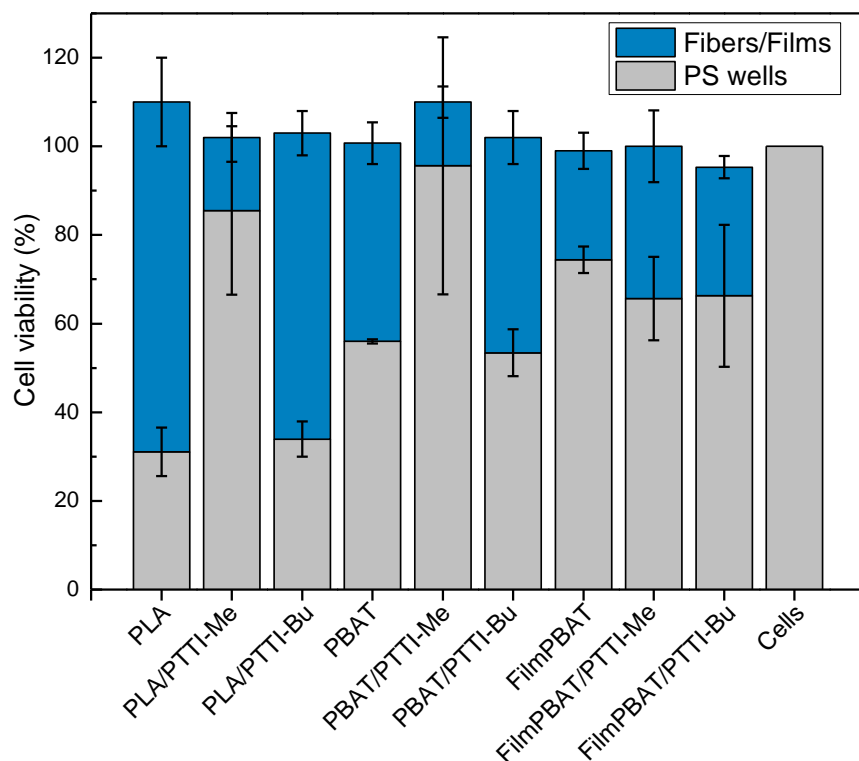


Figure 5. Cell viability of fibroblast seeded onto tested fibers and films assessed by MTS assay using cells seeded in well cell culture plate as negative control 100% viability. Cells adsorbed into the material surfaces are represented in blue, cells remained into cell culture plate are represented in gray. Results are expressed as mean \pm SEM of data obtained by three independent experiments.

This variation in cells adhered on the surface depending on the butylated and methylated sample is not manifested in the prepared films, probably because the surface charge is almost similar. In principle, the incorporation of cationic groups at the surface of biomaterials can enhance cell adhesion and growth due to electrostatic interactions with the negatively charged cell membrane.^{40,41} However, in methylated PLA/PTT1-Me samples with high positive charge density, $6 \times 10^{15} \text{ N}^+ \text{ cm}^{-2}$, the cell adhesion is considerably reduced; showing the best results in the PLA/PTT1-Bu fibers. Similar behavior was obtained for PBAT-based fibers, in which PBAT/PTT1-Bu fiber mat seems to be a more suitable platform for fibroblasts adhesion and proliferation than the methylated sample. It was suggested previously that extremely high interaction between fibroblasts and surface material would alter the cell growth and have a cytostatic effect.¹⁸ Thus, although moderate positive surface charge could have a positive effect on cell adhesion because increases hydrophilicity, high charge density can inhibit cell proliferation.

Next, morphology of the cells seeded on these fiber mats was studied by SEM (Figure 6). Fibroblasts seeded on PLA and PBAT fibers showed a flattened and thin morphology and good spread after 24 h of incubation. However, fibroblasts present more spherical shape when adhered to fibers containing PTTI-Me and PTTI-Bu antimicrobial polymers, indicating limited cell spreading and cell constriction. This rounded and irregular morphology is more evident in the samples with PTTI-Me samples, containing higher number of positive surface charges.

These results seem to indicate, in effect, a cytostatic effect of these positive-charged PLA and PBAT-based materials on human fibroblast cells, which is associated to the strong adhesion of the cells on the surface, reducing the spreading capability and affecting the growth and viability. Cytostatic effect has been observed previously in cationic functionalized surfaces with chitosan¹⁸ and polyethylenimine.⁴² Cells adhere rapidly and strongly to such surfaces and sequester the adhesion molecules in the early steps of cell-surface interaction. This cytostatic property observed in the obtained fiber mats opens the possibility of application in anti-adhesion treatments to reduce, for instance, peritoneal adhesion, which causes numerous complications in postsurgery processes.⁴³

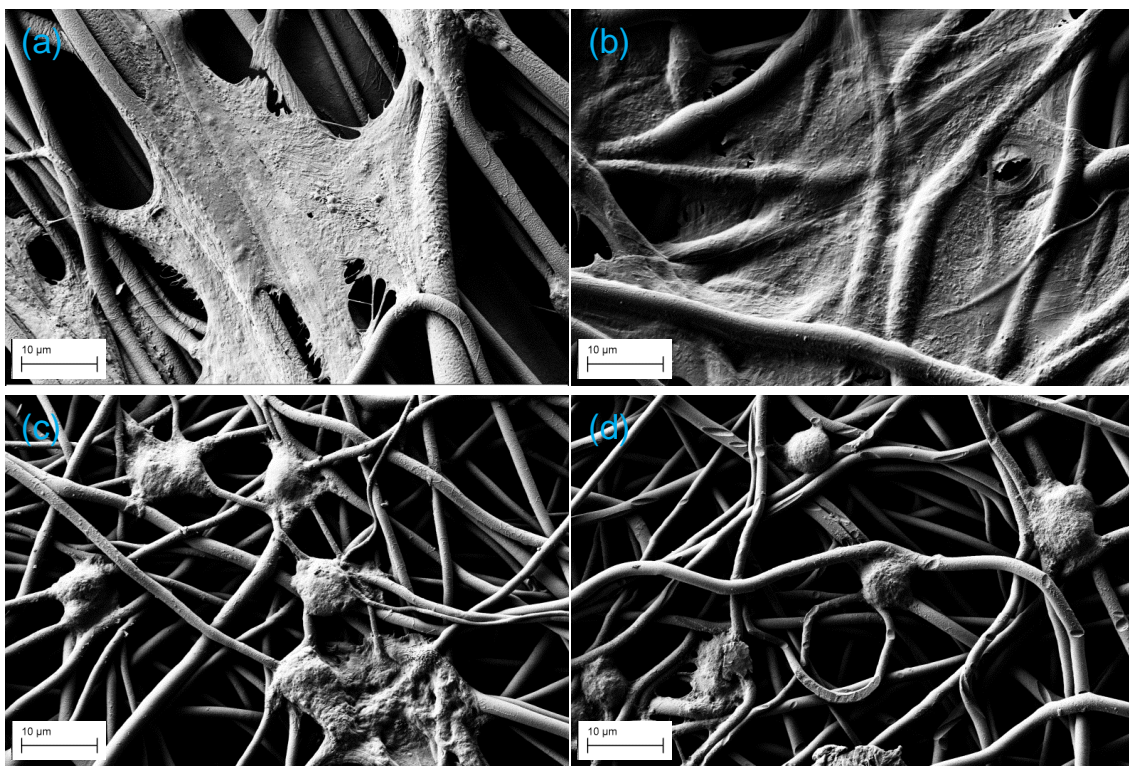


Figure 6. SEM images of Human dermal primary fibroblasts growth for 24 h on a) PLA fiber mat, b) PBAT fiber mat, c) PBAT/PTTI-Bu fiber mat, and d) PBAT/PTTI-Me fiber mat.

3.1.4 Conclusions

In summary, biodegradable PLA and PBAT homogeneous fibers with antibacterial properties were developed incorporating a biobased polyitaconate derivative with thiazole and triazole groups into the electrospinning process. These azole functional groups accessible at the surface of fibers were subjected to *N*-alkylation with either butyl or methyl iodide leading cationic fibers. Lower surface charge density was obtained in butylated fibers in comparison with methylated surfaces due to steric hindrance. The roughness also influences the surface charge of the prepared materials, when we compared electrospun fibers and flat films obtained by compression molding. This surface charge density had a direct correlation with the antibacterial activity, the highest positive charge density the highest the activity. However, when we compared films with similar charge density, those quaternized with iodobutane exhibit better efficiency as long alkylating chains improve hydrophobic/hydrophilic balance, key factor for antimicrobial activity. Although the prepared materials exhibit significant antibacterial activity against Gram-positive bacteria, and non-toxicity against human fibroblast, the morphological analysis of the cells seeded on the surface of cationic fibers showed a cytostatic effect, with potential in anti-adhesion postsurgery treatments.

3.1.5 Experimental part

Materials: Fluorescein sodium salt and cetyltrimethylammonium bromide (CTAB, ≥98%) were purchased from *Merck* and used as received. 3-(4,5-dimethylthiazol-2-yl)-5-(3-carboxymethoxyphenyl)-2-(4-sulfophenyl)-2H-tetrazolium (MTS) was obtained from Promega Corporation. All the organic solvents were of AR grade. *N,N*-dimethylformamide (DMF) and chloroform (CHCl_3) were obtained from *Scharlau*. Polylactic acid (PLA, 6202D) was obtained from *Natureworks* while Ecoflex (PBAT) was provided by BASF. The precursor antibacterial polymer synthesized from itaconic acid, poly(bis((1-(2-(4-methylthiazol-5-yl)ethyl)-1H-1,2,3-triazol-4-yl)methyl) itaconate) (PTI), and the corresponding cationic polymers obtained after *N*-alkylation reaction with methyl and butyl iodide (PTI-Me or PTI-Bu), were synthesized according to the procedure previously described.³⁷

For the antibacterial assay phosphate buffered saline powder (pH 7.4) and sodium chloride solution (NaCl suitable for cell culture, BioXtra) were purchased from *Sigma-Aldrich*. The 96 well microplates were acquired from *BD Biosciences*. Columbia agar (5% sheep blood) plates were obtained from *Fisher Scientific*. For American Type Culture

Collection (ATCC), *Pseudomonas aeruginosa* (*P. aeruginosa*, ATCC 27853), *Staphylococcus aureus* (*S. aureus*, ATCC 29213), and *Staphylococcus aureus* resistant to methicillin and oxacillin (MRSA, ATCC 43300) were used as bacterial strains and purchased from Oxoid.

Electrospinning process: Electrospinning solutions were prepared by dissolving the polymeric blends (PLA/PTTI or PBAT/PTTI) in a 90/10 v/v mixture of CHCl₃/DMF at a concentration of 20% w/w. The polymer ratio was 90% of PLA or PBAT and 10% of PTTI in weight. PLA and PBAT blank solutions were also prepared. From these solutions, electrospun polymeric fibers were obtained using a homemade electrospinner with horizontal configuration equipped with a syringe needle connected to a high voltage power. The fiber mats were collected at room temperature and at 30% of relative humidity, in a grounded aluminum foil collector located perpendicular at 12 cm from the needle tip, at flow rate of 1 mL h⁻¹ and by applying a voltage at 16 kV for 30 min. The obtained PLA/PTTI, PBAT/PTTI, PLA, and PBAT fiber mats were dried under vacuum at room temperature for 24 h to remove any residual solvent.

Preparation of the antimicrobial fiber mats, N-alkylation of the fibers: PLA/PTTI and PBAT/PTTI fibers mats were subjected to N-alkylation of the triazol and thiazol groups available at the surface to obtain antimicrobial functional fibers containing cationic triazolium and thiazolium groups. Briefly, PLA/PTTI and PBAT/PTTI electrospun mats were cut into squares of 1 × 1 cm, and each of these substrates were immersed in 1 mL of methanol solution containing a large excess of methyl iodide or butyl iodide (200 µL). After 10 days of incubation at 37 °C for *N*-alkylation reaction, the mats were rinsed several times with methanol to remove any residual reagents to afford PLA/PTTI-Me, PLA/PTTI-Bu, PBAT/PTTI-Me, and PBAT/PTTI-Bu antimicrobial fibers.

Preparation of the antimicrobial films of PBAT: Antimicrobial films were prepared by melt-extrusion in a microextruder equipped with twin conical co-rotating screws (MiniLab Haake Rheomex CTW5, Thermo Scientific) with a capacity of 7 cm³. PBAT pellets (90 wt %) and antimicrobial polymers (10 wt %) (PTTI-Me or PTTI-Bu) were blended and processed at temperature of 140 °C in the microextruder using a screw rotation rate of 100 rpm, and a residence time of 5 min. Likewise, PBAT pellets were also melt-extruded using similar conditions.

Each extruded sample was subsequently processed into films by compression molding at 140 °C in a hot press (Dr. COLLIN 200 × 200) using a film mold (50 × 50 mm²). The

samples were kept between the plates at atmospheric pressure for 2 min until melting and they were further submitted to the following pressure cycle, 20 kPa for 1 min, 50 kPa for 1 min, and finally the obtained films were quenched to room temperature at 10 kPa for 2 min. The resulting film formulations were labeled as FilmPBAT, FilmPBAT/PTTI-Me, and FilmPBAT/PTTI-Bu.

Characterization: Fourier transform infrared (FTIR) spectra of the fibers were recorded on a Perkin Elmer Spectrum Two instrument equipped with an attenuated total reflection (ATR) module. ^1H NMR spectra were recorded on a Bruker Avance III HD-400AVIII spectrometer at room temperature using DMSO-d₆ purchased from Sigma-Aldrich as solvent.

Surface charge of the obtained films and fibers containing the cationic polymers was determined following a method previously described in literature.^{28,30} Films or mat samples of $1 \times 1 \text{ cm}^2$ (2 cm^2 surface area) were placed in 10 mL of 0.05 wt % aqueous sodium fluorescein solution for 10 min. Then, each sample was rinsed extensively with distilled water and sonicated to remove residual fluorescein. After that, the fluorescein was desorbed from the surface of the samples by treating them with 3 mL of CTAB solution (0.1 wt %) for 20 min under shaking at 300 rpm. Subsequently, the amount of fluorescein recovered in the supernatant was determined by UV-vis spectroscopy (Lamda 35, Perkin Elmer) in solutions prepared by adding 10% v/v of 100 mM phosphate buffer (pH 8.0). The concentration of fluorescein was calculated from the absorbance values at 501 nm with an extinction coefficient of $77 \text{ M}^{-1} \text{ cm}^{-1}$. The accessible cationic groups were determined assuming a relation 1:1 fluorescein: accessible cationic groups.

The surface roughness of the prepared fibers and films was analyzed by optical profilometry using a Zeta-20 optical profiler (Zeta Instruments). Water contact angle measurements were performed with deionized water on a goniometer KSV Theta (KSV Instrument, Ltd., Finland) at room temperature. Water droplets of 3 μL were placed on fiber mats or films and digital images of the water droplets were taken for contact angle determination. The contact angles were measured at least six times on different sites of the surface. Each data reported is the average of measurements \pm SD (standard deviation). The morphology of electrospun fibers based on PLA and PBAT polymers was studied using a scanning electron microscope (SEM) Philips XL30 with an acceleration voltage of 25 kV. The samples were coated with gold prior to scanning.

Antimicrobial assays: The antibacterial activity of the fibers and films was measured following the E2149-13a standard method from the American Society for Testing and Materials (ASTM)⁴⁴ against *P. aeruginosa*, *S. aureus*, and *Methicillin-Resistant S. aureus*. First, bacterial cells were cultured on 5% sheep blood Columbia agar plates for 24 h at 37 °C and then, bacterial suspensions were prepared using the McFarland turbidity scale solution at 10⁸ colony-forming units (CFU) mL⁻¹ in saline. The suspensions were further diluted to 10⁶ CFU mL⁻¹ with PBS. Next, fibers and mats (1 × 1 cm²) were placed in sterile falcon tubes containing 9 mL of PBS and 1 mL of the tested inoculum, reaching a working suspension of ~10⁵ CFU mL⁻¹. Control experiments were also performed in the presence of PLA fiber, PBAT fiber, and PBAT film, and in the absence of sample. These suspensions were shaken at 120 rpm for 24 h. After that, the bacterial colonies were counted by the plate counting method, and the reduction percentage was calculated in comparison with the control. The measurements were made at least in triplicate.

Cell viability assays: Human dermal primary fibroblasts were obtained from adult male patients and isolated as previously reported.⁴⁵ Then, cells were cultured for 3 days in Dulbecco's modified Eagle's medium (DMEM) high glucose, supplemented with 10% fetal bovine serum (FBS), 1% penicillin/streptomycin, 1% L-glutamine, 1% Na-pyruvate, and 1% non-essential amino acids (Sigma-Aldrich, Co. Saint Louis, MO, USA) at 37 °C and 5% CO₂. To study the suitability of the obtained fiber mats and films to human fibroblast cells, cell viability tests were performed. In brief, films and fiber mats (6 mm diameter) were set down into 96-well tissue culture plates and then, cells were added into the wells at a density of 5 × 10³ cells per well and cultured for 24 h at 37 °C and 5% CO₂. As negative control, cells were seeded into a well without sample. After incubation time, the viability of cells seeded on the fibers and films mats as well as of cells growth on the wells was quantified by measuring the mitochondrial dehydrogenase activity using the dye 3-(4,5-dimethylthiazol-2-yl)-5-(3-carboxymethoxyphenyl)2-(4-sulfophenyl)-2H-tetrazolium (MTS). The culture media was removed and fibers and films were put into a clean well. Then, 100 µL the MTS dye solution was added in each well and cells were incubated for 4 h to allow the formation of soluble formazan crystals by viable cells. Color variation was monitored as cell viability and measured at 492 nm using a microplate reader (NB-12-0035, NeBiotech, Holden, MA, USA). All the measurements were performed in triplicate.

Evaluation of morphology of cells seeded onto fibers and films: The cell morphology of cells seeded onto fibers and films was observed by field emission scanning electron microscope (FESEM, AURIGA Zeiss). A total of 2 × 10⁴ fibroblasts were seeded onto

fibers and films as described above and incubated for 24 h. At the end of this incubation, the fibers and films containing the cells were fixed in 2.5 % glutaraldehyde in phosphate buffer saline for 3 h, and then, dehydrated through a graded series of ethyl alcohol. For analysis, samples were fixed onto stubs and gold sputtered and analyzed by FESEM, AURIGA Zeiss.

3.1.6 Acknowledgments

This work was funded by the MICINN (PID2019-104600RB-I00), the Agencia Estatal de Investigación (AEI, Spain) and Fondo Europeo de Desarrollo Regional (FEDER, EU) and by CSIC (LINKA20364). A.C. acknowledges MICIU for his FPU fellowship FPU18/01776.

3.1.7 References

- (1) Agarwal, S.; Wendorff, J. H.; Greiner, A. Use of Electrospinning Technique for Biomedical Applications. *Polymer* **2008**, 49 (26), 5603–5621.
- (2) Deshmukh, S.; Kathiresan, M.; Kulandainathan, M. A. A Review on Biopolymer-Derived Electrospun Nanofibers for Biomedical and Antiviral Applications. *Biomater. Sci.* **2022**, 10 (16), 4424–4442.
- (3) Nayl, A. A.; Abd-Elhamid, A. I.; Awwad, N. S.; Abdelgawad, M. A.; Wu, J.; Mo, X.; Gomha, S. M.; Aly, A. A.; Bräse, S. Recent Progress and Potential Biomedical Applications of Electrospun Nanofibers in Regeneration of Tissues and Organs. *Polymers* **2022**, 14 (8), 1508.
- (4) Maliszewska, I.; Czapka, T. Electrospun Polymer Nanofibers with Antimicrobial Activity. *Polymers* **2022**, 14 (9), 1661.
- (5) Lanno, G.-M.; Ramos, C.; Preem, L.; Putrinš, M.; Laidmāe, I.; Tenson, T.; Kogermann, K. Antibacterial Porous Electrospun Fibers as Skin Scaffolds for Wound Healing Applications. *ACS Omega* **2020**, 5 (46), 30011–30022.
- (6) Hajikhani, M.; Emam-Djomeh, Z.; Askari, G. Fabrication and Characterization of Mucoadhesive Bioplastic Patch via Coaxial Polylactic Acid (PLA) Based Electrospun Nanofibers with Antimicrobial and Wound Healing Application. *Int. J. Biol. Macromol.* **2021**, 172, 143–153.
- (7) Echeverría, C.; Muñoz-Bonilla, A.; Cuervo-Rodríguez, R.; López, D.; Fernández-García, M. Antibacterial PLA Fibers Containing Thiazolium Groups as Wound Dressing Materials. *ACS Appl. Bio Mater.* **2019**, 2 (11), 4714–4719.
- (8) Keirouz, A.; Radacsi, N.; Ren, Q.; Dommann, A.; Beldi, G.; Maniura-Weber, K.; Rossi, R. M.; Fortunato, G. Nylon-6/Chitosan Core/Shell Antimicrobial Nanofibers for the Prevention of Mesh-Associated Surgical Site Infection. *J. Nanobiotechnology* **2020**, 18 (1), 51.
- (9) Shahi, R. G.; Albuquerque, M. T. P. P.; Münchow, E. A.; Blanchard, S. B.; Gregory, R. L.; Bottino, M. C. Novel Bioactive Tetracycline-Containing Electrospun Polymer Fibers as a Potential Antibacterial Dental Implant Coating. *Odontology* **2017**, 105 (3), 354–363.
- (10) Kai, D.; Liow, S. S.; Loh, X. J. Biodegradable Polymers for Electrospinning: Towards Biomedical Applications. *Mater. Sci. Eng. C* **2014**, 45, 659–670.
- (11) Maleki, H.; Azimi, B.; Ismaeilimoghadam, S.; Danti, S. Poly(Lactic Acid)-Based Electrospun Fibrous Structures for Biomedical Applications. *Appl. Sci.* **2022**, 12 (6), 3192.
- (12) DeStefano, V.; Khan, S.; Tabada, A. Applications of PLA in Modern Medicine. *Eng. Regen.* **2020**, 1 (August), 76–87.
- (13) Jalali Dil, E.; Carreau, P. J.; Favis, B. D.; Dil, E. J.; Carreau, P. J.; Favis, B. D. Morphology, Miscibility and Continuity Development in Poly(Lactic Acid)/Poly(Butylene Adipate-Co-Terephthalate) Blends. *Polymer* **2015**, 68, 202–212.
- (14) Chen, J.; Rong, C.; Lin, T.; Chen, Y.; Wu, J.; You, J.; Wang, H.; Li, Y. Stable Co-Continuous PLA/PBAT Blends Compatibilized by Interfacial Stereocomplex Crystallites: Toward Full Biodegradable Polymer Blends with Simultaneously Enhanced Mechanical Properties and Crystallization Rates. *Macromolecules* **2021**, 54 (6), 2852–2861.
- (15) Ribeiro Neto, W. A.; de Paula, A. C. C.; Martins, T. M. M.; Goes, A. M.; Averous, L.; Schlatter, G.; Suman Bretas, R. E. Poly (Butylene Adipate-Co-Terephthalate)/Hydroxyapatite Composite Structures for Bone Tissue Recovery. *Polym. Degrad. Stab.* **2015**, 120, 61–69.
- (16) Santana-Melo, G. F.; Rodrigues, B. V. M. M.; da Silva, E.; Ricci, R.; Marciano, F. R.; Webster, T. J.; Vasconcellos, L. M. R. R.; Lobo, A. O. Electrospun Ultrathin PBAT/NHAp Fibers Influenced the in Vitro and in Vivo Osteogenesis and Improved the Mechanical Properties of Neoformed Bone. *Colloids Surfaces B Biointerfaces* **2017**, 155, 544–552.

- (17) Liu, S.; Qin, S.; He, M.; Zhou, D.; Qin, Q.; Wang, H. Current Applications of Poly(Lactic Acid) Composites in Tissue Engineering and Drug Delivery. *Compos. Part B Eng.* **2020**, 199, 108238.
- (18) Jao, W.-C. C.; Lin, C.-H. H.; Hsieh, J.-Y. Y.; Yeh, Y.-H. H.; Liu, C.-Y. Y.; Yang, M.-C. C. Effect of Immobilization of Polysaccharides on the Biocompatibility of Poly(Butyleneadipate-Co-Terephthalate) Films. *Polym. Adv. Technol.* **2010**, 21 (8), 543–553.
- (19) Persson, M.; Lorite, G. S.; Cho, S.-W.; Tuukkanen, J.; Skrifvars, M. Melt Spinning of Poly(Lactic Acid) and Hydroxyapatite Composite Fibers: Influence of the Filler Content on the Fiber Properties. *ACS Appl. Mater. Interfaces* **2013**, 5 (15), 6864–6872.
- (20) Zhu, D.; Cheng, H.; Li, J.; Zhang, W.; Shen, Y.; Chen, S. S.; Ge, Z.; Chen, S. S. Enhanced Water-Solubility and Antibacterial Activity of Novel Chitosan Derivatives Modified with Quaternary Phosphonium Salt. *Mater. Sci. Eng. C* **2016**, 61, 79–84.
- (21) Unnithan, A. R.; Barakat, N. A. M.; Tirupathi Pichiah, P. B.; Gnanasekaran, G.; Nirmala, R.; Cha, Y.-S.; Jung, C.-H.; El-Newehy, M.; Kim, H. Y. Wound-Dressing Materials with Antibacterial Activity from Electrospun Polyurethane–Dextran Nanofiber Mats Containing Ciprofloxacin HCl. *Carbohydr. Polym.* **2012**, 90 (4), 1786–1793.
- (22) Wattanawong, N.; Aht-Ong, D. Antibacterial Activity, Thermal Behavior, Mechanical Properties and Biodegradability of Silver Zeolite/Poly(Butylene Succinate) Composite Films. *Polym. Degrad. Stab.* **2021**, 183, 109459.
- (23) Ergene, C.; Yasuhara, K.; Palermo, E. F. Biomimetic Antimicrobial Polymers: Recent Advances in Molecular Design. *Polym. Chem.* **2018**, 9 (18), 2407–2427.
- (24) Pham, P.; Oliver, S.; Boyer, C. Design of Antimicrobial Polymers. *Macromol. Chem. Phys.* **2022**, 2200226, 1–28.
- (25) Cramariuc, B.; Cramariuc, R.; Scarlet, R.; Manea, L. R.; Lupu, I. G.; Cramariuc, O. Fiber Diameter in Electrospinning Process. *J. Electrostat.* **2013**, 71 (3), 189–198.
- (26) Konai, M. M.; Bhattacharjee, B.; Ghosh, S.; Haldar, J. Recent Progress in Polymer Research to Tackle Infections and Antimicrobial Resistance. *Biomacromolecules* **2018**, 19 (6), 1888–1917.
- (27) Muñoz-Bonilla, A.; Fernández-García, M. Polymeric Materials with Antimicrobial Activity. *Prog. Polym. Sci.* **2012**, 37 (2), 281–339.
- (28) Murata, H.; Koepsel, R. R.; Matyjaszewski, K.; Russell, A. J. Permanent, Non-Leaching Antibacterial Surfaces-2: How High Density Cationic Surfaces Kill Bacterial Cells. *Biomaterials* **2007**, 28 (32), 4870–4879.
- (29) Kügler, R.; Bouloussa, O.; Rondelez, F. Evidence of a Charge-Density Threshold for Optimum Efficiency of Biocidal Cationic Surfaces. *Microbiology* **2005**, 151 (5), 1341–1348.
- (30) Kliewer, S.; Wicha, S. G.; Bröker, A.; Naundorf, T.; Catmadim, T.; Oellingrath, E. K.; Rohnke, M.; Streit, W. R.; Vollstedt, C.; Kipphardt, H.; Maisom, W. Contact-Active Antibacterial Polyethylene Foils via Atmospheric Air Plasma Induced Polymerisation of Quaternary Ammonium Salts. *Colloids Surfaces B Biointerfaces* **2020**, 186 (July 2019), 110679.
- (31) Navarro-Rodriguez, D.; Frere, Y.; Gramain, P. Kinetics and Steric Limitation of Quaternization of Poly(4-Vinylpyridine) with Mesogenic ω -(4'-Methoxy-4-Biphenylyloxy)Alkyl Bromides. *J. Polym. Sci. Part A Polym. Chem.* **1992**, 30 (12), 2587–2594.
- (32) Milleret, V.; Hefti, T.; Hall, H.; Vogel, V.; Eberli, D. Influence of the Fiber Diameter and Surface Roughness of Electrospun Vascular Grafts on Blood Activation. *Acta Biomater.* **2012**, 8 (12), 4349–4356.
- (33) Sun, L.; Guo, J.; Chen, H.; Zhang, D.; Shang, L.; Zhang, B.; Zhao, Y. Tailoring Materials with Specific Wettability in Biomedical Engineering. *Adv. Sci.* **2021**, 8 (19), 2100126.
- (34) Cui, W.; Li, X.; Zhou, S.; Weng, J. Degradation Patterns and Surface Wettability of Electrospun Fibrous Mats. *Polym. Degrad. Stab.* **2008**, 93 (3), 731–738.

- (35) Zhu, M.; Zuo, W.; Yu, H.; Yang, W.; Chen, Y. Superhydrophobic Surface Directly Created by Electrospinning Based on Hydrophilic Material. *J. Mater. Sci.* **2006**, 41 (12), 3793–3797.
- (36) Chiloeches, A.; Cuervo-Rodríguez, R.; López-Fabal, F.; Fernández-García, M.; Echeverría, C.; Muñoz-Bonilla, A. Antibacterial and Compostable Polymers Derived from Biobased Itaconic Acid as Environmentally Friendly Additives for Biopolymers. *Polym. Test.* **2022**, 109, 107541.
- (37) Chiloeches, A.; Funes, A.; Cuervo-Rodríguez, R.; López-Fabal, F.; Fernández-García, M.; Echeverría, C.; Muñoz-Bonilla, A. Biobased Polymers Derived from Itaconic Acid Bearing Clickable Groups with Potent Antibacterial Activity and Negligible Hemolytic Activity. *Polym. Chem.* **2021**, 12 (21), 3190–3200.
- (38) Sovadnova, I.; Palermo, E. F.; Urban, M.; Mpiga, P.; Caputo, G. A.; Kuroda, K. Activity and Mechanism of Antimicrobial Peptide-Mimetic Amphiphilic Polymethacrylate Derivatives. *Polymers* **2011**, 3 (3), 1512–1532.
- (39) Palermo, E. F.; Kuroda, K. Structural Determinants of Antimicrobial Activity in Polymers Which Mimic Host Defense Peptides. *Appl. Microbiol. Biotechnol.* **2010**, 87 (5), 1605–1615.
- (40) Metwally, S.; Stachewicz, U. Surface Potential and Charges Impact on Cell Responses on Biomaterials Interfaces for Medical Applications. *Mater. Sci. Eng. C* **2019**, 104 (February), 109883.
- (41) Lopreiato, M.; Mariano, A.; Cocchiola, R.; Longo, G.; Dalla Vedova, P.; Scandurra, R.; Scotto d'Abusco, A. Nanostructured TiC Layer Is Highly Suitable Surface for Adhesion, Proliferation and Spreading of Cells. *Condens. Matter V*, 5 (2), 29.
- (42) Alba, A.; Villaggio, G.; Messina, G. M. L.; Caruso, M.; Federico, C.; Cambria, M. T.; Marletta, G.; Sinatra, F. Cytostatic Effects of Polyethyleneimine Surfaces on the Mesenchymal Stromal Cell Cycle. *Polymers* **2022**, 14 (13), 2643.
- (43) Li, J.; Xu, W.; Chen, J.; Li, D.; Zhang, K.; Liu, T.; Ding, J.; Chen, X. Highly Bioadhesive Polymer Membrane Continuously Releases Cytostatic and Anti-Inflammatory Drugs for Peritoneal Adhesion Prevention. *ACS Biomater. Sci. Eng.* **2018**, 4 (6), 2026–2036.
- (44) ASTM D5988, Standard Test Method for Determining Aerobic Biodegradation of Plastic Materials in Soil; ASTM International: West Conshohocken, PA, **2018**.
- (45) Lopreiato, M.; Cocchiola, R.; Falcucci, S.; Leopizzi, M.; Cardone, M.; Di Maio, V.; Brocco, U.; D'Orazi, V.; Calvieri, S.; Scandurra, R.; De Marco, F.; Scotto d'Abusco, A. The Glucosamine-Derivative NAPA Suppresses MAPK Activation and Restores Collagen Deposition in Human Diploid Fibroblasts Challenged with Environmental Levels of UVB. *Photochem. Photobiol.* **2020**, 96 (1), 74–82.

3.1.8 Supporting Information

PLA and PBAT based electrospun fibers functionalized with antibacterial biobased polymers

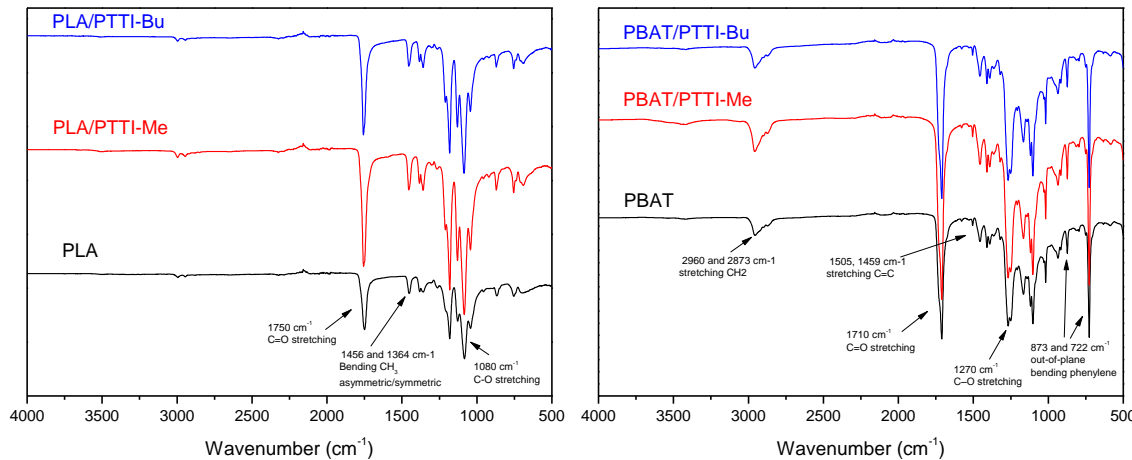


Figure S1. FTIR spectra of PLA and PBAT based fibers.

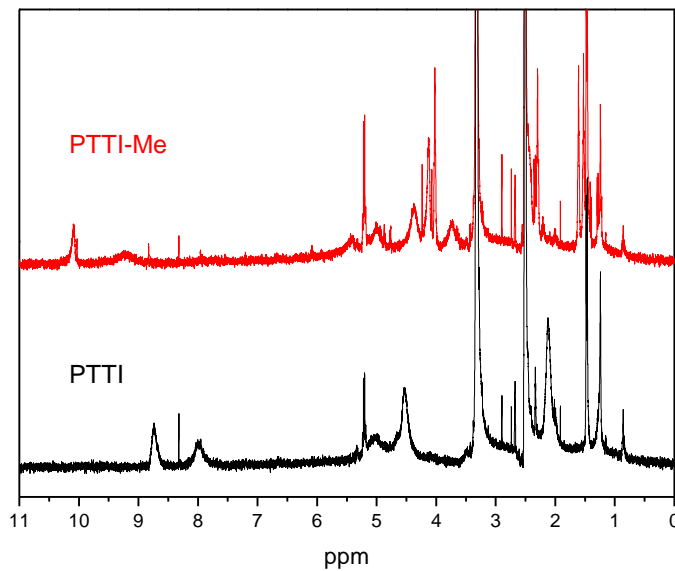


Figure S2. ^1H NMR spectra and signal assignment of PTTI and PTTI-Me extracted in DMSO-d_6 from PLA/PTTI and PLA/PTTI-Me fiber mats.

PTTI. $^1\text{H-NMR (400 MHz, DMSO-d}_6$, δ (ppm): 8.74 (2H, *H*-thiazole), 8.00 (2H, *H*-triazole), 5.01 (4H, O-CH₂-triazole), 4.52 (4H, CH₂-N), 3.26 (4H, CH₂-thiazole), 2.10 (6H, CH₃-thiazole), 3.00-1.50 (6H, CH₂CO and CH₂-chain-).

PTTI-Me. $^1\text{H-NMR (400 MHz, DMSO-d}_6$, δ (ppm): 10.08 (2H, *H*-thiazole), 9.20 (2H, *H*-triazole), 5.42 (4H, O-CH₂-triazole), 5.05 (4H, CH₂-N), 4.38 (6H, N⁺CH₃ triazole), 4.13 (6H, N⁺CH₃ thiazole), 3.72 (4H, CH₂-thiazole), 2.30 (6H, CH₃-thiazole).

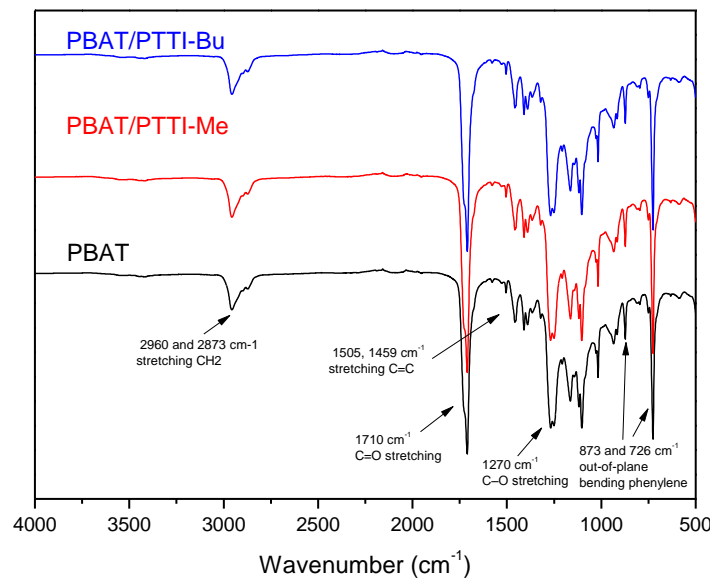


Figure S3. FTIR spectra of PBAT based films.

3.2 Electrospun Polylactic Acid-Based Fibers Loaded with Multifunctional Antibacterial Biobased Polymers

ACS Appl. Polym. Mater. **2022**, *4* (9), 6543-6552

ACS APPLIED
POLYMER MATERIALS
AC ⓘ Article

pubs.acs.org/acspbm
Article

Electrospun Polylactic Acid-Based Fibers Loaded with Multifunctional Antibacterial Biobased Polymers

A. Chiloeches, R. Cuervo-Rodríguez, Y. Gil-Romero, M. Fernández-García, C. Echeverría,* and A. Muñoz-Bonilla*
Cite This: <https://doi.org/10.1021/acspbm.2c00928>
Read Online

ACCESS |
Metrics & More
Article Recommendations
Supporting Information

ABSTRACT: Here, we report the development of antibacterial and compostable electrospun polylactic acid (PLA) fibers by incorporation of a multifunctional biobased polymer in the process. The multifunctional polymer was synthesized from the bio-sourced itaconic acid building block by radical polymerization followed by click chemistry reaction with hydantoin groups. The resulting polymer possesses triazole and hydantoin groups available for further N-alkylation and chlorination reaction, which provide antibacterial activity. This polymer was added to the electrospinning PLA solution at 10 wt %, and fiber mats were successfully prepared. The obtained fibers were surface-modified through the accessible functional groups, leading to the corresponding cationic triazolium and N-halamine groups. The fibers with both antibacterial functionalities demonstrated high antibacterial activity against Gram-positive and Gram-negative bacteria. While the fibers with cationic surface groups are only effective against Gram-positive bacteria (*Staphylococcus epidermidis* and *Staphylococcus aureus*), upon chlorination, the activity against Gram-negative *Escherichia coli* and *Pseudomonas aeruginosa* is significantly improved. In addition, the compostability of the electrospun fibers was tested under industrial composting conditions, showing that the incorporation of the antibacterial polymer does not impede the disintegrability of the material. Overall, this study demonstrates the feasibility of this biobased multifunctional polymer as an antibacterial agent for biodegradable polymeric materials with potential application in medical uses.

KEYWORDS: *poly(lactic acid), polyitaconates, biobased polymers, antimicrobial fibers, triazolium, N-halamine, compostability*

Downloaded via CSIC on August 30, 2022 at 05:57:52 (UTC).
See https://pubs.acs.org/sharingguidelines for options on how to legitimately share published articles.

1. INTRODUCTION

Microbial contamination on surface contacts of solid materials constitutes an important source of infections not only in biomedical devices, implants, and prostheses but also in other fields such as the food industry.^{1,2} Microbial adhesion onto such surfaces and subsequent biofilm formation, together with the emergence of antibiotic resistance, has become one of the more critical public health concerns.^{3–5} Then, surface disinfection and sterilization processes (physical and chemical) in hospitals, food processing facilities, or even in the domestic environment are crucial to reduce and control microbial infections. Typically, both physical and chemical methods are used. Application of chemical disinfectants, such as alcohols, chlorines, or quaternary amines, are effective treatments that, however, have several disadvantages, such as the need for high concentration to achieve sterility standards and the potential hazards to humans and the environment. For instance, common quaternary ammonium compounds such as the disinfectant benzalkonium chloride which generates bacterial resistance,⁶ have been found in sediments and soils.⁷ Similarly, the ethylene oxide chemical sterilization method presents potential hazards, as ethylene oxide is toxic, carcinogenic, and allergenic and can be present after the process.⁸ On the other

Received: June 2, 2022
Accepted: August 18, 2022

© XXXX The Authors. Published by American Chemical Society

ACS Publications

A

<https://doi.org/10.1021/acspbm.2c00928>
ACS Appl. Polym. Mater. XXXX, XXX, XXX-XXX

117

3.2.1 Abstract

Here, we report the development of antibacterial and compostable electrospun polylactic acid (PLA) fibers by incorporation of a multifunctional biobased polymer in the process. The multifunctional polymer was synthesized from the biosourced itaconic acid building block by radical polymerization followed by click chemistry reaction with hydantoin groups. The resulting polymer possesses triazole and hydantoin groups available for further *N*-alkylation and chlorination reaction, which provide antibacterial activity. This polymer was added to the electrospinning PLA solution at 10 wt %, and fiber mats were successfully prepared. The obtained fibers were surface-modified through the accessible functional groups, leading to the corresponding cationic triazolium and *N*-halamine groups. The fibers with both antibacterial functionalities demonstrated high antibacterial activity against Gram-positive and Gram-negative bacteria. While the fibers with cationic surface groups are only effective against Gram-positive bacteria (*Staphylococcus epidermidis* and *Staphylococcus aureus*), upon chlorination, the activity against Gram-negative *Escherichia coli* and *Pseudomonas aeruginosa* is significantly improved. In addition, the compostability of the electrospun fibers was tested under industrial composting conditions, showing that the incorporation of the antibacterial polymer does not impede the disintegrability of the material. Overall, this study demonstrates the feasibility of this biobased multifunctional polymer as an antibacterial agent for biodegradable polymeric materials with potential application in medical uses.

Keywords: poly(lactic acid), polyitaconates, biobased polymers, antimicrobial fibers, triazolium, *N*-halamine, compostability.

3.2.2 Introduction

Microbial contamination on surface contacts of solid materials constitutes an important source of infections not only in biomedical devices, implants, and prostheses but also in other fields such as the food industry.^{1,2} Microbial adhesion onto such surfaces and subsequent biofilm formation, together with the emergence of antibiotic resistance, has become one of the more critical public health concerns.³⁻⁵ Then, surface disinfection and sterilization processes (physical and chemical) in hospitals, food processing facilities, or even in the domestic environment are crucial to reduce and control microbial infections. Typically, both physical and chemical methods are used. Application of chemical disinfectants, such as alcohols, chlorines, or quaternary amines, are effective treatments that, however, have several disadvantages, such as the need for high concentration to achieve sterility standards and the potential hazards to humans and the environment. For instance, common quaternary ammonium compounds such as the disinfectant benzalkonium chloride which generates bacterial resistance,⁶ have been found in sediments and soils.⁷ Similarly, the ethylene oxide chemical sterilization method presents potential hazards, as ethylene oxide is toxic, carcinogenic, and allergenic and can be present after the process.⁸ On the other hand, physical methods such as gamma irradiation, UV-irradiation, and steam sterilization can alter the properties of the materials, in particular polymer materials commonly used for biomedical or packaging applications.⁹⁻¹¹ This is even more critical in biodegradable biopolymers such as polylactic acid (PLA), which typically have hydrolytic and thermal sensitivity, and sterilization can alter the properties of the materials.^{12,13} Nowadays, PLA is widely used as a sustainable alternative to conventional plastics^{14,15} in many applications, including the manufacture of biomedical devices and food packing. Indeed, a large part of plastic waste comes from these sectors, and therefore, the use of biodegradable and renewable polymers in such applications represents a great alternative to protect the environment.^{16,17}

New perspectives to prevent or reduce surface contamination and bacterial growth on these bioplastic materials, maintaining safety requirements and long-term activity, are still challenged. Incorporation of antimicrobial biodegradable polymers into bioplastics is considered a valuable alternative, as these materials retain high long-term antimicrobial activity, do not leakage easily, have low toxicity and low susceptibility for developing resistance, and are able to degrade after their useful lifetime.¹⁸⁻²² Recently, our group has developed antibacterial biobased polymers derived from itaconic acid bearing cationic azonium groups derived from vitamin thiamine (B1). These polymers demonstrate

excellent antibacterial activity against Gram-positive bacteria, negligible toxicity to human cells, and compostability.^{23,24} In addition, these antibacterial cationic copolymers have been studied as active additives in biodegradable films based on poly(butylene adipate-co-terephthalate) for packaging applications.²⁴ However, the activity of these systems against Gram-negative bacteria is limited. Herein and based on our previous itaconate derivatives, we synthesize a biodegradable antibacterial polymer with multifunction, including contact-killing and release-killing mechanisms, with the purpose of improving the antibacterial activity and being more effective against Gram-negative bacteria. The multifunctional itaconate polymer was designed to combine in its structure two functional groups, cationic azonium and *N*-halamine groups. While the cationic groups in the polymer kill bacteria by physically damaging the cell membrane, the activity of *N*-halamine groups is due to the release of oxidative halogen, which can react with the appropriate biological receptors, affecting cell metabolism.²⁵ This antibacterial biobased polymer was subsequently employed to impart antibacterial character to PLA fiber mats obtained by electrospinning in order to achieve “fully-biodegradable” material. Electrospun fibers, widely used for food packages and biomedical materials such as face masks or wound dressing,²⁶⁻²⁸ have a large surface-to-volume ratio so, in principle, low quantities of antimicrobial polymer would be needed to achieve satisfactory results.²⁹

3.2.3 Experimental part

Materials

Itaconic acid (IA, ≥ 99%), propargyl alcohol (≥99%), 4-(dimethylamino) pyridine (DMAP, ≥99%), *N,N'*-dicyclohexylcarbodiimide (DCC, 99%), hydroquinone (99%), 5,5-dimethylhydantoin (97%), 1-bromo-2-chloroethane (98%), potassium hydroxide (KOH, 90%), sodium azide (NaN₃, ≥99%), sodium iodide (NaI, 99.5%) di-tert-butyl dicarbonate (Boc₂O, 99%), copper(I) chloride (CuCl, ≥99.995%), *N,N,N',N'',N''*-pentamethyldiethylenetriamine (PMDTA, 99%), iodomethane (MeI, 99.5%), trifluoroacetic acid (TFA, 99%), tert-butanol (≥99.5%), acetic acid (≥99.7%), neutral aluminum oxide, sodium bicarbonate (NaHCO₃, ≥99.7%), magnesium sulfate anhydrous (MgSO₄, ≥99.5%), fluorescein sodium salt, sodium thiosulfate (Na₂S₂O₃, 99%), cetyltrimethylammonium chloride (CTAC, ≥98%), iodine standard solution, anhydrous tetrahydrofuran (THF, 99.9%), and anhydrous *N,N*-dimethylformamide (DMF, 99.8%) were purchased from Merck and used as received. The radical initiator 2,2'-azobisisobutyronitrile (AIBN, 98%) was purchased from Acros and was recrystallized

twice from methanol. PLA (6202D) was provided by NatureWorks. All the organic solvents were of AR grade; dichloromethane (DCM), THF, DMF, ethanol (EtOH), isopropyl alcohol (iPrOH), hexane, diethyl ether, and chloroform (CHCl₃) were purchased from Scharlau; ethyl acetate (EtOAc) was purchased from Cor Química S.L.; toluene was purchased from Merck; sulfuric acid (H₂SO₄) was purchased from Panreac. Deuterated chloroform (CDCl₃), water (D₂O), and dimethyl sulfoxide (DMSO-d₆) were acquired from Sigma-Aldrich. Cellulose dialysis membranes (CelluSep T1) were purchased from Membrane Filtration Products, Inc.

For the antibacterial assay: phosphate buffered saline powder (pH 7.4) and sodium chloride solution (NaCl suitable for cell culture, BioXtra) were purchased from Sigma-Aldrich. BBL Mueller-Hinton broth used as a microbial growth medium in the determination of the minimum inhibitory concentration (MIC) was acquired from Becton, Dickinson and Company, and the 96 well microplates were purchased from BD Biosciences. Columbia agar (5% sheep blood) plates were obtained from Fisher Scientific. American Type Culture Collection (ATCC): *Pseudomonas aeruginosa* (*P. aeruginosa*, ATCC 27853), *Escherichia coli* (*E. coli*, ATCC 25922), *Staphylococcus epidermidis* (*S. epidermidis*, ATCC 12228), and *Staphylococcus aureus* (*S. aureus*, ATCC 29213) were used as bacterial strains and were purchased from Oxoid.

Synthesis of poly(di(prop-2-yn-1-yl)) itaconate, P(Prl).

The clickable polymer P(Prl) was synthesized as previously described.²³ First, the monomer di(prop-2-yn-1-yl) itaconate (Prl) bearing clickable alkyne groups was synthesized via condensation reaction of itaconic acid with propargyl alcohol. Subsequently, the monomer Prl was polymerized by conventional radical polymerization with 5 mol % of the AIBN initiator, at a total concentration of 2 M in anhydrous DMF, at 70 °C under a nitrogen atmosphere for 24 h. The polymer **P(Prl)** was isolated by precipitation in isopropanol and dried overnight under vacuum at room temperature to afford a white solid (71% yield, M_n = 6700 g/mol, M_w/M_n = 1.58). ¹H-NMR (400 MHz, CDCl₃, δ, ppm): 4.67 (4H, -CH₂C≡CH), 2.49 (2H, -CH₂C≡CH), 1.99-1.00 (8H, CH₂-CO and -CH₂-chain).

Synthesis of tert-butyl 3-(2-azidoethyl)-5,5-dimethylhydantoin-1-carboxylate, Boc-DMH-N3.

First, 3-(2-azidoethyl)-5,5-dimethylhydantoin was synthesized through nucleophilic substitution reaction between 5,5-dimethylhydantoin and 1-bromo-2-chloroethane,³⁰

followed by transformation of chlorine groups to azide groups via a substitution reaction. Briefly, 5,5-dimethylhydantoin (20.0 g, 156 mmol) and potassium hydroxide (8.7 g, 156 mmol) were dissolved in 100 mL of ethanol in a round-bottomed flask. Then, 1-bromo-2-chloroethane (26 mL, 312 mmol) was added, and the mixture was heated under reflux for 6 h. The reaction was cooled to room temperature, and the solvent was removed by rotary evaporation. The resulting white solid was dissolved in EtOAc and washed with water and NaHCO₃ solution (10%) by several extraction steps. The organic fractions were dried over anhydrous magnesium sulfate, filtered, and evaporated under reduced pressure. The white solid was further purified by recrystallization in isopropanol/toluene (9:1) to afford **DMH-Cl** (yield 48%). ¹H-NMR (400 MHz, CDCl₃, δ, ppm): 6.31 (s, 1H, -NH-), 3.85 (t, 2H, -CH₂-Cl), 3.74 (t, 2H, -CH₂-CH₂-Cl), 1.46 (s, 6H, -CH₃).

Later, chlorine-substituted hydantoin (DMH-Cl) (5.0 g, 26 mmol) was dissolved in DMF and deoxygenated by purging with argon. Sodium iodide (3.9 g, 26 mmol) and an excess of sodium azide (2.4 g, 37 mmol) were dissolved in 6 mL of water. Then, both solutions were mixed and heated at 80 °C under an argon atmosphere for 3 h. The resultant mixture was concentrated under reduced pressure and, then, was extracted with EtOAc and washed repeatedly with NaCl aqueous solution. The organic extract was separated, dried over MgSO₄, and filtered, and the solvent was removed under reduced pressure to afford the product **DMH-N₃** as a colorless oil (yield: 88%). ¹H-NMR (400 MHz, CDCl₃, δ, ppm): 6.57 (s, 1H, -NH-), 3.70 (t, 2H, -CH₂-N₃), 3.52 (t, 2H, CH₂-CH₂-N₃), 1.44 (s, 6H, -CH₃).

Subsequently, the amine group of the DMH-N₃ product was protected by di-*tert*-butyl dicarbonate. DMH-N₃ (0.9 g, 4.6 mmol), Boc₂O (1.3 g 6 mmol), DMAP (56 mg, 0.46 mmol), and 25 mL of DCM were added in a round bottom flask. Then, the solution was stirred at room temperature for 4 h. The reaction mixture was washed with water several times. The organic layer was dried over Mg₂SO₄, and filtered, and the solvent was evaporated by rotary evaporation. The residue was purified by silica gel column chromatography using diethyl ether as eluent to give the protected product **Boc-DMH-N₃** (yield: 95%). ¹H-NMR (400 MHz, CDCl₃, δ, ppm): 3.75 (t, 2H, -CH₂-N₃), 3.56 (t, 2H, CH₂-CH₂-N₃), 1.64 (s, 6H, -CH₃), 1.57 (s, 9H, -CH₃ Boc). ¹³C-NMR (100 MHz, CDCl₃, δ, ppm): 174.9 (N-C=O), 151.8 (N-(C=O)-N), 148.4 (N-(C=O)-O), 84.4 (C_{quat}, Boc), 60.3 (C_{quat}, hydantoin), 48.3 (-CH₂-N₃), 38.2 (CH₂-CH₂-N₃), 28.2 (-CH₃, Boc), 23.2 (-CH₃, hydantoin). FTIR: 2097 cm⁻¹ associated with the azide group.

Synthesis of poly(bis((1-(2-(3-(tert-butoxycarbonyl)-4,4-dimethyl-2,5-dioxoimidazolidin-1-yl)ethyl)-1H-1,2,3-triazol-4-yl)methyl)itaconate), P(Boc-DMHI).

The incorporation of the hydantoin Boc-DMH-N₃ into the clickable itaconate polymer P(Prl) was conducted by click chemistry Cu(I)-catalyzed azide-alkyne cycloaddition (CuAAC). In a typical procedure, a mixture of polymer P(Prl) (1.50 g, 7.3 mequiv of alkyne groups), Boc-DMH-N₃ (5.40 g, 18.2 mmol), PMDTA (300 µL, 1.45 mmol), and CuCl (0.072 g, 0.72 mmol) were dissolved in 40 mL of CHCl₃. The mixture was stirred at 40 °C for 24 h and then passed through a neutral alumina column. The resulting polymer **P(Boc-DMHI)** was isolated by precipitation in ethanol, and the degree of modification was almost quantitative (yield: 98%). ¹H-NMR (400 MHz, DMSO-d₆, δ, ppm): 8.08 (2H, H-triazole), 5.04 (4H, O-CH₂-triazole), 4.61 (4H, CH₂-N triazole), 3.85 (4H, CH₂-N hydantoin), 1.49 (s, 18H, -CH₃ Boc), 1.45 (s, 12H, -CH₃), 2.66-1.00 (8H, CH₂-CO and -CH₂-chain).

N-alkylation of P(Boc-DMHI) and deprotection reaction. Synthesis of cationic polymer P(DMHI-Q).

The polymer P(Boc-DMHI) was modified by *N*-alkylation reaction with iodomethane (MeI) leading to the corresponding cationic itaconate polymer. The polymer (1.50 g, 3.75 mequiv of triazole groups) was dissolved in 25 mL of anhydrous DMF, and then, a large excess of MeI was added (1.2 mL, 18.75 mmol; ratio triazole groups/alkyl iodide ≈ 1:5). The mixture was deoxygenated with argon for 15 min, sealed, and then stirred at 70 °C for one week to achieve a high degree of modification. The resulting cationic polymer was purified by precipitation into n-hexane followed by dialysis against distilled water and finally was isolated by freeze-drying. The degree of quaternization was almost quantitative. Subsequently, the deprotection reaction was performed. For this purpose, the polymer was dissolved in trifluoroacetic acid (5 mL) and stirred at 50 °C for 2 h. After cooling down to room temperature, the cationic polymer **P(DMHI-Q)** was purified by dialysis against distilled water and then lyophilized to yield a white solid (96%). ¹H-NMR (400 MHz, DMSO-d₆, δ, ppm): 9.10 (2H, H-triazole), 5.44 (4H, O-CH₂-triazole), 4.78 (4H, CH₂-N triazole), 4.37 (6H, N⁺CH₃ triazole), 3.85 (4H, CH₂-N hydantoin), 1.29 (s, 12H, -CH₃), 2.66-1.00 (8H, CH₂-CO and -CH₂-chain).

Chlorination of P(DMHI-Q). Synthesis of polymer P(DMHICI-Q).

Initially, *tert*-butyl hypochlorite was synthesized.³⁰ Briefly, sodium hypochlorite solution (250 mL, 10 wt %) was placed in a round-bottomed flask and cooled in an ice bath. A

solution of *tert*-butyl alcohol (10 mL) and glacial acetic acid (15.5 mL) was added under stirring. After 10 min, the organic layer of the mixture was extracted with a separatory funnel, and the aqueous layer was discarded. The organic layer was washed successively with an aqueous solution of NaHCO₃ 10% and water, dried over CaCl₂, and filtered (yield: 73%).

The chlorination of the P(DMHI-Q) polymer to afford the **P(DMHICI-Q)** multifunctional polymer was carried out using *tert*-butyl hypochlorite as follows: P(DMHI-Q) (1.50 g, 4.85 equiv of hydantoin groups) and *tert*-butyl hypochlorite (2.25 mL, 19.4 mmol) were dissolved in 20 mL of H₂O/*t*-butanol (1/4 v/v). Then, the mixture was stirred in dark for 24 h at room temperature and dried under a vacuum with a rotary evaporator to obtain the final N-halamine polymer **P(DMHICI-Q)** in a quantitative amount. The polymer was characterized by Fourier transform infrared (FTIR), and the oxidative chlorine (Cl⁺) content of the polymer was quantified through the iodometric/thiosulfate titration method.³¹ Briefly, 1.8 mg of P(DMHICI-Q) was dissolved in 1 mL of 1% aqueous potassium iodide solution for 10 min to form I₂ (the color of the solution changed to yellow). Then, 100 µL of 1% starch solution was added to the polymer solution that changed to blue. This solution was titrated with 0.5 mN sodium thiosulfate solution (the color of the solution changed from blue to colorless). The Cl⁺ content of the polymer was calculated as follows:

$$Cl^+(ppm) = \frac{35.45 \times N \times V}{2 \times m} \times 10^6$$

where Cl⁺ (ppm) is the weight percentage of the oxidative chlorine in the polymer, *N* (equiv/L) is the normality, *V* (L) is the volume of the titrant sodium thiosulfate, and *m* (g) is the weight of the polymer.

Electrospinning process.

Electrospinning solutions were prepared by dissolving the polymeric blends (PLA/P(DMHI) or P(DMHICI-Q)) in a 90/10 v/v mixture of CHCl₃/DMF at a concentration of 18% w/v. Electrospun polymeric fibers were prepared from these solutions using a homemade electrospinner in a horizontal configuration equipped with a syringe needle connected to a high voltage power. The polymer solutions were fed at 1 mL h⁻¹. The electrospun fiber mats were collected in a grounded aluminum foil collector located perpendicular at 12 cm from the needle tip by applying a voltage of 16 kV. Those conditions were selected from the results obtained in our previous works.^{32,33} The

obtained electrospun samples, PLA/P(DMHI) and PLA/(DMHICI-Q), were dried for 48 h under a vacuum to remove any potential residual solvent before their use.

N-alkylation and chlorination of the fibers. Preparation of antimicrobial fiber mats.

PLA/P(DMHI) fiber mats were subjected to *N*-alkylation and chlorination to obtain antimicrobial functional fibers containing triazolium and halamine groups at the surface. First, the PLA/P(DMHI) electrospun mat was cut into several pieces ($1 \times 1 \text{ cm}^2$), and each of them was incubated in 1 mL of methanol. Then, a large excess of methyl iodide (200 μL) was added. The *N*-alkylation reaction was left for 10 days with constant shaking at 37 °C to ensure a complete reaction. After that period, the mats were washed with methanol several times to remove any residual reagent to afford PLA/P(DMHI-Q) fibers. Surface charge determination was performed following a method previously described in the literature.^{34,35} A mat sample of $1 \times 1 \text{ cm}^2$ (2 cm^2 surface area) was placed in 10 mL of 1 wt % aqueous sodium fluorescein solution for 10 min. After that, the sample was rinsed extensively with distilled water and sonicated to remove residual fluorescein. Then, the fluorescein was desorbed from the surface of the sample by treating the mat with 3 mL of 0.1 wt % CTAC solution for 20 min with shaking at 300 rpm. Subsequently, the amount of fluorescein obtained in the supernatant was determined by UV-vis spectroscopy (Lambda 35, PerkinElmer) in a solution prepared by adding 10% v/v of 100 mM phosphate buffer (pH 8.0). The absorbance of the resulting solution was measured at 501 nm, and the concentration of fluorescein was calculated with an extinction coefficient³⁶ of 77 M⁻¹cm⁻¹ assuming a relationship of 1:1 for fluorescein to each accessible cationic triazolium group.

Next, the chlorination reaction of PLA/P(DMHI-Q) fibers was carried out to form N-halamine functional groups at the surface of the cationic fibers. For this reaction, the pieces of fibers obtained after alkylation were immersed in a diluted bleach solution (10% v/v) at room temperature for 2 h. Then, the samples were rinsed with a copious amount of water to reach pH 7 and dried to afford PLA/P(DMHICI-Q) fibers. The chlorine amount in the functionalized fibers was determined by the iodometric/thiosulfate titration method as described above³¹ using mat pieces of $1 \times 1 \text{ cm}^2$ (~2.7 mg).

Characterization

NMR spectra were recorded on a Bruker Avance III HD-400AVIII spectrometer at room temperature using solvents CDCl₃ and DMSO-d₆. FTIR spectra were obtained with a

PerkinElmer Spectrum Two instrument equipped with an attenuated total reflection module. Size exclusion chromatography measurements were performed on a Waters Division Millipore system equipped with a Waters 2414 refractive index detector. DMF stabilized with 0.1 M LiBr (Sigma-Aldrich, >99.9%) was used as eluent at a flow rate of 1 mL min⁻¹ at 50 °C. The calibration was made with poly(methyl methacrylate) standards (Polymer Laboratories LTD). The morphology of electrospun fibers of PLA and PLA/itaconate polymers was studied using a scanning electron microscope (SEM) Philips XL30 with an acceleration voltage of 25-10 kV. The samples were coated with gold prior to scanning. SEM images were analyzed using NIH ImageJ software and measuring at least 100 fibers of each sample from different SEM images. Microhardness (MH) of the electrospun fibers was measured with a Vickers indentor attached to a Leitz microhardness tester. A contact load of 0.96 N and a time of 25 s were employed.

Antibacterial assays

The antibacterial activity of the PLA/P(DMHICI-Q) fibers was measured following the E2149-13a standard method from the American Society for Testing and Materials (ASTM)³⁷ against *P. aeruginosa*, *E. coli*, *S. epidermidis*, and *S. aureus*. First, bacterial cells were cultured on 5% sheep blood Columbia agar plates for 24 h at 37 °C. Then, the bacterial suspensions were prepared in saline using the McFarland turbidity scale and further diluted to 10⁶ colony-forming units (CFU) mL⁻¹ with PBS. Next, PLA/P(DMHICI-Q) fiber mats (1 × 1 cm²) were placed in sterile falcon tubes containing 1 mL of the tested inoculum and 9 mL of PBS to reach a working solution of ~10⁵ CFU mL⁻¹. Control experiments were also performed in the presence of PLA fiber, and also in the absence of mats. The suspensions were shaken at 120 rpm for 30 min or 24 h. After this period, the colonies were counted by the plate counting method, and the reduction percentage was calculated in comparison to the control. The measurements were made at least in triplicate.

Disintegrability under composting conditions test.

The disintegrability test under simulated composting conditions of the prepared PLA and PLA/P(DMHICI-Q) fiber mats was performed at the laboratory scale level following the ISO 20200 standard.³⁸ The synthetic wet compost was prepared by mixing 45 wt % of solid synthetic wet waste [10% of compost (Compo, Spain), 30% rabbit food, 10% starch, 5% sugar, 4% corn oil, 1% urea, and 40% sawdust] and 55 wt % of water contained in a perforated plastic box as composter reactors. Then, several pieces of mats from each

sample (previously weighted) were placed in textile meshes buried in the compost and subjected to an aerobic disintegration process at 58 °C. Samples were withdrawn periodically, cleaned with distilled water, dried in an oven at 37 °C under a vacuum for 24 h, and reweighed. The disintegration degree was calculated by normalizing the sample weight, on different days of composting, to the initial weight. The samples were characterized by SEM and visual inspection.

3.2.4 Results and Discussion

Synthesis and characterization of the P(DMHICl-Q) antibacterial polymer.

In previous studies, biobased and biodegradable polymers derived from itaconic acid containing azonium antibacterial groups were prepared from a clickable polyitaconate developed by our group.²³ These biopolymers bearing cationic thiazolium and triazolium groups demonstrated excellent antibacterial activity against Gram-positive bacteria and negligible toxicity to human cells but were poorly active against Gram-negative bacteria. Based on our previous finding, herein, we design and synthesize a multifunctional antibacterial polyitaconate bearing azonium and *N*-halamine groups to achieve systems with a broad antimicrobial spectrum. Figure 1 displays the synthetic route followed for the preparation of the antibacterial polymer P(DMHICl-Q). Clickable polymer derived from itaconic acid, P(PrI), was employed as a platform to prepare multifunctional polymers by azide-alkyne coupling reactions (CuAAC). For this purpose, Boc-protected 5,5-dimethylhydantoin functionalized with azide group (Boc-DMH-N₃) was incorporated onto the polymer via CuAAC click chemistry, leading to triazole linkages. Subsequently, *N*-alkylating reaction of the triazole groups with methyl iodide provides the corresponding cationic itaconate derivatives. Each of these steps consisted of very efficient reactions and proceeded with high yields and a high degree of conversion of functional groups, as confirmed by FTIR and ¹H-NMR (see Supporting information). After the N-Boc deprotection step, the chlorination reaction changes the amide group of hydantoin into *N*-halamines.

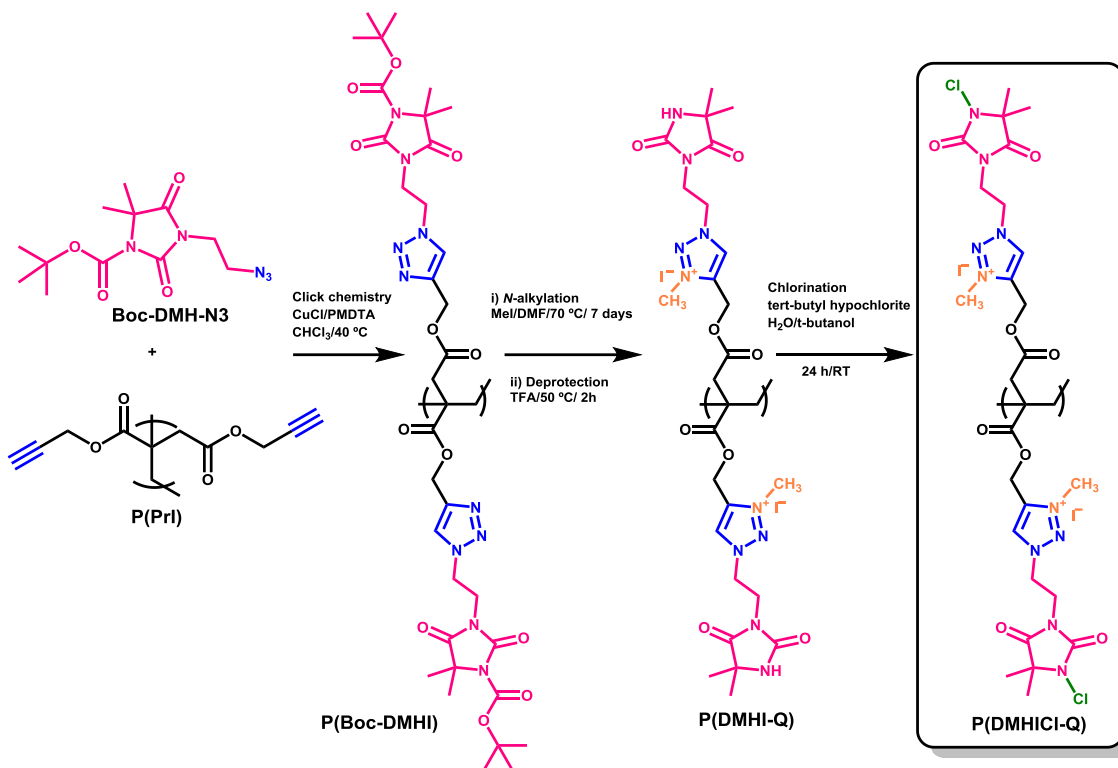


Figure 1. Synthesis route of the antibacterial biobased polymer P(DMHICl-Q).

Figure 2 shows the FTIR spectra of the P(DMHICl-Q) and their precursors. In the spectrum of P(PrI), the bands at 3283 and 2128 cm⁻¹ assigned to the alkyne C-H and C≡C stretching vibrations, respectively, are clearly observed. After the click reaction of P(PrI) with the protected 3-(2-azidoethyl)-5,5-dimethylhydantoin (Boc-DMH-N₃), new bands appear in the spectrum. It can be seen the band at 1810 cm⁻¹ is associated with the ν (C=O) of the Boc group and the band at 1734 cm⁻¹ due to the imide and ester C=O stretching vibrations. Subsequently, *N*-alkylation and deprotection reactions provide the cationic polymer P(DMHI-Q), in whose spectrum the bands assigned to the Boc group disappear and the vibrational band of the imide carbonyl bond is shifted to 1709 cm⁻¹. Also, a new band at 1581 cm⁻¹ corresponding to the ν (C=N⁺) clearly emerges, due to the formation of triazolium groups. The last chlorination step provides a shift of the imide carbonyl group to 1718 cm⁻¹ as a result of the electron-withdrawing effect of the oxidative chlorine.³⁹

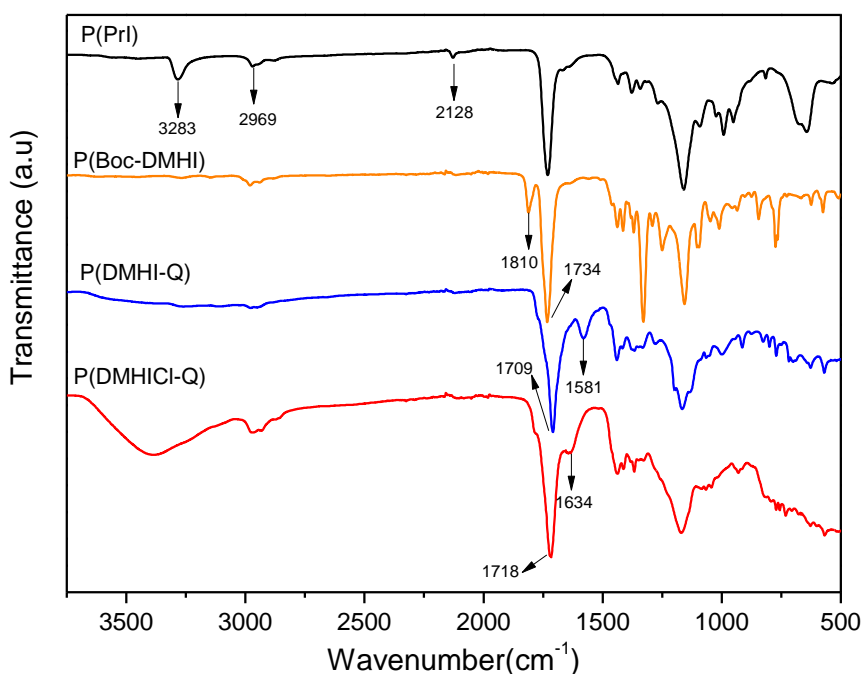


Figure 2. FTIR spectra of the antibacterial biobased polymer P(DMHICI-Q) and its precursors P(PrI), P(Boc-DMHI) and P(DMHI-Q).

It should be mentioned that synthetic *t*-butyl hypochlorite was used for chlorination instead of commercial bleach because, in this way, the polymer can be easily purified, as the excess of *t*-butyl hypochlorite is removed under vacuum.⁴⁰ The content of oxidative chlorine in the polymer was iodometrically titrated and resulted in 7134 ppm for the tested polymer solution. This value corresponds to a degree of chlorination of 9%.

Preparation of antimicrobial electrospun fibers based on PLA/P(DMHICI-Q).

Next, the multifunctional biobased polymer P(DMHICI-Q) was employed to impart antibacterial activity to PLA electrospun fibers. First, the preparation of antimicrobial fibers by electrospinning technique was attempted from CHCl₃/DMF solutions of PLA/P(DMHICI-Q) polymeric blends at a 90/10 ratio. However, the antibacterial polymer P(DMHICI-Q) containing cationic and halamine groups was not soluble in the solvent mixture, and its incorporation as a component of the fibers by the electrospinning process would conduct to maldistribution, aggregation, or leakage problems. It is well known that electrospinning of multiple components using one nozzle is critical and requires careful optimization of the systems. Indeed, this cationic polymer with halamine groups was not soluble in any solvent compatible with PLA or with the electrospinning process and therefore can hardly be electrospun in a direct way. For this reason, we follow an alternative approach consisting of the use of neutrally charged polymer resulting from the

deprotection of P(Boc-DMHI). The P(DMHI) polymer was incorporated into the CHCl₃/DMF solvent mixture at 10 wt % together with PLA 90 wt %, at a total polymer concentration of 18 wt %. Then, PLA-based fibers loaded with the polymer P(DMHI), bearing triazole and hydantoin groups, were prepared by electrospinning leading to antimicrobial precursor fibers. SEM images, shown in Figure 3, illustrate the morphology of the electrospun fiber mats compared to PLA fibers obtained under similar conditions. It is clearly observed that the incorporation of the P(DMHI) polymer affects the morphology of the fibers as it could modify the viscosity and conductivity of the solution, resulting in electrospun fibers with nonuniform size and shape. While the morphology of the electrospun PLA fibers was smooth, uniform, and bead-free, with a diameter of 4.2 ± 0.9 μm, the fiber mats loaded with P(DMHI) are nonuniform in size, with a lower average diameter of 2.3 ± 1.5 μm. Nevertheless, reasonable fiber mats can be obtained by this approach.

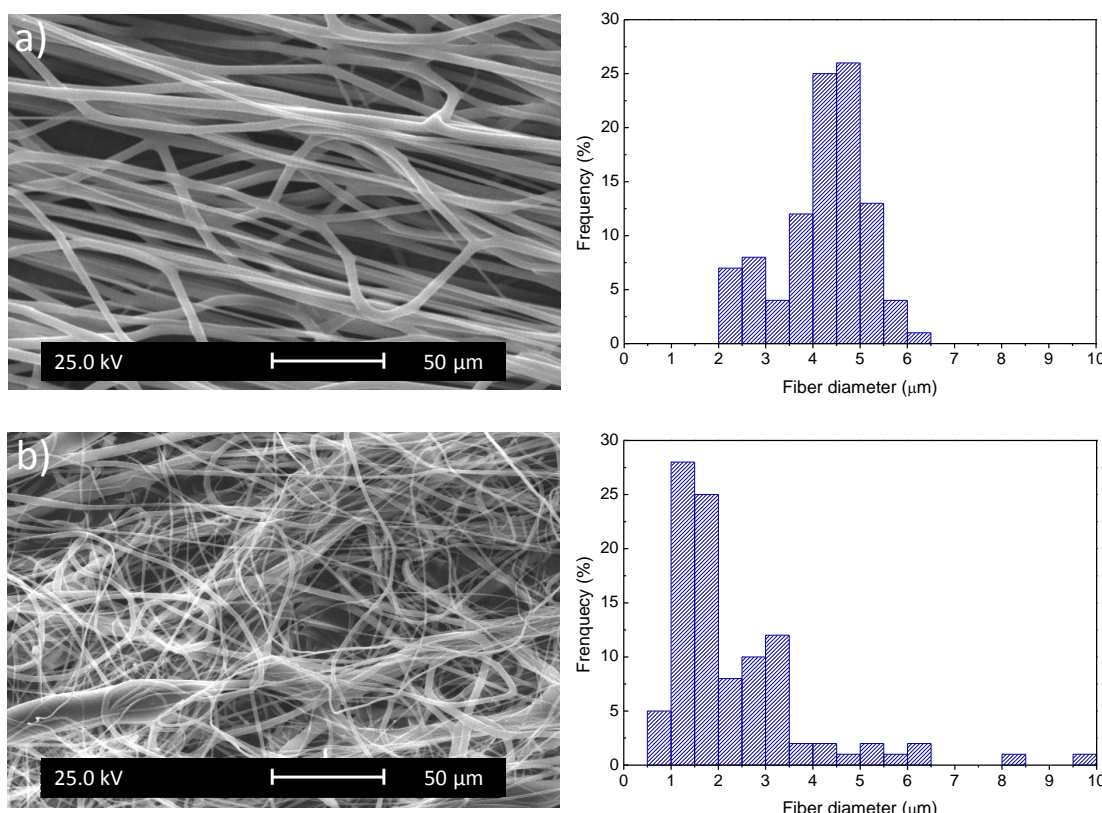


Figure 3. SEM micrographs and its corresponding histograms of fiber diameters of a) PLA and b) PLA/P(DMHI) fiber mats.

The fibers loaded with P(DMHI) polymer precursor were subsequently surface functionalized to provide antimicrobial activity. For this purpose, the *N*-alkylation reaction of the triazole groups was carried out with iodomethane to afford the corresponding

cationic triazolium groups [P(DMHI-Q)], followed by chlorination of the hydantoin groups with bleach to provide *N*-halamine functionalities [P(DMHICI-Q)]. In this case, bleach was employed for the chlorination reaction because the washing steps of the fibers can be easily performed with water. The successful quaternization reaction on the surface was confirmed by measuring the accessible cationic units able to bind fluorescein. In this experiment, the fluorescein adsorbed on the surface, which corresponds to accessible positive surface charges, was desorbed with CTAC and quantified by UV-vis spectroscopy. The estimated cationic groups were found to be $1.4 \times 10^{15} \text{ N}^+/\text{cm}^2$, a value near that previously determined for other contact-active surfaces.^{34,41} Likewise, the active chlorine content of the fiber mat ($1 \times 1 \text{ cm}^2$, 2.7 mg), determined via iodometric titration method, was calculated to be 1654 ppm, an amount enough, in principle, to impart activity to the surface, as has been demonstrated in other *N*-halamine-functionalized surfaces.³¹ These experiments demonstrated the successful functionalization of the fibers with both antimicrobial active groups.

Mechanical properties

Microhardness measurements were carried out on the obtained PLA and PLA/P(DMHICI-Q) fiber mats to evaluate how the incorporation of the polyitaconate derivative and the posterior modification affects the mechanical behavior of PLA material. PLA fiber mats exhibit a MH value of $154 \pm 5 \text{ MPa}$, near other values found in the literature for PLA materials;⁴²⁻⁴⁴ however, in PLA/P(DMHICI-Q) fibers, the MH increases to $171 \pm 6 \text{ MPa}$. As expected, the addition of a glassy polymer such as this polyitaconate derivative results in a slight increase in the hardness of the materials, with values similar to PLA-based composites materials obtained by the incorporation of reinforcing fillers.^{43,44} It is also worth noting that the fibers diameter decreases with the incorporation of P(DMHICI-Q), which could also contribute to the differences in the mechanical properties.

Antibacterial efficacy

Next, the antibacterial activity of the chlorinated and quaternized fiber mats, PLA/P(DMHICI-Q), was evaluated against Gram-positive, *S. epidermidis* and *S. aureus*, and Gram-negative bacteria, *P. aeruginosa* and *E. coli*, and compared with the quaternized fibers before chlorination, PLA/P(DMHI-Q), to analyze the combined action of both functionalities. In the antibacterial test, fiber mats of $1 \times 1 \text{ cm}^2$ were inoculated in 10 mL of bacterial suspension (10^6 CFUs). Controls of PLA fibers alone and inoculum without fibers were also tested. The control samples did not provide any noticeable

reduction of bacteria after 24 h, whereas the fibers containing the antibacterial polyitaconate provoke great reduction (see Figure 2 of Supporting Information). Table 1 summarizes the percentage reduction of bacterial viable counts related to controls upon contact with antibacterial fibers after 30 min or 24 h. The results indicate that the fibers functionalized with cationic triazolium groups after 30 min of contact time are only effective against Gram-positive bacteria, causing 0.59 and 0.75-Log reductions of *S. epidermidis* and *S. aureus*, respectively. These films need a large contact time to achieve high bacterial reduction, 5-Log reductions, as described for other antibacterial systems based on cationic polymers acting through a contact kill mechanism, in which prolonged contacts are necessary to affect bacteria that are not in contact with the surface.⁴⁵ This antibacterial efficacy is considerably reduced against *P. aeruginosa*, a Gram-negative bacteria, by 0.90-Log, whereas no effect on *E. coli* was observed after 24 h of contact time. Remarkably, the chlorination of the fibers considerably improves their activity for both Gram-positive and Gram-negative bacteria. Against Gram-positive bacteria, the chlorinated fibers yield 5-Log reduction after only 30 min of contact, whereas they cause 1.01-Log reduction of *P. aeruginosa* and 2-Log reduction of *E. coli*. The effectivity of these chlorinated PLA/P(DMHICI-Q) fibers practically reaches the highest results after the shortest time tested, 30 min.

Table 1. Antibacterial activity expressed as percentage of bacterial reduction (%) and Log reduction (Log) of PLA/P(DMHI-Q) and PLA/P(DMHICI-Q) against, *S. epidermidis*, *S. aureus*, *P. aeruginosa* and *E. coli* after 30 min or 24 h of contact time.

	<i>S. epidermidis</i>		<i>S. aureus</i>		<i>P. aeruginosa</i>		<i>E. coli</i>	
	%	Log	%	Log	%	Log	%	Log
PLA/P(DMHI-Q) (30 min)	74.6	0.59	82.2	0.75	-	-	-	-
PLA/P(DMHI-Q) (24 h min)	99.999	5	99.999	5	87.5	0.90	-	-
PLA/P(DMHICI-Q) (30 min)	99.999	5	99.999	5	90.2	1.01	99	2
PLA/P(DMHICI-Q) (24 h)	99.999	5	99.999	5	93.2	1.15	98.9	1.96

Thus, the incorporation of *N*-halamine with cationic triazolium groups demonstrates to be a good approach to achieving a broadened antibacterial spectrum of the fibers, improving the activity against both Gram-positive and Gram-negative bacteria.

Biodisintegrability

To study the compostability of the antimicrobial polymeric fibers, a disintegration test was conducted under simulated industrial composting conditions at 58 °C according to the ISO 20200 standard.³⁸ A qualitative evaluation of the physical disintegration of the fiber mats as a function of composting time was performed by taking photographs and by SEM measurements (Figure 4), confirming the biodisintegrable character of PLA and PLA loaded mats in less than 90 days.

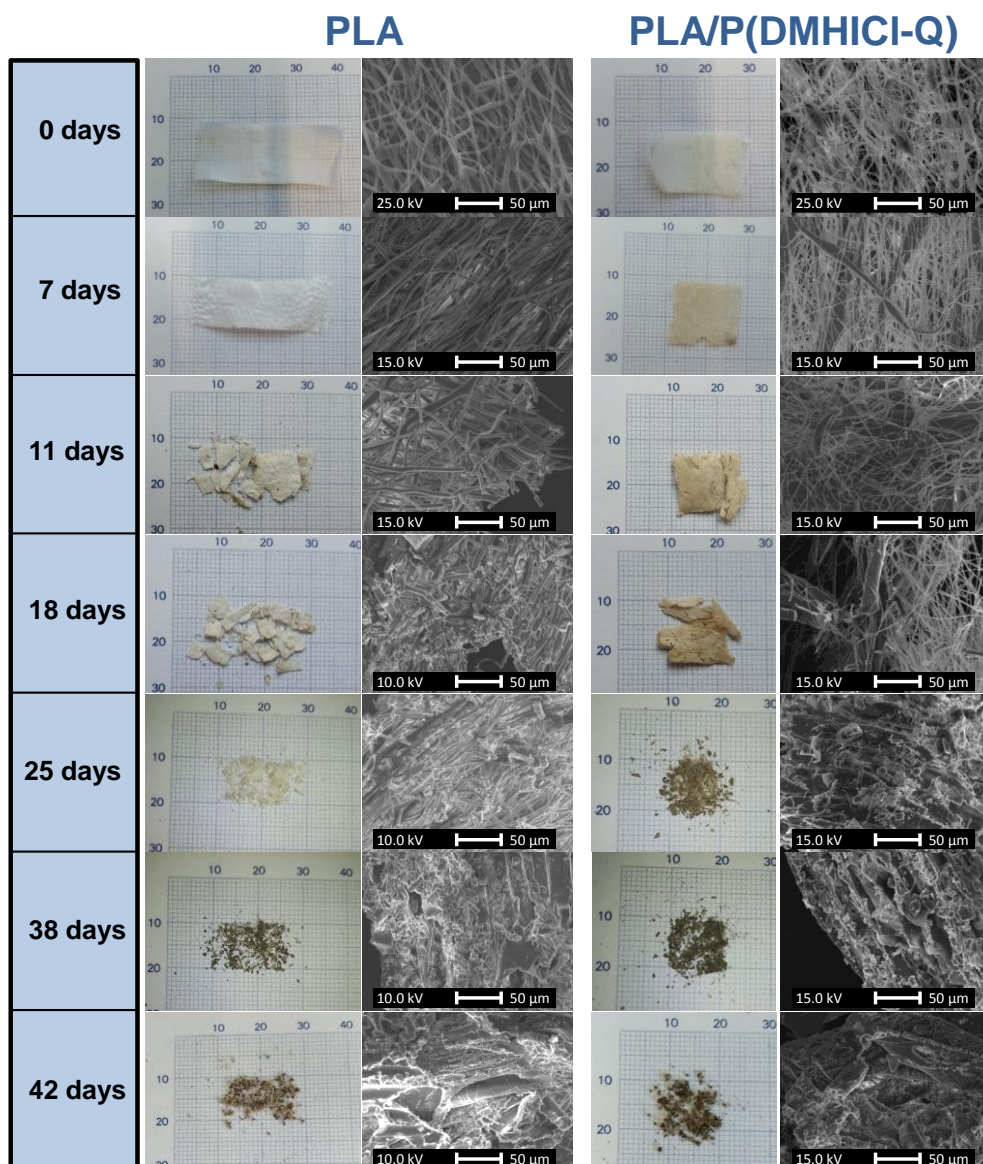


Figure 4. Visual appearance and SEM images of the tested PLA and PLA/P(DMHICl-Q) fiber mats over time under composting conditions.

From the visual appearance of the samples, it is noticeable that the PLA/P(DMHICI-Q) sample turns yellowish on day 7, whereas the coloration becomes evident in PLA on day 11. This change in color may be due to hydrolytic degradation,^{46,47} in addition to the presence of sawdust. After 11 days under composting conditions, both samples exhibited considerable surface deformation and fractures, due to physical and/or chemical degradation of the polymers that cause a loss of flexibility. The PLA/P(DMHICI-Q) sample starts to turn dark brown, suggesting that the disintegration of this sample is faster than the degradation of the PLA mat. From day 25, only small pieces of mats were recovered, mostly smaller than 2 mm in size. At this point it is difficult to separate the polymeric sample from compost particles and, according to the ISO 20200 standard, pieces smaller than 2 mm should be discarded. Finally, after 42 days, samples reached a level of disintegration where no visible polymeric fragments could be easily recovered. Nevertheless, SEM images of the compost particles on day 42 reveal the presence, adhered on the surface, of small pieces of polymeric fibers in the range of micrometric scale (in diameter and length), demonstrating the existence of microplastic particles when apparently the fiber mats are completely disintegrated. Indeed, from SEM micrographs of the mats obtained at different composting times, a considerable fracture of fibers leading to a reduction of the length scale to micron can be appreciated. Figure 5a showed magnified SEM images of the PLA and PLA/P(DMHICI-Q) fibers taken at large incubation composting period, 42 days, in which is appreciated fiber with lengths smaller than 10 µm. Also, during the degradation process, a reduction in the fiber diameter is observed. Figure 5b displays the average fiber diameter as a function of composting time. In both samples, PLA and PLA/P(DMHICI-Q), the fiber diameter diminishes with the incubation periods, as previously observed in PLA fiber mats biodegraded under simulated physiological conditions.⁴⁸ From SEM images of the samples obtained at different incubation times, as seen from visual observation, it seems that the disintegration process is a bit faster in PLA fibers loaded with the antimicrobial polymer P(DMHICI-Q), probably due to the smaller fiber diameter and, therefore, its larger surface area.

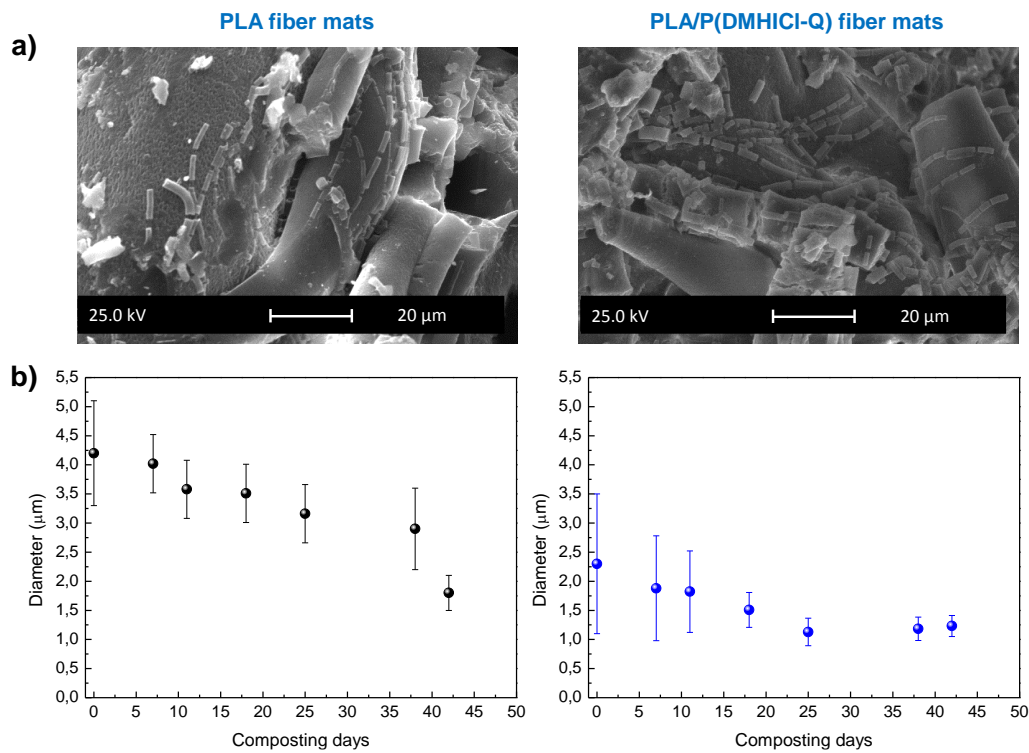


Figure 5. a) SEM image of PLA and PLA/P(DMHICI-Q) fibers taken at large 42 days of composting incubation. b) Average fiber diameter of PLA and PLA/P(DMHICI-Q) fiber mats over time under composting conditions.

The disintegration degree was also analyzed in terms of mass loss as a function of disintegration time (Figure 6). The process seems to be slightly accelerated in the PLA/P(DMHICI-Q) samples, as previously observed in photographs and SEM micrographs. However, statistical analysis using one-way ANOVA followed by Tukey's test ($p < 0.05$) indicates the degradation profile of PLA and PLA/P(DMHICI-Q) fibers are not significantly different.

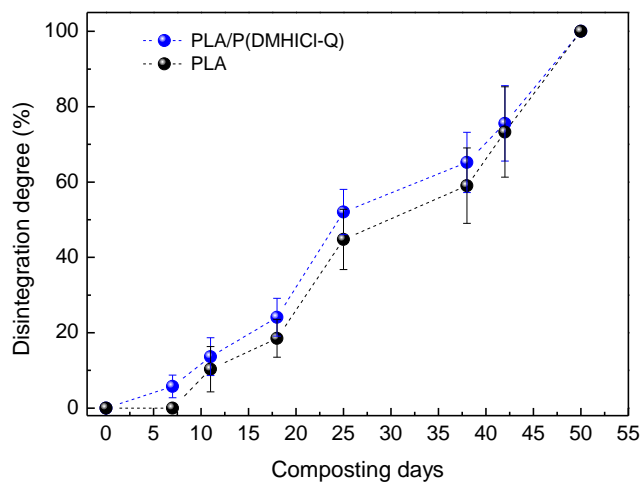


Figure 6. Disintegration degree of PLA and PLA/P(DMHICI-Q) fiber mats over time under composting conditions.

3.2.5 Conclusions

In this study, antibacterial and compostable PLA-based fibers were successfully fabricated by incorporating a multifunctional biobased polymer derived from itaconic acid bearing *N*-halamine and triazolium antibacterial groups, P(DMHICl-Q). In the first attempt, the antibacterial polymer was synthesized by the attachment of both functionalities onto a polyitaconate derivative following efficient and straightforward approaches. However, the polymer exhibits poor solubility in common solvents used in the electrospinning process of PLA, which makes the preparation of homogeneous fibers very difficult. As an alternative, a precursor of such a polymer obtained before *N*-alkylation and chlorination, P(DMHI), was employed and added directly to the electrospinning PLA solution. Subsequent surface functionalization of the accessible triazole and hydantoin groups provides PLA-based fibers with the ability to efficiently inactivate Gram-positive and Gram-negative bacteria. It was demonstrated that the presence of cationic triazolium groups at the surface only provides high efficacy against Gram-positive bacteria, while their combination with *N*-halamine groups extends the effectiveness also to Gram-negative bacteria. Remarkably, due to the small diameter, and therefore high surface area, a minor amount of fibers loaded with antimicrobial is needed for pathogen inactivation. The compostability of the antibacterial electrospun fibers was also tested under simulated industrial composting conditions. It was observed that the incorporation of the antimicrobial biobased polymer apparently did not compromise PLA disintegration under aerobic composting conditions. However, a deep analysis of the compost samples proves the presence of microplastics in both samples (PLA and antimicrobial loaded PLA) after the biodisintegration test following the ISO 20200 standard protocol. Then, more studies are needed in this regard. In addition, these multifunctional biobased polymeric derivatives can be employed as an additive or component not only in electrospun fibers but could also be used in the preparation of films or other devices by different processing methods such as melt extrusion and additive manufacturing in which the solubility problem is avoided.

3.2.6 Acknowledgments

This work was funded by the MICINN (PID2019-104600RB-I00), Agencia Estatal de Investigación (AEI, Spain), Fondo Europeo de Desarrollo Regional (FEDER, EU), and CSIC (LINKA20364). A. Chiloeches acknowledges MICIU for his FPU fellowship FPU18/01776.

3.2.7 References

- (1) Zimmerli, W. Clinical Presentation and Treatment of Orthopaedic Implant-Associated Infection. *J. Intern. Med.* **2014**, 276 (2), 111–119.
- (2) Galié, S.; García-Gutiérrez, C.; Miguélez, E. M.; Villar, C. J.; Lombó, F. Biofilms in the Food Industry: Health Aspects and Control Methods. *Front. Microbiol.* **2018**, 9 (MAY), 898.
- (3) O'Neill, J. Antimicrobial Resistance: Tackling a Crisis for the Health and Wealth of Nations. Review on Antimicrobial Resistance; HM Government: London, **2014**.
- (4) Malheiro, J.; Simões, M. Antimicrobial Resistance of Biofilms in Medical Devices, Biofilms and Implantable Medical Devices. *Infect. Control* **2017**, 97–113.
- (5) Sugden, R.; Kelly, R.; Davies, S. Combatting Antimicrobial Resistance Globally. *Nat. Microbiol.* **2016**, 1 (10), 16187.
- (6) Korsak, D.; Chmielowska, C.; Szuplewska, M.; Bartosik, D. Prevalence of Plasmid-Borne Benzalkonium Chloride Resistance Cassette BcrABC and Cadmium Resistance CadA Genes in Nonpathogenic Listeria spp. Isolated from Food and Food-Processing Environments. *Int. J. Food Microbiol.* **2019**, 290, 247–253.
- (7) Clarke, B. O.; Smith, S. R. Review of ‘Emerging’ Organic Contaminants in Biosolids and Assessment of International Research Priorities for the Agricultural Use of Biosolids. *Environ. Int.* **2011**, 37 (1), 226–247.
- (8) Ribeiro, N.; Soares, G. C.; Santos-Rosales, V.; Concheiro, A.; Alvarez-Lorenzo, C.; García-González, C. A.; Oliveira, A. L. A New Era for Sterilization Based on Supercritical CO₂ Technology. *J. Biomed. Mater. Res. Part B Appl. Biomater.* **2020**, 108 (2), 399–428.
- (9) Tipnis, N. P.; Burgess, D. J. Sterilization of Implantable Polymer-Based Medical Devices: A Review. *Int. J. Pharm.* **2018**, 544 (2), 455–460.
- (10) Horakova, J.; Klicova, M.; Erben, J.; Klapstova, A.; Novotny, V.; Behalek, L.; Chvojka, J. Impact of Various Sterilization and Disinfection Techniques on Electrospun Poly-ε-Caprolactone. *ACS Omega* **2020**, 5 (15), 8885–8892.
- (11) Singh, B.; Sharma, N. Mechanistic Implications of Plastic Degradation. *Polym. Degrad. Stab.* **2008**, 93 (3), 561–584.
- (12) Pérez Davila, S.; González Rodríguez, L.; Chiussi, S.; Serra, J.; González, P. How to Sterilize Polylactic Acid Based Medical Devices? *Polymers* **2021**, 13 (13), 2115.
- (13) Savaris, M.; Santos, V. dos; Brandalise, R. N. Influence of Different Sterilization Processes on the Properties of Commercial Poly(Lactic Acid). *Mater. Sci. Eng. C* **2016**, 69, 661–667.
- (14) Salgado, P. R.; Di Giorgio, L.; Musso, Y. S.; Mauri, A. N. Recent Developments in Smart Food Packaging Focused on Biobased and Biodegradable Polymers. *Front. Sustain. Food Syst.* **2021**, 5 (April), 1–30.
- (15) Joseph, B.; James, J.; Kalarikkal, N.; Thomas, S. Recycling of Medical Plastics. *Adv. Ind. Eng. Polym. Res.* **2021**, 4 (3), 199–208.
- (16) Karan, H.; Funk, C.; Grabert, M.; Oey, M.; Hankamer, B. Green Bioplastics as Part of a Circular Bioeconomy. *Trends Plant Sci.* **2019**, 24 (3), 237–249.
- (17) RameshKumar, S.; Shaiju, P.; O'Connor, K. E.; Babu, R. Bio-Based and Biodegradable Polymers - State-of-the-Art, Challenges and Emerging Trends. *Curr. Opin. Green Sustain. Chem.* **2020**, 21, 75–81.
- (18) Smith, C. A.; Cataldo, V. A.; Dimke, T.; Stephan, I.; Guterman, R. Antibacterial and Degradable Thioimidazolium Poly(Ionic Liquid). *ACS Sustain. Chem. Eng.* **2020**, 8 (22), 8419–8424.

- (19) Cheng, J.; Chin, W.; Dong, H.; Xu, L.; Zhong, G.; Huang, Y.; Li, L.; Xu, K.; Wu, M.; Hedrick, J. L.; Yang, Y. Y.; Fan, W. Biodegradable Antimicrobial Polycarbonates with In Vivo Efficacy against Multidrug-Resistant MRSA Systemic Infection. *Adv. Healthc. Mater.* **2015**, 4 (14), 2128–2136.
- (20) Li, Q.; Tan, W.; Zhang, C.; Gu, G.; Guo, Z. Synthesis of Water Soluble Chitosan Derivatives with Halogeno-1,2,3-Triazole and Their Antifungal Activity. *Int. J. Biol. Macromol.* **2016**, 91, 623–629.
- (21) Arza, C. R.; Ilk, S.; Demircan, D.; Zhang, B. New Biobased Non-Ionic Hyperbranched Polymers as Environmentally Friendly Antibacterial Additives for Biopolymers. *Green Chem.* **2018**, 20 (6), 1238–1249.
- (22) Tan, J.; Tay, J.; Hedrick, J.; Yang, Y. Y. Synthetic Macromolecules as Therapeutics That Overcome Resistance in Cancer and Microbial Infection. *Biomaterials* **2020**, 252 (May), 120078.
- (23) Chiloeches, A.; Funes, A.; Cuervo-Rodríguez, R.; López-Fabal, F.; Fernández-García, M.; Echeverría, C.; Muñoz-Bonilla, A. Biobased Polymers Derived from Itaconic Acid Bearing Clickable Groups with Potent Antibacterial Activity and Negligible Hemolytic Activity. *Polym. Chem.* **2021**, 12 (21), 3190–3200.
- (24) Chiloeches, A.; Cuervo-Rodríguez, R.; López-Fabal, F.; Fernández-García, M.; Echeverría, C.; Muñoz-Bonilla, A. Antibacterial and Compostable Polymers Derived from Biobased Itaconic Acid as Environmentally Friendly Additives for Biopolymers. *Polym. Test.* **2022**, 109, 107541.
- (25) Timofeeva, L.; Kleshcheva, N. Antimicrobial Polymers: Mechanism of Action, Factors of Activity, and Applications. *Appl. Microbiol. Biotechnol.* **2011**, 89 (3), 475–492.
- (26) Aytac, Z.; Huang, R.; Vaze, N.; Xu, T.; Eitzer, B. D.; Krol, W.; MacQueen, L. A.; Chang, H.; Bousfield, D. W.; Chan-Park, M. B.; Ng, K. W.; Parker, K. K.; White, J. C.; Demokritou, P. Development of Biodegradable and Antimicrobial Electrospun Zein Fibers for Food Packaging. *ACS Sustain. Chem. Eng.* **2020**, 8 (40), 15354–15365.
- (27) Amariei, G.; Kokol, V.; Boltes, K.; Letón, P.; Rosal, R. Incorporation of Antimicrobial Peptides on Electrospun Nanofibres for Biomedical Applications. *RSC Adv.* **2018**, 8 (49), 28013–28023.
- (28) Wang, L.; Wu, Y.; Hu, T.; Guo, B.; Ma, P. X. Electrospun Conductive Nanofibrous Scaffolds for Engineering Cardiac Tissue and 3D Bioactuators. *Acta Biomater.* **2017**, 59, 68–81.
- (29) Liang, Y.; Liang, Y.; Zhang, H.; Guo, B. Antibacterial Biomaterials for Skin Wound Dressing. *Asian J. Pharm. Sci.* **2022**, 17 (3), 353–384.
- (30) Fan, X.; Ren, X.; Huang, T. S.; Sun, Y. Cytocompatible Antibacterial Fibrous Membranes Based on Poly(3-Hydroxybutyrate-Co-4-Hydroxybutyrate) and Quaternarized N -Halamine Polymer. *RSC Adv.* **2016**, 6 (48), 42600–42610.
- (31) Chien, H. W.; Chiu, T. H.; Lee, Y. L. Rapid Biocidal Activity of N-Halamine-Functionalized Polydopamine and Polyethylene Imine Coatings. *Langmuir* **2021**, 37 (26), 8037–8044.
- (32) Echeverría, C.; Muñoz-Bonilla, A.; Cuervo-Rodríguez, R.; López, D.; Fernández-García, M. Antibacterial PLA Fibers Containing Thiazolium Groups as Wound Dressing Materials. *ACS Appl. Bio Mater.* **2019**, 2 (11), 4714–4719.
- (33) Echeverría, C.; Limón, I.; Muñoz-Bonilla, A.; Fernández-García, M.; López, D. Development of Highly Crystalline Polylactic Acid with β -Crystalline Phase from the Induced Alignment of Electrospun Fibers. *Polymers* **2021**, 13 (17), 2860.
- (34) Murata, H.; Koepsel, R. R.; Matyjaszewski, K.; Russell, A. J. Permanent, Non-Leaching Antibacterial Surfaces-2: How High Density Cationic Surfaces Kill Bacterial Cells. *Biomaterials* **2007**, 28 (32), 4870–4879.
- (35) Kliewer, S.; Wicha, S. G.; Bröker, A.; Naundorf, T.; Catmadim, T.; Oellingrath, E. K.; Rohnke, M.; Streit, W. R.; Vollstedt, C.; Kipphardt, H.; Maison, W. Contact-Active Antibacterial Polyethylene Foils via Atmospheric Air Plasma Induced Polymerisation of Quaternary Ammonium Salts. *Colloids Surfaces B Biointerfaces* **2020**, 186 (July 2019), 110679.

- (36) Tiller, J.; Liao, C.-J.; Lewis, K.; Klibanov, A. Designing Surface That Kill Bacteria on Contact. *Proc Natl Acad Sci USA* **2001**, 98, 5981–5985.
- (37) ASTM E2149-13a, Standard Test Method for Determining the Antimicrobial Activity of Antimicrobial Agents Under Dynamic Contact Conditions; ASTM International: West Conshohocken, PA, **2019**.
- (38) International Organization for Standardization. ISO 20200: Determination of the Degree of Disintegration of Plastic Materials under Simulated Composting Conditions in a Laboratory-Scale Test; International Organization for Standardization: Geneve, Switzerland.
- (39) Liu, Y.; Ma, K.; Li, R.; Ren, X.; Huang, T. S. Antibacterial Cotton Treated with N-Halamine and Quaternary Ammonium Salt. *Cellulose* **2013**, 20 (6), 3123–3130.
- (40) Li, L.; Zhou, H.; Gai, F.; Chi, X.; Zhao, Y.; Zhang, F.; Zhao, Z. Synthesis of Quaternary Phosphonium N-Chloramine Biocides for Antimicrobial Applications. *RSC Adv.* **2017**, 7 (22), 13244–13249.
- (41) Kügler, R.; Bouloussa, O.; Rondelez, F. Evidence of a Charge-Density Threshold for Optimum Efficiency of Biocidal Cationic Surfaces. *Microbiology* **2005**, 151 (5), 1341–1348.
- (42) Beltrán, F. R.; Gaspar, G.; Dadras Chomachayi, M.; Jalali-Arani, A.; Lozano-Pérez, A. A.; Cenis, J. L.; de la Orden, M. U.; Pérez, E.; Martínez Urreaga, J. M. Influence of Addition of Organic Fillers on the Properties of Mechanically Recycled PLA. *Environ. Sci. Pollut. Res.* **2021**, 28 (19), 24291–24304.
- (43) Vidakis, N.; Petousis, M.; Kourinou, M.; Velidakis, E.; Mountakis, N.; Fischer-Griffiths, P. E.; Grammatikos, S.; Tzounis, L. Additive Manufacturing of Multifunctional Polylactic Acid (PLA)-Multiwalled Carbon Nanotubes (MWCNTs) Nanocomposites. *Nanocomposites* **2021**, 7 (1), 184–199.
- (44) Khammassi, S.; Tarfaoui, M.; Škrlová, K.; Měřinská, D.; Plachá, D.; Erchiqui, F. Poly(Lactic Acid) (PLA)-Based Nanocomposites: Impact of Vermiculite, Silver, and Graphene Oxide on Thermal Stability, Isothermal Crystallization, and Local Mechanical Behavior. *J. Compos. Sci.* **2022**, 6 (4), 112.
- (45) Nigmatullin, R.; Gao, F.; Konovalova, V. Permanent, Non-Leaching Antimicrobial Polyamide Nanocomposites Based on Organoclays Modified with a Cationic Polymer. *Macromol. Mater. Eng.* **2009**, 294 (11), 795–805.
- (46) Fortunati, E.; Armentano, I.; Iannoni, A.; Barbale, M.; Zaccheo, S.; Scavone, M.; Visai, L.; Kenny, J. M. New Multifunctional Poly(Lactide Acid) Composites: Mechanical, Antibacterial, and Degradation Properties. *J. Appl. Polym. Sci.* **2012**, 124, 87–98.
- (47) Elsawy, M. A.; Kim, K. H.; Park, J. W.; Deep, A. Hydrolytic Degradation of Polylactic Acid (PLA) and Its Composites. *Renew. Sustain. Energy Rev.* **2017**, 79 (June 2016), 1346–1352.
- (48) Leonés, A.; Peponi, L.; Lieblich, M.; Benavente, R.; Fiori, S. In Vitro Degradation of Plasticized PLA Electrospun Fiber Mats: Morphological, Thermal and Crystalline Evolution. *Polymers* **2020**, 12 (12), 2975.

3.2.8 Supporting Information

¹H-NMR spectra of the P(Boc-DMHI) and P(DMHIQ) polyitaconate derivatives and photographs of the agar plates of *E. coli* (Gram-negative bacteria) and *S. epidermidis* (Gram-positive bacteria) bacterial colonies after spreading inoculum (at different dilutions) in the previous contact with fibers.

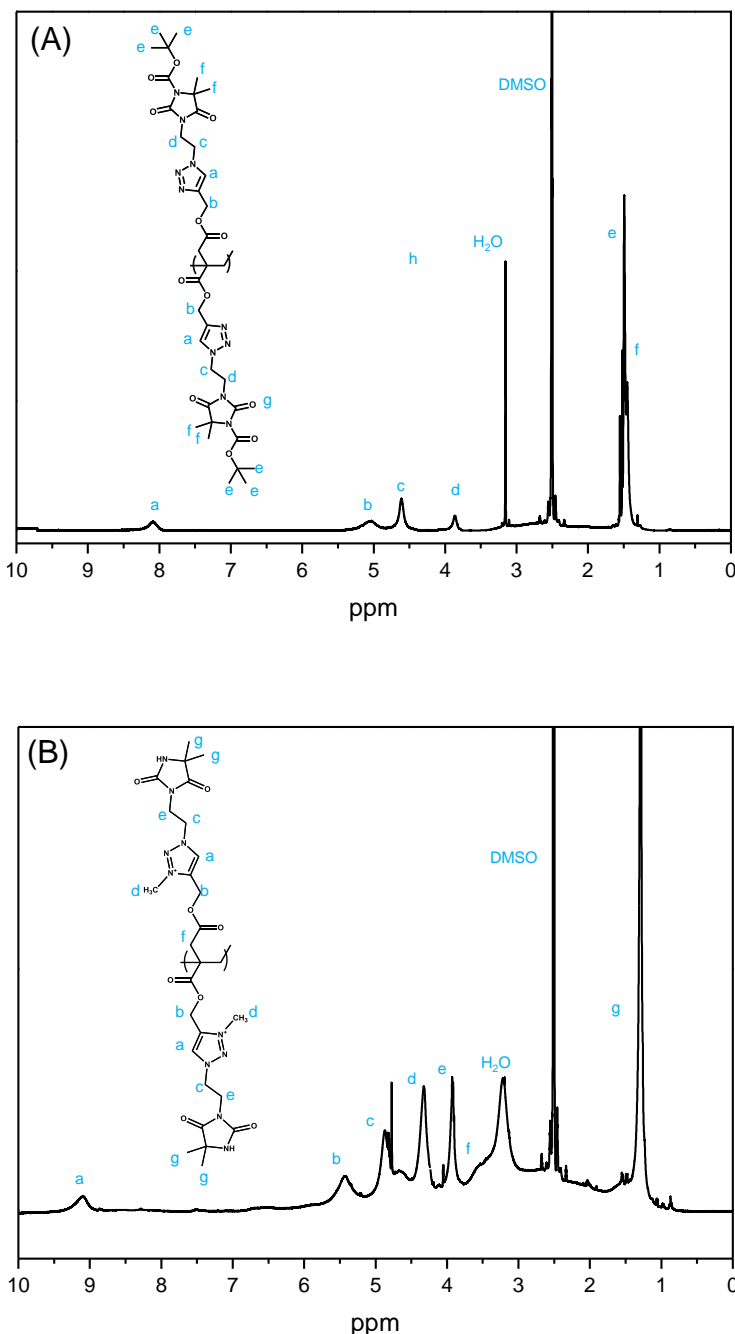


Figure S1. ¹H-NMR spectra of (A) P(Boc-DMHI) and (B) P(DMHI-Q) polyitaconate derivatives obtained in DMSO-d₆ as solvent.

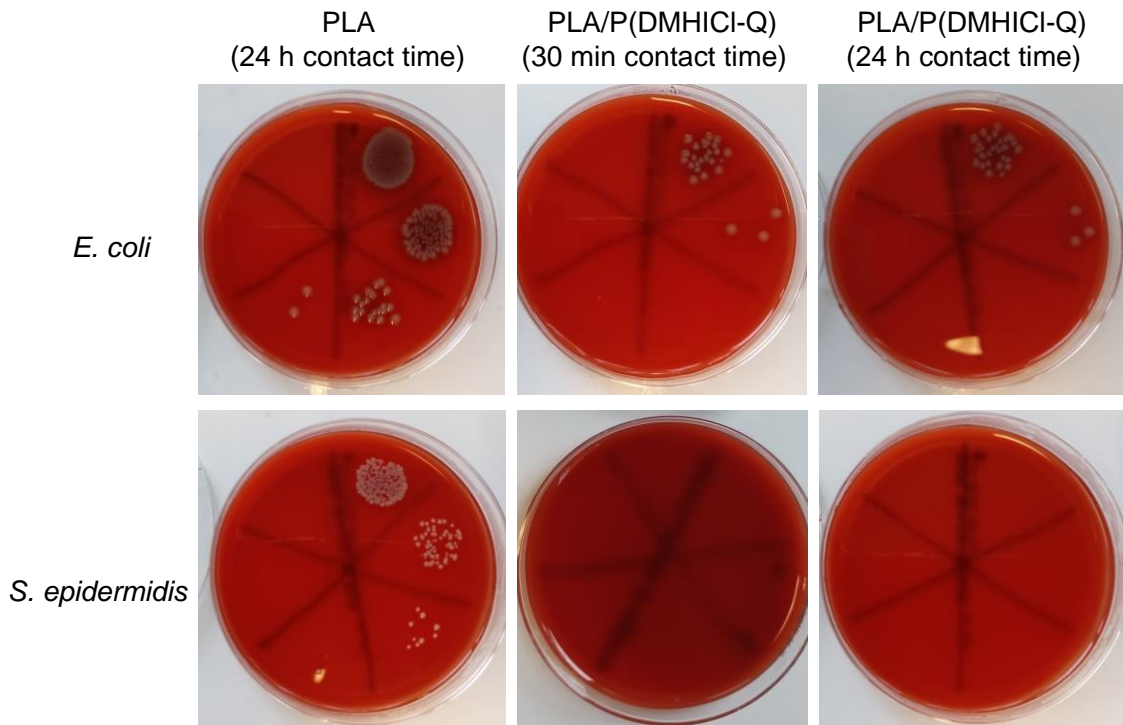


Figure S2. Pictures of the agar plates of *E. coli* (Gram-negative bacteria) and *S. epidermidis* (Gram-positive bacteria) bacterial colonies after spreading inoculum (at different dilutions) in previous contact with PLA fibers (control, left) and incubation during 24 h, and in contact with PLA/(P(DMHICI-Q) fibers and incubation during 30 min (middle) and 24 h (right).

3.3 Synergistic combination of antimicrobial peptides and cationic polyitaconates in multifunctional PLA fibers

ACS Applied Bio Materials

Synergistic combination of antimicrobial peptides and cationic polyitaconates in multifunctional PLA fibers

A. Chiloeches^{1,2} J. Zágora³, D. Plachá³, M.D.T. Torres^{4,5,6}, C. de la Fuente-Nunez^{4,5,6}, F. López-Fabai^{7,8}, Y. Gil-Romero⁷, R. Fernández-García⁷, M. Fernández-García¹, C. Echeverría^{1*}, A. Muñoz-Bonilla^{1*}

¹Instituto de Ciencia y Tecnología de Polímeros (ICTP-CSIC), C/Juan de la Cierva 3, 28006 Madrid, Spain

²Universidad Nacional de Educación a Distancia (UNED), C/ Bravo Murillo 38, 28015 Madrid, Spain

³Nanotechnology Centre, CEET, VSB – Technical University of Ostrava, 17. Listopadu 2172/15, 708 00 Ostrava-Poruba, Czech Republic

⁴Machine Biology Group, Departments of Psychiatry and Microbiology, Institute for Biomedical Informatics, Institute for Translational Medicine and Therapeutics, Perelman School of Medicine, University of Pennsylvania, Philadelphia, PA 19104, USA

⁵Departments of Bioengineering and Chemical and Biomolecular Engineering, School of Engineering and Applied Science, University of Pennsylvania, Philadelphia, PA 19104, USA

⁶Penn Institute for Computational Science, University of Pennsylvania, Philadelphia, PA 19104, USA

⁷Hospital Universitario de Móstoles C/ Dr. Luis Montes, s/n, 28935 Móstoles, Madrid, Spain

⁸Facultad de Ciencias Experimentales, Universidad Francisco de Vitoria, Carretera Pozuelo a Majadahonda, Km 1.800, 28223, Madrid, Spain

mail: cecheverria@ictp.csic.es (C. Echeverría), sbonilla@ictp.csic.es (A. Muñoz-Bonilla)

Abstract

Combining different antimicrobial agents has emerged as a promising strategy to enhance efficacy and address resistance evolution. In this study, we investigated the

3.3.1 Abstract

Combining different antimicrobial agents has emerged as a promising strategy to enhance efficacy and address resistance evolution. In this study, we investigated the synergistic antimicrobial effect of a cationic biobased polymer and the antimicrobial peptide Temporin L, with the goal of developing multifunctional electrospun fibers for potential biomedical applications, particularly in wound dressing. A clickable polymer with pendent alkyne groups was synthesized using a biobased itaconic acid building block. Subsequently, the polymer was functionalized through click chemistry with thiazolium groups derived from vitamin B1 (PTTIQ), as well as a combination of thiazolium and the antimicrobial peptide (AMP) Temporin L, resulting in a conjugate polymer-peptide (PTTIQ-AMP). The individual and combined effects of the cationic PTTIQ, Temporin L, and PTTIQ-AMP were evaluated against Gram-positive and Gram-negative bacteria, as well as Candida species. The results demonstrated that most combinations exhibited an indifferent effect, whereas the covalently conjugated PTTIQ-AMP displayed an antagonist effect, potentially attributed to the aggregation process. Both antimicrobial compounds, PTTIQ and Temporin L, were incorporated into poly(lactic acid) (PLA) electrospun fibers using the supercritical solvent impregnation method. This approach yielded fibers with improved antibacterial performance, as a result of the potent activity exerted by the AMP and the non-leaching nature of the cationic polymer, thereby enhancing long-term effectiveness.

Keywords: Cationic polymers; antimicrobial peptide; fibers; supercritical impregnation; antimicrobial

3.3.2 Introduction

The utilization of antimicrobial and biodegradable compounds derived from renewable resources has gained significant importance in the medical field. Research and development efforts are increasingly focused on materials obtained from sustainable sources. Incorporating antimicrobial biobased polymers into biomaterials offers a promising approach to reduce microbial contamination and decrease reliance on antibiotics, while maintaining biodegradability and sustainability. This is particularly crucial for single-use items like face masks and wound dressings.¹ Electrospinning has emerged as a well-established and versatile technology for producing sub-micron-sized fibers, which provides numerous advantages such as a high surface-to-volume ratio. These electrospun fiber mats serve as physical barriers, preventing microbial penetration while facilitating oxygen and gas transfer, especially important for wound dressing applications.² Moreover, the high surface area of these fiber mats enables the incorporation of bioactive molecules, including antimicrobial compounds, thereby reducing the risk of infections.

In various biomedical applications, including wound dressings, biobased and biodegradable polymers with antimicrobial properties have been successfully incorporated into electrospun fibers.³⁻⁷ Generally, these antimicrobial polymers possess cationic characteristics and exert their antimicrobial activity through contact interactions rather than release-based strategies. This mechanism involves electrostatic interactions with microbial membranes, leading to physical damage to the bacterial wall. Consequently, this approach minimizes the likelihood of bacterial resistance development.

Antimicrobial peptides (AMPs) have emerged as a highly promising class of antibacterial agents due to their low propensity for inducing resistance. These peptides exhibit efficacy against a broad spectrum of microorganisms, including both planktonic bacteria and biofilms.⁸⁻¹¹ AMPs achieve their antimicrobial activity by disrupting the cell membranes of bacteria, a mechanism facilitated by their unique physicochemical properties and amphipathic characteristics. These attributes make AMPs ideal candidates for incorporation into materials designed for various biomedical applications,^{12,13} having been incorporated in fibrous scaffolds to fabricate antimicrobial wound dressings.¹⁴⁻¹⁶ An example of an AMP family is the Temporins, which are derived from the skin of the frog *Rana temporaria* and have shown potential for topical applications.^{17,18} Temporins are short peptides with a low net positive charge and demonstrate effectiveness against both

Gram-positive and Gram-negative bacteria, viruses, and *Candida* spp. Among the approximately 130 isoforms within this family, Temporin L stands out as a particularly promising candidate due to its potent antimicrobial activity (ranging from 0.3-3.6 μ M for different bacterial strains¹⁹). At physiological pH, the cationic net charge of Temporin L, coupled with its amphipathic nature, allows it to adopt an α -helical conformation, facilitating interactions with the phospholipid components of bacterial membranes. Furthermore, synergistic antibacterial effects have been observed when Temporin L is combined with Temporins A and B.²⁰ Notably, investigations combining Temporin L with clinically used antibiotics have yielded varied outcomes, ranging from synergy to antagonism.²¹ In this study, we explore the impact of combining the AMP Temporin L with a cationic polymer on antimicrobial activity.

To investigate the potential synergistic effects of combining antimicrobial compounds, we chose a bio-based polyitaconate containing thiazolium groups based on its advantageous properties, including biobased origin, biodegradability, high antimicrobial activity, low toxicity. Different synthetic approaches were employed to combine this polymer with Temporin L. The antimicrobial activity of the compounds was assessed through determination of minimal inhibitory concentration (MIC) values and calculation of the fractional inhibitory concentration (FIC) index. Additionally, to explore the impact of covalently binding the peptide with the polymer, we synthesized a conjugate using click chemistry and examined its antimicrobial properties. Lastly, both antimicrobial compounds were incorporated into electrospun PLA fibers, and their efficacy against bacteria was evaluated.

Antimicrobial agents can be effectively immobilized into the fibers by incorporation into the solution before the generation of the fibers.¹⁵ However, the processing conditions during electrospinning can significantly impact the stability, activity, and distribution of these compounds within the fibers. The antimicrobials may alter solution properties, such as viscosity or conductivity, which can negatively affect the production of homogeneous fibers. An alternative approach is the direct incorporation of bioactive agents into fibers after the electrospinning process, either through chemical modification reactions or impregnation methods. However, traditional methods often suffer from drawbacks, including the use of toxic organic chemicals, issues of dissolution or compatibility, undesirable reactions and degradation, low loading yields, and heterogeneous incorporation. To address these challenges, supercritical solvent impregnation (SSI) has emerged as a highly advantageous technique for designing functional materials. This

method offers numerous benefits and possibilities while serving as a non-toxic and environmentally friendly alternative, particularly when utilizing carbon dioxide (scCO_2)²². The favorable critical properties of scCO_2 , such as low temperature and critical pressure, along with its non-toxic nature, widespread availability, and ease of removal through decompression, make it an ideal choice for SSI. In this process, the active compound is dissolved in scCO_2 and brought into contact with the materials to be impregnated. Due to the low viscosity and near-zero surface tension of the supercritical solution, it can easily penetrate the polymer matrix, enabling high impregnation yields. SSI methods have been successfully employed to immobilize various antimicrobial agents, particularly essential oils, into polymeric materials.

In this study, we utilized SSI methods to load the antimicrobial peptide Temporin L into electrospun fibers based on poly(lactic acid) (PLA), which also contained a cationic biobased polymer. The objective was to develop multifunctional biobased fibers with antimicrobial activity.

3.3.3 Experimental part

Materials

To prepare antimicrobial polyitaconates, we acquired the following chemicals. Itaconic acid (IA, ≥99%), propargyl alcohol (≥99%), hydroquinone (99%), copper chloride (CuCl, ≥99.995%), N,N,N',N'',N''-pentamethyldiethylenetriamine (PMDETA, 99%), iodomethane (MeI, 99.5%), neutral aluminum oxide, sodium bicarbonate (NaHCO₃, ≥99.7%), magnesium sulfate anhydrous (MgSO₄, ≥99.5%), anhydrous tetrahydrofuran (THF, 99.9%), and anhydrous N,N-dimethylformamide (DMF, 99.8%) were obtained from Merck and used as received. The synthesis of 2-(4-methylthiazol-5-yl)ethanol azide was conducted according to the previously reported method.²³ 2,2'-Azobisisobutyronitrile (AIBN, 98%), used as radical initiator was purchased from Acros. Tetrahydrofuran (THF), N,N-dimethylformamide (DMF), ethanol (EtOH), hexane and chloroform (CHCl₃) were purchased from Scharlau. Ethyl acetate (EtOAc) was procured from Cor Química S.L., toluene from Merck and sulfuric acid (H₂SO₄) from Panreac. Deuterated solvents for NMR measurements, chloroform (CDCl₃) and dimethyl sulfoxide (DMSO-d₆), were acquired from Sigma-Aldrich. Cellulose dialysis membranes (CelluSep T1) were purchased from Membrane Filtration Products, Inc. and PLA (6202D) was provided by NatureWorks.

To conduct the antibacterial assays, the following materials were acquired: phosphate buffered saline powder pH 7.4 (PBS) obtained from Merck and BBL Mueller–Hinton broth purchased from Becton, Dickinson and Company were employed as bacterial medium. 96 well microplates were purchased from BD Biosciences. Columbia agar (5% sheep blood) plates were provided from BioMérieux. Sodium chloride solution (NaCl, BioXtra) was obtained from Merck. *Pseudomonas aeruginosa* (*P. aeruginosa*, ATCC 27853), *Escherichia coli* (*E. coli*, ATCC 25922), *Staphylococcus aureus* (*S. aureus*, ATCC 29213), *Enterococcus faecalis* (*E. faecalis*, ATCC 29212) and *Candida albicans* (*C. albicans*, ATCC 200955) were purchased from Oxoid and used as microbial strains.

Synthesis of clickable polymer, P(Prl)

The P(Prl) polymer bearing alkyne groups was synthesized as previously described from biobased itaconic acid.²⁴ Firstly, itaconic acid was reacted with propargyl alcohol via condensation reaction using H₂SO₄ as catalyst under reflux in THF/toluene. After purification, the monomer (Prl) was polymerized by conventional radical polymerization at a total concentration of 2 M in anhydrous DMF, 5 mol% of AIBN initiator, at 70 °C under nitrogen atmosphere for 24 h. The polymer P(Prl) was purified through precipitation in isopropanol and subsequently dried under vacuum, resulting in the formation of a white solid (M_n= 6700 g/mol, M_w/M_n= 1.6). ¹H-NMR (400 MHz, CDCl₃, δ, ppm): 4.67 (4H, -CH₂C≡CH), 2.49 (2H, -CH₂C≡CH), 1.99-1.00 (8H, CH₂-CO and -CH₂-chain).

Synthesis of thiazolium derivative, M2Q

The 2-(4-methylthiazol-5-yl)ethanol azide (M2) was synthesized from 5-(2-hydroxyethyl)-4-methylthiazole by the formation of the mesylate intermediate followed by the reaction with sodium azide²⁵. Subsequently, the obtained azide-functionalized thiazole was subjected to N-alkylation reaction sing methyl iodide, resulting in the formation of the cationic thiazolium derivative (M2Q). Briefly, M2 (2.000 g, 11.8 mol) was dissolved in 25 mL of acetonitrile and then, a substantial excess of MeI was introduced (110 μL, 17.7 mmol). The reaction mixture was stirred at 90 °C for 24 h. After that, the solvent was partially removed by rota-evaporation and the thiazolium derivative M2Q was purified by precipitation in ether and dried under vacuum (3.570 g, 97% yield). ¹H-NMR (400M Hz, DMSO-d6, δ, ppm): 10.01 (s, 1H, H-thiazole), 4.08 (s, 3H, CH₃-N+), 3.65 (t, 2H, N₃-CH₂-CH₂-thiazole), 3.18 (t, 2H, N₃-CH₂-CH₂-thiazole), 2.45 (s, 3H, CH₃-thiazole).

Synthesis of antimicrobial peptide, AMP

The peptides Temporin-L (FVRWFSRFLGRIL) and azide-Temporin-L ($\text{K}(\text{N}_3)\text{GGGFVRWFSRFLGRIL}$) were purchased from AAPPTec (Kentucky, USA), where $\text{K}(\text{N}_3)$ stands for a lysine residue modified with an azide group in its ϵ -amino group. The purified peptides were characterized by HPLC and mass spectrometry.

Synthesis of polyitaconate derivatives bearing thiazolium groups, PTTIQ

The incorporation of the thiazolium derivative synthesized in section 2.3 to clickable biobased polymer P(Prl) was performed by CuAAC click chemistry. In a typical procedure, P(Prl) polymer bearing alkyne groups (0.150 g, 0.72 mmol), cationic thiazolium derivative functionalized with azide (M2Q) (0.496 g, 1.6 mmol), CuCl (7.2 mg, 0.073 mmol) and PMDETA (30 μL , 0.14 mmol) were dissolved in 5 mL of DMSO and the mixture was stirred at room temperature for 24 h. Following that, the resulting cationic polymer (PTTIQ) was purified via dialysis and was subsequently recovered through lyophilization. (0.366 g, 61% yield). $^1\text{H-NMR}$ (400 MHz, DMSO-d₆, δ , ppm): 10.02 (2H, *H*-thiazolium), 8.20 (2H, *H*-triazole), 5.05 (4H, O-CH₂-triazole), 4.65 (4H, CH₂-N), 4.08 (6H, N⁺CH₃ thiazole), 3.55 (4H, CH₂-thiazolium), 2.44 (6H, CH₃-thiazolium), 2.00-1.00 (4H, CH₂-CO and -CH₂-chain).

Synthesis of polyitaconate derivatives bearing thiazolium groups and antimicrobial peptide, conjugate PTTIQ-AMP

The azide-Temporin-L AMP was incorporated into the polymer chain by CuAAC reaction via alkyne groups. P(Prl) polymer (0.010 g, 0.097 meq), peptide (0.020 g, 0.010 mmol), CuCl (1 mg, 0.01 mmol) and PMDETA (3.8 μL , 0.020 mmol) were dissolved in 5 mL of DMSO and the mixture was stirred at room temperature for 24 h. Subsequently, M2Q (0.027 g, 0.087 mmol) was added to the reaction mixture and the solution was stirred for other 24 h. After that, the conjugated peptide-polymer (PTTIQ-AMP) was purified by dialysis against deionized water and was subsequently lyophilized (0.019 mg, 33% yield). $^1\text{H-NMR}$ (400M Hz, DMSO-d₆, δ , ppm): 10.70 (*NH*- Tryptophan, 10.02 (*H*-thiazolium), 8.4-7.7 (*H*-triazole and *NH* amide of peptide), 7.4 (aromatic protons of peptide) 5.05 (O-CH₂-triazole), 4.65 (4H, CH₂-N), 4.08 (6H, N⁺CH₃ thiazole), 3.55 (4H, CH₂-thiazolium), 2.44 (6H, CH₃-thiazolium), 2.00-1.00 (4H, CH₂-CO and -CH₂-chain), 0.80 (CH₃- Valine, Leucine and Isoleucine).

Preparation of antimicrobial functional fibers via electrospinning

Electrospinning solutions were prepared by dissolving 90 wt% of PLA and 10 wt% of polyitaconate derivative PTTIQ in a mixture of CHCl₃/DMF (90/10 v/v) at a concentration of 20% w/w. We have selected the composition of the fiber mats based on previous works.^{4,5} PLA solutions were also prepared and used as blank sample. These solutions were utilized to produce electrospun polymeric fibers using a custom-made electrospinner with a horizontal configuration. The electrospinner featured a syringe needle connected to a high voltage power source. Fibers mats were collected utilizing a grounded aluminum foil collector positioned perpendicularly at a distance of 12 cm from the needle tip. The electrospinning process involved a flow rate of 1 mL h⁻¹ and the application of a voltage of 16 kV for 30 minutes at room temperature. The resulting fibers were subsequently dried under vacuum at room temperature for 24 hours and labelled as PLA/PTTIQ, and PLA fiber mats.

Functionalization of PLA based fibers by Supercritical Solvent Impregnation

The PLA and PLA/PTTIQ fiber mats were impregnated with the AMP Temporin-L using ScCO₂ as solvent in a commercially supplied device Speed SFE-4 (Applied Separations Inc., USA). Briefly, 6.6 mg of the corresponding fiber mat, 5 mg of AMP and 0.2 mL of ethanol were placed in the high-pressure reactor. The chamber was closed and operated at 40 °C and at 150 bar of pressurized CO₂ for 3 h. Then, depressurization takes place until atmospheric pressure. The mass of impregnated AMP was determined gravimetrically by measuring the weight of samples before and after impregnation. Impregnation yield (I) of PLA and PLA/PTTIQ fibers was calculated according to:

$$I = \frac{m_{AMP}}{m_{AMP} + m_0} \cdot 100$$

where m_0 is the initial mass of fiber mats and m_{AMP} is the mass of impregnated fibers with AMP.

Characterization

NMR spectra were acquired at room temperature using deuterated solvents on a Bruker Avance III HD-400AVIII spectrometer. Size exclusion chromatography (SEC) measurements were conducted using a Waters Division Millipore system, which was equipped with a Waters 2414 refractive index detector. The eluent used was DMF stabilized with 0.1 M LiBr (Sigma-Aldrich, >99.9%) at 50 °C and at a flow rate of 1 mL

min⁻¹. Poly(methyl methacrylate) standards (Polymer Laboratories LTD) were employed for calibration purposes. FTIR spectra were collected utilizing a PerkinElmer Spectrum Two instrument that was equipped with an attenuated total reflection module. Dynamic light scattering (DLS) and Zeta potential measurements in distilled water at 25 °C were performed with a Zetasizer Nano series ZS (Malvern Instruments Ltd). To analyze the morphology of the electrospun fibers, scanning electron microscopy (SEM) was employed on previously gold coated samples using a Philips XL30 microscope with an acceleration voltage of 25-10 kV.

Antimicrobial assays

The antibacterial activities of the cationic polymer PTTIQ and AMP Temporin L were evaluated by determining the minimum inhibition concentrations (MICs) using the standard broth dilution method provided by the Clinical Laboratory Standards Institute (CLSI).²⁶ Bacterial cells were grown on 5% sheep blood Columbia agar plates for 24 h at 37 °C. Then, fresh Mueller Hinton broth was utilized to adjust the bacterial concentration to 10⁶ CFU mL⁻¹. Solutions of the polymer or AMP at a concentration of 20 mg mL⁻¹ (1.9 and 11 mM, respectively) were also obtained in the Mueller–Hinton broth. In the subsequent step, 100 µL from each stock solution were dispensed into the first column of a 96-well round-bottom microplate, while the remaining wells were supplemented with 50 µL of broth. Starting with the first column, a polymer solution (50 µL) was diluted in a 2-fold serial manner across the remaining wells. Subsequently, 50 µL of the bacterial solution was added to achieve a total volume of 100 µL and a bacterial concentration 5 × 10⁵ CFU mL⁻¹. A positive control lacking the antimicrobial and a negative control lacking bacterial strains were also prepared. After incubation at 37 °C for 24 h, and the MIC values against each strain were estimated by checking visually the absence of bacterial growth. All the tests were performed in three biological replicates.

To estimate the antimicrobial combinations, the fractional inhibitory concentration index (FICI) was calculated according to the checkerboard assay.^{27,28} In this assay, a broth dilution method was performed from the stock solutions of both antimicrobial compounds prepared as described below, starting from concentrations of 2×MIC and using bacterial suspension at a final concentration of 5 × 10⁵ CFU mL⁻¹. In a 96-well round-bottom microplate, columns from 1 to 9 contain 2-fold serial dilutions of PTTIQ, while row from A to G contain serial dilutions of AMP. Column 10 contains serial dilutions of PTTIQ alone and row H contains serial dilutions of AMP alone, used to determine de MIC value of each

compound. Column 11 was used as positive growth control without antimicrobial compound and column 12 was used as negative control, containing only the growth medium. The antimicrobial interactions were expressed as the FICI values, which are calculated as:

$$FICI = \frac{MIC_c^{PTTIQ}}{MIC_a^{PTTIQ}} + \frac{MIC_c^{AMP}}{MIC_a^{AMP}}$$

where MIC_c are the MICs of the combinations and MIC_a are the MICs of the antimicrobial alone.

The prepared fiber mats functionalized with the antimicrobial compounds (PTTIQ and/or AMP) were analyzed following the E2149-20 standard method²⁹ from the American Society for Testing and Materials (ASTM) against *E. coli* and *E. faecalis* strains previously cultured for 24 h at 37 °C on 5% sheep blood Columbia agar plates. Next, the bacterial suspensions of 10^6 CFU mL⁻¹ were prepared in PBS. Next, fiber mats (1 mg) were introduced in sterile falcon tubes containing 0.1 mL of the tested inoculum and 0.9 mL of PBS ($\sim 10^5$ CFU mL⁻¹). Control experiments were conducted under two conditions, in the presence of PLA fiber without any antimicrobial compound, and in the absence of mats entirely. The suspensions were subjected to shaking at 120 rpm for 24 hours. Following that, the grown colonies were quantified using the plate counting method, and the reduction percentage was estimated in comparison to the control. The measurements were made at least in triplicate.

The release of the antimicrobial compounds from the PLA fibers to the medium was evaluated by the presence or the absence of zones of inhibition around the sample (6 mm in diameter) when they are placed on agar plates inoculated with *E. coli* ($\sim 10^5$ CFU mL⁻¹) by the spread plate method and after incubation for 24 h at 37 °C.

3.3.4 Results and Discussion

Synthesis of antimicrobial biobased polymers derived from itaconic acid

In our previous study, we successfully developed biobased polymers derived from itaconic acid that incorporate triazolium and thiazolium groups, thus exhibiting antibacterial properties. The synthesis process involved multiple steps. Initially, a clickable polyitaconate was reacted with an azide-modified thiazole molecule, resulting in the formation of a polyitaconate polymer with side chains containing both thiazole and triazole groups via a cycloaddition reaction. Subsequently, an additional step involving N-

alkylation was necessary to obtain the final cationic polymer, which contained thiazolium and triazolium groups (with a total of four cationic groups per monomeric unit).

In this current work, we improved the synthetic approach by quaternizing the azide-modified thiazole molecule prior to the click chemistry reaction. This modification enabled the direct formation of the cationic polyitaconate, with the cationic charge selectively located on the thiazolium moieties. Simultaneously, we explored the incorporation of other functionalities into the clickable polymer to synthesize antimicrobial materials with combined action. Specifically, we successfully attached the antimicrobial peptide Temporin L to the polyitaconate, utilizing the thiazolium group for conjugation. (Figure 1).

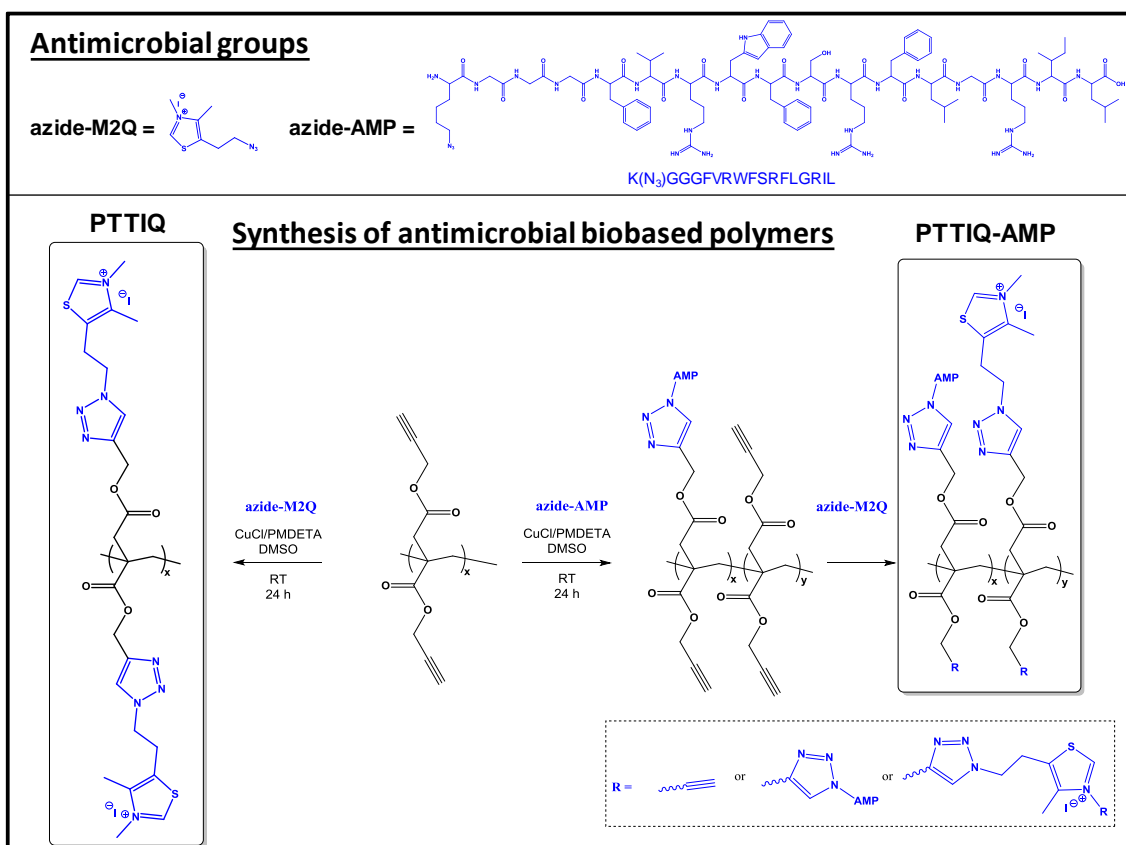


Figure 1. Synthesis of cationic biobased polyitaconate bearing thiazolium groups (PTTIQ) and of the conjugated structure, biobased polyitaconate bearing thiazolium and AMP (PTTIQ-AMP).

Next, we characterized the synthesized polymers by nuclear magnetic resonance (Figure 2). The ¹H-NMR spectra of the synthesized polymers, in which all signals can be assigned to the targeted polymer structures were successfully obtained. Based on the intensity of NMR signals, the composition of the obtained conjugated polymer (PTTIQ-AMP) was estimated to be 70 mol% of M2Q thiazolium and 30 mol% of AMP, thus yielding a higher content of peptide than the content used initially for the synthesis (**N**₃-M2Q/ **N**₃-AMP:

90/10). This can be attributed to the steric hindrance of the AMP, which may have hindered the subsequent reaction of the unreacted alkyne groups from the polyitaconate chain, consequently affecting the attachment of all thiazolium groups.

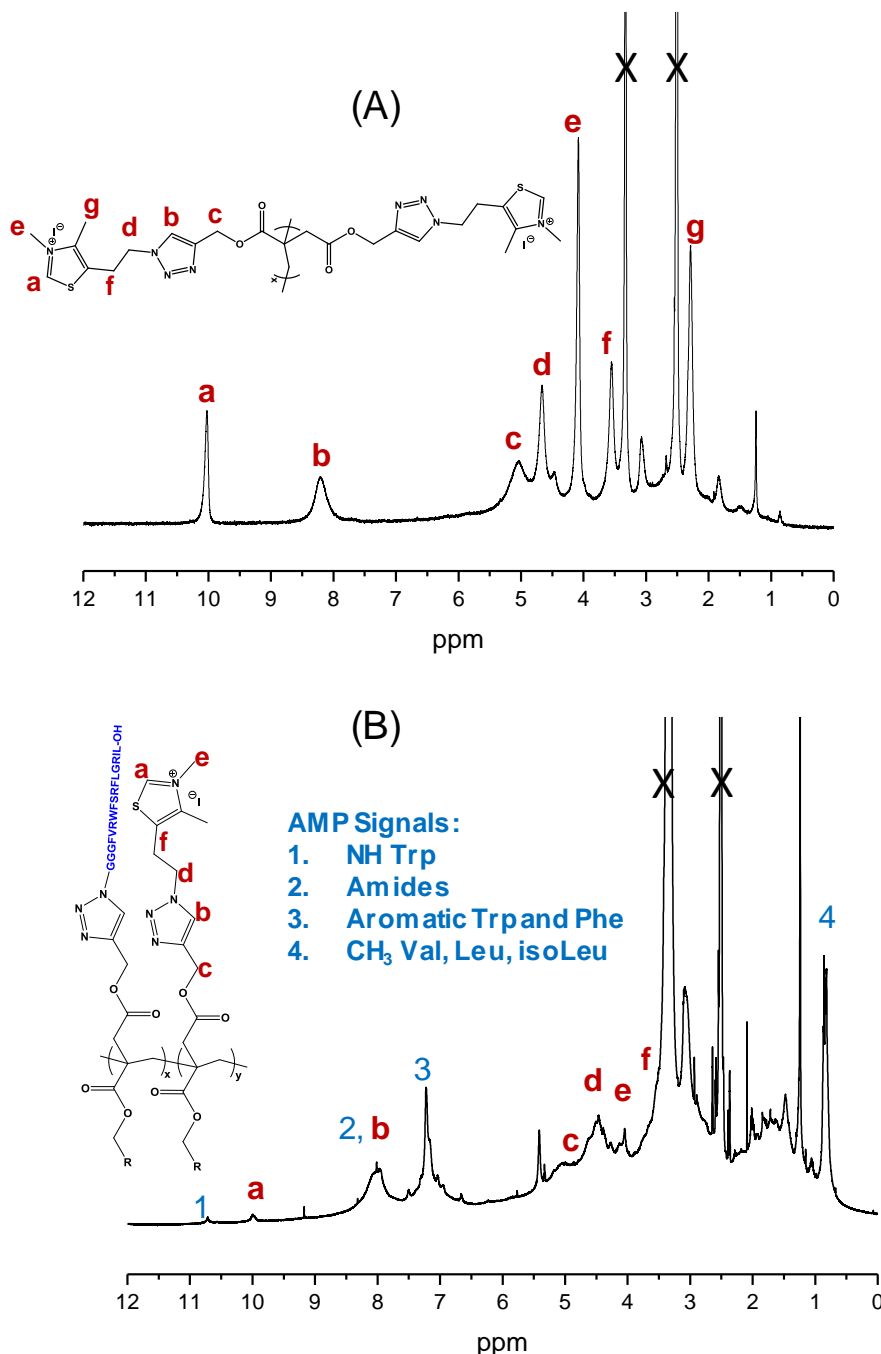


Figure 2. ¹H-NMR spectra of A) PTTIQ and B) PTTIQ-AMP biobased polymer.

FTIR spectra also corroborate the incorporation of both antimicrobial components to the biobased polymer (Figure 3). In the FTIR spectrum of PTTIQ, the bands at 1730 cm⁻¹ assigned to $\nu(\text{C=O})$, 1593 cm⁻¹ corresponding to the $\nu(\text{C=N}^+)$ and 1166 cm⁻¹ due to C-O stretching vibration were observed, whereas in the PTTIQ-AMP FTIR spectrum, new

bands appear associated to the AMP, Temporin L, in addition to the bands of the thiazolium groups. The main bands associated to the peptide appear at 1650 cm^{-1} (amide I, mainly related with the C=O stretching vibration) and at 1541 cm^{-1} (amide II, N–H bending), indicating the presence of amide bonds in the peptide's backbone.

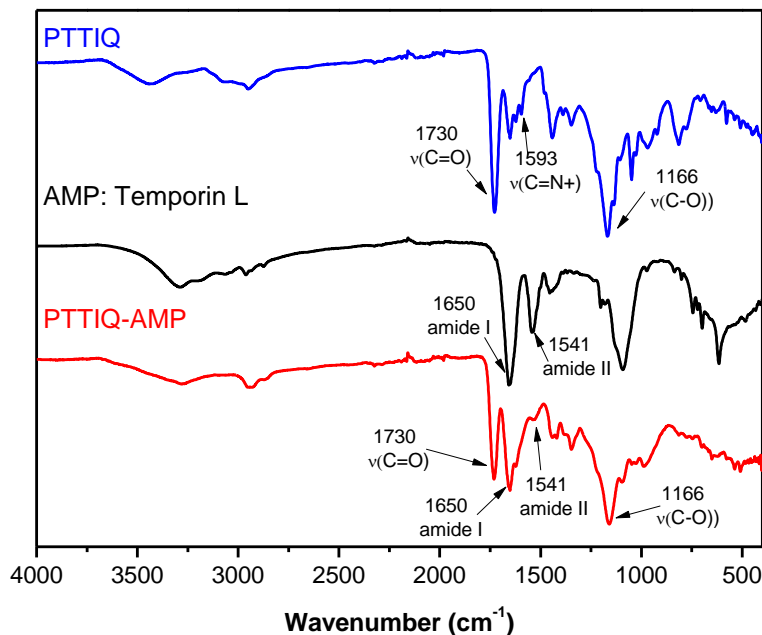


Figure 3. FTIR spectra of PTTIQ, Temporin L peptide, and PTTIQ-AMP conjugated polymer.

Antimicrobial properties of biobased polymers

Subsequently, the antimicrobial activity of the prepared polymers with thiazolium groups, PTTIQ, and with thiazolium and AMP conjugate, PTTIQ-AMP, was assessed by determining the MIC values against *P. aeruginosa*, *E. coli*, *S. aureus*, *E. faecalis*, *C. albicans* strains. We synthesized the polymer-peptide conjugate (PTTIQ-AMP) with the goal of achieving superior antimicrobial activity, stability, and solubility. Conjugating AMP to polymers often provides protection against protease degradation and, in some cases, can reduce cytotoxic effects and increase antibacterial activity.¹⁵ For instance, it has been reported that polylysine AMPs attached to chitosan generated significant damage to bacterial membranes.^{30,31} As shown in Table 1, the cationic polyitaconate bearing thiazolium groups (PTTIQ) is effective against Gram-positive bacteria with MIC values of $64\text{ }\mu\text{g mL}^{-1}$ and has moderate activity against the fungus *C. albicans*, whereas is not active against Gram-negative bacteria. In contrast, the AMP Temporin L has a broad antimicrobial spectrum, effectively targeting both Gram-positive and Gram-negative bacteria, and *C. albicans*. However, upon conjugation of the thiazolium group with the

AMP within the polyitaconate chains (PTTIQ-AMP), significantly higher MIC values were observed compared to both the corresponding polymer with only thiazolium groups and the standalone Temporin L peptide. This observation can be attributed to the aggregation of the polymeric chain, leading to reduced solubility in this case, and consequently limiting the availability of functional antimicrobial groups for interaction with microorganisms. In effect, Zeta potential measurements indicated a significant decrease in the value of the PTTIQ-AMP conjugate (31 ± 5 mV) compared to the values obtained for the cationic polymer (52 ± 5 mV) and the peptide (41 ± 5 mV). These findings could be an indicative of an aggregation process occurring within the PTTIQ-AMP conjugate, which could hinder the positive charges and then reduce the antimicrobial efficacy.

Table 1. MIC values of PTTIQ, Temporin L AMP and PTTIQ-AMP.

Sample	MICs ($\mu\text{g mL}^{-1}$)					MICs in combination ($\mu\text{g mL}^{-1}$)	
	<i>C. albicans</i>	<i>P. aeruginosa</i>	<i>S. aureus</i>	<i>E. coli</i>	<i>E. faecalis</i>	<i>E. coli</i>	<i>E. faecalis</i>
PTTIQ	125	>500	64	500	64	250	64
AMP	32	125	4	16	8	8	8
PTTIQ-AMP	500	>500	125	>500	125	-	-

For this reason, we decided to assess the impact on antimicrobial activity of the combination of the cationic polymer PTTIQ and the AMP Temporin L without conjugation in the same polymeric structure. The fractional inhibitory concentration index (FICI) values of the combination (PTTIQ-AMP) against the Gram-positive *E. faecalis* and the Gram-negative *E. coli* bacterial strains were determined using the checkerboard method.

In this assay, the combination is considered synergistic when $\text{FICI} \leq 0.5$, additive if $0.5 < \text{FICI} \leq 1$, indifferent when $1 < \text{FICI} \leq 2$, and antagonistic when $\text{FICI} > 2$.³² The FICI against *E. faecalis* and *E. coli* was found to be 2 and 1.5, respectively; thus, an indifferent effect is observed meaning that a combination of cationic polymer and antimicrobial peptide has an identical effect to that of the most active constituent. In principle, the mechanism of action of the cationic polymer and Temporin L is mainly through interactions with the negatively charged bacterial membranes leading to insertion, destabilization, and consequent, disruption of the membrane.³³ Temporin L's ability to

damage and penetrate the bacterial membrane is associated to its highly stable secondary amphipathic α -helical conformation. Although it has been studied that synergistic interactions could be probable with antimicrobial agent combinations that act on a similar manner,^{34,35} in this case, the combination had no synergistic effect.

Preparation of antimicrobial fiber mats via electrospinning

Subsequently, the antimicrobial biobased polymer and the AMP Temporin L were employed to confer activity to fiber mats based on PLA. Due to the significantly low antimicrobial activity exhibited by the PTTIQ-AMP conjugated structure, this polymer was excluded from the experimental investigations. Despite the combination of PTTIQ and Temporin showing indifferent effects when exposed to the bacterial suspension medium, we proceeded to test the combination of PTTIQ and the AMP Temporin L, which was immobilized in PLA fibers. This decision was based on the understanding that the availability of both antimicrobial compounds to interact with the bacteria might vary due to differences in diffusion, migration, and release processes. Initially, PLA fibers and PLA/PTTIQ (90/10 wt%) fibers were directly electrospun from solutions containing CHCl₃ and DMF. Next, we analyzed the morphology of the obtained fibers in both cases (Figure 4), in which it is evident that the incorporation of 10 wt% of PTTIQ did not induce changes in the resulting fibers, albeit a slight reduction in diameter is observed, from 1.6 ± 0.6 μ m for PLA to 1.2 ± 0.5 μ m for PLA/PTTIQ fibers.

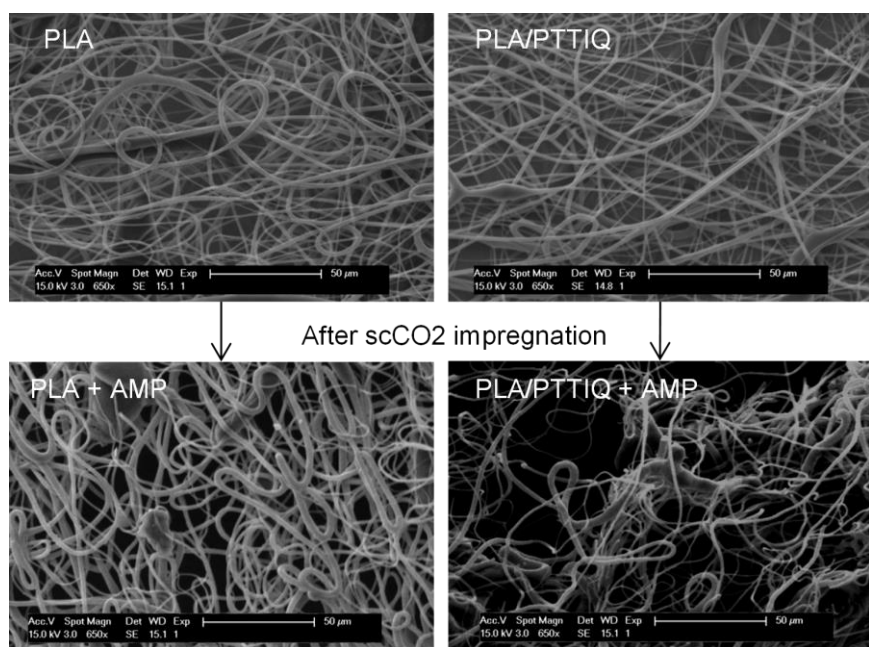


Figure 4. SEM images of prepared fiber mats before (PLA and PLA/PTTIQ) and after (PLA + AMP and PLA/PTTIQ +AMP) scCO₂ impregnation with AMP.

In a second step, the AMP Temporin L was incorporated to both fiber mats (PLA and PLA/PTTIQ) by supercritical solvent impregnation. This technique allows the use of low amount of peptide to impregnate a relative high volume of solid sample without the use of any toxic organic solvent at moderate experimental conditions. It is well known, that both, the operating conditions and the structure of the polymer strongly affect the impregnation yield. In this study, we compared the supercritical solvent impregnation efficiency of PLA and PLA/PTTIQ fibers by applying fixed conditions of 40 °C, 150 bar for 3 h. The AMP impregnation yields were determined gravimetrically, 27% and 6%, for PLA and PLA/PTTIQ, respectively. We hypothesize that the lower impregnation yield obtained in the PLA/PTTIQ fibers in comparison to the PLA fibers is associated with the presence of the cationic polymer that might hinder the incorporation of the peptide by electrostatic repulsion or because the cationic polymer impedes the swelling of the PLA fibers. SEM images of the impregnated fibers (Figure 4) confirm that, under the chosen temperature and pressure conditions, the scCO₂ impregnation process does not significantly alter the morphology of the fibers, although some fiber breakages are observed. However, both fiber mats exhibit an increase in diameter, indicating the swelling effect induced by carbon dioxide on the polymeric fibers. The diameter of the PLA+AMP fibers, 2.5 ± 0.9 µm is larger compared to PLA/PTTIQ+AMP impregnated fibers, 2 ± 1. Nonetheless, the swelling percentage relative to the non-impregnated fibers is slightly lower for the latter case. Therefore, the low loaded yield observed in PLA/PTTIQ may be attributed to repulsive interactions with the cationic polymer.

FTIR spectra were recorded to evaluate the chemical structure of PLA and PLA/PTTIQ fibers before and after peptide impregnation using scCO₂ (Figure 5). The spectra of PLA and PLA/PTTIQ reveal the characteristic absorption bands for PLA, at 1756 cm⁻¹ due to the stretching of carbonyl group –C=O, and bands at 1450 cm⁻¹ assigned to the CH₃ asymmetric bending vibration, at 1183 cm⁻¹ corresponding to the C–O–C stretching vibration and at 1083 cm⁻¹ associated to C-O stretching. In the FTIR spectrum of the fibers several new bands appeared after impregnation. The presence of the AMP is confirmed by the bands associated to the amide I and amide II, at 1650 cm⁻¹ and 1541 cm⁻¹, respectively.

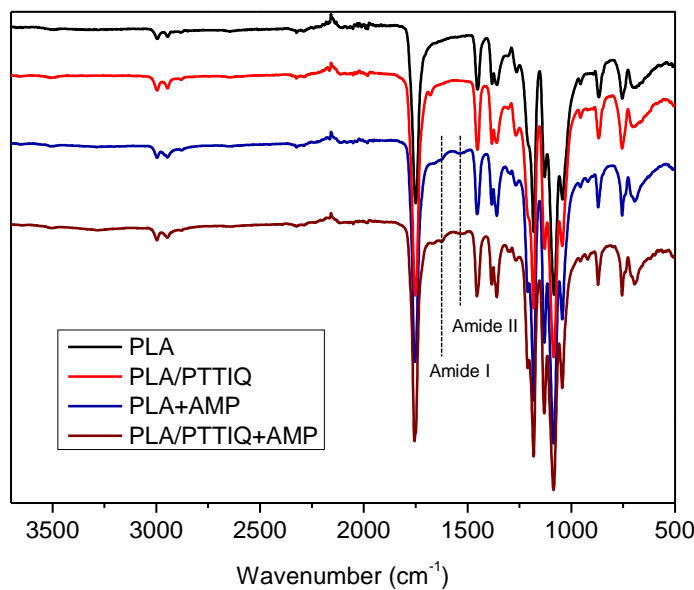


Figure 5. FTIR spectra of non-impregnated fibers (PLA and PLA/PTTIQ) and impregnated fibers with AMP (PLA+AMP and PLA/PTTIQ+AMP).

After confirming the success of the AMP impregnation, we investigated the antimicrobial activity of PLA and PLA/PTTIQ fibers impregnated with the AMP (PLA+AMP and PLA/PTTIQ+AMP) in comparison with the corresponding non-impregnated samples against *E. coli* and *E. faecalis*. The results obtained from the tested fibers, using the ASTM E2149 method that determines the percentage of bacteria reduction after incubation in dynamic conditions related to an initial inoculum, are summarized in Table 2.

It is evident that the fibers impregnated with the AMP Temporin L exhibits high antimicrobial activity, achieving a Log reduction up to 5 against both bacterial strains. In contrast, the fibers containing only the cationic polyitaconate yield log reductions of 1.58 and 1.39 against *E. coli* and *E. faecalis*, respectively. These findings confirm the potential of Temporin L as antimicrobial agent in PLA based fibers.

Subsequently, the antibacterial efficacy of the fibers was retested in a second cycle. The fiber mats were subjected to sequential washing with ethanol, PBS, and water, and subsequently dried overnight in a vacuum oven. The antibacterial test against both bacterial strains was then repeated as described above. The fibers experienced a significant decrease in activity, which can be attributed to the leaching of the antimicrobial component during the first antimicrobial test, resulting in a reduction of the available antimicrobial agent for the second cycle (Table 2). This effect is more pronounced in fibers mats impregnated with AMP (PLA +AMP and PLA/PTTIQ + AMP), suggesting that the

loss/leaching of the AMP during incubation is greater than that of the cationic polyitaconate, probably because the scCO₂ impregnation of AMP occurs mostly at the surface of the fiber mats. In contrast, the cationic polyitaconate mostly remains embedded in the fibers, maintaining its antimicrobial performance likely due to its higher molecular weight and lower diffusion capacity.

Table 2. Antimicrobial activity of non-impregnated fibers (PLA and PLA/PTTIQ) and of impregnated fibers with AMP (PLA+AMP and PLA/PTTIQ+AMP) against *E. coli* and *E. faecalis*.

Sample	<i>E. coli</i>		<i>E. faecalis</i>	
	Bacterial reduction (%)	Log reduction	Bacterial reduction (%)	Log reduction
PLA/PTTIQ	97	1.58	96	1.39
PLA/PTTIQ+AMP	99.999	5	99.999	5
PLA +AMP	99.999	5	99.999	5
PLA/PTTIQ*	83	0.77	77	0.63
PLA/PTTIQ+AMP*	84	0.78	92	1.10
PLA +AMP*	0	0	45	0.26

*Results obtained in a second cycle of the antibacterial test.

Disk diffusion test was performed to confirm the release of the AMP from the fiber mats. As can be seen in Figure 6 for the test with Gram-negative *E. coli*, only the fibers mats impregnated with AMP (PLA +AMP and PLA/PTTIQ + AMP) form an inhibition zone revealing the diffusion of the peptide out of the fibers. Nevertheless, as PLA is a biodegradable material, the cationic polymers and the AMP could be released from the fibers during its degradation process.^{36,37}



Figure 6. Photographs of disk diffusion assays on agar plates cultivated with Gram-negative *E. coli* of non-impregnated fibers (PLA and PLA/PTTIQ) and impregnated fibers with AMP (PLA+AMP and PLA/PTTIQ+AMP).

3.3.5 Conclusions

In conclusion, we have shown that the combination of a cationic biobased polyitaconate incorporating thiazolium moieties with the AMP Temporin L did not improve the antibacterial activity against various microorganisms. In fact, an indifferent effect was observed, and even a negative effect was noticed when Temporin L was covalently conjugated as a side chain of the cationic polyitaconate. However, the clickable biobased polymer has demonstrated its suitability and versatility as a platform for specific tethering bioactive groups, enabling the development of multifunctional systems with the aim of identifying synergistic combinations.

On the other hand, the incorporation of both the cationic polymer and Temporin L into PLA fibers has shown improved antibacterial performance. This enhancement can be attributed to their different diffusion capacities and leaching behaviors, which contribute to a more effective and sustained release of antimicrobial agents.

3.3.6 Acknowledgments

This work was funded by the MICINN (PID2019-104600RB-I00 and PID2021-123553OA-I00), the Agencia Estatal de Investigación (AEI, Spain) and Fondo Europeo de Desarrollo Regional (FEDER, EU) and by CSIC (LINKA20364). A. Chiloeches acknowledges MICIU for his FPU fellowship FPU18/01776. Cesar de la Fuente-Nunez holds a Presidential Professorship at the University of Pennsylvania and acknowledges funding from the Procter & Gamble Company, United Therapeutics, a BBRF Young Investigator Grant, the Nemirovsky Prize, Penn Health-Tech Accelerator Award, and the Dean's Innovation Fund

from the Perelman School of Medicine at the University of Pennsylvania. Research reported in this publication was supported by the Langer Prize (AIChE Foundation), the National Institute of General Medical Sciences of the National Institutes of Health under award number R35GM138201, and the Defense Threat Reduction Agency (DTRA; HDTRA11810041, HDTRA1-21-1-0014, and HDTRA1-23-1-0001). D. Placha and J. Zagora acknowledge to the Doctoral grant competition VSB -Technical University of Ostrava, reg. no. CZ.02.2.69/0.0/0.0/19_073/0016945 within the Operational Programme Research, Development and Education, under project DGS/INDIVIDUAL/2020-001 "Development of antimicrobial biobased polymeric material using supercritical fluid technology".

3.3.7 References

- (1) Chowdhury, M. A.; Shuvho, M. B. A.; Shahid, M. A.; Haque, A. K. M. M.; Kashem, M. A.; Lam, S. S.; Ong, H. C.; Uddin, M. A.; Mofijur, M. Prospect of Biobased Antiviral Face Mask to Limit the Coronavirus Outbreak. *Environ. Res.* **2021**, 192, 110294.
- (2) Uhljar, L. É.; Ambrus, R. Electrospinning of Potential Medical Devices (Wound Dressings, Tissue Engineering Scaffolds, Face Masks) and Their Regulatory Approach. *Pharmaceutics*. MDPI February **2023**.
- (3) Adeli, H.; Khorasani, M. T.; Parvazinia, M. Wound Dressing Based on Electrospun PVA/Chitosan/Starch Nanofibrous Mats: Fabrication, Antibacterial and Cytocompatibility Evaluation and in Vitro Healing Assay. *Int. J. Biol. Macromol.* **2019**, 122, 238–254.
- (4) Chiloeches, A.; Cuervo-Rodríguez, R.; Gil-Romero, Y.; Fernández-García, M.; Echeverría, C.; Muñoz-Bonilla, A. Electrospun Polylactic Acid-Based Fibers Loaded with Multifunctional Antibacterial Biobased Polymers. *ACS Appl. Polym. Mater.* **2022**, 4 (9), 6543–6552.
- (5) Chiloeches, A.; Fernández-García, R.; Fernández-García, M.; Mariano, A.; Bigioni, I.; Scotto d'Abusco, A.; Echeverría, C.; Muñoz-Bonilla, A. PLA and PBAT-Based Electrospun Fibers Functionalized with Antibacterial Bio-Based Polymers. *Macromol. Biosci.* **2023**, 23 (1), 2200401.
- (6) Chen, K.; Nikam, S. P.; Zander, Z. K.; Hsu, Y.-H.; Dreger, N. Z.; Cakmak, M.; Becker, M. L. Continuous Fabrication of Antimicrobial Nanofiber Mats Using Post-Electrospinning Functionalization for Roll-to-Roll Scale-Up. *ACS Appl. Polym. Mater.* **2020**, 2 (2), 304–316.
- (7) Xu, J.-W.; Wang, Y.; Yang, Y.-F.; Ye, X.-Y.; Yao, K.; Ji, J.; Xu, Z.-K. Effects of Quaternization on the Morphological Stability and Antibacterial Activity of Electrospun Poly(DMAEMA-Co-AMA) Nanofibers. *Colloids Surf. B* **2015**, 133, 148–155.
- (8) Torres, M. D. T.; Sothiselvam, S.; Lu, T. K.; de la Fuente-Nunez, C. Peptide Design Principles for Antimicrobial Applications. *J. Mol. Biol.* **2019**, 431 (18), 3547–3567.
- (9) Cesaro, A.; Torres, M. D. T.; de la Fuente-Nunez, C. Chapter Thirteen - Methods for the Design and Characterization of Peptide Antibiotics. In *Antimicrobial Peptides*; Hicks, L. M. B. T.-M. in E., Ed.; Academic Press, **2022**; Vol. 663, pp 303–326.
- (10) Magana, M.; Pushpanathan, M.; Santos, A. L.; Leanse, L.; Fernandez, M.; Ioannidis, A.; Julianotti, M. A.; Apidianakis, Y.; Bradfute, S.; Ferguson, A. L.; et al. The Value of Antimicrobial Peptides in the Age of Resistance. *Lancet Infect. Dis.* **2020**, 20 (9), e216–e230.
- (11) Torres, M. D. T.; Cao, J.; Franco, O. L.; Lu, T. K.; de la Fuente-Nunez, C. Synthetic Biology and Computer-Based Frameworks for Antimicrobial Peptide Discovery. *ACS Nano* **2021**, 15 (2), 2143–2164.
- (12) Riool, M.; de Breij, A.; Drijfhout, J. W.; Nibbering, P. H.; Zaaij, S. A. J. Antimicrobial Peptides in Biomedical Device Manufacturing. *Front. Chem.* **2017**, 5.
- (13) Li, X.; Wang, X.; Subramaniyan, S.; Liu, Y.; Rao, J.; Zhang, B. Hyperbranched Polyesters Based on Indole- and Lignin-Derived Monomeric Aromatic Aldehydes as Effective Nonionic Antimicrobial Coatings with Excellent Biocompatibility. *Biomacromolecules* **2022**, 23 (1), 150–162.
- (14) Amariei, G.; Kokol, V.; Boltes, K.; Letón, P.; Rosal, R. Incorporation of Antimicrobial Peptides on Electrospun Nanofibres for Biomedical Applications. *RSC Adv.* **2018**, 8 (49), 28013–28023.
- (15) Dart, A.; Bhave, M.; Kingshott, P. Antimicrobial Peptide-Based Electrospun Fibers for Wound Healing Applications. *Macromol. Biosci.* **2019**, 19 (9), 1800488.
- (16) Yu, L.; Dou, S.; Ma, J.; Gong, Q.; Zhang, M.; Zhang, X.; Li, M.; Zhang, W. An Antimicrobial Peptide-Loaded Chitosan/Polyethylene Oxide Nanofibrous Membrane Fabricated by Electrospinning Technology. *Front. Mater.* **2021**, 8.
- (17) Simonetti, O.; Cirioni, O.; Goteri, G.; Ghiselli, R.; Kamysz, W.; Kamysz, E.; Silvestri, C.; Orlando, F.;

- Barucca, C.; Scalise, A.; et al. Temporin A Is Effective in MRSA-Infected Wounds through Bactericidal Activity and Acceleration of Wound Repair in a Murine Model. *Peptides* **2008**, *29* (4), 520–528.
- (18) Koohzad, F.; Asoodeh, A. Cross-Linked Electrospun PH-Sensitive Nanofibers Adsorbed with Temporin-Ra for Promoting Wound Healing. *ACS Appl. Mater. Interfaces* **2023**, *15* (12), 15172–15184.
- (19) Rinaldi, A. C.; Mangoni, M. L.; Rufo, A.; Luzi, C.; Barra, D.; Zhao, H.; Kinnunen, P. K. J.; Bozzi, A.; Di Giulio, A.; Simmaco, M. Temporin L: Antimicrobial, Haemolytic and Cytotoxic Activities, and Effects on Membrane Permeabilization in Lipid Vesicles. *Biochem. J.* **2002**, *368* (Pt 1), 91–100.
- (20) Ferguson, P. M.; Clarke, M.; Manzo, G.; Hind, C. K.; Clifford, M.; Sutton, J. M.; Lorenz, C. D.; Phoenix, D. A.; Mason, A. J. Temporin B Forms Hetero-Oligomers with Temporin L, Modifies Its Membrane Activity, and Increases the Cooperativity of Its Antibacterial Pharmacodynamic Profile. *Biochemistry* **2022**, *61* (11), 1029–1040.
- (21) Ulvatne, H.; Karoliussen, S.; Stiberg, T.; Rekdal, Ø.; Svendsen, J. S. Short Antibacterial Peptides and Erythromycin Act Synergically against Escherichia Coli. *J. Antimicrob. Chemother.* **2001**, *48* (2), 203–208.
- (22) Kankala, R. K.; Zhang, Y. S.; Wang, S.-B.; Lee, C.-H.; Chen, A.-Z. Supercritical Fluid Technology: An Emphasis on Drug Delivery and Related Biomedical Applications. *Adv. Healthc. Mater.* **2017**, *6* (16), 1700433.
- (23) Tejero, R.; López, D.; López-Fabal, F.; Gómez-Garcés, J. L.; Fernández-García, M. Antimicrobial Polymethacrylates Based on Quaternized 1,3-Thiazole and 1,2,3-Triazole Side-Chain Groups. *Polym. Chem.* **2015**, *6* (18).
- (24) Chiloeches, A.; Funes, A.; Cuervo-Rodríguez, R.; López-Fabal, F.; Fernández-García, M.; Echeverría, C.; Muñoz-Bonilla, A. Biobased Polymers Derived from Itaconic Acid Bearing Clickable Groups with Potent Antibacterial Activity and Negligible Hemolytic Activity. *Polym. Chem.* **2021**, *12* (21), 3190–3200.
- (25) Tejero, R.; López, D.; López-Fabal, F.; Gómez-Garcés, J. L.; Fernández-García, M. Antimicrobial Polymethacrylates Based on Quaternized 1,3-Thiazole and 1,2,3-Triazole Side-Chain Groups. *Polym. Chem.* **2015**, *6* (18), 3449–3459.
- (26) Mercer, D. K.; Torres, M. D. T.; Duay, S. S.; Lovie, E.; Simpson, L.; von Köckritz-Blickwede, M.; de la Fuente-Nunez, C.; O’Neil, D. A.; Angeles-Boza, A. M. Antimicrobial Susceptibility Testing of Antimicrobial Peptides to Better Predict Efficacy. *Front. Cell. Infect. Microbiol.* **2020**, *10*.
- (27) Balouiri, M.; Sadiki, M.; Ibsouda, S. K. Methods for in Vitro Evaluating Antimicrobial Activity: A Review. *J. Pharm. Anal.* **2016**, *6* (2), 71–79.
- (28) Berditsch, M.; Jäger, T.; Strempel, N.; Schwartz, T.; Overhage, J.; Ulrich, A. S. Synergistic Effect of Membrane-Active Peptides Polymyxin B and Gramicidin S on Multidrug-Resistant Strains and Biofilms of *Pseudomonas Aeruginosa*. *Antimicrob. Agents Chemother.* **2015**, *59* (9), 5288–5296.
- (29) ASTM International. ASTM E2149-20, Stand. Test Method Determ. Antimicrob. Act. Antimicrob. Agents Under Dyn. Contact Cond. ASTM E2149-20, Stand. *Test Method Determ. Antimicrob. Act. Antimicrob. Agents Under Dyn. Contact Cond. ASTM Int.* www.astm.org. **2020**.
- (30) Li, P.; Zhou, C.; Rayatpisheh, S.; Ye, K.; Poon, Y. F.; Hammond, P. T.; Duan, H.; Chan-Park, M. B. Cationic Peptidopolysaccharides Show Excellent Broad-Spectrum Antimicrobial Activities and High Selectivity. *Adv. Mater.* **2012**, *24* (30), 4130–4137.
- (31) Hyldgaard, M.; Mygind, T.; Vad, B. S.; Stenvang, M.; Otzen, D. E.; Meyer, R. L. The Antimicrobial Mechanism of Action of Epsilon-Poly-L-Lysine. *Appl. Environ. Microbiol.* **2014**, *80* (24), 7758–7770.
- (32) Odds, F. C. Synergy, Antagonism, and What the Chequerboard Puts between Them. *J. Antimicrob. Chemother.* **2003**, *52* (1), 1.
- (33) Maione, A.; Bellavita, R.; de Alteriis, E.; Galdiero, S.; Albarano, L.; La Pietra, A.; Guida, M.; Parrilli,

- E.; D'angelo, C.; Galdiero, E.; et al. WMR Peptide as Antifungal and Antibiofilm against Albicans and Non-Albicans Candida Species: Shreds of Evidence on the Mechanism of Action. *Int. J. Mol. Sci.* **2022**, 23 (4).
- (34) Brochado, A. R.; Telzerow, A.; Bobonis, J.; Banzhaf, M.; Mateus, A.; Selkrig, J.; Huth, E.; Bassler, S.; Zamarreño Beas, J.; Zietek, M.; et al. Species-Specific Activity of Antibacterial Drug Combinations. *Nature* **2018**, 559 (7713), 259–263.
- (35) Namivandi-Zangeneh, R.; Sadrearhami, Z.; Dutta, D.; Willcox, M.; Wong, E. H. H.; Boyer, C. Synergy between Synthetic Antimicrobial Polymer and Antibiotics: A Promising Platform To Combat Multidrug-Resistant Bacteria. *ACS Infect. Dis.* **2019**, 5 (8), 1357–1365.
- (36) Kumar, S.; Singh, S.; Senapati, S.; Singh, A. P.; Ray, B.; Maiti, P. Controlled Drug Release through Regulated Biodegradation of Poly(Lactic Acid) Using Inorganic Salts. *Int. J. Biol. Macromol.* **2017**, 104, 487–497.
- (37) Sun, Q.; Sheng, J.; Yang, R. Controllable Biodegradation and Drug Release Behavior of Chitosan-Graft-Poly(D, L-Lactic Acid) Synthesized by an Efficient Method. *Polym. Degrad. Stab.* **2021**, 186, 109458.

Capítulo 4

Conclusiones

Conclusiones

En la presente tesis doctoral se han logrado novedosos sistemas poliméricos bioactivos a partir del monómero de origen natural, el ácido itacónico. Aprovechando la capacidad que tiene la química click en la síntesis química, el monómero se ha modificado con dos grupos alquino, para posteriormente añadir mediante cicloadición azida-alquino catalizada con cobre (CuAAC) diferentes grupos funcionales (tiazol, dimetilhidantoina y AMPs) que proporcionan actividad antimicrobiana a los polímeros. Además, estos polímeros son biodegradables en condiciones de compostaje. Adicionalmente, estos polímeros se han introducido en matrices poliméricas biobasadas tales como el PLA y el PBAT para la obtención de diferentes tipos de materiales, como fibras o films, que mostraron en general buenas capacidades antimicrobianas frente a bacterias, manteniendo sus propiedades térmicas, biodegradabilidad y su baja toxicidad.

Las conclusiones por capítulos más significativas se describen a continuación:

Conclusiones derivadas del Capítulo 2

- Se ha logrado crear copolímeros a partir del monómero derivado del ácido itacónico con grupos alquino con la capacidad de modificarse con cualquier azida mediante química click. Estos se han funcionalizado con un grupo tiazol y posteriormente se han cuaternizado para la obtención de polímeros antimicrobianos con grupos catiónicos tiazolio y triazolio.
- Los polímeros obtenidos tienen una buena actividad frente a bacterias Gram-positivas, pero son poco eficientes frente a Gram-negativas. Además, tienen una nula o baja hemotoxicidad. De todas las composiciones evaluadas en los copolímeros, se puede concluir que el polímero P100T es el que mejores resultados presenta.
- Todos los copolímeros se biodegradan en menos de 80 días, siendo el polímero P100T el que más rápido se biodegrada debido probablemente a su mayor solubilidad en agua.

Conclusiones derivadas del Capítulo 3

- Los polímeros con grupos triazolio y tiazolio se han incorporado en fibras de PLA y PBAT exitosamente mediante eletrohilado. Las fibras presentan escasa citotoxicidad frente fibroblastos humanos, pero se produce un efecto citostático. En cuanto a la actividad antimicrobiana han resultado ser muy efectivas frente a

S. aureus y MRSA (Gram-positiva) pero no muy activas contra *E. coli* (Gram-negativa).

- La incorporación de grupos N-halamina a los polímeros itacónicos da lugar a un polímero con dos funcionalizaciones antimicrobianas distintas, N-halamina y triazolio. Estos polímeros multifuncionales se incorporan con éxito a fibras de PLA, que han demostrado tener buena actividad frente a bacterias Gram-positiva, pero además mejoran considerablemente la actividad frente a las Gram-negativa, que es lo que se buscaba con la incorporación de N-halamina. Además, se ha determinado que la degradación de las fibras en condiciones de compostaje sucede en solo 28 días.
- La incorporación de un péptido antimicrobiano (AMP) a las fibras antimicrobianas para mejorar la actividad antimicrobiana no produce ninguna mejora cuando se incorporan juntos en disolución; no se da la sinergia esperada en ninguna de las dos estrategias utilizadas. Sin embargo, sí que se observa una buena sintonía cuando el AMP es depositado sobre las fibras antimicrobianas mediante fluido supercrítico. Este sistema ofrece por un lado una acción antimicrobiana inmediata gracias al AMP, y, por otro lado, una acción a largo plazo gracias a las fibras antimicrobianas funcionalizadas con el politaconato con grupos tiazolio.

En resumen, se ha diseñado un polímero muy versátil a partir de un compuesto de origen natural como es el ácido itacónico, que ha servido como plataforma para el desarrollo de nuevos sistemas antimicrobianos. Este nuevo polímero presenta una capacidad para la creación y modulación de las características deseadas, gracias a la química click. La incorporación de diferentes grupos funcionales antimicrobianos brinda buenas propiedades para la contención de infecciones. Además, se ha demostrado la biodegradación de estos polímeros, y su potencial como componentes de materiales biobasados tales como films y fibras de PLA y PBAT.

Anexo

Publicaciones científicas derivadas de esta tesis doctoral

	Revista	Año de publicación	Factor de impacto
Biobased polymers derived from itaconic acid bearing clickable groups with potent antibacterial activity and negligible hemolytic activity	<i>Polymer Chemistry</i>	2021	5.364 Q1 (86.11)
Antibacterial and compostable polymers derived from biobased itaconic acid as environmentally friendly additives for biopolymers	<i>Polymer Testing</i>	2022	5.1 Q1 (84.30)
PLA and PBAT based electrospun fibers functionalized with antibacterial biobased polymers	<i>Macromolecular Bioscience</i>	2022	4.6 Q1 (79.70)
Electrospun polylactic acid-based fibers loaded with multifunctional antibacterial biobased polymers	<i>ACS Applied Polymer Materials</i>	2022	5.0 Q1 (82.00)
Multifunctional PLA fibers loaded with antimicrobial peptides and cationic polyitaconates	<i>ACS Applied Bio Materials</i>	2023	4.7 Q3 (41.67)

Reported in Journal Citation Reports (JCR). Journal Impact Factor (JIF) Category: Polymer science

Otras contribuciones

Proyectos de investigación

- I-LINK1191 Graphene-based hybrid materials as antimicrobial systems effective against antibiotic resistant bacteria. CSIC, Convocatoria “I-LINK+ 2017”.
Fecha: 1/01/2018-31/12/2019
- PID2019-104600RB-I00. Polímeros sostenibles biobasados con actividad antimicrobiana. MICINN
Fecha: 01/06/2020-31/05/2023
- I-LINKA 20364 Design of novel antimicrobial biobased materials using supercritical fluids processes. CSIC, Convocatoria “I-LINK+2020”
Fecha: Fecha: 1/01/2021-31/12/2022
- PID2021-123553OA-I00 Generación de polímeros antimicrobianos biobasados electroactivos para aplicaciones biomédicas. MICINN
Fecha: 01/09/2022-31/08/2025

Estancias de investigación

- Estancia en la Universidad de Roma La Sapienza, Roma (Italia), de septiembre a diciembre de 2021.
- Estancia en la Universidad Técnica-VSB de Ostrava (República Checa), noviembre de 2022.

Congresos

- Participación en el congreso con un poster: XVI Reunión del Grupo Especializado de Polímeros (GEP), XVII Simposio Latinoamericano de Polímeros (SLAP) y XV Congreso Iberoamericano de Polímeros. San Sebastián (2022).
- Jornadas de Jóvenes Investigadores en Materiales Funcionales UCO-SECV (JIMAF 2023). Córdoba.
- Participación en el congreso “Jóvenes Investigadores en Polímeros” (JIP 2023), Alicante.

Actividades divulgativas

- Polímeros divertidos 2018, 2019 y 2022. Talleres científicos para estudiantes de primaria (CEIP Nuestra Señora de la Paloma) llevado a cabo en el ICTP-CSIC, Madrid.
- 4ºde la ESO+EMPRESA 2023. Talleres científicos para estudiantes de secundaria llevado a cabo en el ICTP-CSIC, Madrid.

Esta tesis ha sido financiada por el programa FPU del Ministerio de Universidades en colaboración con el Instituto de Ciencia y Tecnología de Polímeros del Consejo Superior de Investigaciones Científicas (ICTP-CSIC)

